Journal of Oncology

Clinical and Basic Progress on Head and Neck Cancer

Lead Guest Editor: Zhien Feng
Guest Editors: Qian Li, Qihong Li, Wei Cao, and Tiancheng Li

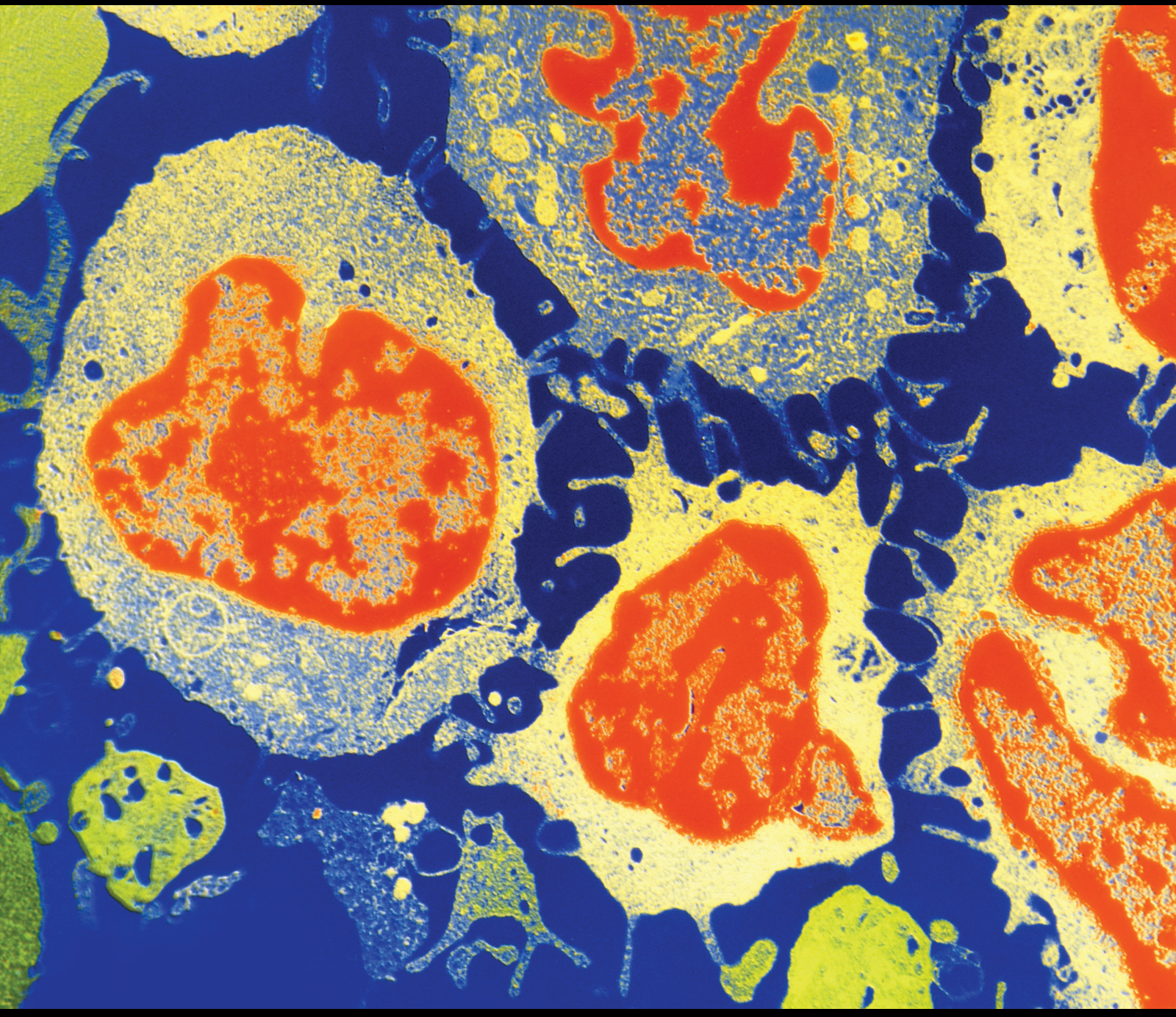

Clinical and Basic Progress on Head and Neck Cancer

Journal of Oncology

Clinical and Basic Progress on Head and Neck Cancer

Lead Guest Editor: Zhien Feng
Guest Editors: Qian Li, Qihong Li, Wei Cao, and Tiancheng Li

Contents

Hindawi
Journal of Oncology
Volume 2023, Article ID 6027860, 15 pages
https://doi.org/10.1155/2023/6027860

Research Article

The Long Noncoding RNA Cytoskeleton Regulator RNA (CYTOR)/miRNA-24-3p Axis Facilitates Nasopharyngeal Carcinoma Progression by Modulating GAD1 Expression

Jingwei Du,[1,2] Wangbo Yu,[3] Lijuan Peng,[4] and Tao Zhang[1]

[1]*Department of Otolaryngology-Head and Neck Surgery, The First Affiliated Hospital of Jinan University, Guangzhou 510630, China*
[2]*Department of Otolaryngology-Head and Neck Surgery, Nanchong Central Hospital, The Second Clinical Medical College, North Sichuan Medical College, Nanchong 637000, Sichuan, China*
[3]*Department of Otolaryngology-Head and Neck Surgery, Affiliated Hospital of North Sichuan Medical College, Nanchong 637000, Sichuan, China*
[4]*Department of Pathogen Biology, School of Basic Medical Sciences and Forensic Medicine, North Sichuan Medical College, Nanchong 637000, Sichuan, China*

Correspondence should be addressed to Tao Zhang; tzhangt@126.com

Received 28 July 2022; Revised 11 October 2022; Accepted 24 November 2022; Published 13 February 2023

Academic Editor: Wei Cao

Nasopharyngeal carcinoma (NPC) is a head and neck epithelial carcinoma that is unusually prevalent in Southeast Asia. Noncoding RNAs, including lncRNA and miRNA, and their target genes are considered vital regulators of tumorigenesis and the progression of NPC. However, the detailed underlying mechanisms of GAD1 involved in the regulation of NPC need to be further elucidated. In the present study, we identified that GAD1 was significantly upregulated in NPC tissues. GAD1 overexpression is promoted, while genetic knockdown of GAD1 suppresses proliferation, colony formation, migration, and invasion of NPC cells. Bioinformatics analysis and a luciferase reporter assay demonstrated that GAD1 is a direct target gene of miR-24-3p. In NPC tissues, miR-24-3p was downregulated and the lncRNA CYTOR was upregulated. CYTOR was sponged to suppress the function of miR-24-3p. CYTOR regulates GAD1 expression via modulating miR-24-3p. The CYTOR/miR-24-3p/GAD1 axis is converged to modulate the growth, migration, and invasion of NPC cells. In conclusion, the study identified a novel axis for the regulation of NPC cell growth, providing new insights into the understanding of NPC.

1. Introduction

Nasopharyngeal carcinoma (NPC), a carcinoma originating from the nasopharyngeal mucosa epithelium, is one of the most severe head and neck tumors [1, 2]. The global incidence of NPC is over 120,000 cases annually, with over 70% of the cases occurring in Southeast Asia, especially southern China [3]. There are three primary pathogenic factors for NPC, including Epstein–Barr virus (EBV) infection, genetic susceptibility, and environmental factors [4]. Early diagnosis of NPC is generally not possible, and radical surgical resection is prohibitive due to the anatomical structure of the nasopharyngeal mucosa and its proximity to vital organs [5, 6]. Because most pathological types of NPC are nonkeratinizing undifferentiated carcinomas, which are highly malignant and prone to cervical lymph node metastasis, 20% of patients develop local-regional recurrence or distant metastasis due to tumor radio-resistance or chemotherapy resistance, resulting in treatment failure [2, 7]. Delineating the molecular mechanisms of NPC recurrence and metastasis is imperative for the identification of potential targets to increase the sensitivity of the NPC to treatment and improve its prognosis.

Glutamate decarboxylase 1 (GAD1) is a rate-limiting enzyme of glutamate and gamma-aminobutyric acid (GABA) [8, 9]. GAD1 and GABA are important neural

regulators in adult mammals, but studies have found that GAD1 and GABA are also present in many nonneural tissues. For example, GAD1 expression is significantly upregulated in many tumor tissues, such as rectal cancer, breast cancer, lymphoma, and gastric cancer [10, 11]. GAD1 is significantly overexpressed in patients with metastatic prostate cancer, suggesting its potential application as a prostate-specific biomarker [12, 13]. As a target of the β-catenin/TCF pathway, GAD1 is highly expressed in Wilms' tumors [14]. In addition, GAD1 expression is significantly elevated in microsatellite unstable (MSI) colon cancer compared to microsatellite stable (MSS) cancer [15]. Recent studies have demonstrated that GAD1 and GABA regulate tumor cell proliferation, especially that of stem cells [16]. However, the role of GAD1 and the detailed regulatory mechanisms of NPC remain incompletely understood.

LncRNA and miRNA are small noncoding RNAs that play critical roles in regulating the development and metastasis of NPC [17, 18]. miR-24-3p is downregulated in NPC and targets Jab1/CSN5 to modulate NPC cell function [19]. miR-24-3p-enriched exosomes impede T-cell function by targeting GFG11, which is a potential biomarker for NPC [20]. Furthermore, the lncRNA cytoskeleton regulator RNA (CYTOR) is elevated in NPC tissues and cells and promotes NPC development via miR-163-targeted ANXA2 [21]. However, the potential regulation of GAD1 by miR-24-3p or CYTOR has not been explored.

2. Materials and Methods

2.1. Bioinformatic Analysis of NPC Dataset. To identify the key genes that play critical roles in NPC, we reanalyzed the NPC dataset published in GEO (GSE12452), which contains 10 nontumor nasopharyngeal epithelial tissue samples and 31 NPC tissue samples [22–24]; and GSE64634, which contains four normal nasopharyngeal tissue samples and 12 nasopharyngeal carcinoma specimens [25]. Briefly, raw CEL files from the Affymetrix Human Genome U133 Plus 2.0 microarray platform were downloaded and imported, along with the 32 GSM samples, into R (version 3.6). Gene expression levels were then analyzed, and differentially expressed genes were identified using the limma package [26]. Data were then plotted in a volcano plot with $P < 0.01$ and a log2-transformed expression fold change >1.0 for further evaluation.

2.2. Cell Culture and Transfection. Human NPC cell lines (CNE-1 and 5-8F) were purchased from the American Type Culture Collection (ATCC, Manassas, VA, USA). The cells were cultured in Dulbecco's modified Eagle medium (DMEM; Thermo Scientific, Waltham, MA), containing 10% fetal bovine serum (FBS; Gibco, Grand Island, MA, USA), 0.5% penicillin, and 0.5% streptomycin (Gibco), and cultured in a humidified incubator under 5% CO_2 at 37°C. The GAD1 and CYTOR genes were extracted and cloned into the pEGFP-C1 vector (Addgen), and siRNA fragments against GAD1 and miR-24-3p mimics and inhibitors were purchased from GenePharma (Shanghai, China). For transfection, the media was changed to DMEM without FBS, and the cells were then transfected with Lipofectamine 2000 reagent (Invitrogen, Grand Island, NY, USA) for 48 h, with the exception to the MTT assays, which were performed at 24 h, 48 h, and 72 h.

2.3. Immunohistochemistry. We collected 36 pairs of adjacent tumor and NPC tumor tissues from 36 patients who received surgical treatment in the Nanchong Central Hospital from Jan 2007 to Dec 2009. Written consents were signed by the patients, and the study protocol was approved by the ethics committee of Nanchong Central Hospital in accordance with the Declaration of Helsinki. For immunohistochemistry analysis, the samples embedded in paraffin were cut into sections of 5 βM. The following procedures were conducted as reported [27, 28]. Briefly, sections were dewaxed and heat-treated to retrieve epitopes by immersing in a citrate buffer solution at pH 6.0 in an autoclave at 121°C for 1 min. Then, the sections were washed and incubated with 3% hydrogen peroxide for 1 h and blocked with normal goat serum for 1 h. For immunostaining with GAD1, the sections were incubated with anti-GAD1 antibody (1 : 1000, Abcam, Cambridge, MA, USA) overnight at 4°C. Sections with no primary antibody were used as the negative control. Then, sections were incubated with an HRP-labeled secondary antibody for 1 h at room temperature. Then, the sections were visualized with microscopy (BX51, Olympus, Germany). For the GAD1 score in IHC staining, the percentage of neoplastic cells with clear staining were used for quantification: 0, no staining; 1, less than 30% of cells stained in scattered individual cells; 2, less than 50% of cells stained; 3, 50–80% of cells stained; and 4, greater than 80% of cells stained.

2.4. Quantitative RT-PCR (qRT-PCR). For qRT-PCR [29], the total RNA of clinical or cell samples was reverse-transcribed with EasyScript cDNA Synthesis SuperMix, and qRT-PCR was performed with SYBR Premix Ex Taq™ II (TaKaRa, Japan), according to the manufacturer's protocol. Primer sequences are presented in Table 1. Gene expression levels were normalized to U6 or actin.

2.5. Western Blot Analysis. The procedure was performed as reported [30]. Total protein cell lysates were isolated with RIPA buffer (Beyotime, Shanghai, China) on ice and centrifuged for 15 min at 14000 rpm. Thirty microliters of total protein from each sample were subjected to SDS-PAGE. The separated proteins were then transferred to PVDF membranes. Subsequently, the membranes were sealed with 5% skim milk for 1 h, and after washing, the membranes were incubated with primary antibodies against GAD1 (#ab228710, 1 : 1000; Abcam, MA, USA) or Actin (#ab8227, Abcam) overnight at 4°C. After washing three times with TBST, membranes were incubated with HRP-conjugated secondary antibodies at room temperature for 1 h. After washing, an ECL kit (Beyotime, cat. no. #P0018S) was used to label the protein bands, and band intensity was quantified using ImageJ and normalized to control.

Table 1: Primers used for qRT-PCR.

Gene	Fwd primer 5′-3′	Rev primer 5′-3′
miR-24-3p	AACACACCTATTCAAGGATTCA	mRQ 3′primer (clontech)
CYTOR	AGAATGAAGGCTGAGGTGTG	CAGCGACCATCCAGTCATTTA
U6	CTCGCTTCGGCAGCACA	AACGCTTCACGAATTTGCGT
Actin	TCACCCACACTGTGCCCATCTACGA	GGATGCCACAGGATTCCATACCCA

2.6. MTT Assay. For the MTT assay, transfected cells were seeded on a 96-well plate (1×10^4 cells/well) and then incubated with the MTT kit (#C0009 M; Beyotime) for 4 h at 1 day, 2 days, and 3 days. Prior to harvest, 100 μl Formazan solution was added to each well and incubated for an additional 4 h. The absorbance of each well was measured at 570 nm. The values were normalized to those of day 0 control.

2.7. Colony Formation Assay. For the colony formation assay, 500 transfected cells/well were plated on a 6-well plate and cultured for 7 days. Colonies were then stained with 0.5% crystal violet (Beyotime) and fixed with 4% paraformaldehyde (Beyotime) for colony quantification.

2.8. Transwell Assay for Migration and Invasion. Transfected or untransfected cells were collected and replanted in the upper chamber of a Transwell system (Corning, MA, USA). The chamber was coated with Matrigel (BD Biosciences) for the invasion assay but not the migration assay. The lower chamber contained a full culture medium. After 24 h, migrated or invaded cells were stained with 0.5% crystal violet. Images were then taken, and cell numbers were counted.

2.9. Dual-Luciferase Reporter Assay. The sequence of wild-type GAD1 or the CYTOR 3′UTR with a potential recognition site targeting miR-24-3p was synthesized and cloned into luciferase reporter vectors (Promega, Madison, WI, USA), as was a mutant 3′UTR. NPC cells were then transfected with miR-24-3p mimic or the indicated plasmids and cotransfected with Renilla luciferase plasmids as an internal control. After 48 h transfection, cells were harvested and luciferase activity was measured using the Dual-Luciferase Reporter System (Promega), according to the manufacturer's instructions.

2.10. Statistical Analysis. All data were presented as the mean ± SD from at least three independent experiments. The statistical analysis was conducted with GraphPad Prism. A student's *t*-test was used for pairwise comparison between two groups, and an ANOVA was used for comparison between multiple groups. $P < 0.05$ was considered statistically significant.

3. Results

3.1. GAD1 is Upregulated in Nasopharyngeal Cancer Tissues. To explore the role of GAD1 in NPC, we first reanalyzed the transcriptome datasets GSE12452 and GSE64634 published in GEO. Differentially expressed genes were analyzed (Figures 1(a) and 1(b)). GAD1 expression was upregulated in both datasets. Scaled expression between the two datasets is represented as a heatmap (Figure 1(c)). These data indicate that GAD1 is upregulated in nasopharyngeal cancer tissues.

3.2. GAD1 is Critical for the Growth, Migration, and Invasion of Nasopharyngeal Cancer Cells. Elevated GAD1 expression in NPC tissues suggests GAD1 as a potential oncogene. To further explore its function, we designed and synthesized genetic knockdown fragments (siRNAs) against GAD1. Knockdown was first validated in two NPC cancer cell lines, CNE-1 and 5-8F, and was confirmed in both cell lines (Figures 2(a) and 2(b)). Subsequently, we determined the effects of GAD1 on NPC cell function. Transfection of siRNA fragments targeting GAD1 significantly suppressed cell differentiation in both cell lines, as indicated by an MTT assay (Figures 2(c) and 2(d)). Furthermore, transfection of GAD1-targeting siRNAs markedly suppressed the colony formation ability of both cell lines, as revealed by a colony formation assay (Figures 2(e) and 2(f)), and inhibited cell migration and invasion in both CNE-1 and 5-8F cells (Figures 2(g) and 2(h)), as demonstrated by the Transwell assay. These data suggest that GAD1 inhibition suppresses proliferation, colony formation, cell migration, and cell invasion in NPC cells. To overexpress GAD1, we cloned the GAD1 gene and transfected GAD1-encoding plasmids. GAD1 overexpression was confirmed in both cell lines (Figures 3(a) and 3(b)). GAD1 overexpression significantly promoted NPC proliferation (Figures 3(c) and 3(d)), colony formation (Figures 4(e) and 4(f)), and migration and invasion (Figures 3(g) and 3(h)) in both CNE-1 and 5-8F cells. Taken together, these data indicate that GAD1 functions as an oncogene, promoting the development of NPC cells.

3.3. GAD1 is the Target of miR-24-3p in Nasopharyngeal Cancer Cells. After determining the role of GAD1 in NPC, we sought to delineate the detailed regulatory mechanism for GAD1-mediated NPC development. Using online bioinformatics tools, we screened miRNAs that could target GAD1, identifying that miR-24-3p potentially targets GAD1. The potential targeting site in the GAD1 3′ UTR that matched the miR-24-3p targeting sequence is shown in Figure 4(a). The target sites of the GAD1 3′UTR were highly conserved among species (Figure 4(b)). To determine the direct targeting relationship between miR-24-3p and GAD1, we synthesized a mimic and an inhibitor of miR-24-3p and constructed reporter gene plasmids containing the wild-type (WT) or mutant (MUT) GAD1 3′UTR sequence

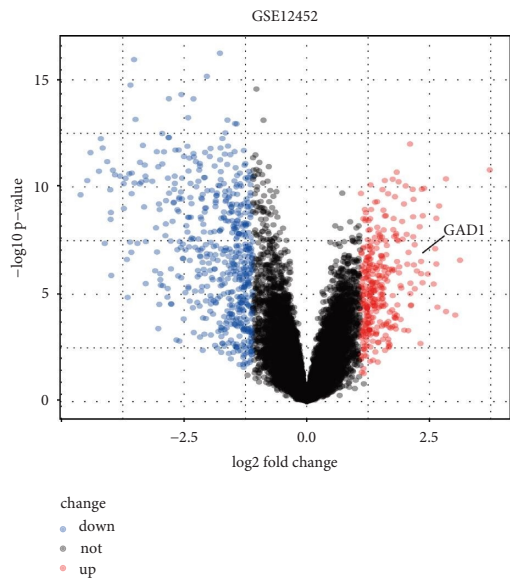

(a)

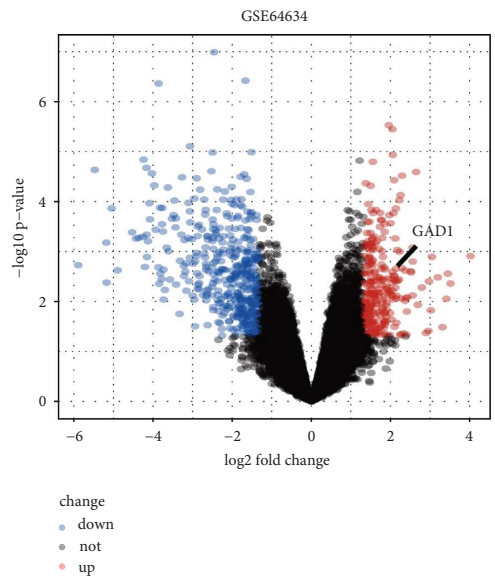

(b)

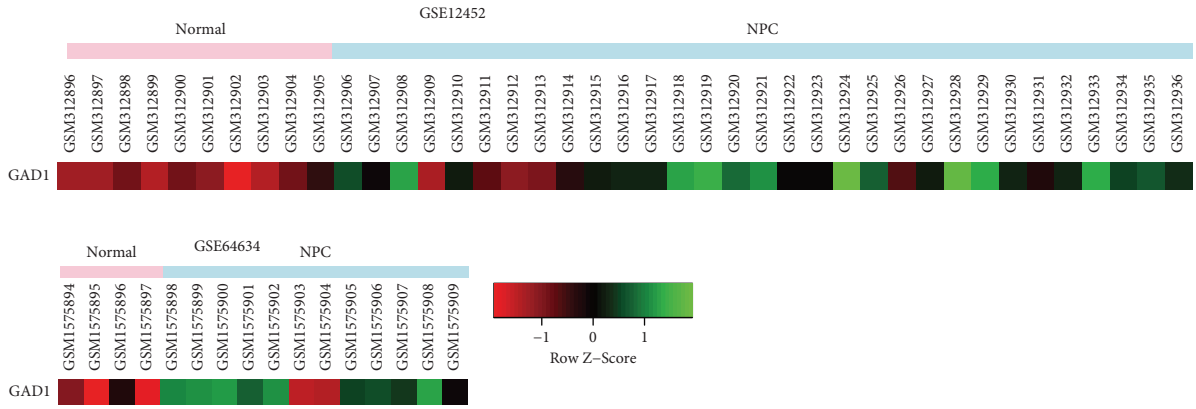

(c)

Figure 1: Continued.

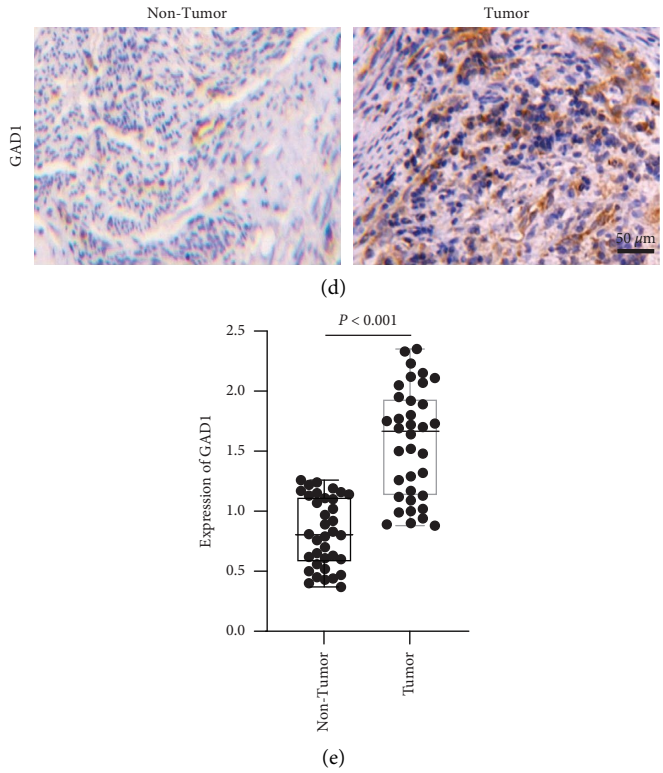

Figure 1: GAD1 is upregulated in NPC tissues. The differentiated expressed genes in public datasets of GSE12452 and GSE64634. The volcanos are shown in (a, b), the normalized expression levels of GAD1 in the two datasets are shown in (c), the expression of GAD1 in our collected samples of NPC is shown in (d) by histochemistry, and the statistical data are shown in (e).

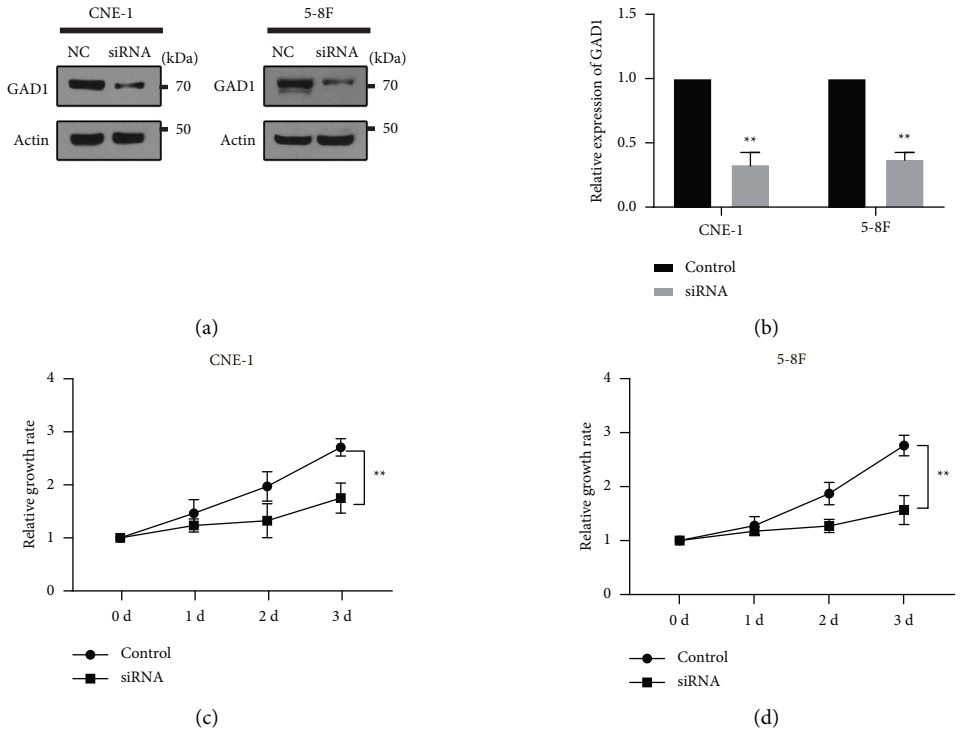

Figure 2: Continued.

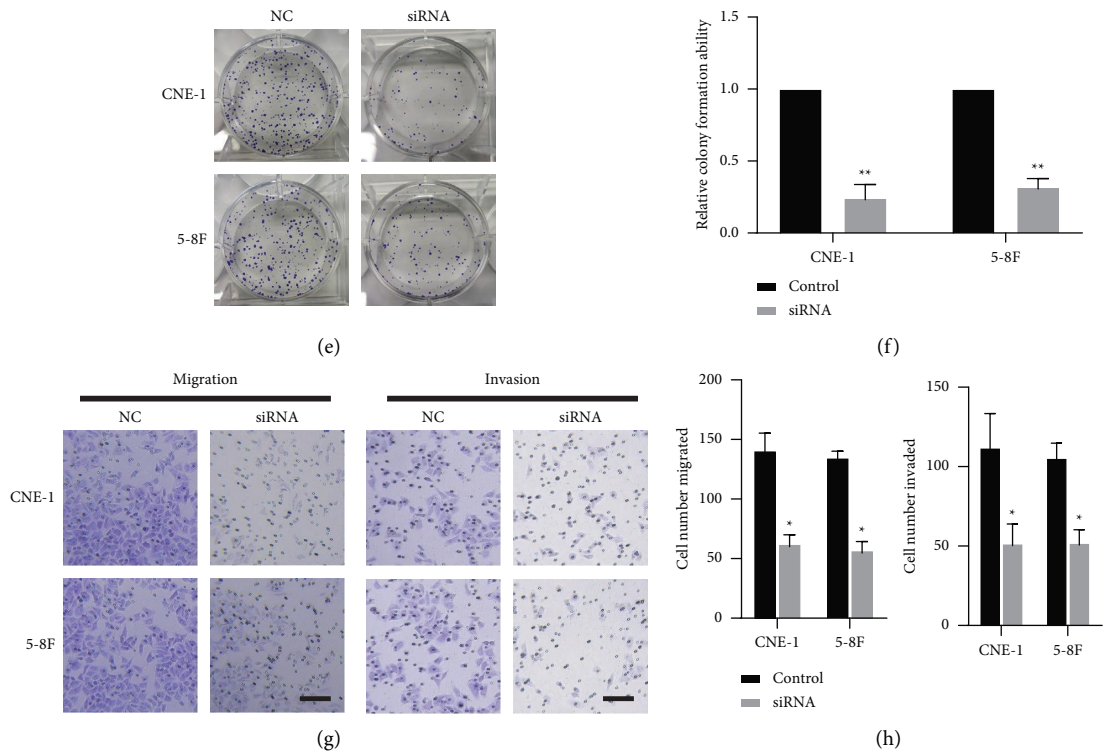

Figure 2: GAD1 is necessary for the development of NPC cells. (a) siRNA fragments against GAD1 were synthesized and transfected into two NPC cell lines, CNE-1 and 5-8F. Then, the lysates were subjected for western blotting for the detection of GAD1. The statistical data are shown in (b). NPC cells were transfected with siRNA fragments against GAD1 for 24 h, and then the cells were subjected to the MTT assay to detect the cell growth rate (c, d), to colony formation assay (e, f), and to the Transwell assay to detect cell migration and invasion (g, h). Scale bar, 20 βm; * denotes $P < 0.05$; ** denotes$P < 0.01$; *** denotes $P < 0.001$.

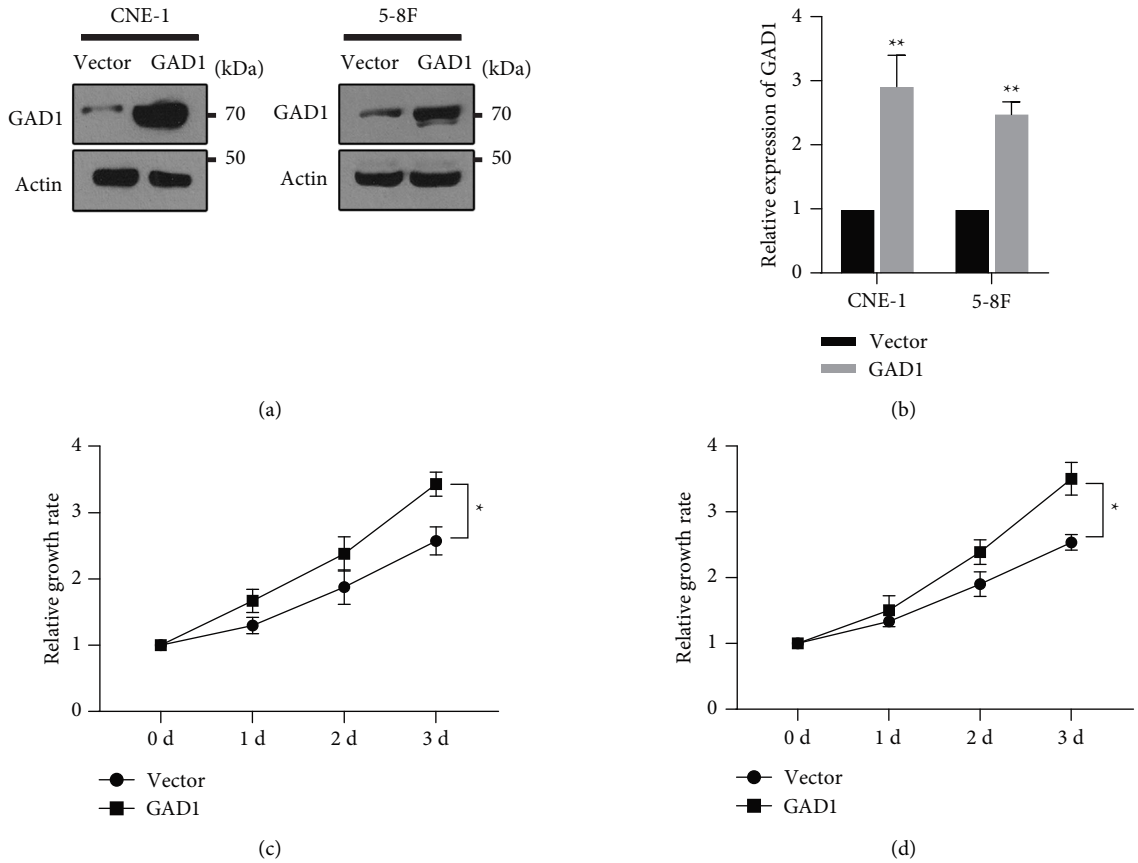

Figure 3: Continued.

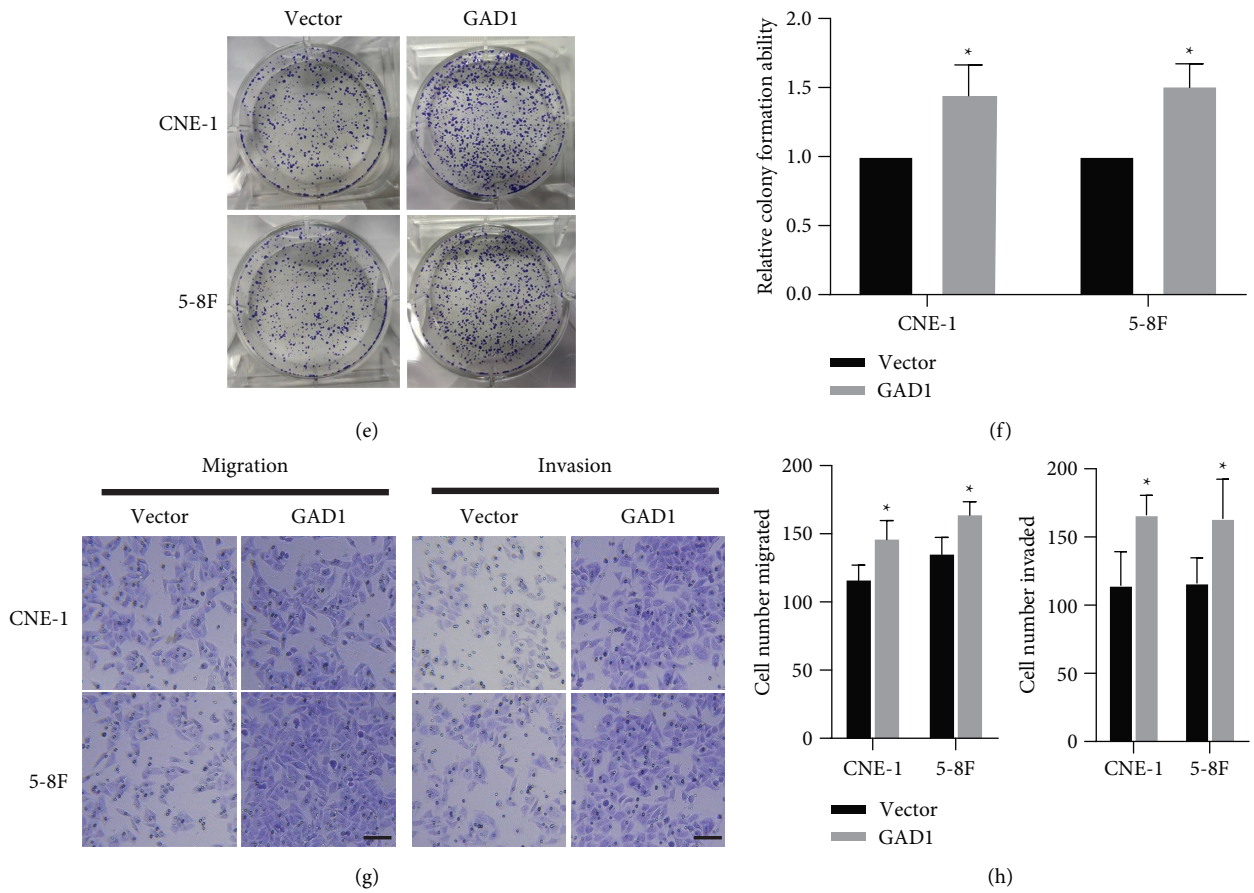

Figure 3: GAD1 is sufficient to promote the development of NPC cells. (a, b) GAD1 encoding plasmid was constructed and verified via transfection in NPC cells by western blotting. Then, the cells were subjected to MTT assay (c, d), colony formation assay (e, f) and Transwell assay (g, h) as in Figure 2. Scale bar, 20 μm; * denotes $P < 0.05$; ** denotes $P < 0.01$.

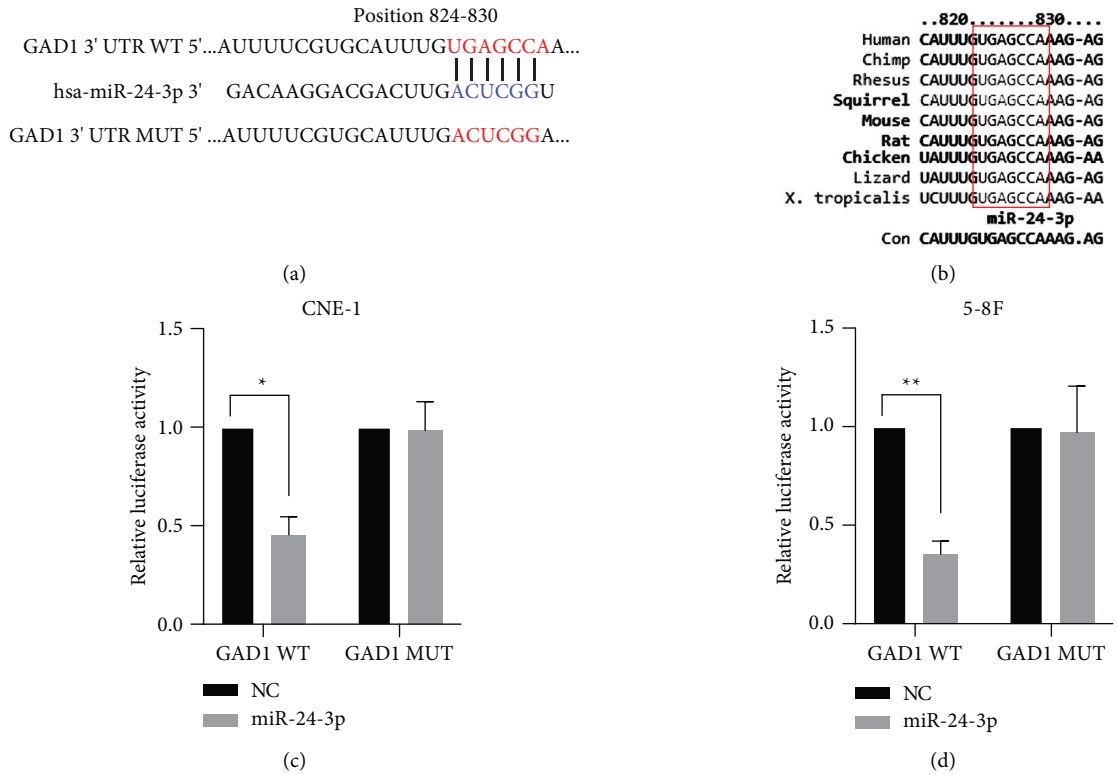

Figure 4: Continued.

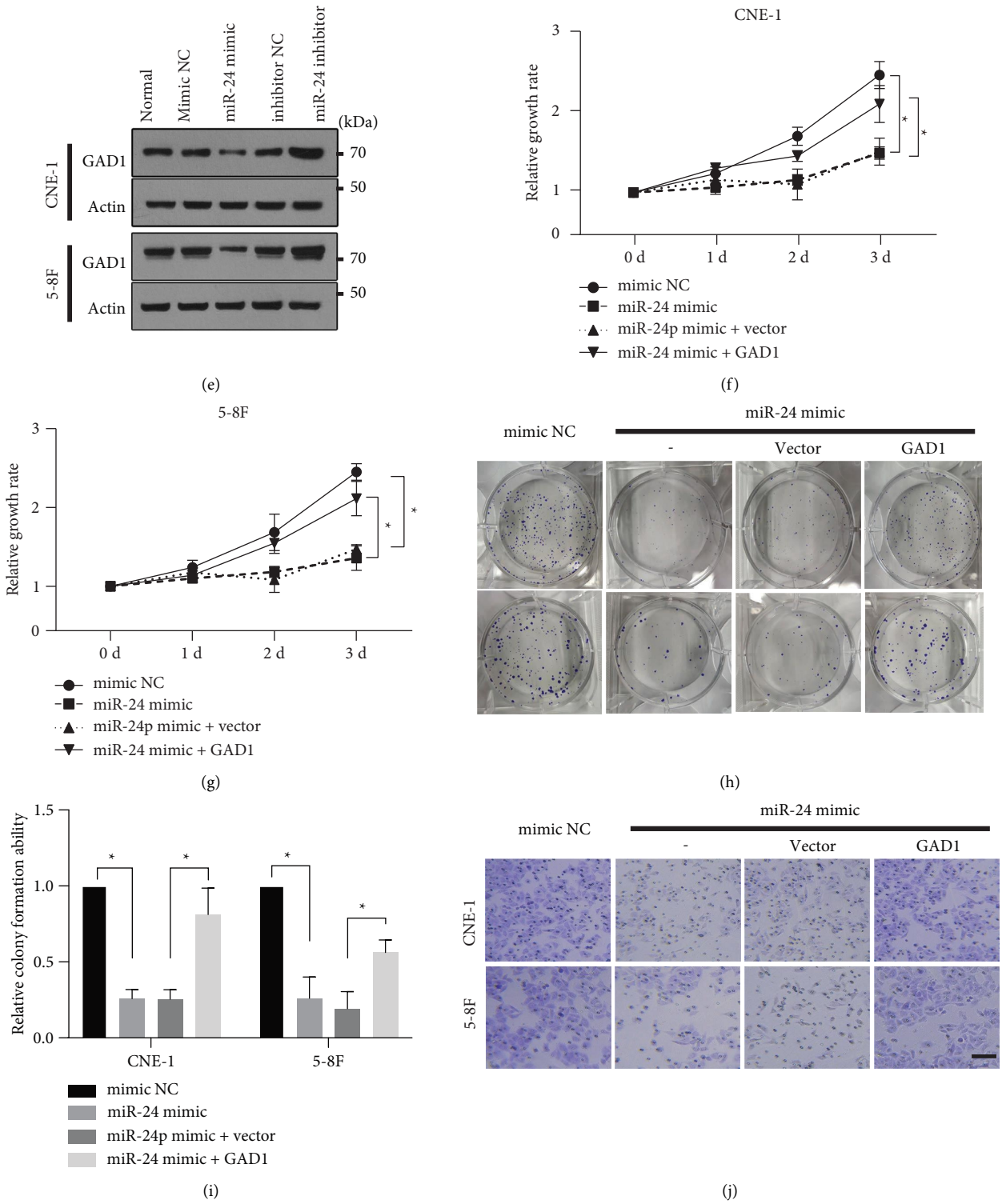

Figure 4: Continued.

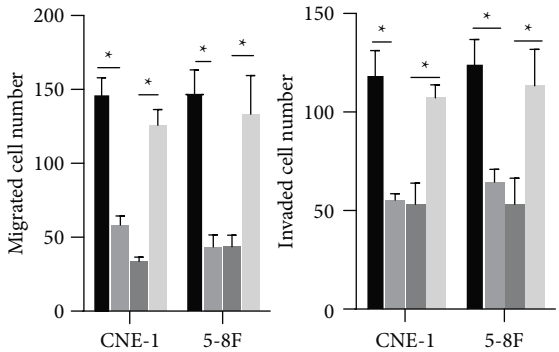

(k)

Figure 4: GAD1 is a target of miR-24-3p. (a) Bioinformatics analysis showed the matching site of GAD1 3′UTR to miR-24-3p, and the mutation form was constructed. (b) The homogenous of 3′UTR site of GAD1 between different species, (c, d) NPC cells were transfected with GAD1 3′UTR WT or MUT luciferase reporter, with miR-24-3p or the NC control. Then, the relative luciferase activity was determined and shown. (e) NPC cells were transfected with indicated miR-24-3p mimic or inhibitor, with mimic NC or inhibitor NC as controls. The endogenous level of GAD1 was determined by western blotting. NPC cells were transfected with miR-24-3p mimic, with or without GAD1 encoding plasmids. Then, the cells were subjected to MTT assay (f, g), colony formation assay (h, i) and Transwell assay (j, k) as in Figure 2. Scale bar, 20 μm; * denotes $P < 0.05$; ** denotes $P < 0.01$.

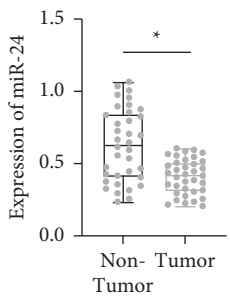

(a)

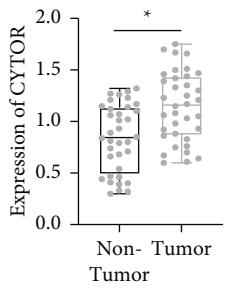

(b)

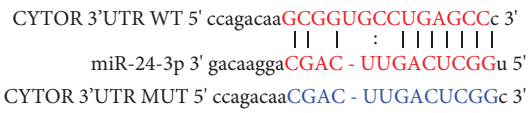

(c)

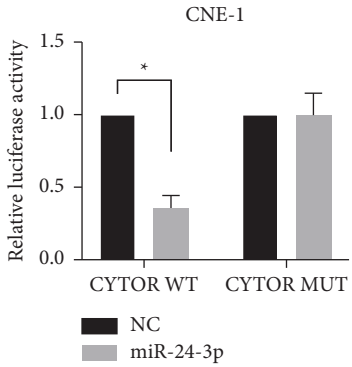

(d)

Figure 5: Continued.

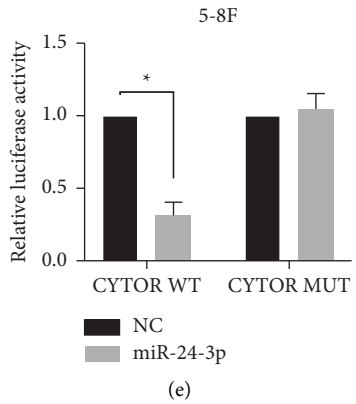

Figure 5: CYTOR sponges miR-24-3p. The expression levels of miR-24-3p (a) and lncRNA CYTOR (b) in our collected NPC samples were determined by RT-qPCR. (c) The bioinformatics analysis showed that CYTOR 3′UTR site matched with miR-24-3p. (d, e) NPC cells were transfected with CYTOR 3′UTR WT or MUT, together with or without miR-24-3p. Then, the luciferase activity in each group was determined and shown. *denotes $P < 0.05$.

(Figure 4(a)). For the dual-luciferase reporter gene assay, NPC cells were transfected with GAD1 reporter plasmids and the miR-24-3p mimic or empty control. Cotransfection of the miR-24-3p mimic significantly suppressed luciferase activity of the GAD1 WT reporter, but not the GAD1 MUT reporter (Figures 4(c) and 4(d)). Further, NPC cells were transfected with the miR-24-3p mimic or inhibitor, using mimic NC and inhibitor NC as controls. Transfection of the miR-24-3p mimic significantly downregulated, while transfection of the miR-24-3p inhibitor upregulated endogenous GAD1 expression in both CNE-1 and 5-8F cells (Figure 4). These findings suggested that GAD1 is a miR-24-3p target in NPC cells. Furthermore, CNE-1 and 5-8F cells were transfected with the miR-24-3p mimic with or without GAD1, and an MTT assay demonstrated that miR-24-3p suppressed NPC growth, while cotransfection with the GAD1-encoding plasmid partially restored proliferation (Figures 4(f) and 4(g)). Further, colony formation (Figures 4(h) and 4(i)), cell migration, and cell invasion (Figures 4(j) and 4(k)) were decreased by the miR-24-3p mimic, and this effect was attenuated by cotransfection with the GAD1-encoding plasmid in both CNE-1 and 5-8F cells. These data indicate that GAD1 is a direct target of miR-24-3p, and that the miR-24-3p/GAD1 axis regulates the development of NPC cells.

3.4. CYTOR Sponges miR-24-3p. We next sought to identify the upstream regulator of miR-24-3p and GAD1. LncRNA is a novel regulator that promotes NPC [31, 32]. However, the role of the lncRNA CYTOR remains unclear. We measured miR-24-3p and CYTOR expression in clinical samples of NPC and paracancerous control tissues. miR-24-3p was significantly downregulated in NPC tumor samples relative to paracancerous controls, while CYTOR was upregulated (Figure 5(a)). We conducted predictive analysis with the bioinformatics online tool starBase [33] to identify that the CYTOR 3′UTR could be matched by miR-24-3p. WT and mutant CYTOR 3′UTR sequences were constructed (Figure 5(c)). Gene reporters were cotransfected into NPC cells with either the miR-24-3p mimic or NC. miR-24-3p overexpression significantly suppressed luciferase activity of the CYTOR WT but not the CYTOR MUT reporter vector in both CNE-1 and 5-8F cells (Figures 5(d) and 5(e)). These data suggest that CYTOR could function as a sponge to suppress miR-24-3p function.

3.5. CYTOR/miR-24-3p Promotes Development of Nasopharyngeal Cancer Cells. Subsequently, we determined whether the CYTOR/miR-24-3p axis affected GAD1 expression. Transfection of miR-24-3p suppressed the luciferase signal of the GAD1 WT, but not the GAD1 MUT vector (Figures 6(a)). Furthermore, cotransfection of a CYTOR-encoding plasmid rescued luciferase activity in both cell lines (Figures 6(a) and 6(b)). Overexpression of the miR-24-3p mimic significantly downregulated endogenous GAD1, and cotransfection of a CYTOR-encoding plasmid abolished this inhibitory effect (Figures 6(c) and 6(d)). These data indicate that the CYTOR/miR-24-3p axis modulates GAD1 expression.

Finally, we determined if CYTOR/miR-24-3p affected cell function via modulation of GAD1. Both NPC cell lines were transfected with miR-24-3p mimic fragments, with or without the CYTOR-encoding plasmid. Transfection of miR-24-3p significantly suppressed NPC cell proliferation, which was rescued by cotransfection of CYTOR (Figures 7(a) and 7(b)). Colony formation ability (Figures 7(c) and 7(d)) and cell migration and invasion ability (Figures 7(e) and 7(f)) were decreased by miR-24-3p, and this effect was counteracted by overexpression of CYTOR. These data indicate that the CYTOR/miR-24-3p axis regulates NPC cell development via modulation of GAD1 expression.

4. Discussion

In the present study, we demonstrated that GAD1 was upregulated in NPC tissues and functioned as an oncogene in the context of NPC. Genetic GAD1 knockdown significantly suppressed, while GAD1 overexpression promoted the growth, colony formation, migration, and invasion of

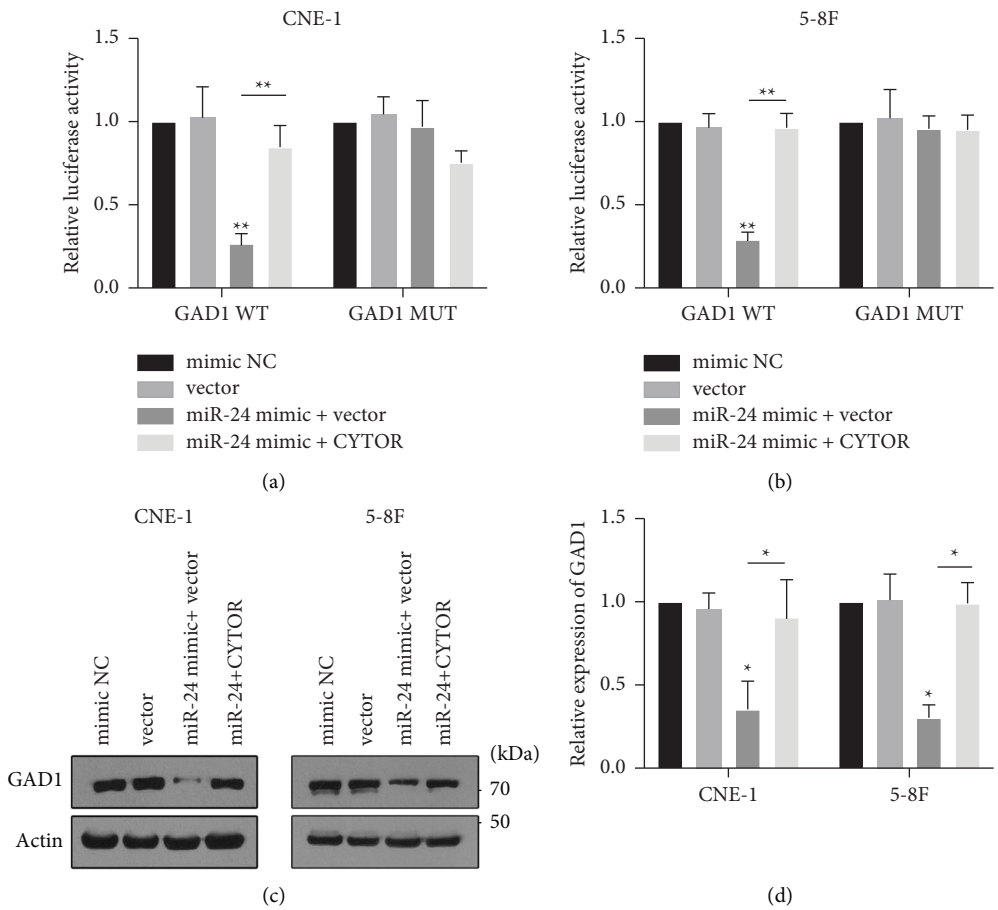

Figure 6: CYTOR/miR-24-3p regulates the expression of GAD1. (a, b) NPC cells were transfected with GAD1 3′UTR WT or MUT luciferase plasmid, with miR-24-3p mimic, with or without CYTOR-encoding plasmids, then the relative luciferase activity was detected. (c, d) NPC cells were treated with miR-24-3p mimic, with or without CYTOR-encoding plasmids, and the endogenous expression level of GAD1 was determined by western blotting. *denotes $P < 0.05$; **denotes $P < 0.01$.

NPC cells. Bioinformatics analyses and luciferase activity assays demonstrated that GAD1 was a miR-24-3p target gene. The miR-24-3p/GAD1 axis regulated the proliferation, colony formation, migration, and invasion of NPC cells. Furthermore, miR-24-3p was downregulated and the lncRNA CYTOR was upregulated in NPC tissues. CYTOR functioned as a sponge to suppress miR-24-3p activity. Thus, CYTOR regulates GAD1 luciferase activity and expression by modulating miR-24-3p. Taken together, these findings demonstrated that CYTOR/miR-24-3p/GAD1 is a critical axis for NPC development and pathogenesis.

GAD1 and GABA were first identified in neural systems and play critical roles in many neurological diseases, including Parkinson's disease, bipolar disorder, and schizophrenia [15, 34]. However, recent studies have identified that GAD1 and GABA play active roles in non-neural systems, especially in promoting cancers, including oral, breast, gastric, prostate, and colorectal cancers [8, 10, 15]. GAD1 is activated by DNA methylation in cancer cells to increase its expression, which is pivotal for the development of mucinous colon cancer [15, 35, 36]. Increased GABA and GAD1 expression are involved in prostate cancer cell migration [10, 13], and GAD1 is a specific marker for prostate cancer tissues because GAD1 expression is positively correlated with a higher Gleason score and poorer prognosis [12, 37]. GAD1 plays a crucial role and has been identified as a potential target for oral squamous cell carcinoma, due to its interaction with the Wnt/β-catenin/MMP7 pathway [8]. Furthermore, GAD1 influences GABA metabolism via the glutamine-glutamate/GABA cycle [38], which is important for hepatocellular carcinoma [39]. A recent study reported that GAD1 is overexpressed in NPC and is closely associated with the AJCC stage, and thus could be used as a prognosticator of poor outcomes in NPC [40]. However, the function of GAD1 in NPCs remains to be explored. In the present study, we identified that GAD1 was upregulated in NPC tissues and constructed GAD1 overexpression plasmids and siRNA fragments to elucidate the effect of GAD1 on the development of NPC cells. Furthermore, the upstream miR-24-3p/CYTOR regulator targeted GAD1 during NPC development. Further in vivo studies will be imminently conducted to elucidate the in vivo role of GAD1 and the impact of the CYTOR/miR-24-3p/GAD1 axis.

Noncoding RNAs play an important role in the occurrence, development, and malignant progression of human tumors, particularly miRNAs, lncRNAs, and circular

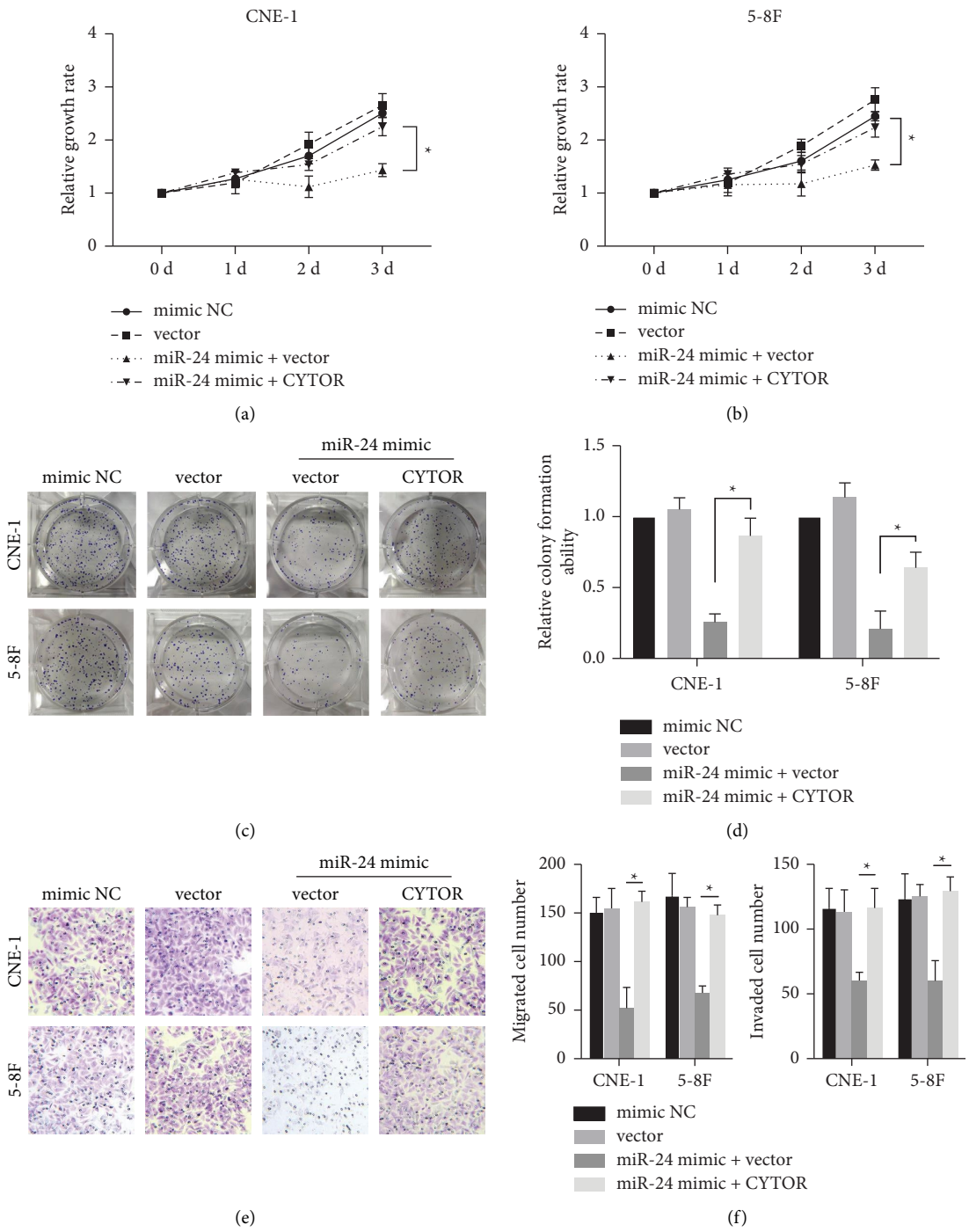

Figure 7: CYTOR/miR-24-3p/GAD1 axis regulates the development of NPC cells. NPC cells were treated as in Figures 6(c) and 6(d), and then the cells were subjected to MTT assay (a, b), colony formation assay (c, d), and Transwell assay (e, f). Scale bar, 20 μm; * denotes $P < 0.05$.

RNAs. miRNA is a type of noncoding RNA that typically contains 20 to 25 nucleotides and binds the 3′- or 5′-UTR regions of target gene mRNA, decreasing the translation and potentially the stability of mRNA [41]. miR-24-3p promotes tumor proliferation, growth, and metastasis in the human lung, bladder, colorectal adenocarcinoma, hepatocellular carcinoma, and other tumors [42–47]. In lung cancer, miR-24-3p is upregulated and targets SOX7 to promote cancer cell development in vitro and in vivo [42]. In bladder cancer, miR-24-3p is also upregulated and targets the DEDD protein to regulate proliferation, apoptosis, migration, invasion, and autophagy [43]. In colorectal cancer (CRC), elevated expression of miR-24-3p promotes tumor growth and is closely correlated with poor disease-free survival and overall survival in colorectal adenocarcinoma patients, indicating its potential value as a prognosticator [44, 47]. In hepatocellular carcinoma (HCC), miR-24-3p is significantly upregulated and decreases metallothionein 1M expression to promote

the initiation and progression of HCC [46]. The lncRNA CASC2 inhibits cell viability and induces apoptosis by targeting miR-24-3p, suppressing HCC [45]. However, miR-24-3p also has a tumor suppressive effect in colon cancer, lacrimal gland adenoid cystic carcinoma, non-small cell lung cancer, and other malignancies [48–50]. miR-24 and miR-101 are downregulated in gastric cancer [50], and Gao et al. reported that miR-24-3p is reduced in CRC samples from patients that underwent radical resection and is associated with CRC cell proliferation, migration, and invasion [48]. Pan et al. reported that decreased miR-24-3p expression favors small-cell lung cancer cells for VP16-DDP treatment by modulating its downstream target ATG4A protein during autophagy [49].

The role of miR-24-3p in human malignant tumors is therefore controversial and likely to be tissue-specific. In NPCs, the role of miR-24-3p is incompletely understood. Ye et al. reported that miR-24-3p levels are increased in exosomes from patient sera or NPC cells [51, 52], and exosomal miR-24-3p impedes T-cell function by targeting FGF11 in NPC [20]. However, in the present study, we demonstrated that miR-24-3p was downregulated in NPC tissues, unlike previous reports. We demonstrated that miR-24-3p was downregulated by the lncRNA CYTOR to promote the development of NPC cells. We did not measure circulating or exosomal miR-24-3p levels in NPC patients. To better elucidate the role of miR-24-3p, larger sample sizes should be analyzed, and the distribution of miR-24-3p expression in human organs should be characterized.

CYTOR (synonymous with C2orf59, LINC00152, and NCRNA00152) is a long noncoding RNA that is overexpressed in tumor cells and promotes cell proliferation and the epithelial-mesenchymal transition [53]. CYTOR is abnormally expressed in many tumors. Want et al. reported that CYTOR expression is positively correlated with BCL6 protein levels in ovarian cancer tissues and cell lines, in which CYTOR promotes polyubiquitination of BCL6 to support carcinogenesis [54]. CYTOR downregulation inhibits the invasiveness of cancer cells in vitro and in vivo by interacting with miR-139-5p [55–57]. In CRC, CYTOR functions as a sponge to suppress the expression and function of miRNA [58], and CYTOR inhibition upregulates miR-215, which targets CKD13 to suppress the development of liver cancer [59]. Also, lncRNAs play important roles in the development of NPCs [17]. LncRNA CYTOR regulates mitochondrial metabolism and glycolysis of oral cancer cells via HNRNPC-mediated ZEB1 stabilization in oral squamous cell carcinoma [60], and the level of CYTOR could be upregulated by forkhead box D1 to promote EMT and chemoresistance in oral squamous cell carcinoma [61]. In NPC, CYTOR titrates miR-613 to regulate ANXA2 to promote cell invasion and metastasis [21]. In the present study, we identified that CYTOR was upregulated in NPC tissues. Further, CYTOR acted as a sponge to suppress the expression of miR-24-3p and increase GAD1 levels. The CYTOR/miR-24-3p/GAD1 axis contributes to the proliferation, colony formation, migration, and invasion of NPC cells.

In summary, the present study identified the upregulation of GAD1 in NPC tissues and public databases of NPC arrays. CYTOR and GAD1 are oncogenes that promote the development of NPC cells. GAD1 is a miR-24-3p target, and CYTOR suppresses the expression of miR-24-3p to increase GAD1 levels. These data identify a novel mechanism by which the CYTOR/miR-24-3p/GAD1 axis regulates NPC development, which could provide new insights into the identification, treatment, and prognostication of NPC.

Data Availability

The datasets used during the present study are available from the corresponding author upon reasonable request.

Ethical Approval

All the protocols were approved by the ethics committee of Nanchong Central Hospital, the Second Clinical Medical College, North Sichuan Medical College (No. 200903265), in accordance with the Declaration of Helsinki.

Conflicts of Interest

The authors declare that they have no conflicts of interest.

Authors' Contributions

JD and WY performed the experiments; LP performed the data analysis; JD wrote the manuscript drafting; WY and LP contributed to the interpretation of the results and the critical revision of the manuscript; and TZ conceptualized the study and revised the manuscript. All the authors have read and approved the final version of the manuscript and agreed to be accountable for all aspects of the work.

Acknowledgments

This work was supported by the Nanchong 2020 City-School Science and Technology Strategic Cooperation Special Project (North Sichuan Medical College) (grant no. 20SXQT0105).

References

[1] K. C. W. Wong, E. P. Hui, K. W. Lo et al., "Nasopharyngeal carcinoma: an evolving paradigm," *Nature Reviews Clinical Oncology*, vol. 18, no. 11, pp. 679–695, 2021.

[2] N. J. Campion, M. Ally, B. J. Jank, J. Ahmed, and G. Alusi, "The molecular march of primary and recurrent nasopharyngeal carcinoma," *Oncogene*, vol. 40, no. 10, pp. 1757–1774, 2021.

[3] H. Q. Mai, Q. Y. Chen, D. Chen et al., "Toripalimab or placebo plus chemotherapy as first-line treatment in advanced nasopharyngeal carcinoma: a multicenter randomized phase 3 trial," *Nature Medicine*, vol. 27, no. 9, pp. 1536–1543, 2021.

[4] Z. Liu, Y. Chen, Y. Su, X. Hu, and X. Peng, "Nasopharyngeal carcinoma: clinical achievements and considerations among treatment options," *Frontiers Oncology*, vol. 11, Article ID 635737, 2021.

[5] S. Li, Y. Q. Deng, Z. L. Zhu, H. L. Hua, and Z. Z. Tao, "A comprehensive review on radiomics and deep learning for

nasopharyngeal carcinoma imaging," *Diagnostics*, vol. 11, no. 9, p. 1523, 2021.

[6] X. Zhou, P. Liu, and X. Wang, "Temporal lobe necrosis following radiotherapy in nasopharyngeal carcinoma: new insight into the management," *Frontiers Oncology*, vol. 10, Article ID 593487, 2020.

[7] M. Li, B. Zhang, Q. Chen et al., "Concurrent chemoradiotherapy with additional chemotherapy for nasopharyngeal carcinoma: a pooled analysis of propensity score-matching studies," *Head & Neck*, vol. 43, no. 6, pp. 1912–1927, 2021.

[8] R. Kimura, A. Kasamatsu, T. Koyama et al., "Glutamate acid decarboxylase 1 promotes metastasis of human oral cancer by beta-catenin translocation and MMP7 activation," *BMC Cancer*, vol. 13, p. 555, 2013.

[9] D. F. Bu, M. G. Erlander, B. C. Hitz et al., "Two human glutamate decarboxylases, 65-kDa GAD and 67-kDa GAD, are each encoded by a single gene," *Proceedings of the National Academy of Sciences of the U S A*, vol. 89, no. 6, pp. 2115–2119, 1992.

[10] K. Maemura, H. Yamauchi, H. Hayasaki et al., "Gamma-amino-butyric acid immunoreactivity in intramucosal colonic tumors," *Journal of Gastroenterology and Hepatology*, vol. 18, no. 9, pp. 1089–1094, 2003.

[11] M. Matuszek, M. Jesipowicz, and Z. Kleinrok, "GABA content and GAD activity in gastric cancer," *Medical Science Monitor*, vol. 7, no. 3, pp. 377–381, 2001.

[12] S. J. Jaraj, M. Augsten, L. Haggarth et al., "GAD1 is a biomarker for benign and malignant prostatic tissue," *Scandinavian Journal of Urology and Nephrology*, vol. 45, no. 1, pp. 39–45, 2011.

[13] H. Azuma, T. Inamoto, T. Sakamoto et al., "Gamma-aminobutyric acid as a promoting factor of cancer metastasis; induction of matrix metalloproteinase production is potentially its underlying mechanism," *Cancer Research*, vol. 63, no. 23, pp. 8090–8096, 2003.

[14] C. M. Li, C. E. Kim, A. A. Margolin et al., "CTNNB1 mutations and overexpression of wnt/β-catenin target genes in WT1-mutant Wilms' tumors," *American Journal Of Pathology*, vol. 165, no. 6, pp. 1943–1953, 2004.

[15] H. Yan, G. Tang, H. Wang et al., "DNA methylation reactivates GAD1 expression in cancer by preventing CTCF-mediated polycomb repressive complex 2 recruitment," *Oncogene*, vol. 35, no. 30, pp. 3995–4008, 2016.

[16] M. Andang, J. Hjerling-Leffler, A. Moliner et al., "Histone H2AX-dependent GABA(A) receptor regulation of stem cell proliferation," *Nature*, vol. 451, no. 7177, pp. 460–464, 2008.

[17] H. Wang, W. Wang, and S. Fan, "Emerging roles of lncRNA in Nasopharyngeal Carcinoma and therapeutic opportunities," *International Journal of Biological Sciences*, vol. 18, no. 7, pp. 2714–2728, 2022.

[18] C. X. Zhao, W. Zhu, Z. Q. Ba et al., "The regulatory network of nasopharyngeal carcinoma metastasis with a focus on EBV, lncRNAs and miRNAs," *Am J Cancer Res*, vol. 8, no. 11, pp. 2185–2209, 2018.

[19] S. Wang, Y. Pan, R. Zhang et al., "Hsa-miR-24-3p increases nasopharyngeal carcinoma radiosensitivity by targeting both the 3'UTR and 5'UTR of Jab1/CSN5," *Oncogene*, vol. 35, no. 47, pp. 6096–6108, 2016.

[20] S. B. Ye, H. Zhang, T. T. Cai et al., "Exosomal miR-24-3p impedes T-cell function by targeting FGF11 and serves as a potential prognostic biomarker for nasopharyngeal carcinoma," *The Journal of Pathology*, vol. 240, no. 3, pp. 329–340, 2016.

[21] W. Chen, M. Du, X. Hu et al., "Long noncoding RNA cytoskeleton regulator RNA promotes cell invasion and metastasis by titrating miR-613 to regulate ANXA2 in nasopharyngeal carcinoma," *Cancer Medicine*, vol. 9, no. 3, pp. 1209–1219, 2020.

[22] S. Sengupta, J. A. den Boon, I. H. Chen et al., "Genome-wide expression profiling reveals EBV-associated inhibition of MHC class I expression in nasopharyngeal carcinoma," *Cancer Research*, vol. 66, no. 16, pp. 7999–8006, 2006.

[23] Y. E. Lee, H. L. He, T. J. Chen et al., "The prognostic impact of RAP2A expression in patients with early and locoregionally advanced nasopharyngeal carcinoma in an endemic area," *Am J Transl Res*, vol. 7, no. 5, pp. 912–921, 2015.

[24] L. E. Dodd, S. Sengupta, I. H. Chen et al., "Genes involved in DNA repair and nitrosamine metabolism and those located on chromosome 14q32 are dysregulated in nasopharyngeal carcinoma," *Cancer Epidemiology, Biomarkers & Prevention*, vol. 15, no. 11, pp. 2216–2225, 2006.

[25] H. Bo, Z. Gong, W. Zhang et al., "Upregulated long noncoding RNA AFAP1-AS1 expression is associated with progression and poor prognosis of nasopharyngeal carcinoma," *Oncotarget*, vol. 6, no. 24, pp. 20404–20418, 2015.

[26] M. E. Ritchie, B. Phipson, D. Wu et al., "Limma powers differential expression analyses for RNA-sequencing and microarray studies," *Nucleic Acids Research*, vol. 43, no. 7, p. e47, 2015.

[27] Z. Chen, H. Wang, B. Hu et al., "Transcription factor nuclear factor erythroid 2 p45-related factor 2 (NRF2) ameliorates sepsis-associated acute kidney injury by maintaining mitochondrial homeostasis and improving the mitochondrial function," *European Journal of Histochemistry*, vol. 66, no. 3, p. 3412, 2022.

[28] Y. Wang, J. Sun, and N. Yao, "Correlation of the AKT/mTOR signaling pathway with the clinicopathological features and prognosis of nasopharyngeal carcinoma," *European Journal of Histochemistry*, vol. 65, no. 4, p. 3304, 2021.

[29] N. Marziliano, E. Arbustini, M. Rossi de Gasperis, and S. Crovella, "Detection of Epstein Barr virus in formalin-fixed paraffin tissues by fluorescent direct in situ PCR," *European Journal of Histochemistry*, vol. 49, no. 3, pp. 309–312, 2009.

[30] C. Casali, S. Siciliani, L. Zannino, and M. Biggiogera, "Histochemistry for nucleic acid research: 60 years in the European Journal of Histochemistry," *European Journal of Histochemistry*, vol. 66, no. 2, p. 3409, Apr 20 2022.

[31] Z. Tang, X. Zeng, J. Li et al., "LncRNA HOXC-AS1 promotes nasopharyngeal carcinoma (NPC) progression by sponging miR-4651 and subsequently upregulating FOXO6," *Journal of Pharmacological Sciences*, vol. 147, no. 3, pp. 284–293, 2021.

[32] L. Zhou, R. Liu, X. Liang et al., "lncRNA RP11-624l4.1 is associated with unfavorable prognosis and promotes proliferation via the CDK4/6-cyclin D1-Rb-E2F1 pathway in NPC," *Molecular Therapy - Nucleic Acids*, vol. 22, pp. 1025–1039, 2020.

[33] J. H. Li, S. Liu, H. Zhou, L. H. Qu, and J. H. Yang, "starBase v2.0: decoding miRNA-ceRNA, miRNA-ncRNA and protein-RNA interaction networks from large-scaleCLIP-Seq data," *Nucleic Acids Research*, vol. 42, no. D1, pp. D92–D97, 2014.

[34] T. H. Joh, E. E. Baetge, M. E. Ross et al., "Genes for neurotransmitter synthesis, storage, and uptake," *Federation Proceedings*, vol. 44, no. 12, pp. 2773–2779, 1985.

[35] F. V. Negri, A. Wotherspoon, D. Cunningham, A. R. Norman, G. Chong, and P. J. Ross, "Mucinous histology predicts for reduced fluorouracil responsiveness and survival in advanced

colorectal cancer," *Annals of Oncology*, vol. 16, no. 8, pp. 1305–1310, 2005.

[36] R. Maisano, D. Azzarello, M. Maisano et al., "Mucinous histology of colon cancer predicts poor outcomes with FOLFOX regimen in metastatic colon cancer," *Journal of Chemotherapy*, vol. 24, no. 4, pp. 212–216, 2012.

[37] J. E. Ippolito and D. Piwnica-Worms, "A fluorescence-coupled assay for gamma aminobutyric acid (GABA) reveals metabolic stress-induced modulation of GABA content in neuroendocrine cancer," *PLoS One*, vol. 9, no. 2, p. e88667, 2014.

[38] A. B. Walls, H. S. Waagepetersen, L. K. Bak, A. Schousboe, and U. Sonnewald, "The glutamine-glutamate/GABA cycle: function, regional differences in glutamate and GABA production and effects of interference with GABA metabolism," *Neurochemical Research*, vol. 40, no. 2, pp. 402–409, 2015.

[39] Y. H. Li, Y. Liu, Y. D. Li et al., "GABA stimulates human hepatocellular carcinoma growth through overexpressed GABAA receptor theta subunit," *World Journal of Gastroenterology*, vol. 18, no. 21, pp. 2704–2711, 2012.

[40] Y. Y. Lee, T. B. Chao, M. J. Sheu et al., "Glutamate decarboxylase 1 overexpression as a poor prognostic factor in patients with nasopharyngeal carcinoma," *Journal of Cancer*, vol. 7, no. 12, pp. 1716–1723, 2016.

[41] X. Du, J. Zhang, J. Wang, X. Lin, and F. Ding, "Role of miRNA in lung cancer-potential biomarkers and therapies," *Current Pharmaceutical Design*, vol. 23, no. 39, pp. 5997–6010, 2018.

[42] L. Yan, J. Ma, Y. Zhu et al., "miR-24-3p promotes cell migration and proliferation in lung cancer by targeting SOX7," *Journal of Cellular Biochemistry*, vol. 119, no. 5, pp. 3989–3998, 2018.

[43] G. Yu, Z. Jia, and Z. Dou, "miR-24-3p regulates bladder cancer cell proliferation, migration, invasion and autophagy by targeting DEDD," *Oncology Reports*, vol. 37, no. 2, pp. 1123–1131, 2017.

[44] D. Kerimis, C. K. Kontos, S. Christodoulou, I. N. Papadopoulos, and A. Scorilas, "Elevated expression of miR-24-3p is a potentially adverse prognostic factor in colorectal adenocarcinoma," *Clinical Biochemistry*, vol. 50, no. 6, pp. 285–292, 2017.

[45] J. C. Fan, F. Zeng, Y. G. Le, and L. Xin, "LncRNA CASC2 inhibited the viability and induced the apoptosis of hepatocellular carcinoma cells through regulating miR-24-3p," *Journal of Cellular Biochemistry*, vol. 119, no. 8, pp. 6391–6397, 2018.

[46] X. Dong, W. Ding, J. Ye et al., "MiR-24-3p enhances cell growth in hepatocellular carcinoma by targeting metallothionein 1M," *Cell Biochemistry and Function*, vol. 34, no. 7, pp. 491–496, 2016.

[47] Y. Yin, J. Zhong, S. W. Li et al., "TRIM11, a direct target of miR-24-3p, promotes cell proliferation and inhibits apoptosis in colon cancer," *Oncotarget*, vol. 7, no. 52, pp. 86755–86765, 2016 27.

[48] Y. Gao, Y. Liu, L. Du et al., "Down-regulation of miR-24-3p in colorectal cancer is associated with malignant behavior," *Medical Oncology*, vol. 32, no. 1, p. 362, 2015.

[49] B. Pan, Y. Chen, H. Song, Y. Xu, R. Wang, and L. Chen, "Mir-24-3p downregulation contributes to VP16-DDP resistance in small-cell lung cancer by targeting ATG4A," *Oncotarget*, vol. 6, no. 1, pp. 317–331, 2015.

[50] X. Dong and Y. Liu, "Expression and significance of miR-24 and miR-101 in patients with advanced gastric cancer," *Oncology Letters*, vol. 16, no. 5, pp. 5769–5774, 2018.

[51] S. B. Ye, Z. L. Li, D. H. Luo et al., "Tumor-derived exosomes promote tumor progression and T-cell dysfunction through the regulation of enriched exosomal microRNAs in human nasopharyngeal carcinoma," *Oncotarget*, vol. 5, no. 14, pp. 5439–5452, 2014.

[52] X. Zou, D. Zhu, H. Zhang et al., "MicroRNA expression profiling analysis in serum for nasopharyngeal carcinoma diagnosis," *Gene*, vol. 727, Article ID 144243, 2020.

[53] S. Zhang, W. Liao, Q. Wu et al., "LINC00152 upregulates ZEB1 expression and enhances epithelial-mesenchymal transition and oxaliplatin resistance in esophageal cancer by interacting with EZH2," *Cancer Cell International*, vol. 20, no. 1, p. 569, 2020.

[54] S. Wang, W. Weng, T. Chen et al., "LINC00152 promotes tumor progression and predicts poor prognosis by stabilizing BCL6 from degradation in the epithelial ovarian cancer," *Frontiers Oncology*, vol. 10, Article ID 555132, 2020.

[55] M. Li, N. Jun, Z. Li, W. Jing, Z. Cong, and W. Lei, "LINC00152 promotes the growth and invasion of oral squamous cell carcinoma by regulating miR-139-5p," *OncoTargets and Therapy*, vol. 11, pp. 6295–6304, 2018.

[56] Z. Bian, J. Zhang, M. Li et al., "Long non-coding RNA LINC00152 promotes cell proliferation, metastasis, and confers 5-FU resistance in colorectal cancer by inhibiting miR-139-5p," *Oncogenesis*, vol. 6, no. 11, p. 395, 2017.

[57] K. Sun, P. Hu, and F. Xu, "LINC00152/miR-139-5p regulates gastric cancer cell aerobic glycolysis by targeting PRKAA1," *Biomedicine & Pharmacotherapy*, vol. 97, pp. 1296–1302, 2018.

[58] M. Li, Q. Wang, F. Xue, and Y. Wu, "lncRNA-CYTOR works as an oncogene through the CYTOR/miR-3679-5p/MACC1 Axis in colorectal cancer," *DNA and Cell Biology*, vol. 38, no. 6, pp. 572–582, 2019.

[59] J. Wang, Y. Zhang, L. Lu, Y. Lu, Q. Tang, and J. Pu, "Insight into the molecular mechanism of LINC00152/miR-215/CDK13 axis in hepatocellular carcinoma progression," *Journal of Cellular Biochemistry*, vol. 120, no. 11, pp. 18816–18825, 2019.

[60] W. Zhu, J. Wang, X. Liu et al., "lncRNA CYTOR promotes aberrant glycolysis and mitochondrial respiration via HNRNPC-mediated ZEB1 stabilization in oral squamous cell carcinoma," *Cell Death & Disease*, vol. 13, no. 8, p. 703, 2022.

[61] S. Chen, M. Yang, C. Wang et al., "Forkhead box D1 promotes EMT and chemoresistance by upregulating lncRNA CYTOR in oral squamous cell carcinoma," *Cancer Letters*, vol. 503, pp. 43–53, 2021.

Hindawi
Journal of Oncology
Volume 2023, Article ID 4616682, 11 pages
https://doi.org/10.1155/2023/4616682

Review Article

Advances in the Histone Acetylation Modification in the Oral Squamous Cell Carcinoma

Ying Lu,[1,2] **Jinjin Yang**,[2] **Junwen Zhu**,[3] **Yao Shu**,[2] **Xuan Zou**,[2] **Qiao Ruan**,[4] **Shuyuan Luo**,[2] **Yong Wang**,[2] **and Jun Wen**[4]

[1]*School of Stomatology, Southern Medical University, Guangzhou 510515, China*
[2]*Department of Stomatology, The Fifth Medical Center of PLA General Hospital, Beijing 100071, China*
[3]*Harbin Medical University Cancer Hospital, Harbin, Helongjiang 150081, China*
[4]*Stomatological Hospital, Southern Medical University, Guangzhou 510280, China*

Correspondence should be addressed to Yong Wang; fgwangyong@163.com and Jun Wen; drwenjun@sina.com

Received 26 September 2022; Revised 23 October 2022; Accepted 29 November 2022; Published 9 February 2023

Academic Editor: Zhi-En Feng

Oral squamous cell carcinoma (OSCC) is one of the common malignant tumors in the head and neck, characterized by high malignancy, rapid growth and metastasis, high invasive ability, and high mortality. In recent years, surgery combined with chemotherapy or radiotherapy remains the preferred clinical treatment for OSCC, despite considerable advances in diagnostic and therapeutic techniques. Hence, new targeted therapy is urgently needed. Histone modification affects the function of massive cells through histone acetyltransferase and histone deacetylase. Accompanied by the progress of some diseases, especially tumors, these proteins often show abnormal functions, and by reversing these abnormalities with drugs or gene therapy, the cancer phenotype can even be restored to normal. As a result, they are potential drug targets. This article reviewed the role of the histone dynamic process of acetylation modifications and their associated active modifying enzymes in the pathogenesis and progress of OSCC. Moreover, we explored the value of histone acetylation modification as a potential therapeutic target and the new progress of related drugs in clinical treatment.

1. Introduction

Oral cancer is one of the most common malignancies occurring in the maxillofacial region, with a mortality rate close to 50% and an overall 5-year survival rate of about 60%. 90% of them are squamous cell carcinoma. Oral squamous cell carcinoma (OSCC) is the sixth most common malignant tumor in the world. It occurs mostly in adults aged 40–60 years in China, with more males than females. Alcohol, tobacco, and HPV infection are the most important risk factors for OSCC [1]. In recent years, the conventional therapies for OSCC have evolved into various modalities, including surgery, chemotherapy, radiotherapy, and combination therapy based on the diagnostic stage [2], but none of them has brought significant outcomes to the prognosis of OSCC. This is mainly due to the special anatomical structure of the oral cavity that provides great ease for metastasis. Most of the administered patients with progression to the middle and late stage have already missed the best treatment opportunities, with serious prognostic implications. Hence, the early diagnosis, treatment, and inhibition of metastasis are critical to control this disease. Moreover, it has great clinical significance to investigate the molecular biological mechanisms of occurrence, development, and metastasis of the disease and to discover new therapeutic targets for the intervention in those critical molecules and processes to achieve early diagnosis and treatment and suppress metastasis.

The progression of OSCC is mainly caused by the genetic or epigenetic alterations in proto-oncogenes, antioncogenes, and dysregulation of molecular networks. Histone modification is one of the most critical epigenetic regulations for gene expression by posttranslational modification of the histones [3, 4]. Posttranslational modifications of proteins are essential for organisms, while the metabolism and

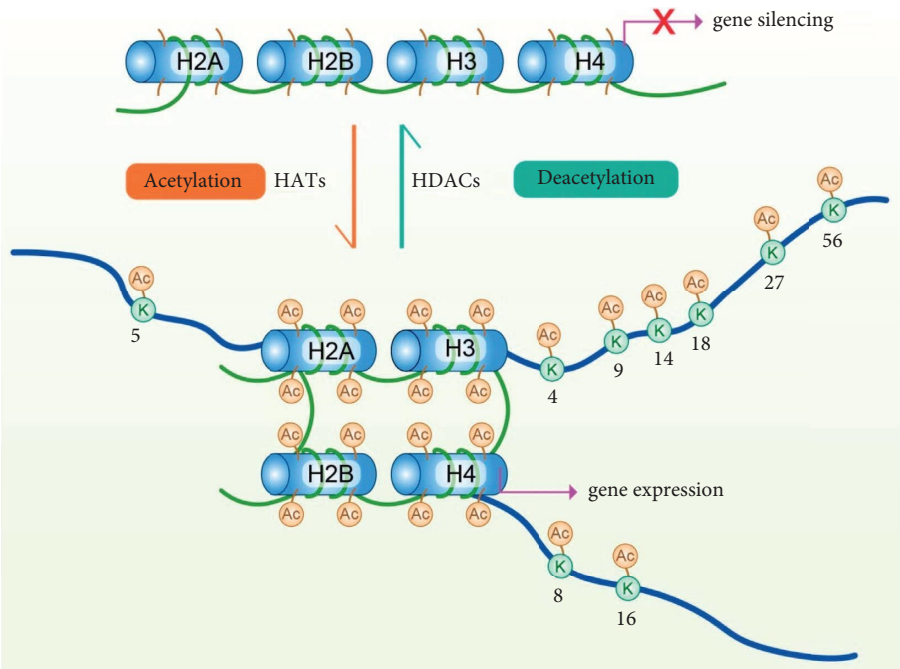

Figure 1: The dynamic process of reversible acetylation. Commonly functioning acetylation sites in oral squamous carcinoma.

metabolites can control the activity of growth-related signaling pathways to regulate cell growth through covalent modifications of proteins [5]. The histone acetyltransferases (HATs) and the histone deacetylases (HDACs) are responsible for controlling the histone acetylation level and chromatin accessibility [3, 6]. Acetylation of the ε-amino group on the histone lysine residues plays a key role in cell growth activity and gene transcription. Epigenetic and posttranslational modifications have emerged as new targets for anticancer therapy. This review focused on the relationship between the acetylation/deacetylation of histones and the OSCC and the potential therapeutic targets. Figure 1 shows the pattern of acetylation function and lists the reported sites in OSCC.

2. Histone Modification

The concept that epigenetic abnormality is a possible sign of cancer has now been verified over the past decades. Several studies have suggested that the multimutations and the copy number alterations in the epigenetic modifiers (including acetyltransferase, deacetylase, methyltransferase, demethylase, and kinase) might jointly promote the progression of OSCC [7]. The nucleosome made up of approximately 147 bp of DNA is the basic unit of chromatin. It envelops a 2-copy histone octamer containing 4 kinds of histones (i.e., H2A, H2B, H3, and H4). Chromatin-modifying enzymes dynamically perform the posttranslational modifications of histones and DNA through tightly regulated mechanism [4, 8]. Posttranslational modification of histone is also an important mechanism regulating the structure and function of chromatin, which acts as a critical role in the emergence and progression of cancer through regulating the genetic transcription, chromatin remodeling, and nuclear structure [9]. Various posttranslational modifications exist in the eukaryotic animal cells, which usually include phosphorylation, ubiquitination, glycosylation, methylation, and acetylation. The histone tail projection of the nucleosome octamer experiences several posttranslational modifications including the added chemical groups like acetyl, phosphate, and methyl. Less common modifications include ubiquitination, sulfonation, and ribosylation, occurring on the residues of lysine, arginine, and serine on histones [10].

2.1. Acetylation. Various posttranslational modifications can regulate the function of histones, including the reversible acetylation of lysine terminal 1 group on histones. Acetylation is a universal protein modification that modulates a variety of cellular events including the cell cycle, cell metabolism, gene transcription, signal transduction, and RNA splicing [11]. Histone acetylation can disrupt or remove the nucleosomes from the transcription region and loosen the chromatin to facilitate the entry of proteins to the DNA to be replicated or transcribed. Studies of proteomics stated that acetylation can occur in every corner of the cell on thousands of proteins [12]. Histone acetylation is a widely studied posttranslational modification that can be reversed through the transfer of acetyl groups to lysine residues by HATs and its further removal by HDACs.

Histone acetyltransferase can attach the acetyl groups to the lysine residues in both histones and nonhistones, which can be divided into 2 groups according to their intracellular location and substrate specificity. The first group, named HAT, is located only in the nucleosomes and that has the effect on chromatin remodeling by modifying the chromatin-related histones. The other group, named B HAT, is located both in nucleosomes and cytoplasm and that can

acetylate free soluble histones [13]. The common HATs are mainly composed of three families: the GCN5/PCAF family, the CBP/p300 subfamily, and the MYST family (MOZ, MOF, TIP60, and HBO1) [14] (see Table 1). The largest subfamily of histone acetyltransferase (MYST family) contains a high conserved MYST domain, and this structure consists of a zinc finger and an acetyl-CoA binding motif. The histone acetyltransferase has some extra structures including the plant homologous structural domain-linked zinc fingers (MORF and MOZ) and chromophores (TIP60 and MOF) [15], which are parts of the protein-complexes involved in the pro- and anticancer activities [16]. Another group of N-acetyltransferase (GNAT) family related to GCN5 is represented by the p300/CREB binding protein (CBP), binding factor (PCAF), HAT1, and GCN5, which contains bromo polysaccharides and adds an acetylated group of lysine to histone H2B, H3, and H4 [17, 18]. The CBP/p300 subfamily contains many small domains that interact with many other proteins containing disordered domains, including p53 and NF-κB [19].

HATs catalyze the transfer of acetyl groups to the target lysine (Lys/K) residues on the histone tail, thereby neutralizing the positive lysine charge, loosening condensed chromatin, promoting activation of gene transcription, and exposing binding sites for "binding motif proteins" that recognize the modifications on the histone [20]. Apart from the histone charge modification, histone acetylation can regulate the intracellular pH. Interestingly, many tumor cells show low histone acetylation levels and the acidic internal environment. Besides, poor prognosis in cancer patients has also been associated with low intracellular pH [21]. Different HATs can simultaneously act as tumor suppressors and oncogenes, which mean the balance of acetylation is critical to the stability of cells [22]. For example, as a kind of HAT, Tip60 can regulate ataxia-telangiectasia mutated (ATM) and DNA damage response pathways to participate in tumorigenesis, and it can also activate the transcription of p53 and Myc. ATM is a key regulator of DNA double strand break repair. Upregulated Tip60 can activate ATM through acetylation to promote DNA damage repair and inhibit tumor cell growth [23]. The reduction of Tip60 expression leads to genomic instability and apoptotic signaling cascade impairment, promoting the onset of malignant transformation of tumors [24] (see Tables1 and 2).

2.2. Deacetylation. Contrary to the HATs, the HDACs remove acetyl groups from the high acetylated histones and repress the gene transcription. There are 4 HDACs in mammals, including the Zn^{2+}-dependent class I (i.e., Rpd3-like enzyme) consisting of HDAC1, HDAC2, HDAC3, and HDAC8; the class II (i.e., Hda1-like enzyme) consisting of a subclass of IIa (HDAC4, HDAC5, HDAC7, and HDAC9 belong to class IIa) and IIb (HDAC6 and HDAC10 belong to class IIb); the class III (i.e., Sir-like enzyme) consisting of 7 SIRTs referred as the NAD-dependent deacetylase; the class IV of only HDAC11 with homologous sequences of class I and II [24](see Table 2).

HDAC regulates tumorigenesis through mechanisms like activating oncogene signaling pathways and downregulating tumor suppressor genes. HDACs have low substrate specialty with each kind of them deacetylating multiple sites on histone. Although mutation of HDACs is rare, overexpression of HDACs is still common in cancer [10, 25]. HDACs interfere with the transcription of oncogenes and antioncogenes by removing the acetyl groups from histones and reversing the acetylation of chromatins. Furthermore, HDACs can catalyze the deacetylation of many nonhistone proteins, which control a series of biological processes including the development and progression of cancer [26]. These processes are involved in the cell cycle, apoptosis, DNA damage response, metastasis, angiogenesis, autophagy, and other honeycomb shaping process [27].

2.3. Histone Acetylation and Oral Cancer. Accumulating scientific evidence have presented that epigenetic alterations, including chromatin remodeling, noncoding RNAs, DNA methylation, and histone covalent modifications, are generally involved in oral carcinogenesis and treatment tolerance. Epigenetic modifications contribute to the formation of cell plasticity and cancer stem cells (CSCs) during tumor progression [3]. Especially the dysregulation of histone acetylation leads to the disorder of the activity of different genes, resulting in malignant transformation-related events. Due to the reversibility and low-abundance of acetylation, it is a challenge to identify a large number of acetylation sites. Few literature have indicated changes in histone acetylation on specific lysine residues in head and neck squamous cell carcinoma (HNSCC) [28]. The reported main acetylation sites are listed in Table 3.

Most theories confirmed that in HNSCC, low level histone acetylation makes the nucleus smaller, which reduces the DNA damage repair proteins flowing into the nucleus and enhances the resistance to intercalation agents [34], with the most studied being H3K9ac. Some studies have demonstrated that the deletion of histone H3K9ac indicates the occurrence of chemoresistance and is associated with the NF-κB signaling and the accumulation of CSC [35]. The decrease of H3K9ac is related to the activation of epithelial-mesenchymal transition (EMT) and the increased cell proliferation during the process of oral carcinogenesis, indicating the H3K9ac is involved in the progression of HNSCC and is coexpressed with the mesenchymal vimentin prior to the invasion of HNSCC [30]. In oral cancer, the low level of H3K9 acetylation indicates a bad prognosis. The expression level of H3K9Ac is expressed at lower levels in OSCC than in oral leukoplakia, an oral precancerous lesion. In survival analysis, low expression of H3K9Ac was associated with a poorer prognosis in OSCC [31]. Interestingly, in contrast, some studies have found the hyperacetylation of histone H3 (mainly H3K14 and H3K9) in samples from patients with OSCC as well as the hyperacetylation of H2AK5 and H3K56 and hypoacetylation of H4K8 and H4K16 [29]. Several reports have reported the acetylation of special lysine residues in oral cancer. For example, both low and high levels of H3K4ac have been

Table 1: The major HAT families.

Family	Dominant members	Characteristics
GANAT	HAT1 GCN5 PCAF	Contains bromo polysaccharides and conducts the acetylation of lysine on histone H2B, *H*3, and *H*4
MYST	TIP60 MOF MOZ MORF HBO1	Contains a high conserved MYST domain, which consists of a zinc finger and an acetyl coenzyme, a binding motif
P300/CPB	P300/CPB	Contains many small domains that interact with many other proteins containing disordered transactivation domains

Table 2: The major HDAC families.

Family	Dominant members	Characteristics
I	HDAC1, 2, 3, 8	Widely expressed in human cell lines and nuclear tissues
II	IIa: HDAC4, 5, 7, 9 IIb: HDAC6, 10	Tissue specific expression, shuttling between nucleus and cytoplasm
III	Sirt1, 2, 3, 4, 5, 6, 7	NAD^+ dependent, with a very unique catalytic mechanism for deacetylation
IV	HDAC11	Deacetylate different histone sites, resulting in reduced substrate specificity

reported to be correlated with the progression and the poor prognosis of OSCC. The hypoacetylation of H3K4 is associated with the advanced OSCC tumor staging, primary tumor (*T*), regional lymph nodes (*N*), and perineural infiltration (PNI), while the H3K18ac is positively correlated with tumor stage [28]. Upregulation of H3K27ac was found to be associated with the activation of the placenta-specific protein 2 (PLAC2) gene in OSCC. PLAC2 promoted the progression of OSCC by modulating the Wnt/β-catenin signaling pathway. Compared with normal oral epithelial keratinocytes, PLAC2 is more abundant in oral squamous cell carcinoma cells (CAL-27 and SCC-9) [33]. Moreover, the non-long-strand coding RNA lncRNA MX1-215 can directly interact with the H3K27 acetylase GCN5, interrupting the combination of GCN5 and H3K27, interfering the transcription of PD-L1 and LGALS9 mediated by the acetylation of H3K27, and decreasing the acetylation level and expression level of PD-L1 and galectin-9 on the tumor cells [32]. It is also found that the hMOF (males absent on the first) can participate in the activation of transcription through acetylation of H4K16 and regulate the growth of cancer cells by the multicomb histone enhancer of zeste homolog 2 in OSCC. The upregulation of hMOF indicates poorer overall survival and disease-free survival [36].

2.4. Histone Deacetylation and Oral Cancer. Changes in the expression of multiple HDACs have been reported to be closely related to the regulation of cell cycle-related genes, cell invasion, apoptosis, angiogenesis, differentiation, and migration in a variety of cancers [37, 38]. For example, several studies have shown that the HDAC2 is overexpressed in OSCC, leading to increased stability of HIF-1α and the increased invasion and migration of HNSCC. The high abundance of HDAC2 is associated with the *T* and *N* states in the late stage [39]. Sakuma et al. [40] also found that HDAC6 is overexpressed in late HNSCC, indicating the activity of HDAC6 may associate with the tumor invasiveness of oral cancer. Besides, some researchers also found that HDAC6 catalyzes the deacetylation of α-tubulin and increases cell mobility and tumor metastasis [41]. The HDAC7 is also overexpressed in head and neck tumor, whose accumulation can activate proto oncogene c-MYC and promote cell proliferation [42]. The accumulation of HDAC8 induces the proliferation of cancer cells by inhibiting the activation and autophagy of Caspase in OSCC. In contrast, silencing of HDAC8 significantly inhibited OSCC cell proliferation, invasion, and metastasis [42]. HDAC9 has been reported to have oncogenic effects in OSCC by targeting proapoptotic genes to promote tumor growth. The low expressed HDAC9 inhibited the proliferation of SCC116 cells, increased apoptosis, and induced the *G*0/*G*1 arrest. The overexpressed HDAC9 positively correlates with the OS and promotes OSCC by targeting the transcription factors of MEF2D and NR4A1/Nur77 (proapoptotic MEF2 targets) [43].

The SIRT family belongs to the NAD^+-dependent histone deacetylase class III and is involved in the cell cycle, transcriptional regulation, and metabolism [44]. Contrary to the HDAC, the SIRT acts as a tumor suppressor in cancer, preventing the occurrence of DNA damage and oxidative stress [45]. The SIRT1, SIRT2, SIRT3, SIRT5, and SIRT7 are reduced in advanced HNSCC and have the potential to be used as prognostic markers [46]. While SIRT6 accumulates in peripheral blood of HNSCC patients [47], SIRT1 is the mammalian homolog of the chromatin silencing factor Sir2 in *S. cerevisiae*, which is expressed at elevated levels and catalytic activity in OSCC cells [48]. The latest study has presented that the SIRT7 inhibits the EMT in the metastasis

Table 3: Histone acetylation sites and expression in OSCC.

Sites	Expression	Acetylase	Function	References
H2AK5	Hyperacetylation	Tip60	Hyperacetylation is associated with cancer promotion	[29]
H3K4	Hypoacetylation	P300/Tip60	Low acetylation level is positively correlated with malignancy	[28]
H3K9	Hypoacetylation	P300	CSC accumulation leads to hypoacetylation and promotes tumor; its absence is a hallmark of chemoresistance	[30, 31]
	Hyperacetylation		High acetylation expression detected in oral cancer	[29]
H3K14	Hyperacetylation	MOZ/ MORF	P300-mediated hyperacetylation promotes tumor growth	[29]
H3K18	Hyperacetylation	P300	High acetylation levels are associated with poor prognosis	[28]
H3K27	Hyperacetylation	GCN5	Hyperacetylation enhances PD-L1 expression to promote tumor infiltration, metastasis, and recurrence	[32]
	Hyperacetylation		Hyperacetylation activates PLAC2 to promote tumor proliferation	[33]
H3K56	Hyperacetylation	P300/CPB	Hyperacetylation is associated with cancer promotion	[29]
H4K8	Hypoacetylation	P300/CPB	Hypoacetylation is associated with cancer promotion	[29]
H4K16	Hypoacetylation	hMOF/ Tip60	Hypoacetylation is associated with cancer promotion	[29]
	Hyperacetylation		hMOF promotes acetylation to enhance oral cancer cell growth	[33]

of OSCC by promoting the deacetylation of SMAD4, therefore, reducing the proliferation and invasion of OSCC cells in vitro [49]. In OSCC, the posttranscriptional regulation of SIRT3 is induced by miR-31, which targets the SIRT3 to destroy the mitochondrial structure and increase the oxidative stress response in oral cancer. The downregulation of SIRT3 reduces the migration and invasion of cancer cells enhanced by miR-31 [50]. The reported main histone deacetylase are listed in Table 4.

3. The Role of Histone Deacetylase Inhibitors in the Treatment of Oral Squamous Carcinoma

Owing to the reversibility of acetylation modifications, it is clear that the changes observed in the development of cancer have become attractive targets for therapy with the thriving research on the histone deacetylase inhibitor (HDACi)-related drugs. Although the HDACi has been applied to the treatment of hematologic malignancies successfully, its clinical efficacy as an independent drug in the treatment of solid tumors remains limited. The HDACi is able to achieve the best clinical efficacy only by combining with other treatments, including radiotherapy and chemotherapy, for synergistic or additive effects [51]. Current research data suggested that the HDACi has the best effect on HNSCC when administered together with other therapeutic drugs [52, 53].

The HDACi counteracts the abnormal acetylation state of proteins in cancer cells and reactivates the expression of tumor suppressors, thus inducing cell cycle arrest, apoptosis, differentiation, and inhibiting angiogenesis and metastasis [8]. Besides, the tumor cells are more sensitive to the apoptosis induced by HDACi than normal cells [54]. Based on their chemical structures, HDACi is classified into four classes, including hydroxamic acid, cyclic peptides, short-chain fatty acids, and benzamide. Most of them have already been developed as anticancer drugs with different specificity, efficiency, and pharmacokinetic and toxicological properties [8, 51–53, 55, 56]. Studies on the anticancer effects of HDAC in oral squamous cell carcinoma are presented in Table 5.

3.1. The Class of Hydroxamic Acid. The hydroxamic acid class of HDACi has been extensively studied in recent years, which mainly consists of rings, aliphatic chains, and hydroxamic acids for the surface recognition region, linkage region, and metal binding region (zinc combining region), respectively. It mainly contains SAHA (suberoylanilide hydroxamic acid), trichostatin A (TSA), and panobinostat, belinostat.

SAHA is a nonselective HDACi and the first FDA-approved HDACi that can be used alone or in combination as clinical treatment since October 2006 [77]. A research report found that SAHA can enhance the acetylation of H2A and H3 and inhibit the anticancer activity in vitro and xenotransplantation models by inducing cell activity reduction, caspase dependent apoptosis, and tumor growth inhibition [57]. In addition, powerful antiproliferative and synergistic effects of SAHA and gefitinib were noted. The SAHA enhances the antitumor function of gefitinib by upregulating the E-cadherin and ErbB3, downregulating the vimentin, EGFR, and ErbB2, and the restoration of mesenchyme to an epithelial phenotype [58]. Studies also reflected that the SAHA can enhance the cellular chemosensitivity to cisplatin, thereby mediating apoptosis in oral squamous carcinoma cells [78].

It has been verified that TSA is a natural inhibitor of HDAC class I and II. The changes in chromatin acetylation of HNSCC unexpectedly triggered a decrease in CSC. The hyperacetylation of chromatin in HNSCC induced by TSA can interrupt the generation of CSC and destroy the ability of stem cells to maintain tumor globules. It is also demonstrated that the TSA can decrease the enzyme activity of ALDH (a recognized marker of CSCs) [30]. The SAHA and TSA also reduce the CSC markers of CD44 and ABCG2, the expression of genes related to cell stemness, and the EMT phenotype in the oral cancer [79]. The combined application of TSA and PS-341 (bortezomib), a proteasome inhibitor, was also studied in HNSCC. Although TSA alone did not induce apoptosis, it can activate cystathionine to significantly enhance the degree of apoptosis induced by PS-341 [59]. The combination therapy of TSA and all-trans retinoic

Table 4: Histone deacetylase and expression in OSCC.

Name	Expression	Function	References
HDAC2	High expression	Overexpressed in OSCC, resulting in protein HIF-1 α, resulting in increased invasion and migration of HNSCC	[39]
HDAC6	High expression	Send α-tubulin deacetylation, thus promoting the process of tumor metastasis development	[40, 41]
HDAC7	High expression	Activate c-myc and promote the proliferation of oral tumor cells	[42]
HDAC8	High expression	Inhibition of caspase activation and autophagy in OSCC	[42]
HDAC9	High expression	Promote tumor growth by targeting proapoptotic genes	[43]
SIRT1, 2, 3, 5, 7	Low expression	Inhibit tumor and prevent DNA damage and oxidative stress	[45, 46]

acid (ATRA) synergistically inhibited the growth of tumor cells and strongly induced transcriptional and activation of target genes, thereby restoring the tumor sensitivity of HNSCC cell lines to retinoic acid [60]. HDACi reportedly appears to be valuable in the treatment of radiosensitized tumors in solid tumors, including HNSCC. TSA, SAHA, M344 (SAHA analogue), and desmethyl peptide (FR90228) regulate the cellular response to ionizing radiation and promote apoptosis and cell cycle arrest in HNSCC [80]. Recent treatments have shown that the TSA combined with 5-Aza-dC or RG108 can significantly reduce the vitality of HSC-2 cells and Ca922 cells. The TSA combined with DZNep also reduces the vitality of Ca922 cells, and the combination of TSA and the combination of TSA with other epigenetic inhibitors is also therapeutic for OSCC [81].

Panobinostat, an FDA-approved hydroxamic acid analogue (LBH589) for the treatment of refractory/recurrent multiple myeloma, induces hyperacetylation of histones *H*3 and *H*4 [82]. The LBH589 can inhibit cell growth and induce the *G*1 arrest and the apoptosis of OSCC by increasing the inhibition of transcription factor specificity protein 1 [61]. In vitro studies performed by flow cytometry on laryngopharyngeal (FaDu) and oral (CAL-27, SCC-15, UM-SCC-1, and UM-SCC-47) OSCC cell lines showed that treatment of these cells with LBH589 upregulated p21 and induced G2/M phase block and cell death [62].

3.2. The Class of Cyclic Peptide. The cyclic peptide class of HDACi can be divided into 2 categories according to the functional groups: one category contains (2S, 9S)-2-amino-9, 10-epoxy-8-oxodecanoic acid (Aoe), and epoxy ketone, while the other category does not contain the Aoe structure, which is mainly represented by apicidin, FK228, and trapoxin.

Apicidin is a cyclic tetrapeptide isolated from *Fusarium*, whose decanoic acid side chain, macrocyclic structure, and tryptophan side chain competitively bind HDAC. It has a significant antitumor function involving the antiproliferative activity and differentiation inducing activity toward the cancer cells [63]. Moreover, the OSCC cell lines treated with apicidin presented elevated levels of LC3-II, *G*2/*M* arrest, apoptosis, and autophagy as assessed by the MTT, DAPI staining, and flow cytometry [64].

Romidepsin (FK228) is a natural HDACi separated from *Chromobacterium violaceum*, which can induce the inhibition of HDAC with the characteristics of p21 (Waf1/Cip1) and reduce the staining of Ki67. Despite the limitations of single romidepsin treatment in the treatment of HNSCC, it still can effectively inhibit the tumor-related HDAC [65]. As an HDAC inhibitor, the FK228 induces the telomerase reverse transcriptase (hTERT) gene through a complex mechanism that involves the inhibition of histone deacetylation and other transcription factors except for the c-myc [66].

Trapoxin, a fungal product, was found to induce morphological reversion from transformed to normal in sis-transformed NIH3T3 fibroblasts [83]. Low concentration of trapoxin irreversibly inhibited the deacetylation of acetylated histone molecules through the covalent binding of epoxides and histone deacetylase. The process caused accumulation of highly acetylated core histone in a variety of mammalian cell lines [84]. Other findings have found that the product of binding trapoxin to histone deacetylase HDAC8 helps inhibit tumor cell proliferation as a potential anticancer compound [67].

3.3. The Class of Short-Chain Fatty Acid. The short-chain fatty acid class of HDACi has a relatively simple structure including a carboxyl group that binds the metal ions. It mainly contains sodium butyrate, valproic acid, and phenylbutyric acid.

Valproic acid (VPA), which is often widely used as a broad-spectrum antiepileptic drug and mood stabilizer in clinical practice, has been reported to be a class I and II HDAC inhibitor that promotes hyperacetylation of the *N*-terminal chains of histones *H*3 and *H*4 and nonhistones, thereby altering chromatin structure and preventing restricted expression of oncogenes. Moreover, several researchers have reported that the enhanced function of HDAC can stabilize the DNMT, while the VPA degrades the DNMT1 by multiple biochemical mechanisms including acetylation [68]. Because of its HDAC inhibitory activity, VPA has been a safe treatment for epilepsy for many years, and therefore, VPA is considered a good candidate for antitumor therapy in patients with metastatic or recurrent HNCs. In a clinical study, Gan et al. [52] have found that VPA inhibits the growth of HNSCC cell lines as a monotherapy or in combination with other anticancer drugs at physiological doses. The VPA therapy can increase the *G*1 arrest, apoptosis, and the expression of small ubiquitin-related modifiers. VPA treatment resulted in reduced tumor volume and increased apoptosis in xenograft models [69].

Table 5: Antitumor effects of HDACis in OSCC.

Class	Name	Target	Mechanism	References
Hydroxamic acids	SAHA	HDAC I, HDAC II, HDAC IV	Induces hyperacetylation of H2A and *H*3 and inhibits tumor activity	[57]
			Upregulate E calcineurin and ErbB3, downregulate vimentin, EGFR and ErbB2, and enhance the antitumor effect of defibrotide	[58]
	TSA	HDAC I, HDAC II	Induced apoptosis of tumor cells in combination with PS-341	[59]
			Combine with ATRA to inhibit tumor growth	[60]
	LBH589	HDAC I, HDAC II, HDAC IV	Induce high acetylation of *H*3 and *H*4, inhibit tumor growth and induce apoptosis, and lead to *G*1 phase block	[61]
			Upregulate the expression of p21 and induce *G*2/*M* arrest and cancer cell apoptosis	[62]
Cyclopeptides	Apicidin	HDAC1, HDAC3	Competitive combination of HDAC and antitumor proliferation	[63]
			Increase the level of LC3-II and increase the apoptosis and autophagy of tumor cells	[64]
	FK228	HDAC1, HDAC2	Reduce Ki67 staining and inhibit tumor growth	[65]
			Induce high expression of hTERT and inhibit tumor growth	[66]
	Trapoxin	HDAC8	Inhibit tumor cell proliferation as a potential anticancer compound	[67]
Short-chain fatty acids	VPA	HDAC I, HDAC II	Promote *H*3, *H*4 acetylation and inhibit oncogene expression	[68]
			Increase *G*1 arrest and apoptosis of tumor cells	[69]
	PBA	HDAC I, HDAC II	Promote tumor cell apoptosis and inhibit EMT transformation	[70]
			Reduce TNF-α level and promote DNA repair	[71]
	NaBu	HDAC I, HDAC IIa	Induce cell cycle arrest, related to the increased expression of kip1	[72]
Benzamides	MS-275	HDAC I	Make tumor cells stagnate in *G*0/*G*1 phase, enhance *H*3 and *H*4 acetylation, and promote apoptosis	[73]
			Increase cisplatin cytotoxicity	[74]
			Inhibit tumor migration and invasion by activating mir-107 and miR-138	[75]
	MGCD0103	HDAC I, HDAC IV	Has better radiotherapy sensitization effect	[76]

As an ammonia scavenger in the treatment of urea cycle diseases, phenylbutyric acid (PBA) leads to cell apoptosis, differentiation, and cell cycle arrest. Radiation-exposed patients receiving PBA have relatively low levels of mucosal oxidative stress and TNF-α, accompanied by mild oral mucositis, which promotes DNA repair and survival [71]. Sodium phenylbutyrate has a proapoptotic effect on tumor cells, inhibiting transforming growth factor-β-related epithelial-mesenchymal transition, with a decrease in the mesenchymal marker N-calmodulin and an increase in the epithelial marker E-calmodulin [70]. The PBA-derived HDACs (S)-HDAC42 present a higher activity of antiproliferation than SAHA, which can induce cell apoptosis by elevating the p21and p27, reducing the levels of CDK6 in the $G1$ phase, the cyclin D1 and the phosphorylation of Akt. Accordingly, it showed high potency in inhibiting the growth of OSCC in a Ca922 xenograft nude mouse model [85].

The short-chain fatty acid derivative sodium butyrate (NaBu) is another class I and IIa HDAC inhibitor belonging to aliphatic fatty acids. It is presented by the flow cytometry and immunocytochemical analysis that the NaBu significantly inhibits the proliferation of Tca8113 in a time and dose-dependent manner, and the NaBu therapy can inhibit the in vitro growth of OSCC cell lines and induce the cell cycle arrest, which may be related to the increased expression of p27 [72].

3.4. The Class of Benzamide. The benzamide class of HDACi has not been extensively studied as the first three HDAC inhibitors, which mainly contain the MS-275 (entinostat) and MGCD0103 (mocetinostat).

Entinostat is a bioavailable class I HDACi with a long half-life. In vitro and in vivo studies suggested that entinostat alone or in combination may be a promising agent for the treatment of OSCC due to its antiproliferative and proapoptotic effects. Administration of entinostat could reduce the proliferation of OSCC cells, leading to the $G0/G1$ arrest and massive apoptosis of tumor cells. Meanwhile, an increase in reactive oxygen species and a significant reduction in CSCs was observed as well. Entinostat also caused an increase in acetylated histone $H3$ or $H4$ and changes in the expression of cell cycle-related proteins (e.g., p21) [73]. The synergistic effect of HDACi and cisplatin enhanced the induction of cytotoxicity and apoptosis compared with using cisplatin alone, while the MS-275 also played the same role in the cytotoxicity of cisplatin during the treatment of OSCC. [74]. Combination treatment also activated the miR-138 and miR-107, leading to interrupting the following migration and invasion of tumor cells [75].

Preprocessing of the OSCC cell lines with the MGCD0103 and 5-aza20-deoxycytidine prior to radiotherapy resulted in better radiosensitization compared to the preprocessing by 5-Aza-dC alone [76].

4. Summary and Outlook

Histones have many common epigenetic modifications, and acetylation is one of the most common, which regulates DNA transcription and interferes with gene expression. The deacetylation is opposite of acetylation. The balance of those two reactions is necessary to ensure the integrity of chromatin. Therefore, histone acetylation in cancer cells can play a double role in cancer progression, which may be involved in suppressing the silencing of oncogenes and enhancing the expression of oncogenes. Evidence accumulated from a large amount of experimental data suggests that overexpression of HDAC may be closely associated with the development and progression of OSCC, and HDAC can be considered as a potential anticancer agent for OSCC. Further study on histone acetylation modification may be helpful to discover new therapies for oral cancer.

Data Availability

The data used to support the findings of this study are available from the corresponding authors upon request.

Conflicts of Interest

The authors declare that they have no conflicts of interest.

Authors' Contributions

Ying Lu collected the related studies and drafted the manuscript. Jinjin Yang participated in the design of the review. Junwen Zhu and Shuyuan Luo helped to publish the review. Yao Shu, Xuan Zou, and Qiao Ruan prepared the tables and the figure. Jun Wen and Yong Wang reviewed and revised the first manuscript. All authors read and approved the final manuscript. Ying Lu and Jinjin Yang contributed equally to this work.

Acknowledgments

This work was supported by the Beijing Natural Science Foundation (7222177) and National Natural Science Foundation of China (81602534).

References

[1] M. Hashibe, P. Brennan, S. C. Chuang et al., "Interaction between tobacco and alcohol use and the risk of head and neck cancer: pooled analysis in the International Head and Neck Cancer Epidemiology Consortium," *Cancer Epidemiology Biomarkers & Prevention*, vol. 18, no. 2, pp. 541–550, 2009.

[2] A. P. Algazi and J. R. Grandis, "Head and neck cancer in 2016: a watershed year for improvements in treatment?" *Nature Reviews Clinical Oncology*, vol. 14, no. 2, pp. 76–78, 2017.

[3] R. M. Castilho, C. H. Squarize, and L. O. Almeida, "Epigenetic modifications and head and neck cancer: implications for tumor progression and resistance to therapy," *International Journal of Molecular Sciences*, vol. 18, no. 7, p. 1506, 2017.

[4] J. E. Audia and R. M. Campbell, "Histone modifications and cancer," *Cold Spring Harbor Perspectives in Biology*, vol. 8, no. 4, Article ID a019521, 2016.

[5] G. Figlia, P. Willnow, and A. A. Teleman, "Metabolites regulate cell signaling and growth via covalent modification of proteins," *Developmental Cell*, vol. 54, no. 2, pp. 156–170, 2020.

[6] A. C. West and R. W. Johnstone, "New and emerging HDAC inhibitors for cancer treatment," *Journal of Clinical Investigation*, vol. 124, no. 1, pp. 30–39, 2014.
[7] D. Martin, M. C. Abba, A. A. Molinolo et al., "The head and neck cancer cell oncogenome: a platform for the development of precision molecular therapies," *Oncotarget*, vol. 5, no. 19, pp. 8906–8923, 2014.
[8] M. A. Dawson and T. Kouzarides, "Cancer epigenetics: from mechanism to therapy," *Cell*, vol. 150, no. 1, pp. 12–27, 2012.
[9] S. B. Rothbart and B. D. Strahl, "Interpreting the language of histone and DNA modifications," *Biochimica et Biophysica Acta (BBA) - Gene Regulatory Mechanisms*, vol. 1839, no. 8, pp. 627–643, 2014.
[10] P. Chi, C. D. Allis, and G. G. Wang, "Covalent histone modifications--miswritten, misinterpreted and mis-erased in human cancers," *Nature Reviews Cancer*, vol. 10, no. 7, pp. 457–469, 2010.
[11] Q. Wang, Y. Zhang, C. Yang et al., "Acetylation of metabolic enzymes coordinates carbon source utilization and metabolic flux," *Science*, vol. 327, no. 5968, pp. 1004–1007, 2010.
[12] S. Zhao, W. Xu, W. Jiang et al., "Regulation of cellular metabolism by protein lysine acetylation," *Science*, vol. 327, no. 5968, pp. 1000–1004, 2010.
[13] D. R. Friedmann and R. Marmorstein, "Structure and mechanism of non-histone protein acetyltransferase enzymes," *FEBS Journal*, vol. 280, no. 22, pp. 5570–5581, 2013.
[14] T. Narita, B. T. Weinert, and C. Choudhary, "Functions and mechanisms of non-histone protein acetylation," *Nature Reviews Molecular Cell Biology*, vol. 20, no. 3, pp. 156–174, 2019.
[15] J. Su, F. Wang, Y. Cai, and J. Jin, "The functional analysis of histone acetyltransferase MOF in tumorigenesis," *International Journal of Molecular Sciences*, vol. 17, no. 1, p. 99, 2016.
[16] N. Avvakumov and J. Côté, "The MYST family of histone acetyltransferases and their intimate links to cancer," *Oncogene*, vol. 26, no. 37, pp. 5395–5407, 2007.
[17] A. I. Salah Ud-Din, A. Tikhomirova, and A. Roujeinikova, "Structure and functional diversity of GCN5-relatedN-acetyltransferases (GNAT)," *International Journal of Molecular Sciences*, vol. 17, no. 7, p. 1018, 2016.
[18] L. Ngo, T. Brown, and Y. G. Zheng, "Bisubstrate inhibitors to target histone acetyltransferase 1," *Chemical Biology & amp; Drug Design*, vol. 93, no. 5, pp. 865–873, 2019.
[19] H. J. Dyson and P. E. Wright, "Role of intrinsic protein disorder in the function and interactions of the transcriptional coactivators CREB-binding protein (CBP) and p300," *Journal of Biological Chemistry*, vol. 291, no. 13, pp. 6714–6722, 2016.
[20] N. D. Heintzman, R. K. Stuart, G. Hon et al., "Distinct and predictive chromatin signatures of transcriptional promoters and enhancers in the human genome," *Nature Genetics*, vol. 39, no. 3, pp. 311–318, 2007.
[21] S. H. Stricker, A. Köferle, and S. Beck, "From profiles to function in epigenomics," *Nature Reviews Genetics*, vol. 18, no. 1, pp. 51–66, 2017.
[22] R. H. Jacobson, A. G. Ladurner, D. S. King, and R. Tjian, "Structure and function of a human TAFII250 double bromodomain module," *Science*, vol. 288, no. 5470, pp. 1422–1425, 2000.
[23] K. Zhang, Q. Wu, W. Liu et al., "FAM135B sustains the reservoir of Tip60-ATM assembly to promote DNA damage response," *Clinical and Translational Medicine*, vol. 12, no. 8, p. e945, 2022.
[24] S. M. Sykes, H. S. Mellert, M. A. Holbert et al., "Acetylation of the p53 DNA-binding domain regulates apoptosis induction," *Molecular Cell*, vol. 24, no. 6, pp. 841–851, 2006.
[25] A. J. Bannister and T. Kouzarides, "Regulation of chromatin by histone modifications," *Cell Research*, vol. 21, no. 3, pp. 381–395, 2011.
[26] Y. Li and E. Seto, "HDACs and HDAC inhibitors in cancer development and therapy," *Cold Spring Harb Perspect Med*, vol. 6, no. 10, Article ID a026831, 2016.
[27] N. Reichert, M. A. Choukrallah, and P. Matthias, "Multiple roles of class I HDACs in proliferation, differentiation, and development," *Cellular and Molecular Life Sciences*, vol. 69, no. 13, pp. 2173–2187, 2012.
[28] Y. W. Chen, S. Y. Kao, H. J. Wang, and M. H. Yang, "Histone modification patterns correlate with patient outcome in oral squamous cell carcinoma," *Cancer*, vol. 119, no. 24, pp. 4259–4267, 2013.
[29] M. Arif, B. M. Vedamurthy, R. Choudhari et al., "Nitric oxide-mediated histone hyperacetylation in oral cancer: target for a water-soluble HAT inhibitor, CTK7A," *Chemistry & Biology*, vol. 17, no. 8, pp. 903–913, 2010.
[30] F. S. Giudice, D. S. Pinto, J. E. Nör, C. H. Squarize, and R. M. Castilho, "Inhibition of histone deacetylase impacts cancer stem cells and induces epithelial-mesenchyme transition of head and neck cancer," *PLoS One*, vol. 8, no. 3, Article ID e58672, 2013.
[31] L. P. Webber, V. P. Wagner, M. Curra et al., "Hypoacetylation of acetyl-histone H3 (H3K9ac) as marker of poor prognosis in oral cancer," *Histopathology*, vol. 71, no. 2, pp. 278–286, 2017.
[32] H. Ma, H. Chang, W. Yang, Y. Lu, J. Hu, and S. Jin, "A novel IFNα-induced long noncoding RNA negatively regulates immunosuppression by interrupting H3K27 acetylation in head and neck squamous cell carcinoma," *Molecular Cancer*, vol. 19, no. 1, p. 4, 2020.
[33] F. Chen, S. Qi, X. Zhang, J. Wu, X. Yang, and R. Wang, "lncRNA PLAC2 activated by H3K27 acetylation promotes cell proliferation and invasion via the activation of Wnt/β catenin pathway in oral squamous cell carcinoma," *International Journal of Oncology*, vol. 54, no. 4, pp. 1183–1194, 2019.
[34] L. O. Almeida, A. C. Abrahao, L. K. Rosselli-Murai et al., "NFκB mediates cisplatin resistance through histone modifications in head and neck squamous cell carcinoma (HNSCC)," *FEBS Open Bio*, vol. 4, no. 1, pp. 96–104, 2013.
[35] D. M. Guimarães, L. O. Almeida, M. D. Martins et al., "Sensitizing mucoepidermoid carcinomas to chemotherapy by targeted disruption of cancer stem cells," *Oncotarget*, vol. 7, no. 27, pp. 42447–42460, 2016.
[36] Q. Li, H. Sun, Y. Shu, X. Zou, Y. Zhao, and C. Ge, "hMOF (human males absent on the first), an oncogenic protein of human oral tongue squamous cell carcinoma, targeting EZH2 (enhancer of zeste homolog 2)," *Cell Proliferation*, vol. 48, no. 4, pp. 436–442, 2015.
[37] S. Ropero and M. Esteller, "The role of histone deacetylases (HDACs) in human cancer," *Molecular Oncology*, vol. 1, no. 1, pp. 19–25, 2007.
[38] O. Witt, H. E. Deubzer, T. Milde, and I. Oehme, "HDAC family: what are the cancer relevant targets?" *Cancer Letters*, vol. 277, no. 1, pp. 8–21, 2009.
[39] H. H. Chang, C. P. Chiang, H. C. Hung, C. Y. Lin, Y. T. Deng, and M. Y. P. Kuo, "Histone deacetylase 2 expression predicts poorer prognosis in oral cancer patients," *Oral Oncology*, vol. 45, no. 7, pp. 610–614, 2009.

[40] T. Sakuma, K. Uzawa, T. Onda et al., "Aberrant expression of histone deacetylase 6 in oral squamous cell carcinoma," *International Journal of Oncology*, vol. 29, no. 1, pp. 117–124, 2006.

[41] J. A. Gasche and A. Goel, "Epigenetic mechanisms in oral carcinogenesis," *Future Oncology*, vol. 8, no. 11, pp. 1407–1425, 2012.

[42] M. Y. Ahn and J. H. Yoon, "Histone deacetylase 7 silencing induces apoptosis and autophagy in salivary mucoepidermoid carcinoma cells," *Journal of Oral Pathology & Medicine*, vol. 46, no. 4, pp. 276–283, 2017.

[43] B. Rastogi, S. K. Raut, N. K. Panda, V. Rattan, B. D. Radotra, and M. Khullar, "Overexpression of HDAC9 promotes oral squamous cell carcinoma growth, regulates cell cycle progression, and inhibits apoptosis," *Molecular and Cellular Biochemistry*, vol. 415, no. 1-2, pp. 183–196, 2016.

[44] M. C. Haigis and L. P. Guarente, "Mammalian sirtuins--emerging roles in physiology, aging, and calorie restriction," *Genes & Development*, vol. 20, no. 21, pp. 2913–2921, 2006.

[45] A. Noguchi, X. Li, A. Kubota et al., "SIRT1 expression is associated with good prognosis for head and neck squamous cell carcinoma patients," *Oral Surgery, Oral Medicine, Oral Pathology and Oral Radiology*, vol. 115, no. 3, pp. 385–392, 2013.

[46] C. C. Lai, P. M. Lin, S. F. Lin et al., "Altered expression of SIRT gene family in head and neck squamous cell carcinoma," *Tumor Biology*, vol. 34, no. 3, pp. 1847–1854, 2013.

[47] J. F. Lv, L. Hu, W. Zhuo, C. M. Zhang, H. H. Zhou, and L. Fan, "Epigenetic alternations and cancer chemotherapy response," *Cancer Chemotherapy and Pharmacology*, vol. 77, no. 4, pp. 673–684, 2016.

[48] P. Xiong, Y. X. Li, Y. T. Tang, and H. G. Chen, "Proteomic analyses of Sirt1-mediated cisplatin resistance in OSCC cell line," *The Protein Journal*, vol. 30, no. 7, pp. 499–508, 2011.

[49] W. Li, D. Zhu, and S. Qin, "SIRT7 suppresses the epithelial-to-mesenchymal transition in oral squamous cell carcinoma metastasis by promoting SMAD4 deacetylation," *Journal of Experimental & Clinical Cancer Research*, vol. 37, no. 1, p. 148, 2018.

[50] Y. Y. Kao, C. H. Chou, L. Y. Yeh et al., "MicroRNA miR-31 targets SIRT3 to disrupt mitochondrial activity and increase oxidative stress in oral carcinoma," *Cancer Letters*, vol. 456, pp. 40–48, 2019.

[51] M. D. Martins and R. M. Castilho, "Histones: controlling tumor signaling circuitry," *Journal of Carcinogenesis & Mutagenesis*, vol. 1, no. 5, pp. 1–12, 2013.

[52] C. P. Gan, S. Hamid, S. Y. Hor et al., "Valproic acid: growth inhibition of head and neck cancer by induction of terminal differentiation and senescence," *Head & Neck*, vol. 34, no. 3, pp. 344–353, 2012.

[53] A. M. Gillenwater, M. Zhong, and R. Lotan, "Histone deacetylase inhibitor suberoylanilide hydroxamic acid induces apoptosis through both mitochondrial and Fas (Cd95) signaling in head and neck squamous carcinoma cells," *Molecular Cancer Therapeutics*, vol. 6, no. 11, pp. 2967–2975, 2007.

[54] J. S. Ungerstedt, Y. Sowa, W. S. Xu et al., "Role of thioredoxin in the response of normal and transformed cells to histone deacetylase inhibitors," *Proceedings of the National Academy of Sciences of the United States of America*, vol. 102, no. 3, pp. 673–678, 2005.

[55] C. Lindsay, H. Seikaly, and V. L. Biron, "Epigenetics of oropharyngeal squamous cell carcinoma: opportunities for novel chemotherapeutic targets," *Journal of Otolaryngology - Head & Neck Surgery*, vol. 46, no. 1, p. 9, 2017.

[56] E. Ceccacci and S. Minucci, "Inhibition of histone deacetylases in cancer therapy: lessons from leukaemia," *British Journal of Cancer*, vol. 114, no. 6, pp. 605–611, 2016.

[57] B. Kumar, A. Yadav, J. C. Lang, T. N. Teknos, and P. Kumar, "Suberoylanilide hydroxamic acid (SAHA) reverses chemoresistance in head and neck cancer cells by targeting cancer stem cells via the downregulation of nanog," *Genes Cancer*, vol. 6, no. 3-4, pp. 169–181, 2015.

[58] F. Bruzzese, A. Leone, M. Rocco et al., "HDAC inhibitor vorinostat enhances the antitumor effect of gefitinib in squamous cell carcinoma of head and neck by modulating ErbB receptor expression and reverting EMT," *Journal of Cellular Physiology*, vol. 226, no. 9, pp. 2378–2390, 2011.

[59] J. Kim, J. Guan, I. Chang, X. Chen, D. Han, and C. Y. Wang, "PS-341 and histone deacetylase inhibitor synergistically induce apoptosis in head and neck squamous cell carcinoma cells," *Molecular Cancer Therapeutics*, vol. 9, no. 7, pp. 1977–1984, 2010.

[60] Y. M. Whang, E. J. Choi, J. H. Seo, J. S. Kim, Y. D. Yoo, and Y. H. Kim, "Hyperacetylation enhances the growth-inhibitory effect of all-trans retinoic acid by the restoration of retinoic acid receptor beta expression in head and neck squamous carcinoma (HNSCC) cells," *Cancer Chemotherapy and Pharmacology*, vol. 56, no. 5, pp. 543–555, 2005.

[61] Y. J. Jeon, S. M. Ko, J. H. Cho, J. I. Chae, and J. H. Shim, "The HDAC inhibitor, panobinostat, induces apoptosis by suppressing the expresssion of specificity protein 1 in oral squamous cell carcinoma," *International Journal of Molecular Medicine*, vol. 32, no. 4, pp. 860–866, 2013.

[62] M. B. Prystowsky, A. Adomako, R. V. Smith et al., "The histone deacetylase inhibitor LBH589 inhibits expression of mitotic genes causing G2/M arrest and cell death in head and neck squamous cell carcinoma cell lines," *The Journal of Pathology*, vol. 218, no. 4, pp. 467–477, 2009.

[63] J. W. Han, S. H. Ahn, S. H. Park et al., "Apicidin, a histone deacetylase inhibitor, inhibits proliferation of tumor cells via induction of p21WAF1/Cip1 and gelsolin," *Cancer Research*, vol. 60, no. 21, pp. 6068–6074, 2000.

[64] M. Y. Ahn, S. G. Ahn, and J. H. Yoon, "Apicidin, a histone deaceylase inhibitor, induces both apoptosis and autophagy in human oral squamous carcinoma cells," *Oral Oncology*, vol. 47, no. 11, pp. 1032–1038, 2011.

[65] M. Haigentz Jr, M. Kim, C. Sarta et al., "Phase II trial of the histone deacetylase inhibitor romidepsin in patients with recurrent/metastatic head and neck cancer," *Oral Oncology*, vol. 48, no. 12, pp. 1281–1288, 2012.

[66] J. Murakami, J. Asaumi, N. Kawai et al., "Effects of histone deacetylase inhibitor FR901228 on the expression level of telomerase reverse transcriptase in oral cancer," *Cancer Chemotherapy and Pharmacology*, vol. 56, no. 1, pp. 22–28, 2005.

[67] N. J. Porter and D. W. Christianson, "Binding of the microbial cyclic tetrapeptide trapoxin A to the class I histone deacetylase HDAC8," *ACS Chemical Biology*, vol. 12, no. 9, pp. 2281–2286, 2017.

[68] S. A. Brodie, G. Li, A. El-Kommos et al., "Class I HDACs are mediators of smoke carcinogen-induced stabilization of DNMT1 and serve as promising targets for chemoprevention of lung cancer," *Cancer Prevention Research*, vol. 7, no. 3, pp. 351–361, 2014.

[69] Z. Sang, Y. Sun, H. Ruan, Y. Cheng, X. Ding, and Y. Yu, "Anticancer effects of valproic acid on oral squamous cell

carcinoma via SUMOylation in vivo and in vitro," *Experimental and Therapeutic Medicine*, vol. 12, no. 6, pp. 3979–3987, 2016.

[70] K. Qian, L. Sun, G. Zhou et al., "Sodium phenylbutyrate inhibits tumor growth and the epithelial-mesenchymal transition of oral squamous cell carcinoma in vitro and in vivo," *Cancer Biotherapy and Radiopharmaceuticals*, vol. 33, no. 4, pp. 139–145, 2018.

[71] Y. L. Chung, M. Y. Lee, and N. N. Pui, "Epigenetic therapy using the histone deacetylase inhibitor for increasing therapeutic gain in oral cancer: prevention of radiation-induced oral mucositis and inhibition of chemical-induced oral carcinogenesis," *Carcinogenesis*, vol. 30, no. 8, pp. 1387–1397, 2009.

[72] L. Gong, W. M. Wang, Y. Ji, Y. Wang, and D. W. Li, *Zhonghua Kou Qiang Yi Xue Za Zhi*, vol. 45, no. 10, pp. 619–622, 2010.

[73] A. E. M. Marques, C. H. V. Nascimento Filho, T. M. Marinho Bezerra, E. N. S. Guerra, R. M. Castilho, and C. H. Squarize, "Entinostat is a novel therapeutic agent to treat oral squamous cell carcinoma," *Journal of Oral Pathology & Medicine*, vol. 49, no. 8, pp. 771–779, 2020.

[74] H. Rikiishi, F. Shinohara, T. Sato, Y. Sato, M. Suzuki, and S. Echigo, "Chemosensitization of oral squamous cell carcinoma cells to cisplatin by histone deacetylase inhibitor suberoylanilide hydroxamic acid," *International Journal of Oncology*, vol. 30, no. 5, pp. 1181–1188, 2007.

[75] J. Datta, M. Islam, S. Dutta, S. Roy, Q. Pan, and T. N. Teknos, "Suberoylanilide hydroxamic acid inhibits growth of head and neck cancer cell lines by reactivation of tumor suppressor microRNAs," *Oral Oncology*, vol. 56, pp. 32–39, 2016.

[76] H. De Schutter, M. Kimpe, S. Isebaert, and S. Nuyts, "A systematic assessment of radiation dose enhancement by 5-Aza-2'-deoxycytidine and histone deacetylase inhibitors in head-and-neck squamous cell carcinoma," *International Journal of Radiation Oncology, Biology, Physics*, vol. 73, no. 3, pp. 904–912, 2009.

[77] S. Rangwala, C. Zhang, and M. Duvic, "HDAC inhibitors for the treatment of cutaneous T-cell lymphomas," *Future Medicinal Chemistry*, vol. 4, no. 4, pp. 471–486, 2012.

[78] M. Suzuki, M. Endo, F. Shinohara, S. Echigo, and H. Rikiishi, "Enhancement of cisplatin cytotoxicity by SAHA involves endoplasmic reticulum stress-mediated apoptosis in oral squamous cell carcinoma cells," *Cancer Chemotherapy and Pharmacology*, vol. 64, no. 6, pp. 1115–1122, 2009.

[79] K. Chikamatsu, H. Ishii, T. Murata et al., "Alteration of cancer stem cell-like phenotype by histone deacetylase inhibitors in squamous cell carcinoma of the head and neck," *Cancer Science*, vol. 104, no. 11, pp. 1468–1475, 2013.

[80] Y. Zhang, M. Jung, A. Dritschilo, and M. Jung, "Enhancement of radiation sensitivity of human squamous carcinoma cells by histone deacetylase inhibitors," *Radiation Research*, vol. 161, no. 6, pp. 667–674, 2004.

[81] R. Ushio, M. Hiroi, A. Matsumoto, K. Mori, N. Yamamoto, and Y. Ohmori, "Enhanced cytotoxic effects in human oral squamous cell carcinoma cells treated with combined methyltransferase inhibitors and histone deacetylase inhibitors," *Biomedicines*, vol. 10, no. 4, p. 763, 2022.

[82] M. Xu, L. Yin, Y. Cai et al., "Epigenetic regulation of integrin $\beta 6$ transcription induced by TGF-$\beta 1$ in human oral squamous cell carcinoma cells," *Journal of Cellular Biochemistry*, vol. 119, no. 5, pp. 4193–4204, 2018.

[83] H. Yoshida and K. Sugita, "A novel tetracyclic peptide, trapoxin, induces phenotypic change from transformed to normal in sis-oncogene-transformed NIH3T3 cells," *Japanese Journal of Cancer Research*, vol. 83, no. 4, pp. 324–328, 1992.

[84] M. Kijima, M. Yoshida, K. Sugita, S. Horinouchi, and T. Beppu, "Trapoxin an antitumor cyclic tetrapeptide, is an irreversible inhibitor of mammalian histone deacetylase," *Journal of Biological Chemistry*, vol. 268, no. 30, pp. 22429–22435, 1993.

[85] S. H. Baek, "When signaling kinases meet histones and histone modifiers in the nucleus," *Molecular Cell*, vol. 42, no. 3, pp. 274–284, 2011.

Hindawi
Journal of Oncology
Volume 2023, Article ID 7487306, 6 pages
https://doi.org/10.1155/2023/7487306

Research Article

Radiofrequency Coblation-Assisted Transoral Surgery for the Treatment of Oropharyngeal Squamous Cell Carcinoma: A Comparative Study with Open Surgery

Xiaowan Du,[1] **Xin Zhao**,[2] **Junbo Zhang**,[1] **Chi Zhang**,[1] **Shuifang Xiao**,[1] **and Tiancheng Li**[1]

[1]*Department of Otolaryngology, Head and Neck Surgery, Peking University First Hospital, Beijing, China*
[2]*Department of Otolaryngology, Head and Neck Surgery, Qingdao University Medical College Affiliated Yantai Yuhuangding Hospital, Qingdao, Shandong, China*

Correspondence should be addressed to Shuifang Xiao; xiao_ent@163.com and Tiancheng Li; litianchengltc@163.com

Received 21 August 2022; Revised 17 September 2022; Accepted 27 January 2023; Published 8 February 2023

Academic Editor: Guan-Jun Yang

Objective. Radiofrequency coblation (RFC) is a relatively new method that has opened up new perspectives in treating oropharyngeal squamous cell carcinoma (OPSCC). Our study was designed to explore the feasibility and effectiveness of RFC-assisted transoral surgery (RFC-TOS) for primary OPSCC. *Methods*. Sixty-nine cases of OPSCC from February 2005 to November 2020 were retrospectively analyzed, including 31 in the RFC-TOS group and 38 in the open surgery group. No difference was observed in demographic and oncological characteristics. *Results*. The significance between the RFC-TOS group and the open surgery group was proved in intraoperative bleeding volume (34.10 ± 10.10 ml vs. 193.68 ± 21.00 ml, $P < 0.001$), durations of surgery (79.58 ± 8.45 min vs. 217.87 ± 17.65 min, $P < 0.001$), time to resume oral feeding (1.64 ± 0.41 d vs. 11.58 ± 1.41 d, $P < 0.001$), duration of hospitalization (7.84 ± 0.66 d vs. 15.66 ± 1.62 d, $P < 0.001$), and the total costs (22846.22 ± 1821.55¥ vs. 41792.24 ± 4150.86¥, $P < 0.001$). The rates of 5-year overall survival (OS), 5-yeardisease-specific survival (DSS), and 5-year local control rate (LC) were 69.1%, 71.7%, and 75.7%, respectively, in the RFC-TOS group and 71.0%, 73.4%, and 73.7% in the open surgery group ($P > 0.05$). *Conclusions*. RFC-TOS is a feasible alternative transoral approach for OPSCC. The reported perioperative and oncologic outcomes are satisfactory.

1. Introduction

Oropharyngeal squamous cell carcinoma (OPSCC) accounts for 90% of oropharyngeal malignancies [1], and the number of OPSCC patients is still increasing [2]. According to the National Comprehensive Cancer Network (NCCN) guidelines, the therapeutic options for OPSCC are surgery with or without adjuvant therapy and radiotherapy with or without chemotherapy. The adverse effects of nonsurgical treatments and recent technical innovations have prompted a new trend in surgical approaches [3]. Surgical treatment approaches have changed dramatically with a trend of minimally invasive surgery, especially for early-stage OPSCC. Traditional open surgery for such malignancies is associated with high complication rates, affecting speech and swallowing and changing appearance [4, 5]. During the past decades, transoral surgeries, including transoral laser microsurgery (TLM) and transoral robotic surgery (TORS), have altered the surgical landscape for resecting oropharyngeal malignancies. Such procedures are characterized by less trauma, excellent function preservation, fewer complications, and improved quality of life [3–6].

Laser, though widely used in TLM for the treatment of selectable tumors located in multiple regions of the upper aerodigestive tract [6–10], has its own limitations, including low efficiency in hemostasis and tissue manipulation, resulting in surgical difficulties and prolonged operation time [11–13]. These limitations are more obviously observed

when treating oropharyngeal tumors, as these tumors are always associated with large volumes and abundant blood supplies [5]. The other limitations included the 2-dimensional cutting plane, serious thermal damage, and the risk of a catastrophic laser fire [12, 13]. TORS is another minimally invasive procedure that was approved by the FDA for treating early-stage OPSCC in 2009, with excellent visualization, decreased line of sight issues (using a 30° endoscope), improved range of motion (360° robotic arm movement), precise cutting, and easier en bloc resection [14–20]. Nevertheless, it lacks haptic feedback, and it is hard to popularize due to its extremely high cost of purchase and maintenance.

Radiofrequency coblation (RFC) is a relatively new method that has been widely used in several pharyngeal surgical procedures [18], including tonsillectomy, uvulopalatopharyngoplasty, and some tongue or tongue base procedures [21–24]. Its advantages include high cutting and hemostatic efficiency, less thermal damage, good haptic feedback, relief of postoperative pain, and lack of charring, making it an attractive choice in transoral surgery for treating OPSCC.

Currently, only very small clinical study data supported the feasibility of RFC-assisted transoral surgery (RFC-TOS) in treating oropharyngeal cancer [12, 25]. This retrospective study was conducted to further explore the safety, feasibility, and effectiveness of RFC-TOS in treating OPSCC compared with open surgery.

2. Materials and Methods

2.1. Patients. Between January 2005 and December 2020, a total of 31 patients with *T*1–3 stage OPSCC who successfully underwent RFC-TOS with or without postoperative adjunct radiotherapies at Peking University First Hospital were included for analysis (RFC-TOS group). Meanwhile, an additional 38 patients with *T*1–3 stage OPSCC who underwent open surgery with or without postoperative adjunct radiotherapies during the same period at Peking University School of Stomatology were included in the control group (open surgery group). The inclusion criteria were patients aged ≥18 years with no previous treatment history. The exclusion criteria included patients with a prior history of head and neck aerodigestive tract malignancy, distant metastasis, or multiple primary tumors outside the oropharynx during the presentation. The baseline, perioperative, and prognostic data of these two groups of patients were collected for analysis. The study has been approved by the Institutional Ethics Committee of Peking University First Hospital (approval number 2019-264) and was carried out following the Declaration of Helsinki.

2.2. Surgical Procedure. Open surgery procedures included transcervical, trans-hyoid approaches, or even partial mandible resection. In the RFC-TOS procedure, patients underwent surgery by transnasal endotracheal intubation under general anesthesia. Boyle-Davis mouth gag, molar mouth gag, or FK retractor were used to expose the surgical fields. EIC8870-01 coblation wand (Arthrocare Corp.; Austin, Texas, USA) or MC401 coblation wand (MECHAN; Chengdu, Sichuan Province, China) were used for tumor resection. The console was set for 7-8 (coblation) or 5 (coagulation). Primary tumors were removed by transoral "en bloc" resection. Frozen sections were applied to ensure surgical margins of at least 5 mm and, if possible, 10 mm for all intraoperative tumor resections. In certain cases with large tumors, it is not possible to ensure 5–10 mm margins; therefore, *R*0 resection status should be ensured. To prevent persistent postoperative nasopharyngeal reflux, patients with large oropharyngeal defects underwent reconstructive procedures using a buccal mucosal flap or hard palate flap. All patients staged cN + underwent concurrent selective neck dissections.

2.3. Adjunct Therapies and Follow-Up. Postoperative radiotherapy was suggested when the incisional margin was reported to be less than 5 mm from the tumor edge or when extranodal extension (ENE) was positive. There were 13 patients in the RFC-TOS group and 15 patients in the open surgery group who received postoperative radiotherapy with a dose of 50–60 Gy. All patients were regularly followed up in the outpatient department with physical examinations, neck ultrasounds, endoscopes, and enhanced CT. Meanwhile, the patients were also followed up by telephone regularly regarding the postoperative quality of life and potential complications that affect their speech and swallowing.

2.4. Statistical Analysis. Pearson's chi-square test or Fischer's exact test was applied to compare categorical variables. The *t*-test or nonparametric test was used for continuous variables. The Kaplan–Meier method was employed to analyze the survival outcomes, and the comparison was assessed by a log-rank test. Statistics significance exists when $P < 0.05$. Statistical analyses were performed using MedCalc software (MedCalc version 18.11.3; MedCalc Software, Ostend, Belgium).

3. Results

The comparisons of baseline characteristics between RFC-TOS and open surgery group patients are shown in Table 1. No significant differences were found in gender, age, tumor sites, tumor stages, pathological differentiation, p16 positive rate, and postoperative adjuvant radiotherapy (all $P > 0.05$).

Perioperative data were analyzed and compared between these two groups, as shown in Table 2. The mean intraoperative bleeding volume, operation time, recovery of oral feeding time, hospital stay days, and total costs in the RFC-TOS group were significantly lower than those in the open surgery group (all $P < 0.05$).

Only one patient in the RFC-TOS group dropped out in the sixth month. The median follow-up periods were 42 months (6–151 months) in the RFC-TOS group and 50.5 months (6–142 months) in the open surgery group. As shown in Figure 1, no significant differences were found

Table 1: The baseline patient characteristics and comparison between the RFC-TOS and open surgery groups.

	RFC-TOS ($n = 31$)	Open surgery ($n = 38$)	P value
Gender			
Male	24 (77.4%)	29 (76.3%)	0.91
Female	7 (22.6%)	9 (23.7%)	
Age	56.3 ± 7.9	58.2 ± 10.6	0.41
Tumor site			
Tonsil/lateral wall	20 (64.5%)	22 (57.9%)	0.74
Soft palate	5 (16.1%)	9 (23.7%)	
Base of tongue	6 (19.4%)	7 (18.4%)	
T stage			
$T1$	8 (25.8%)	8 (21.1%)	0.63
$T2$	21 (67.7%)	25 (65.8%)	
$T3$	2 (6.5%)	5 (13.2%)	
N stage			
$N0$	22 (70.9%)	28 (73.7%)	0.80
$N+$	3 (9.7%)	10 (26.3%)	
Clinical stage			
I-II stage	20 (64.5%)	23 (60.5%)	0.74
III-IV stage	11 (35.5%)	15 (39.5%)	
Differentiation			
High	15 (48.4%)	15 (39.5%)	0.76
Moderate	12 (38.7%)	17 (44.7%)	
Poor	4 (12.9%)	6 (15.8%)	
p16 result			
p16+	18 (58.1%)	21 (55.3%)	0.82
p16−	13 (41.9%)	17 (44.7%)	
Radiotherapy			
Yes	13 (41.9%)	15 (39.5%)	0.84
No	18 (58.1%)	23 (60.5%)	

between the RFC-TOS and open surgery groups (all $P > 0.05$) regarding 5-year overall survival (OS) (69.1% vs. 71.0%), 5-yeardisease-specific survival (DSS) (71.7% vs. 73.4%), and 5-year local control rate (LC) (75.7% vs. 73.7%).

Postoperative complications in the open surgery group included 1 case of asphyxia (2.6%) because of a swollen tongue base (emergency tracheotomy needed). No short-term complications were found in the RFC-TOS group. At the end of the follow-up period, there were 3 cases of mild nasopharyngeal reflux (7.9%) and 1 case of taste loss (2.6%) in the open surgery group, while in the RFC-TOS group, 2 cases (6.5%) of mild nasopharyngeal reflux occurred occasionally and 1 case of taste loss (3.2%) was recorded. No long-term complications that affected speech, swallowing, or breathing were reported in both groups.

4. Discussion

RFC is considered a relatively new technique applied in transoral surgeries. Since its first technical descriptions and feasibility reports, only a few studies have reported perioperative outcomes for OPSCC. Among them, Carney et al. and Hofauer et al. included 10 and 12 cases of oropharyngeal malignancy resection, respectively [12, 25]. Neither of them reported long-term oncological results. Our study, while retrospective, is the first one focusing on OPSCC with a substantial population ($N = 69$), including 31 in the RFC-TOS group, and a relatively long follow-up.

The present study confirmed that, compared to open surgery, RFC-TOS evidently had favorable outcomes in terms of less intraoperative blood loss, shorter surgical time, rapid recovery of oral feeding, shorter length of hospital stays, and an economically friendly cost. Oncologic outcomes were also proven to be comparable to open surgery. These results suggest the feasibility and effectiveness of RFC-TOS in treating OPSCC.

Similar surgical data of TLM and TORS for $T1$ to $T3$ stage OPSCC resection were seldom published previously. Sievert et al. reported the blood losses of TLM and TORS as 121.5 ± 109.3 ml and 102.2 ± 76.9 ml, respectively [13]. Hofauer et al. reported a mean value of bleeding of 2.31 (SD = 0.82) for RFC-TOS treating oral and oropharyngeal tumors ($n = 25$) and described it as self-limiting in most of the cases [25]. In this study, the blood loss was 34.10 ± 10.10 ml ($n = 31$). Although the precise values of the blood loss and operation time are incomparable, they might suggest the correlations with hemostasis efficiency in different cutting instruments. The sealing capacities of the CO_2 laser, monopolar scalpel, and RFC were reported, separately, as 1-2 mm, 2 mm, and 7 mm, measured by vessel diameters [3]. Because of the abundant blood supply in the oropharynx, it might be possible that RFC-TOS is more favorable for OPSCC, partially due to its better hemostasis capacity. In addition, operation times of TLM and TORS were reported as 140 ± 59 min ($n = 10$) and 186 ± 54 min ($n = 9$)[13], while in this study, it was 79.58 ± 8.45 min in RFC-TOS ($n = 31$). Carney et al. suggested that RFC allowed for a much faster resection time than the CO_2 laser for the resection of head and neck malignancies ($P = 0.017$), especially in the oropharynx ($P = 0.007$) [12]. RFC-TOS also showed sufficient competence in tissue manipulation without high thermal damage [11]. This suggested RFC-TOS is an attractive alternative technique in transoral surgery for oropharyngeal lesions [3, 12].

Cost is one of the important factors that determine whether a treatment can be widely accepted by patients, which is mostly influenced by equipment [26]. Analyses of costs were rare. Sievert et al. reported incurred costs of a significantly higher average amount of 5719.20 ± 3611.79 euros for TORS and 2856.35 ± 1439.75 euros for TLM ($P = 0.002$) treating OPSCC [13]. Dombrée et al. analyzed the total costs for supraglottic open, TLM, and TORS approaches and confirmed them to be 3,349 euros (3,193–3,499 euros), 3,461 euros (3,207–3,664 euros), and 5,650 euros (4,297–5,974 euros), respectively [26]. These may suggest that the order of costs from highest to lowest would be TORS, TLM, and open surgery. Our study showed the total costs for open surgery and RFC-TOS are 22846.22 ± 1821.55¥ and 41792.24 ± 4150.86¥ ($P < 0.001$), respectively. It might indirectly indicate that RFC could be the most economical and practical method of all, which would greatly help the popularization of this method.

Less precise cutting is one major disadvantage of RFC. Carney et al. first proposed that the RFC probe design limits evaluating the surgical margin [12]. Hofauer et al. reported

Table 2: Perioperative results and comparison between the RFC-TOS and open surgery groups.

	RFC-TOS ($n = 31$)	Open surgery ($n = 38$)	P value
Bleeding volume (ml)	34.10 ± 10.10	193.68 ± 21.00	<0.001
Duration of surgery (min)	79.58 ± 8.45	217.87 ± 17.65	<0.001
Time to resume oral feeding (d)	1.64 ± 0.41	11.58 ± 1.41	<0.001
Duration of hospitalization (d)	7.84 ± 0.66	15.66 ± 1.62	<0.001
Total hospital cost (¥)	22846.22 ± 1821.55	41792.24 ± 4150.86	<0.001

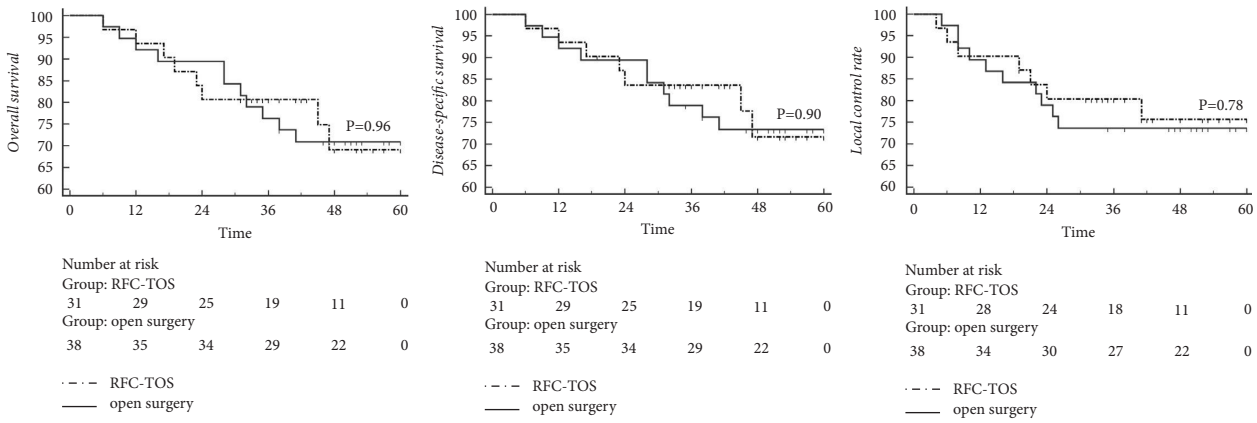

Figure 1: The KM curves of OS, DSS, and LC and the oncologic comparison between the RFC-TOS and open surgery groups.

an average width of 1593.75 μm of the coagulation zones of RFC in resecting oral and oropharyngeal lesions [25]. Wider margins are needed in OPSCC, where the most frequent identification of a clear margin was >5 mm on microscopic examination [18, 27]. The definition is also included in the National Comprehensive Cancer Network (NCCN) guidelines for head and neck cancer. Therefore, the disadvantage of RFC is acceptable for OPSCC resection.

In general, the oncological results of RFC-TOS treating $T1$ to $T3$ stage OPSCC (5-OS 69.1%, 5-DSS 71.7%, and 5-LC 75.7%) are in line with the prognosis of current publications of other transoral surgeries [13, 28–30]. Besides, the oncological results showed no significant difference compared with open surgery, namely the standard procedure.

However, RFC-TOS for OPSCC is considered a challenging and skilled procedure suitable for selected OPSCC patients. Rigorous indication, adaptation, and regulation of operation are strongly recommended.

The limitations of our investigation need to be addressed. The study was designed to evaluate the feasibility and oncological prognosis of RFC-TOS for OPSCC as a retrospective study and therefore was not planned as a blinded and controlled clinical trial, which might decrease the power of this investigation. In addition, data were collected from two different medical centers, which could have an impact on the comparison of perioperative and oncological results. Another limitation is that the comparison of RFC-TOS directly with TLM or TORS, instead of open surgery, could be more illustrative, which is the direction of our future work.

5. Conclusions

RFC could be an alternative tool for resecting OPSCC. Compared with traditional open surgery, RFC-TOS could offer comparable oncologic outcomes. OPSCC patients who underwent such surgery also showed rapid recovery, a low complication rate, and excellent functional outcomes. The superiority in economical cost and operation difficulty also makes RFC-TOS an attractive choice for treating OPSCC.

Data Availability

The data supporting the findings of this data are available from the corresponding authors upon reasonable request.

Ethical Approval

The study was approved by the Institutional Ethics Committee of Peking University First Hospital (approval number 2019-264).

Disclosure

Shuifang Xiao and Tiancheng Li are the corresponding authors.

Conflicts of Interest

The authors declare that they have no conflicts of interest.

Authors' Contributions

Shuifang Xiao and Tiancheng Li contributed equally to this work.

Acknowledgments

The study was supported by the Capital's Funds for Health Improvement and Research (grant no. 2022-2-4076), the Beijing Municipal Science and Technology Commission (grant no. Z171100001017094), and the Scientific Research Seed Fund of Peking University First Hospital (grant no. 2021SF21).

References

[1] J. S. Cooper, K. Porter, K. Mallin et al., "National Cancer Database report on cancer of the head and neck: 10-year update," *Head & Neck*, vol. 31, no. 6, pp. 748–758, 2009.

[2] F. Bray, J. Ferlay, I. Soerjomataram, R. L. Siegel, L. A. Torre, and A. Jemal, "Global cancer statistics 2018: GLOBOCAN estimates of incidence and mortality worldwide for 36 cancers in 185 countries," *CA: A Cancer Journal for Clinicians*, vol. 68, no. 6, pp. 394–424, 2018.

[3] G. Tirelli, F. Boscolo Nata, M. Piovesana, E. Quatela, N. Gardenal, and R. E. Hayden, "Transoral surgery (TOS) in oropharyngeal cancer: different tools, a single mini-invasive philosophy," *Surgical Oncology*, vol. 27, no. 4, pp. 643–649, 2018.

[4] W. Golusiński and E. Golusińska-Kardach, "Current role of surgery in the management of oropharyngeal cancer," *Frontiers Oncology*, vol. 9, p. 388, 2019.

[5] A. S. Ibrahim, F. J. Civantos, J. M. Leibowitz et al., "Meta-analysis comparing outcomes of different transoral surgical modalities in management of oropharyngeal carcinoma," *Head & Neck*, vol. 41, no. 6, pp. 1656–1666, 2019.

[6] B. G. Weiss, F. Ihler, M. Z. Anczykowski et al., "Transoral laser microsurgery for treatment of oropharyngeal cancer in 368 patients," *Head & Neck*, vol. 41, no. 9, pp. 3144–3158, 2019.

[7] W. Steiner, P. Ambrosch, C. F. Hess, and M. Kron, "Organ preservation by transoral laser microsurgery in piriform sinus carcinoma," *Otolaryngology - Head and Neck Surgery*, vol. 124, no. 1, pp. 58–67, 2001.

[8] M. Canis, A. Martin, F. Ihler et al., "Transoral laser microsurgery in treatment of pT2 and pT3 glottic laryngeal squamous cell carcinoma - results of 391 patients," *Head & Neck*, vol. 36, no. 6, pp. 859–866, 2014.

[9] M. Canis, F. Ihler, A. Martin, C. Matthias, and W. Steiner, "Transoral laser microsurgery for T1a glottic cancer: review of 404 cases," *Head & Neck*, vol. 37, no. 6, pp. 889–895, 2015.

[10] B. G. Weiss, F. Ihler, Y. Pilavakis et al., "Transoral laser microsurgery for T1b glottic cancer: review of 51 cases," *European Archives of Oto-Rhino-Laryngology*, vol. 274, no. 4, pp. 1997–2004, 2017.

[11] J. Howard, L. Masterson, R. C. Dwivedi et al., "Minimally invasive surgery versus radiotherapy/chemoradiotherapy for small-volume primary oropharyngeal carcinoma," *Cochrane Database of Systematic Reviews*, vol. 12, Article ID CD010963, 2016.

[12] A. S. Carney, M. S. Timms, C. N. Marnane, S. Krishnan, G. Rees, and S. Mirza, "Radiofrequency coblation for the resection of head and neck malignancies," *Otolaryngology - Head and Neck Surgery*, vol. 138, no. 1, pp. 81–85, 2008.

[13] M. Sievert, M. Goncalves, A. Zbidat et al., "Outcomes of transoral laser microsurgery and transoral robotic surgery in oropharyngeal squamous cell carcinoma," *Auris Nasus Larynx*, vol. 48, no. 2, pp. 295–301, 2021.

[14] J. G. Frederiksen, H. I. Channir, M. H. H. Larsen et al., "Long-term survival outcomes after primary transoral robotic surgery (TORS) with concurrent neck dissection for early-stage oropharyngeal squamous cell carcinoma," *Acta Oto-Laryngologica*, vol. 141, no. 7, pp. 714–718, 2021.

[15] Y. Chillakuru, D. A. Benito, D. Strum et al., "Transoral robotic surgery versus nonrobotic resection of oropharyngeal squamous cell carcinoma," *Head & Neck*, vol. 43, no. 7, pp. 2259–2273, 2021.

[16] P. M. Bunch, H. S. Patwa, R. T. Hughes, M. Porosnicu, and J. D. Waltonen, "Patient selection for transoral robotic surgery (TORS) in oropharyngeal squamous cell carcinoma: what the surgeon wants to know," *Topics in Magnetic Resonance Imaging*, vol. 30, no. 2, pp. 117–130, 2021.

[17] H. Li, S. J. Torabi, H. S. al Park et al., "Clinical value of transoral robotic surgery: nationwide results from the first 5 years of adoption," *The Laryngoscope*, vol. 129, no. 8, pp. 1844–1855, 2019.

[18] E. J. Moore, K. M. Van Abel, D. L. al Price et al., "Transoral robotic surgery for oropharyngeal carcinoma: surgical margins and oncologic outcomes," *Head & Neck*, vol. 40, no. 4, pp. 747–755, 2018.

[19] B. Dhanireddy, N. P. Burnett, S. Sanampudi et al., "Outcomes in surgically resectable oropharynx cancer treated with transoral robotic surgery versus definitive chemoradiation," *American Journal of Otolaryngology*, vol. 40, no. 5, pp. 673–677, 2019.

[20] H. S. Parhar, C. M. Yver, and R. M. Brody, "Current indications for transoral robotic surgery in oropharyngeal cancer," *Otolaryngologic Clinics of North America*, vol. 53, no. 6, pp. 949–964, 2020.

[21] H. Y. Li, L. A. Lee, and E. J. Kezirian, "Coblation endoscopic lingual lightening (CELL) for obstructive sleep apnea," *European Archives of Oto-Rhino-Laryngology*, vol. 273, no. 1, pp. 231–236, 2016.

[22] M. R. Elbadawey, H. M. Hegazy, A. E. Eltahan, and J. Powell, "A randomised controlled trial of coblation, diode laser and cold dissection in paediatric tonsillectomy," *Journal of Laryngology & Otology*, vol. 129, no. 11, pp. 1058–1063, 2015.

[23] B. Simunjak, J. Slipac, P. Krmpotić, and S. Dubravcić-Simunjak, "Efficiency of radiofrequency assisted uvulopalatopharyngoplasty in the treatment of snoring," *Acta Clinica Croatica*, vol. 50, no. 3, pp. 357–360, 2011.

[24] L. Wang, J. X. Liu, X. L. Yang, C. W. Yang, and Y. X. Qin, "Z-palatoplasty and tongue radiofrequency for patients with small tonsils," *Otolaryngology - Head and Neck Surgery*, vol. 148, no. 5, pp. 873–877, 2013.

[25] B. Hofauer, A. Knopf, U. Strassen et al., "Radiofrequency resection in oral and oropharyngeal tumor surgery," *Auris Nasus Larynx*, vol. 47, no. 1, pp. 148–153, 2020.

[26] M. Dombrée, R. Crott, G. Lawson, P. Janne, A. Castiaux, and B. Krug, "Cost comparison of open approach, transoral laser microsurgery and transoral robotic surgery for partial and total laryngectomies," *European Archives of Oto-Rhino-Laryngology*, vol. 271, no. 10, pp. 2825–2834, 2014.

[27] J. D. Meier, D. A. Oliver, and M. A. Varvares, "Surgical margin determination in head and neck oncology: current clinical practice. The results of an International American Head and Neck Society Member Survey," *Head & Neck*, vol. 27, no. 11, pp. 952–958, 2005.

[28] F. De Felice, L. Humbert-Vidan, M. Lei, A. King, and T. Guerrero Urbano, "Analyzing oropharyngeal cancer survival outcomes: a decision tree approach," *British Journal of Radiology*, vol. 93, no. 1111, Article ID 20190464, 2020.

[29] D. Blanchard, J.-P. Rame, M. Y. Louis et al., "Oropharyngeal cancer," *Bulletin du Cancer*, vol. 101, no. 5, pp. 429–437, 2014.

[30] C. M. Yver, D. Shimunov, G. S. Weinstein et al., "Oncologic and survival outcomes for resectable locally-advancedHPV-related oropharyngeal cancer treated with transoral robotic surgery," *Oral Oncology*, vol. 118, Article ID 105307, 2021.

Hindawi
Journal of Oncology
Volume 2022, Article ID 2208176, 15 pages
https://doi.org/10.1155/2022/2208176

Review Article

Chemokine/GPCR Signaling-Mediated EMT in Cancer Metastasis

Xutengyue Tian,[1] Jiayi Wang,[1] Lanxin Jiang,[1] Yuchen Jiang,[1] Juan Xu,[2] and Xiaodong Feng[1]

[1]*State Key Laboratory of Oral Diseases, National Clinical Research Center for Oral Diseases, Research Unit of Oral Carcinogenesis and Management, Chinese Academy of Medical Sciences, West China Hospital of Stomatology, Sichuan University, Chengdu, Sichuan 610041, China*
[2]*Department of Stomatology, Sijing Hospital, Shanghai 210061, China*

Correspondence should be addressed to Yuchen Jiang; jiangyuchen16@126.com, Juan Xu; doctorxue@126.com, and Xiaodong Feng; fengxiaodong84@126.com

Received 25 June 2022; Revised 8 August 2022; Accepted 23 August 2022; Published 11 October 2022

Academic Editor: Zhi-En Feng

Metastasis, the chief cause of cancer-related deaths, is associated with epithelial-mesenchymal transition (EMT). In the tumor microenvironment, EMT can be triggered by chemokine/G-protein-coupled receptor (GPCR) signaling, which is closely associated with tumor progression. However, the functional links between chemokine/GPCR signaling-mediated EMT and metastasis remain unclear. Herein, we summarized the mechanisms of chemokine/GPCR signaling-mediated EMT with an insight into facilitating metastasis and clarified the role of chemokine in the local invasion, intravasation, circulation, extravasation, and colonization, respectively. Moreover, several potential pathways that might contribute to EMT based on the latest studies on GPCR signaling were proposed, including signaling mediated by G protein, β-arrestin, intracellular, dimerization activation, and transactivation. However, there is still limited evidence to support the EMT programme functional contribution to metastasis, which keeps a key question still open whether we should target EMT programme of cancer cells. Answers to that question might help develop an anticancer strategy or guide new directions for anticancer metastasis therapy.

1. Introduction

Chemokines are a group of small (8~14 kDa) structurally related molecules that participate mainly in leukocyte trafficking via GPCR signaling. Approximately 48 ligands are found to bind to 19 different chemokine receptors nowadays[1]. And most chemokine receptors are Gαi-coupled GPCRs regulating directed cell migration, adhesion, and cell-cell interactions. In the tumor microenvironment, chemokines are major drivers of tumor progression, angiogenesis, metastasis, and even EMT in multiple cancers.

EMT was first proposed by Elizabeth Hay in the field of development, where cells undergoing EMT remodel their cytoskeletons, gain front-back polarity, and abandon tight junctions [2]. Interestingly, in neoplasms, a complete-EMT (c-EMT) is rare; instead, it is often "hijacked" partly by malignant cells, termed the partial-EMT (p-EMT). Those programmes were recognized as important in the context of cancer, owing to their potential in conferring malignant cells with motility, stemness, and invasiveness, which allows malignant cells to find a new place to colonize [3].

Metastasis is the chief cause of cancer-related death (about 90% [4]). However, metastatic dissemination is not efficient; once cancer cells leave their favorable surroundings, they are exposed to various threats such as shear stress, which may lead to death [5]. Only a few cancer cells succeed in forming metastases, and they must complete metastatic processes, including local invasion, intravasation, transportation through circulation, extravasation, and colonization. They have the traits to exploit the microenvironment, transform themselves for adaptation, survive, and form distant metastases [6, 7]. Currently, one of the key phenotypes discovered in cancer cells throughout metastatic

dissemination is the mesenchymal phenotype, regarded as a consequence of EMT [8]. However, whether chemokine/GPCR mediates metastasis through EMT programmes or should we focus on targeting EMT programmes for anti-cancer metastasis therapies development remains unclear.

2. EMT and Metastasis in Brief

EMT is a cellular programme in which epithelial cells acquire mesenchymal phenotypes with a loss of epithelial phenotypes [2]. This programme is known to be associated with tumor initiation, invasion, migration, stemness, proliferation, and chemoresistance and has received extraordinary attention for EMT-associated protein markers for their clinical significance in evaluating the malignancy of cancer. In the tumor microenvironment, cancer cells tend to undergo a partial-EMT (p-EMT) programme instead of a complete-EMT (c-EMT) programme [3]. Unlike the c-EMT programme, the p-EMT programme is used to describe cancer cells in an epithelial-mesenchymal intermediate state, manifesting as simultaneously expressing both epithelial and mesenchymal markers or simply loss of epithelial markers with no change in mesenchymal markers [9]. To date, the EMT programme is believed to be triggered by the stroma in the malignant tissue, which is mainly composed of carcinoma-associated fibroblasts (CAFs), tumor-associated macrophages (TAMs), T lymphocytes, and myeloid-derived suppressor cells [10]. Together, they employ paracrine or direct contacts to induce EMT in carcinoma cells, which transduce signaling ending up at EMT-TFs (Snail, Slug, Twist1/2, and Zeb1/2) [10].

EMT programmes have been reported to be associated with multiple steps. In primary tumor, EMT cells are reported to localize at the leading edge of the tumor, which is in proximity to stroma [11, 12], exhibiting invasive features that secrete matrix metalloproteases (MMPs) and form invadopodia [13, 14] to remodel ECM. Twist has been reported specifically enhanced in intravasation [14, 15]. Circulating tumor cells (CTCs) have been reported to have mesenchymal characteristics and express EMT regulators, such as components of the TGF-β pathway and FOXC1 [16]. Notably, the source of TGF-β in circulation is likely to be platelets that attach to CTCs and help these cells survive in circulation [16, 17]. Attachment of cancer cells to endothelial cells is the first step in extravasation.And N-cadherin, a marker of mesenchymal cells, expressed both by endothelial and some cancer cells, is important for attachment and extravasation [18]. Interestingly, even the relationship between EMT and metastasis was carefully reviewed by Mittal [11], and most studies successfully established the association of them, but still, very limited concrete experimental evidence has proven the EMT programme a potent regulator of cancer cell dissociation from the primary tumor and crossing the endothelial barrier.

Clinically, the EMT-TFs have been found critical prognostic value in head and neck squamous cell carcinoma (HNSCC) [19]. Overexpression of Twist1, Snail1, Snail2, and ZEB1 indicated a poor overall survival (OS) of HNSCC [19]. And EMT status of circulating tumor cells (CTCs) is also associated with HNSCC recurrence [20]. Single-cell transcriptomic analysis revealed that head and neck squamous cells mainly undergo the p-EMT programme instead of the c-EMT programme. Notably, among the classical EMT-TFs, only Snail2 was detected, hinting at a post-transcriptional regulation [12]. Immunohistochemistry stained these p-EMT cancer cells at the leading edge of the tumor, closely interacting with CAFs [12]. And, flow cytometry has confirmed the significance abundance of CAFs in human HNSCC [21]. These studies indicated the possible critical role of CAFs in mediating EMT in HNSCC. However, the influence of TAMs cannot be excluded even though there are limited studies.

3. Chemokine-Mediated EMT and Associated Metastasis

The chemokine superfamily comprises a large number of ligands and receptors. In further studies, the confusing ligand-receptor relationships were gradually unveiled and categorized into two subgroups: "inflammatory" and "homeostatic". A plethora of literature has shown that chemokines from both subgroups are able to induce EMT (see Table 1) and promote metastasis. In addition to mediating EMT, chemokines also contribute to directed migration and transendothelial migration of cancer cells and recruitment of non-cancer cells in the whole dissemination process (Figure 1).

CXCL12-CXCR4 axis has been well studied in cancer, with a significant effect on mediating EMT in a variety of cancers, such as gastric cancer, breast cancer, head and neck cancer, and lung cancer (see Table 1). In the context of metastasis, CXCL12 as a typical homeostatic chemokine regulates directional metastasis, which might be a result of its function in mediating EMT, directing cell migration. Signaling through CXCL12-CXCR4 could mediate intracellular actin polymerization and induce typical pseudopodia formation after 20 minutes of stimulation, suggesting an active mesenchymal transition [83]. MCF-7 cells stably expressing SDF-1 (CXCL12) observed significant downregulation of E-cadherin and enhanced expression of Slug, fibronectin, and vimentin through the NF-κB pathway [84]. In a 2D environment, MCF-7 expressing constitutively active CXCR4 exhibited upregulation of ZEB1 and cadherin 11, loss of E-cadherin, and p120 isoform switching [32]. Interestingly, MCF-7 CXCR4 WT cells displayed epithelial characteristics under 2D condition but mesenchymal characteristics under 3D culture. This structural discrepancy between 3D and 2D cultures indicates that confinement may be critical for regulating EMT [32].

CXCL12 is mostly recognized to be secreted by CAF in a paracrine way [85]. Accordingly, cancer cells upregulate the expression of CXCR4 with increased vimentin and decreased E-cadherin upon sensing CAF-produced CXCL12 in a coculture system [86]. These CXCR4-positive cells thus migrate directionally along the CXCL12 gradient toward their destination, such as blood vessels [85, 87]. Additionally, CXCR4-positive

Table 1: Summary of literature regarding chemokine-mediated EMT.

Chemokine-receptor axis	Category	Cancer type	Marker used	Signaling pathway	Method	Refs
CXCL1-CXCR1	Inflammatory	Glioma	N-cadherin, vimentin	NF-κB/Snail	WB, IF	[22]
CXCL1-CXCR1/CXCR2		Prostate cancer	E-cadherin	Src pathway	WB	[23]
		Ovarian cancer	E-cadherin, vimentin	Wnt/β/catenin	WB	[24]
CXCL2-CXCR2		Colon cancer	EpCAM, Snail, Twist, vimentin	Gαi-2 and Gαq/11 pathway	WB	[25]
CXCR2		Breast cancer	E-cadherin	P85α/Akt1	WB	[26]
		Colorectal cancer	E-cadherin, ZO-1 N-cadherin, vimentin	MAPK/Elk-1/Snail	WB, IF	[27]
		Papillary thyroid cancer	E-cadherin, N-cadherin, vimentin	β-catenin signaling	WB, IF	[28]
CXCL5-CXCR2		Head and neck cancer	E-cadherin, vimentin, Snail	MAPK/GSK-3β/Snail	Morphology, WB, qPCR	[29]
		Hepatocellular cancer	E-cadherin, vimentin	PI3K/Akt/GSK-3β/Snail	Morphology, IF, WB, IHC	[30]
CXCR4/CXCR2		Gastric cancer	E-cadherin, N-cadherin, vimentin, Snail	CXCR2/NF-κB/p65-CXCR4 CXCR4/JAK/STAT3/CXCR2	WB	[31]
		Breast cancer	ZEB1, cadherin 11, E-cadherin	PI3K/Akt/mTOR Raf/MEK/MAPK	WB	[32]
CXCL8-CXCR1/CXCR2		Breast cancer	E-cadherin, N-cadherin, vimentin, MMP9	Unreported	qPCR	[33]
		Colon cancer	E-cadherin, N-cadherin, vimentin, α-SMA	PI3K/Akt/NF-κB	WB, qPCR	[34]
		Thyroid cancer	Zeb, Slug, Snail	Akt/Slug	Morphology, WB	[35]
		Triple-negative breast cancer	E-cadherin. MMP2	PI3K/Akt	WB	[36]
CXCL9-CXCR3		Head and neck cancer	E-cadherin, vimentin	Akt pathway	IF, WB	[37]
CXCL10-CXCR3		Colon cancer	E-cadherin, ZO-1, cytokeratin, occludin, desmoplakin, fibronectin, N-cadherin, vimentin, Snail	PI3K/Akt/GSK-3β/Snail	Morphology, qPCR, IF, WB	[38]
CXCL12-CXCR4	Homeostatic	Colorectal cancer	E-cadherin, Snail, vimentin, MMP7	CXCR4/miR-133a/RhoA Wnt/β-catenin	IHC, WB	[39, 40]
		Papillary thyroid cancer	E-cadherin, N-cadherin, vimentin	NF-κB pathway	Morphology, WB, IF	[41]
		Gastric cancer	ZEB1/2, Twist2, Snail, E-cadherin, vimentin	STAT3-ZEB1 and Cav-1-c-EMT	Morphology, WB, IF	[42, 43]
		Hepatocellular cancer	E-cadherin, N-cadherin, vimentin	Wnt-β-catenin	IHC, WB	[40, 44]
		Ovarian cancer	E-cadherin, N-cadherin	Wnt-β-catenin	WB	[45]
		Non-small-cell lung cancer	E-cadherin	Akt pathway or MAPK pathway	IHC	[46]
		Pancreatic cancer	E-cadherin, vimentin	Non-canonical hedgehog pathway (SDF-1/CXCR4/SMO)	WB	[47]
		Lung cancer	E-cadherin, vimentin N-cadherin, Slug	CXCR4/β-catenin/PPARδ	WB, IF	[48]
		Head and neck cancer	E-cadherin, keratin, N-cadherin, vimentin, MMP2, MMP9	PI3K/Akt	WB, IHC, IF, qPCR, morphology	[49–51]
		Sacral chondrosarcoma	Snail, N-cadherin	MEK/MAPK and PI3K/Akt	WB	[52]
CXCL13-CXCR5	Homeostatic	Breast cancer	E-cadherin, N-cadherin, vimentin, Slug, Snail	Src/PI3K	WB, qPCR, IF, morphology	[53]
		Renal cell carcinoma	E-cadherin, N-cadherin, vimentin	Akt pathway	WB	[54]
CXCL16-CXCR6	Homeostatic	Gastric cancer	E-cadherin, ZO-1N-cadherin, Snail, Slug	Akt pathway MAPK pathway	WB, IF, morphology	[55, 56]
CCL2-CCR2	Inflammatory	Hepatocellular cancer	E-cadherin, vimentin, Snail	Hedgehog pathway (CCR2/SMO/Gli-1)	WB, qPCR	[57, 58]
		Gastric cancer	E-cadherin, vimentin, ZEB2	CCR2/MAPK/ELK1/EGR1/ZEB2	IF, WB, qPCR	[59]
		Breast cancer	E-cadherin, vimentin, fibrinogen	MAPK/GSK-3β/Snail	Morphology, WB, IF	[60]
		Prostate cancer	E-cadherin, Snail, MMP9	CCR2-STAT3	WB	[61]
		Head and neck cancer	E-cadherin, Snail, vimentin	Unreported	WB, IF	[62]
CCR4	Dual	Hepatocellular cancer	E-cadherin, N-cadherin, vimentin, Slug, Snail	MAPK-akt-MMP2	WB, IF	[63]
CCL17-CCR4		Hepatocellular cancer	E-cadherin, N-cadherin vimentin, Snail	Wnt/β-catenin	WB	[64]

Table 1: Continued.

Chemokine-receptor axis	Category	Cancer type	Marker used	Signaling pathway	Method	Refs
CCR5	Inflammatory	Melanoma	E-cadherin, N-cadherin, vimentin, Snail, Slug	PI3K/AKT/GSK3β	WB, IF, IHC	[65]
CCL18-CCR6		Pancreatic ductal adenocarcinoma	Snail, E-cadherin	Unreported	qPCR, WB	[66]
		Colon cancer	E-cadherin, vimentin, N-cadherin, Snail1, ZEB1, β-catenin, α-SMA	Unreported	WB, qPCR	[67]
CCL20-CCR6		Gastric cancer	N-cadherin, vimentin, MMP2	CCR6/CrkL/MAPK1/2	WB	[68]
		Breast cancer	E-cadherin, ZO-1, N-cadherin, vimentin, Snail	NF-κb/Snail, mTOR/S6 kinase, PKCδ ccr6/VEGF	WB, qPCR	[69]
CCL20-CCR6		Head and neck cancer	E-cadherin, vimentin	Unreported	WB, qPCR	[70]
CCL19-CCR7	Homeostatic	Breast cancer	E-cadherin, N-cadherin, vimentin	Akt pathway	WB	[71]
		Gastric cancer	Snail, E-cadherin, MMP9	MAPK/Snail and PI3K/Snail	WB	[72]
		Ovarian cancer	E-cadherin, N-cadherin, Snail, MMP9	CCR7-CrkL-MAPK	WB	[73]
CCL21-CCR7		Head and neck cancer	E-cadherin, N-cadherin, vimentin	JAK/STAT	WB, IF, morphology	[74]
		Pancreatic cancer	E-cadherin, N-cadherin, LYVE-1	MAPK/NF-κB	WB	[75]
		Lung cancer	E-cadherin, vimentin, Slug	MAPK pathway	WB, qPCR	[76]
		Breast carcinoma	E-cadherin, vimentin, N-cadherin, Slug	Unreported	WB, qPCR	[77]
		Chondrosarcoma	E-cadherin, N-cadherin, Slug	MAPK/Slug and PI3K/Akt/Slug	WB	[78]
CCL18-CCR8		Bladder cancer	E-cadherin, MMP2	MMP2 pathway	WB	[79]
CCR9		Osteosarcoma	E-cadherin, N-cadherin, vimentin, Twist, Snail, MMP-1	Wnt/β-catenin	WB qPCR	[80]
CCL28-CCR10		Head and neck cancer	E-cadherin, β-catenin, Slug, Twist1, Snail	Inhibit EMT CCR10/RARβ	WB, IF	[81]
XCL1-XCR1	Dual	Breast cancer	E-cadherin, N-cadherin, vimentin	MAPK/HIF-1α	WB	[82]

tumor cells might exploit interstitial fluid to form autologous gradients that direct them to blood vessels [88, 89].

The role of CXCL12 in effective vascular barrier crossing and distal colonization has been extensively studied. For example, CXCL12 can directly promote the adhesion of cancer cells to endothelial cells or induce morphological changes via GTPase-mediated signaling [90, 91]. After extravasation to metastasized tissues, the main problem is how to adapt and thrive in new microenvironments. Zhang et al. proposed a view that stromal signals resembling those of a distant organ select for cancer cells that are primed for metastasis in that organ. For example, triple-negative breast tumor cells that tend to thrive on the CAFs-derived CXCL12 and IGF are primed for metastasis in the CXCL12-rich microenvironment [92].

CCL2-CCR2 axis not only acts on cancer cells to mediate EMT and transendothelial migration but also recruits TAMs to assist tumor progression and metastasis. CCL2 is an inflammatory chemokine that attracts monocytes, natural killer cells, and memory T cells to mediate multiple inflammatory processes. In neoplasms, CCL2 is well recognized to have a promalignant effect with TAMs. A recent study indicates that CCL2 attracts circulating monocytes into the tumor and triggers their acquisition of a TAM phenotype [93]. In turn, the TAMs display a tumor-promoting effect in the tumor microenvironment. A recent study indicated that ZEB1 expression is required for the activation of macrophages toward a protumor TAM phenotype, which enhances the expression of CCR2 and MMP9. Through MMP9, TAMs activate CCL2 expression in cancer cells. Together they form a CCR2-MMP9-CCL2 positive loop that drives tumor progression and are probably critical in triggering the EMT programme [94]. In addition to cancer cells, CCL2 is also secreted by TAMs. In colorectal cancer, TAMs secrete CCL2 via Wnt5a/CaMKII/ERK/CCL2 axis, and those CCL2 molecules act on cancer cells and drive tumor progression [95].

CCL2-CCR2 axis has been reported to mediate EMT in various cancers, including hepatocellular, gastric, prostate, breast, head, and neck cancer (Table 1). Like CXCL12, most researchers incubated carcinoma cells, which have been starved overnight, with CCL2 for about 48 h, and witnessed alterations in cell morphology and EMT markers. For example, in breast cancer, MCF-7 incubated with CCL2 (50 ng/ml) observed spindle morphology and increased Snail, E-cadherin, and vimentin expression. The MEK1/2 and GSK-3 beta could reverse the CCL2-induced EMT phenotype, indicating that MAPK/GSK-3-beta/Snail signaling is involved in EMT regulation [60]. Interestingly, no apparent changes in Snail mRNA levels were shown during CCL2 treatment. This might be a result of post-transcriptional regulation of CCL2.

Study about CCL2 in metastatic dissemination is limited. Current studies have reported CCL2 attracting monocytes to the primary tumor that facilitate migration. These monocytes subsequently differentiate into migratory TAMs that carry cancer cells along the CXCL12 gradient secreted by perivascular fibroblasts toward blood vessels [96]. In further process, the CCL2 secreted by cancer cells can also interact with CCR2 on endothelial cells to facilitate the transendothelial process [6].

CCL19/CCL21-CCR7 axis also plays a vital role in EMT (see Table 1) and lymphatic metastasis. CCL19 and CCL21, two known ligands of CCR7, display nonoverlapping roles in the homing of the immune system, including trafficking of T cells and dendritic cells [97]. For example, CCL19 functions in the thymic emigration of mature T cells from fetal thymic organ cultures, but not CCL21 [98]. Therefore, even if they share the same receptor, their roles in EMT or tumor progression might be slightly different. Cancer cells incubated with CCL19 (50 ng/ml) or CCL21 (100 ng/ml) showed increased expression of N-cadherin and vimentin and decreased expression of E-cadherin. In this process, adverse signaling pathways were involved such as PI3K/Akt, JAK/STAT, and MAPK pathways.

The specific origin of CCL19 and CCL21 in the tumor microenvironment remains unclear. Studies have found CCL21 expression in the high endothelial venules of lymph nodes, which connects it with lymphatic metastasis. For now, several studies have found a correlation between CCR7 expression and lymph node metastasis [99, 100].

Studies on the mechanism of which CCL19/CCL21 attracts cancer cells toward lymph nodes are unclear. A study proposed that CCL21/CCL19-CCR7 axis mediated the directional migration of cancer cells to lymphatics with an autocrine fashion. Specifically, CCL21/CCL19 secreted by tumor cells with membrane CCR7 generates an autologous gradient, along which tumor cells migrate to lymphatics [89]. Additionally, CCL21 secreted by lymphatic can also guide lymphatic metastasis [101, 102].

The deregulation of chemokines has been observed in HNSCC via bioinformatics analysis of The Cancer Genome Atlas (TCGA). Chemokines such as CXCL1, CXCL8, CXCL13, CCL3, and CCL5 are reported upregulation in mRNA levels [103]. Interestingly, the well-studied chemokines such as CXCL12, CCL2, and CCL7 were not obviously deregulated in mRNA levels, indicating a post-transcriptional modification. CXCL12 is well studied in HNSCC and has prognostic value. Patients with higher expression of CXCL12/CXCR4 have higher risk of regional recurrence [104]. CXCL12 secreted by CAFs or malignant cells can activate the EMT programme via the PI3K-Akt pathway (Table 1) and promote invasion via MAPK-AP1 and NF-κb pathways [105, 106]. CCL2 can be secreted by CAFs and malignant cells to assist tumor progression, EMT, and migration [107].

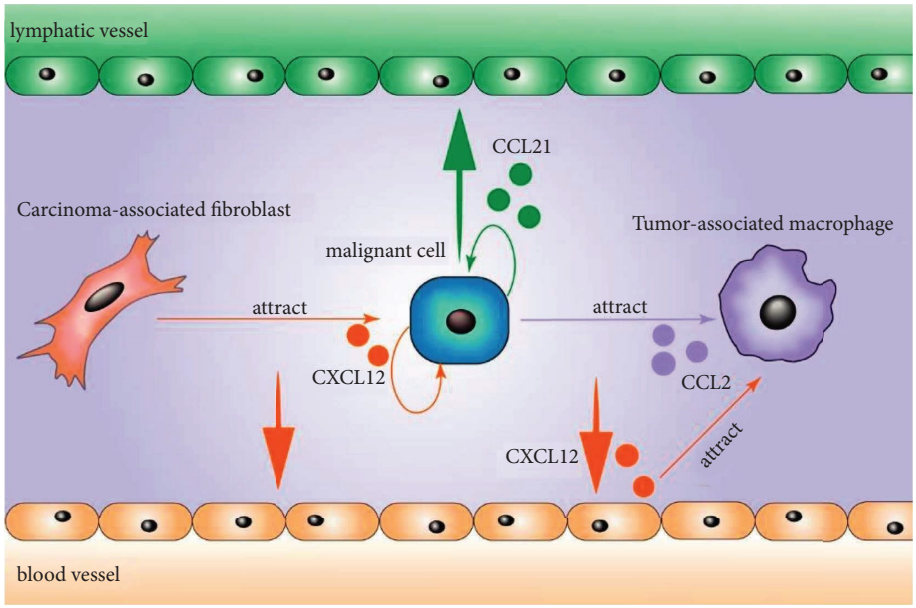

Figure 1: Interaction between cancer cells and non-cancer cells via chemokine. CXCL12 is secreted by CAFs, malignant cells, and endothelial cells. Malignant cells migrate along CXCL12 gradient to blood vessels with the help of CAFs or independently. CCL2 is secreted by malignant cells to recruit TAMs. They migrate toward blood vessels with the help of TAMs. CCL21 gradient directs malignant cells to lymphatic vessels via autocrine way. CAFs, carcinoma-associated fibroblasts and TAMs, tumor-associated macrophages.

CCL2-CCR4 axis, not the CCL2-CCR2 axis, is reported to facilitate cell migration via Vav guanine nucleotide exchange factor 2 (Vav2) Rac family small GTPase1 (Rac1) complex-myosin light chain (MLC) signaling [108]. However, we still have few clues on how CCL2 contributes to EMT in HNSCC. CCR7 in HNSCC is associated with lymph node metastasis [109]. CCL19-CCR7 axis facilitates migration, invasion, and adhesion with the involvement of PI3K-cdc42, MMP9, RhoA/ROCK, and β-1 integrin [110–113], while JAK-STATs and MAPK pathways have been reported correlated with EMT activation (Table 1).

Above all, these studies reflect the complexity of chemokine/GPCR-mediated EMT-associated metastatic dissemination of cancer cells, in which cancer cells, non-cancer cells, cytokines, and the ECM should be considered. Further studies are required to clarify how these factors work together to promote metastasis. Only a few studies demonstrated morphological changes among cells under microscopes, perhaps because the p-EMT programme rather than the c-EMT programme is more common in cancer.

4. Signaling Pathways Inducing EMT by Chemokines

EMT can be induced by several intracellular signaling pathways in neoplastic epithelial cells when they receive chemokine/GPCR signaling from the tumor microenvironment. Regarding to the signaling pathways that are triggered by chemokines, we need to refer to literature about GPCRs to deduce them. To date, as new biological techniques and research pop out, the modes of GPCR become a more complex picture [114]. Wang et al. proposed new insights into modes of GPCR activation, including biased, intracellular, dimerization, transactivation, and biphasic activation. These patterns are applicable in explaining the biological effects of chemokines [114]. Herein, we refer to these modes; categorize the signaling of chemokine receptors into G protein, β-arrestin, intracellular, dimerization transactivation, and MAPK signaling; and summarize each function in mediating EMT (Figure 2).

4.1. G-Protein Signaling. Most chemokine receptors have been identified to be Gαi-dependent, since the first chemokine CXCL8 was found to mediate signaling via Gαi subunit [115, 116]. Gαi protein, a direct inhibitor of ACs, which subsequently suppresses cAMP and alters PKA and EPAC activation, has been shown to possess the ability to mediate the neoplastic transformation of normal cells when constitutively activated. In contrast, the Gαs protein, a direct stimulator of ACs, has a tumor-suppressive role [117]. For example, conditional deletion of Gαs results in the formation of basal-cell carcinoma by releasing PKA-mediated inhibition of sonic hedgehog (SHH) and YAP signaling pathways [118]. Moreover, Pattabiraman et al. uncovered a role of PKA in mesenchymal-to-epithelial transition and loss of tumor-initiating ability [119]. Notably, they used immortalized human mammary epithelial cells to model tumor-initiating cells in basal-like breast cancers rather than cancer cells [119]. This might explain why the in vitro model exhibited distinct c-EMT. These studies imply that Gαi protein, which has an opposite effect to the Gαs protein might be critical in maintaining the balance of epithelial and mesenchymal states. So far, few studies have directly elucidated the correlation between Gαi protein and the EMT programme.

G$\beta\gamma$ subunits, once thought to be only negative regulators of Gα-dependent signaling, are now recognized to be more critical in GPCR signaling (reviewed in [120]), as well as chemokine receptors, because of their indispensability in chemotaxis [121]. In the early event, G$\beta\gamma$ dimmers are required by many downstream effectors. Phospholipase Cβ (PLCβ) is an effector directly activated by G$\beta\gamma$ subunits. PLCβ activation leads to the production of inositol-1,4,5-trisphosphate (Ins (1,4,5) P3) and diacylglycerol (DAG), which regulate the release of intracellular calcium (Ca2+) and activation of protein kinase C (PKC). The role of calcium flux in EMT was firstly described by Davis et al. EGF-mediated EMT was calcium-signal-dependent, partially owing to the effect of TRPM7 [122]. Reminiscent of the effect of Gαq-coupled GPCRs, which can directly stimulate PLCβ and induce calcium flux, Norgard et al. provided concrete evidence that Gαq-coupled GPCRs mobilize calcium through Ca^{2+}-calmodulin-Camk2b axis to assist cells in achieving a p-EMT state [123]. Interestingly, E-cadherin expression was not found to be downregulated in this study. Instead, it was translocated from the cell membrane to the cytoplasm [123]. However, the role of calcium signaling by G$\beta\gamma$ subunits in mediating EMT remains to be explored. PI3Kγ, a critical regulator of survival signaling, is also a direct effector of G$\beta\gamma$ subunits [120]. Several studies have reported the participation of PI3K downstream chemokine receptors in mediating EMT. The CXCL12/CXCR4 axis mediates EMT via activation of PI3K-Akt/PKB in human sacral chondrosarcoma, breast cancer, and oral carcinoma cells [32, 50, 52]. Commonly, the PI3K-Akt signaling pathway works together with the MEK-MAPK pathway to induce EMT, and inhibition of either can only partially reverse the transition. In the context of CCR7, its ligand CCL19 was reported to upregulate Snail through MAPK and PI3K in gastric cancer, whereas CCL21 was reported to upregulate Slug through the same pathway in human chondrosarcoma [72, 78]. These studies highlighted G$\beta\gamma$ subunits regulating MAPK and PI3K mediated EMT by chemokine receptor stimulation, and we will further discuss the role of MAPK signaling in the EMT programme in the latter part of this review.

4.2. β-Arrestin Signaling. Current studies on GPCRs indicate that β-arrestins not only can induce GPCRs internalization and desensitization but also can activate a novel pathway that is distinct from pathways induced by G proteins [124]. From the traditional point of view, most chemokine receptors hold the characteristic of inducing short and transient signals. They tend to rapidly terminate their signals and refresh themselves with the help of regulators of G-protein signaling (RGS) proteins, G-protein-coupled receptor serine/threonine kinases (GRKs), and β-arrestins [125, 126]. When chemokine receptors are internalized, they either become ubiquitinated or simply recycled to the membrane for resensitization. This hallmark of chemokine receptors has biological significance in sensing direction and chemotaxis [127, 128]. The internalization and desensitization processes are mainly regulated by GRKs and β-arrestins. Chemokine receptors phosphorylated by GRKs at multiple sites on the cytoplasmic COOH-terminus [126, 129] promote their binding affinity to β-arrestins. To date, β-arrestins have been found to serve as scaffold proteins that recruit several signaling molecules and emit signals parallel to G-protein-dependent signals [130]. For example, β-arrestins potently activate the MAPK kinase pathway by forming a CXCR4-β-arrestin complex that interacts with Raf [131]. Moreover, β-arrestin signaling may switch the coupling of GPCRs from canonical Gα proteins to other Gα proteins. For example, PKA-phosphorylatedβ2-adrenergic receptor switches Gαs to Gαi [132]. This switch of coupling G proteins can be well explained by recent research conducted by Smith et al. [133]. They discovered Gαi:β-arrestin signaling complexes that formed downstream not only Gαi-coupled GPCRs but also Gαs- or Gαq-coupled GPCRs at the plasma membrane. Moreover, the complexes are capable of forming scaffolds with ERK and promoting PTX-sensitive cell migration, which can also explain why Gαi activation is necessary but probably not sufficient for chemotaxis [121, 134]. However, whether β-arrestin contributes to GPCR signaling remains controversial. O'Hayre et al. provided evidence that the loss of β-arrestins enhanced the potency and efficacy of isoproterenol- and epinephrine-induced ERK phosphorylation, suggesting that β-arrestins are not required for MAPK activation [135]. Notably, silencing β-arrestin-1 can reverse the EMT process initiated by the endothelin A receptor of ovarian cancer cells, while elevated β-arrestin-1 expression can promote EMT in prostate cancer cells via the Wnt/β-catenin pathway [136, 137]. β-Arrestin-1 has also been reported necessary in nicotine-induced EMT and protease-activated receptor 2 (PAR2) induced migration in lung cancer cells, with the involvement of Src kinase activity and MAPK signaling [138–140]. However, it still remains unclear whether or how β-arrestin downstream chemokine receptors play a role in the EMT programme. Since, even MAPK signaling, which is associated with various pathways, has been widely reported to be involved in EMT regulation. Further studies are required to identify novel mechanisms of dissection and phenotypic conformations.

4.3. Intracellular Signaling. Accumulated evidence indicates that some GPCRs can be activated not only on the cell surface but also inside the cell and trigger specific signals, suggesting that GPCR activation may be a result of intracellular events [114]. This phenomenon can be explained in two ways. GPCRs located in the cytoplasm can be activated intracellularly. And GPCRs located at the cell surface provide sustained signals after internalization. Chemokine receptors are primarily localized and activated at the cell surface. More importantly, they belong to the class A GPCRs, a group of GPCRs that form unstable endocytic complexes with β-arrestins. Chemokine receptors and β-arrestins disassociate rapidly after internalization and recycle back to the cell surface with MAPK activated in this transient process [141]. Together with G-protein signaling, we can conclude that signals induced by chemokine receptors from activation to resensitization are rapid and transient. Typically, the induction of EMT requires long-term cultivation (for days or weeks) and sustained signaling. This may explain why tyrosine kinase receptors are more

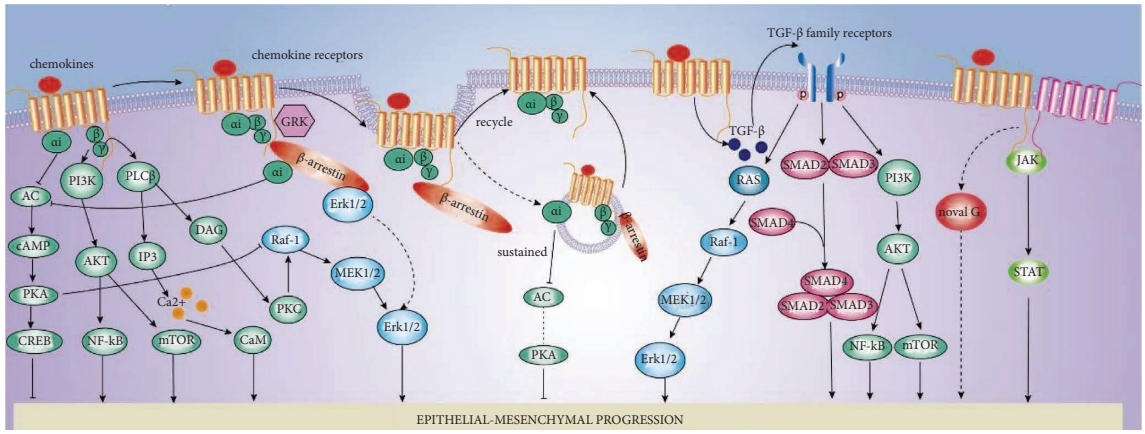

Figure 2: Signaling pathways to EMT initiated by chemokine receptors. Binding chemokines with their cognate receptors triggers G-protein signaling and JAK/STAT signaling at the very beginning if receptors are dimerized. Subsequently, β-arrestins bind to chemokine receptors, resulting in Gαi-β-arrestin complexes and stimulation of Gαi and Erk signaling. Most chemokine receptors lose their connection with β-arrestins after they are dragged into the cytoplasm and simply recycle back to the plasma membrane. During transactivation, chemokine receptors may stimulate receptor tyrosine kinases by elevating the expression of their ligands in the cytoplasm, such as TGF-β, EGF, and IGF.

popular at inducing EMT, since tyrosine kinase receptors seldom internalize and desensitize, thus providing stable signals to cells. Recent findings suggest that some GPCRs can (mostly class B GPCRs) mediate sustained Gα signaling after internalization, such as vasopressin type 2 receptor (V2R) [142], parathyroid hormone receptor type 1 (PTHR) [143], TSH receptors (TSHRs) [144], and Sphingosine-1-phosphate (S1P) receptors [145]. One explanation for this sustained Gα signaling is the recent discovery of an internalized GPCR-G protein:β-arrestin megaplex [146]. This megaplex architecture allows GPCRs to promote GDP-GTP exchange and Gα activation, resulting in prolonged G protein signaling [146]. Few studies have reported sustained G protein signaling in chemokine receptors. Here, we use S1P receptors, a group of GPCRs that resemble chemokine receptors, as a reference. They belong to class A GPCRs, coupled to Gαi protein, and regulate essential processes, such as adaptive immune cell trafficking, vascular development, and homeostasis [147]. However, as members of class A GPCRs, they demonstrate persistent signaling after the activation of FTY720P, a "functional antagonist," by promoting the efficient internalization of S1P1 receptors. In conclusion, certain ligands of chemokine receptors might trigger long-lasting Gαi signaling and bring massive influence on epithelial versus mesenchymal balance in cancer cells.

4.4. Dimerization Signaling. GPCRs were originally considered monomers. To date, much evidence has shown that these receptors exist as homodimers or heterodimers [148]. Surprisingly, these dimers can activate tyrosine kinase signaling pathways [149]. Using a sensitive bioluminescence resonance energy transfer system (BRET), Percherancier et al. found that CXCR4 exists as constitutive homo- and heterodimers [150]. Chemokine receptors can form dimers with different receptors. For example, CXCR4 forms heterodimers with CXCR7 [151], CCR5 [152], CD4 [153], CCR2 [154], and even δ-opioid receptor [155]. Heterodimers may conduct a β-arrestin switching or G protein switching. For instance, CXCR4-CXCR7 heterodimers block Gαi activation and induce β-arrestin signaling pathway [156], and costimulation of CCR2-CCR5 with their cognate ligands leads to novel Gαq/11 signaling, instead of the classical Gαi signaling [157]. Changes in the balance of homo- and heterodimers, as well as the formation of novel heterodimers, could have significant effects on signaling [124], and whether there is a typical heterodimer in cancer that exclusively manages the EMT programme requires further discussion.

4.5. Transactivation Signaling. Transactivation means several GPCR agonists induce rapid tyrosine phosphorylation and activation of receptor tyrosine kinases. Currently, two mechanisms of RTKs and GPCRs interaction have been identified as "ligand-dependent" and "ligand-independent" mechanisms. A typical example of ligand-dependent mechanisms is GPCRs that activate EGFR. GPCRs first activate the Src kinase. Activated Src then elevates the expression of matrix metalloproteinases (MMPs), which shed and cleave HB-EGF, a classical endogenous ligand for EGFR, from the membrane and subsequently captured by EGFR [114]. In the context of chemokine receptors, the CXCL12-CXCR4 axis mediates TGF-β formation and activates TGF-β signaling, which in turn mediates CXCL12 formation through the pSmad2/3 pathway. Together, CXCL12 and TGF-β form autocrine signaling loops in myofibroblasts of invasive human breast cancers [158]. In a ligand-independent mechanism, GPCRs can transactivate EGFR by forming GPCR-EGFR heterodimers or complexes (reviewed in [114]). Similarly, CXCR4 transactivated by insulin-like growth factor receptor (IGF-1R) and S1P1 receptor by platelet-derived growth factor (PDGF) are both activated by forming GPCR-RTK complexes [159, 160]. As mentioned above, RTKs can be important regulators of the EMT programme. For example, TGF-β can induce EMT

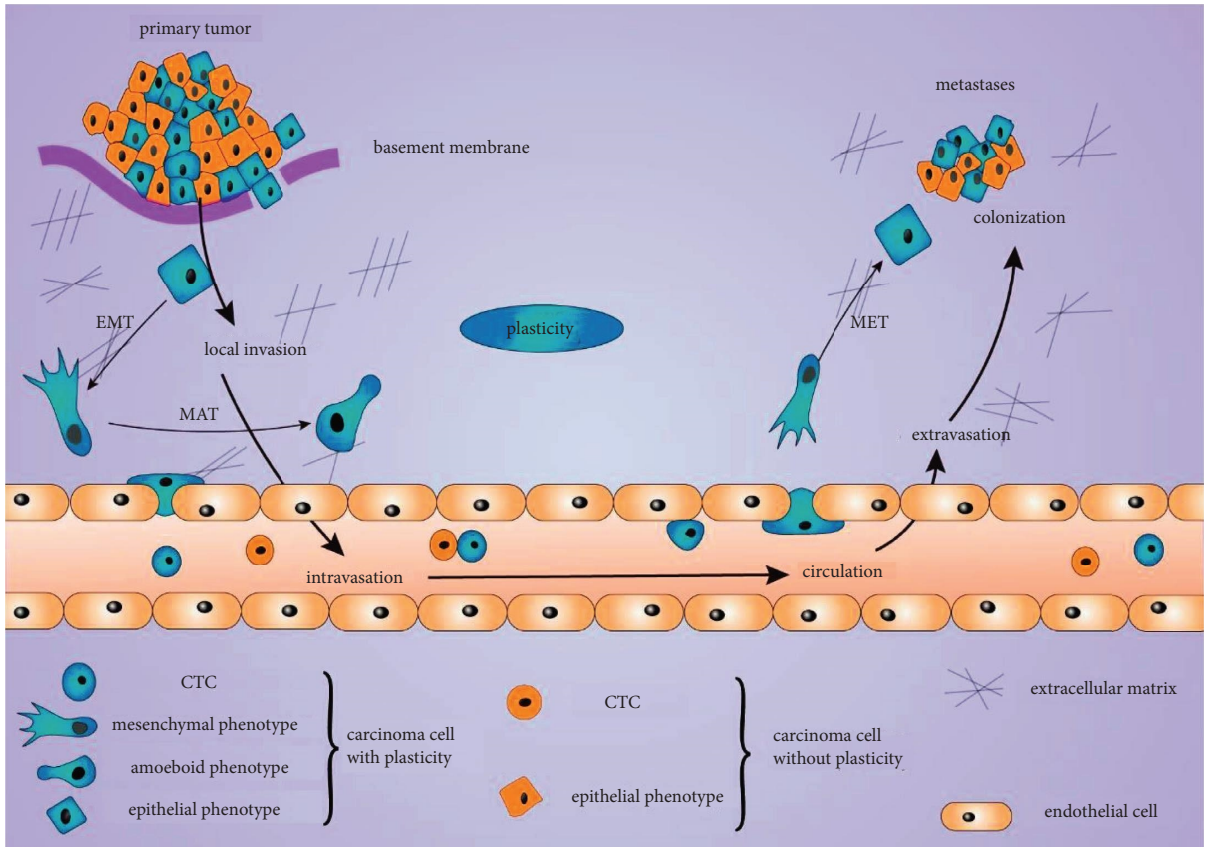

Figure 3: Depiction of epithelial-mesenchymal plasticity in metastasis. Carcinoma cells with plasticity or without plasticity were primarily outlined by a basement membrane. Carcinoma cells with plasticity undergo EMT or MAT, resulting in local invasion, intravasation, circulation, extravasation, and colonization. In this process, carcinoma cells with plasticity decide which morphology (mesenchymal or amoeboid) to transform in response to their circumstances. As carcinoma cells colonize, EMT cells may transform back to epithelial phenotype by MET to proliferate. Abbreviations: EMT, epithelial-mesenchymal transition; MAT, mesenchymal-amoeboid transition; and MET, mesenchymal-epithelial transition.

through the RAS-RAF-MEK-MAPK pathway or SMAD2-SMAD4-SMAD3 complexes [10]. Thus, the induction of EMT may be a joint effort by both chemokine receptors and RTKs.

4.6. MAPK Signaling. MAPK is phosphorylated by multiple signaling induced by chemokines. In the context of G protein signaling, the Gαi subunits activate MAPK through the cAMP-PKA-cRaf pathway and Rap1-cRaf pathway. $\beta\gamma$ subunits activate MAPK through PLCβ/PI3K-Src-Shc-Sos pathway (reviewed in [161]). In the case of the β-arrestin pathway, β-arrestin not only functions as scaffolds to enhance cRaf-1 and MEK-dependent activation of MAPK [131, 162] but also forms Gαi:β-arrestin complexes to activate MAPK [133]. However, β-arrestin-mediated Erk MAPK activation and MAPK regulation EMT are all required further mechanistic and phenotypic studies. Studies have found biphasic activation of GPCRs. AT1R-mediated MAPK phosphorylation has two peaks. The first peak is transient and appears at 2 min after activation, while the last peak is sustained and appears at 120–150 min. The appearance of the first peak might be a result of Gα:β-arrestin signaling complexes, while the last might be stimulated by G$\beta\gamma$ subunits or from intracellular signaling. The inhibitors of MAPK might inhibit all the sources of MAPK phosphorylation, which lead us to miss the effect of β-arrestins.

Above all, multiple chemokine/GPCR signaling pathways have been proven correlated with EMT. Among them, the MAPK and PI3K signaling from G$\beta\gamma$ subunits, JAK/STAT signaling form dimerization signaling, and crosstalk between chemokine receptor and Wnt signaling are well focused. And their inhibitors have been proven to reverse or inhibit the EMT process. However, signaling the effect of Gαi and β-arrestin has long been ignored. Indeed, we believe EMT is a result of complicated signaling networks. Further study should complete these networks and distinguish them from each other if possible.

5. Conclusion and Perspective

The chemokine family is one of the pivotal regulators of EMT in the tumor microenvironment with an array of signaling pathways that can activate the EMT programme. However, the limited pathway has been proven to be dominating in the EMT programme and available in all types

of cancer cells. Inspired by calcium-mediated p-EMT [123], we can deduce that different signals emitted by chemokine receptors may activate different EMT programmes. Our knowledge of chemokine-triggered signaling and the EMT programme has advanced, but still little is known about how different chemokines and signaling pathways work in combination to drive EMT in different tumors. Chemokines play a pivotal role in metastatic dissemination due to their functions in directing cell migration, facilitating trans-endothelial migration, mediating cell adhesion, and recruiting stromal and immune cells. Uncovering how cancer cells "hijack" chemokine receptors to mediate cell migration highways will be an exciting and promising direction.

EMT and EMT-TFs are associated with metastasis. However, whether the EMT programme is critically involved in metastasis or merely casual requires concrete experimental evidence. EMT-TFs have a common function in the activation of the EMT programme with each having non-redundant functions [163]. Therefore, the appearance of the EMT phenotype in cancer indicates the activation of certain EMT-TFs. For example, Snail2 was detected in p-EMT malignant cells at the leading edge of cancer [12]. To date, EMT-TFs have been proven to play a critical role in metastasis with a tissue-specific property and spatiotemporal expression patterns [3, 164]. However, the EMT programme has long been associated with the metastasis process, and EMT-TFs functions should not be simply extrapolated as functions of the EMT programme.

EMT programmes have been shown strongly associated with the processes of primary tumor invasion and dissemination, which are considered the first step in the metastatic cascade. Without dissemination, metastases do not develop, but highly invasive cancer cells also need epithelial characteristics to settle and resume tumor growth at metastatic sites. Thus, EMT programmes might not always positively contribute to the whole process of complex cancer metastasis. For example, EMT programme-targeted therapy may activate the MET programme, which encourages colonization of cancer cells [164]. In addition, the transiency of EMT-TFs and effectors, abundance of EMT receptors, and redundant function of EMT pathways make EMT difficult to target experimentally and clinically.

Notably, only a few cancer cells could undergo complex processes of metastasis, including local invasion, dissemination, intravasation, transportation through circulation, extravasation, and final colonization. Interestingly, those cells must go through not only the EMT process during dissemination at the very beginning of metastasis but also the MET process at final colonization [3], suggesting that cancer cells could not be in a certain consistent statements to achieve final metastasis. The key abilities include switching statements from one to another, such as EMT or MET, which as known as "plasticity," one of the hallmark features of cancer cells [165]. Therefore, plasticity might be a more constant property of metastatic cancer cells, and targeting plasticity might be a suitable strategy for cancer metastasis therapy (Figure 3).

Conflicts of Interest

The authors declare that there are no conflicts of interest.

Acknowledgments

The authors thank the National Natural Science Foundations of China (82170971 and 82002888), Fundamental Research Funds for the Central Universities (YJ201987), Sichuan Science and Technology Program (2021ZYD0090 and 2022YFS0207), Scientific Research Foundation, West China Hospital of Stomatology Sichuan University (QDJF2019-3 and RD-03-202110), and CAMS Innovation Fund for Medical Sciences (CIFMS and 2019-I2M-5-004).

References

[1] A. Zlotnik, O. Yoshie, and H. Nomiyama, "The chemokine and chemokine receptor superfamilies and their molecular evolution," *Genome Biology*, vol. 7, no. 12, p. 243, 2006.

[2] J. Yang, P. Antin, G. Berx et al., "Guidelines and definitions for research on epithelial–mesenchymal transition," *Nature Reviews Molecular Cell Biology*, vol. 21, no. 6, pp. 341–352, 2020.

[3] T. Brabletz, R. Kalluri, M. A. Nieto, and R. A. Weinberg, "Epithelial to mesenchymal transition in cancer," *Nature Reviews Cancer*, vol. 18, no. 2, pp. 128–134, 2018.

[4] K. Ganesh and J. MASSAGUé, "Targeting metastatic cancer," *Nat Med*, vol. 27, no. 1, pp. 34–44, 2021.

[5] G. Follain, D. Herrmann, S. Harlepp et al., "Fluids and their mechanics in tumour transit: shaping metastasis," *Nature Reviews Cancer*, vol. 20, no. 2, pp. 107–124, 2020.

[6] N. Reymond, B. B. D'Água, and A. J. Ridley, "Crossing the endothelial barrier during metastasis," *Nature Reviews Cancer*, vol. 13, no. 12, pp. 858–870, 2013.

[7] D. F. Quail and J. A. Joyce, "Microenvironmental regulation of tumor progression and metastasis," *Nat Med*, vol. 19, no. 11, pp. 1423–1437, 2013.

[8] V. Graziani, I. Rodriguez-Hernandez, O. Maiques, and V. Sanz-Moreno, "The amoeboid state as part of the epithelial-to-mesenchymal transition programme," *Trends in Cell Biology*, vol. 32, no. 3, pp. 228–242, 2022.

[9] B. Bakir, A. M. Chiarella, J. R. Pitarresi, and A. K. Rustgi, "EMT, MET, plasticity, and tumor metastasis," *Trends in Cell Biology*, vol. 30, no. 10, pp. 764–776, 2020.

[10] A. Dongre and R. A. Weinberg, "New insights into the mechanisms of epithelial–mesenchymal transition and implications for cancer," *Nature Reviews Molecular Cell Biology*, vol. 20, no. 2, pp. 69–84, 2019.

[11] V. Mittal, "Epithelial mesenchymal transition in tumor metastasis," *Annual Review of Pathology: Mechanisms of Disease*, vol. 13, no. 1, pp. 395–412, 2018.

[12] S. V. Puram, I. Tirosh, A. S. Parikh et al., "Single-cell transcriptomic analysis of primary and metastatic tumor ecosystems in head and neck cancer," *Cell*, vol. 171, no. 7, pp. 1611–1624.e24, 2017.

[13] M. Yilmaz and G. Christofori, "EMT, the cytoskeleton, and cancer cell invasion," *Cancer Metastasis Rev*, vol. 28, no. 1-2, pp. 15–33, 2009.

[14] M. A. Eckert, T. M. Lwin, A. T. Chang et al., "Twist1-Induced invadopodia formation promotes tumor metastasis," *Cancer Cell*, vol. 19, no. 3, pp. 372–386, 2011.

[15] J. Yang, S. A. Mani, J. L. Donaher et al., "Twist, a master regulator of morphogenesis, plays an essential role in tumor metastasis," *Cell*, vol. 117, no. 7, pp. 927–939, 2004.

[16] M. Yu, A. Bardia, B. S. Wittner et al., "Circulating breast tumor cells exhibit dynamic changes in epithelial and mesenchymal composition," *Science*, vol. 339, no. 6119, pp. 580–584, 2013.

[17] M. Labelle, S. Begum, and R. O. Hynes, "Direct signaling between platelets and cancer cells induces an epithelial-mesenchymal-like transition and promotes metastasis," *Cancer Cell*, vol. 20, no. 5, pp. 576–590, 2011.

[18] J. Qi, N. Chen, J. Wang, and C. H. Siu, "Transendothelial migration of melanoma cells involves N-Cadherin-mediated adhesion and activation of the β-catenin signaling pathway," *Molecular Biology of the Cell*, vol. 16, no. 9, pp. 4386–4397, 2005.

[19] Y. Wan, H. Liu, M. Zhang et al., "Prognostic value of epithelial mesenchymal transition inducing transcription factors in head and neck squamous cell carcinoma: a meta analysis," *Head & Neck*, vol. 42, no. 5, pp. 1067–1076, 2020.

[20] H. Tada, H. Takahashi, S. Ida, Y. Nagata, and K. Chikamatsu, "Epithelial–mesenchymal transition status of circulating tumor cells is associated with tumor relapse in head and neck squamous cell carcinoma," *Anticancer Research*, vol. 40, no. 6, pp. 3559–3564, 2020.

[21] A. Obradovic, D. Graves, M. Korrer et al., "Immunostimulatory cancer-associated fibroblast Subpopulations can Predict Immunotherapy response in head and neck cancer," *Clinical Cancer Research*, vol. 28, no. 10, pp. 2094–2109, 2022.

[22] B. Zhang, L. Shi, S. Lu et al., "Autocrine IL-8 promotes F-actin polymerization and mediate mesenchymal transition via ELMO1-NF-κB-Snail signaling in glioma," *Cancer Biology & Therapy*, vol. 16, no. 6, pp. 898–911, 2015.

[23] Y. Lu, B. Dong, F. Xu et al., "CXCL1-LCN2 paracrine axis promotes progression of prostate cancer via the Src activation and epithelial-mesenchymal transition," *Cell Communication and Signaling*, vol. 17, no. 1, p. 118, 2019.

[24] J. Wen, Z. Zhao, L. Huang, L. Wang, Y. Miao, and J. Wu, "IL 8 promotes cell migration through regulating EMT by activating the Wnt/β catenin pathway in ovarian cancer," *Journal of Cellular and Molecular Medicine*, vol. 24, no. 2, pp. 1588–1598, 2020.

[25] M. C. Chen, R. Baskaran, N. H. Lee et al., "CXCL2/CXCR2 axis induces cancer stem cell characteristics in CPT 11 resistant LoVo colon cancer cells via Gαi 2 and Gαq/11," *Journal of Cellular Physiology*, vol. 234, no. 7, Article ID 11822, 2019.

[26] H. Xu, F. Lin, Z. Wang et al., "CXCR2 promotes breast cancer metastasis and chemoresistance via suppression of AKT1 and activation of COX2," *Cancer Letters*, vol. 412, pp. 69–80, 2018.

[27] J. Zhao, B. Ou, D. Han et al., "Tumor-derived CXCL5 promotes human colorectal cancer metastasis through activation of the ERK/Elk-1/Snail and AKT/GSK3β/β-catenin pathways," *Molecular Cancer*, vol. 16, no. 1, p. 70, 2017.

[28] D. Cui, Y. Zhao, and J. Xu, "Activated CXCL5-CXCR2 axis promotes the migration, invasion and EMT of papillary thyroid carcinoma cells via modulation of β-catenin pathway," *Biochimie*, vol. 148, pp. 1–11, 2018.

[29] W. Z. Qiu, H. B. Zhang, W. X. Xia et al., "The CXCL5/CXCR2 axis contributes to the epithelial-mesenchymal transition of nasopharyngeal carcinoma cells by activating ERK/GSK-3β/snail signalling," *Journal of Experimental & Clinical Cancer Research*, vol. 37, no. 1, p. 85, 2018.

[30] S. L. Zhou, Z. J. Zhou, Z. Q. Hu et al., "CXCR2/CXCL5 axis contributes to epithelial–mesenchymal transition of HCC cells through activating PI3K/Akt/GSK-3β/Snail signaling," *Cancer Letters*, vol. 358, no. 2, pp. 124–135, 2015.

[31] Z. Xiang, Z. J. Zhou, G. K. Xia et al., "A positive crosstalk between CXCR4 and CXCR2 promotes gastric cancer metastasis," *Oncogene*, vol. 36, no. 36, pp. 5122–5133, 2017.

[32] T. Sobolik, Y. J. Su, S. Wells, G. D. Ayers, R. S. Cook, and A. Richmond, "CXCR4 drives the metastatic phenotype in breast cancer through induction of CXCR2 and activation of MEK and PI3K pathways," *Molecular Biology of the Cell*, vol. 25, no. 5, pp. 566–582, 2014.

[33] G. Nie, X. Cao, Y. Mao, Z. Lv, M. Lv, and Y Wang, H. Wang and C. Liu, "Tumor-associated macrophages-mediated CXCL8 infiltration enhances breast cancer metastasis: suppression by Danirixin," *Int Immunopharmacol*, vol. 95, Article ID 107153, 2021.

[34] T. Shen, Z. Yang, X. Cheng et al., "CXCL8 induces epithelial-mesenchymal transition in colon cancer cells via the PI3K/Akt/NF-κB signaling pathway," *Oncology Reports*, vol. 37, no. 4, pp. 2095–2100, 2017.

[35] C. Visciano, F. Liotti, N. Prevete et al., "Mast cells induce epithelial-to-mesenchymal transition and stem cell features in human thyroid cancer cells through an IL-8–Akt–Slug pathway," *Oncogene*, vol. 34, no. 40, pp. 5175–5186, 2015.

[36] F. Deng, Y. Weng, X. Li, T. Wang, M. Fan, and Q. Shi, "Overexpression of IL-8 promotes cell migration via PI3K-Akt signaling pathway and EMT in triple-negative breast cancer," *Pathology, Research & Practice*, vol. 223, Article ID 152824, 2021.

[37] Z. Li, J. Liu, L. Li et al., "Epithelial mesenchymal transition induced by the CXCL9/CXCR3 axis through AKT activation promotes invasion and metastasis in tongue squamous cell carcinoma," *Oncology Reports*, vol. 39, no. 3, pp. 1356–1368, 2018.

[38] Z. Wang, X. Ao, Z. Shen et al., "TNF-α augments CXCL10/CXCR3 axis activity to induce Epithelial-Mesenchymal Transition in colon cancer cell," *International Journal of Biological Sciences*, vol. 17, no. 11, pp. 2683–2702, 2021.

[39] X. Yu, D. Wang, X. Wang et al., "CXCL12/CXCR4 promotes inflammation-driven colorectal cancer progression through activation of RhoA signaling by sponging miR-133a-3p," *Journal of Experimental & Clinical Cancer Research*, vol. 38, no. 1, p. 32, 2019.

[40] T. H. Hu, Y. Yao, S. Yu et al., "SDF-1/CXCR4 promotes epithelial–mesenchymal transition and progression of colorectal cancer by activation of the Wnt/β-catenin signaling pathway," *Cancer Letters*, vol. 354, no. 2, pp. 417–426, 2014.

[41] Y. Lin, Q. Ma, L. Li, and H. Wang, "The CXCL12–CXCR4 axis promotes migration, invasiveness, and EMT in human papillary thyroid carcinoma B-CPAP cells via NF-κB signaling," *Biochemistry and Cell Biology*, vol. 96, no. 5, pp. 619–626, 2018.

[42] Y. Cheng, Y. Song, J. Qu et al., "The chemokine receptor CXCR4 and c-MET cooperatively promote epithelial-mesenchymal transition in gastric cancer cells," *Translational Oncology*, vol. 11, no. 2, pp. 487–497, 2018.

[43] Y. Qin, F. Wang, H. Ni et al., "Cancer-associated fibroblasts in gastric cancer affect malignant progression via the CXCL12-CXCR4 axis," *Journal of Cancer*, vol. 12, no. 10, pp. 3011–3023, 2021.

[44] X. Li, P. Li, Y. Chang et al., "The SDF-1/CXCR4 axis induces epithelial–mesenchymal transition in hepatocellular carcinoma," *Molecular and Cellular Biochemistry*, vol. 392, no. 1-2, pp. 77–84, 2014.

[45] F. Zhang, J. Y. Cui, H. F. Gao et al., "Cancer-associated fibroblasts induce epithelial-mesenchymal transition and cisplatin resistance in ovarian cancer via CXCL12/CXCR4 axis," *Future Oncology*, vol. 16, no. 32, pp. 2619–2633, 2020.

[46] N. F. Saba, Y. Wang, H. Fu et al., "Association of cytoplasmic CXCR4 with loss of epithelial marker and activation of ERK1/2 and AKT signaling pathways in non–small-cell Lung Cancer," *Clinical Lung Cancer*, vol. 18, no. 3, pp. e203–e210, 2017.

[47] X. Li, Q. Ma, Q. Xu et al., "SDF-1/CXCR4 signaling induces pancreatic cancer cell invasion and epithelial–mesenchymal transition in vitro through non-canonical activation of Hedgehog pathway," *Cancer Letters*, vol. 322, no. 2, pp. 169–176, 2012.

[48] Y. Wang, W. Lan, M. Xu et al., "Cancer-associatedfibroblast-derived SDF-1 induces epithelial-mesenchymal transition of lung adenocarcinoma via CXCR4/β-catenin/PPARδ signalling," *Cell Death & Disease*, vol. 12, no. 2, p. 214, 2021.

[49] Y. Duan, S. Zhang, L. Wang et al., "Targeted silencing of CXCR4 inhibits epithelial-mesenchymal transition in oral squamous cell carcinoma," *Oncology Letters*, vol. 12, no. 3, pp. 2055–2061, 2016.

[50] T. Onoue, D. Uchida, N. M. Begum, Y. Tomizuka, H. Yoshida, and M. Sato, "Epithelial-mesenchymal transition induced by the stromal cell-derived factor-1/CXCR4 system in oral squamous cell carcinoma cells," *International Journal of Oncology*, vol. 29, no. 5, pp. 1133–1138, 2006.

[51] M. Taki, K. Higashikawa, S. Yoneda et al., "Up-regulation of stromal cell-derivedfactor-1alpha and its receptor CXCR4 expression accompanied with epithelial-mesenchymal transition in human oral squamous cell carcinoma," *Oncology Reports*, vol. 19, no. 4, pp. 993–998, 2008.

[52] P. Yang, G. Wang, H. Huo, Q. Li, Y. Zhao, and Y. Liu, "SDF-1/CXCR4 signaling up-regulates survivin to regulate human sacral chondrosarcoma cell cycle and epithelial–mesenchymal transition via ERK and PI3K/AKT pathway," *Medical Oncology*, vol. 32, no. 1, p. 377, 2015.

[53] S. Biswas, S. Sengupta, S. Roy Chowdhury et al., "CXCL13–CXCR5 co-expression regulates epithelial to mesenchymal transition of breast cancer cells during lymph node metastasis," *Breast Cancer Research and Treatment*, vol. 143, no. 2, pp. 265–276, 2014.

[54] Y. Xie, Z. Chen, Q. Zhong et al., "M2 macrophages secrete CXCL13 to promote renal cell carcinoma migration, invasion, and EMT," *Cancer Cell International*, vol. 21, no. 1, p. 677, 2021.

[55] J. Han, R. Fu, C. Chen et al., "CXCL16 promotes gastric cancer tumorigenesis via ADAM10-dependent CXCL16/CXCR6 Axis and activates akt and MAPK signaling pathways," *International Journal of Biological Sciences*, vol. 17, no. 11, pp. 2841–2852, 2021.

[56] J. J. Jin, F. X. Dai, Z. W. Long et al., "CXCR6 predicts poor prognosis in gastric cancer and promotes tumor metastasis through epithelial-mesenchymal transition," *Oncology Reports*, vol. 37, no. 6, pp. 3279–3286, 2017.

[57] H. Zhuang, G. Cao, C. Kou, and T. Liu, "CCL2/CCR2 axis induces hepatocellular carcinoma invasion and epithelial-mesenchymal transition in vitro through activation of the Hedgehog pathway," *Oncology Reports*, vol. 39, no. 1, pp. 21–30, 2018.

[58] H. Li, H. Li, X. P. Li et al., "C C chemokine receptor type 2 promotes epithelial to mesenchymal transition by upregulating matrix metalloproteinase 2 in human liver cancer," *Oncology Reports*, vol. 40, no. 5, pp. 2734–2741, 2018.

[59] J. Yan, Y. Gao, S. Lin, Y. Li, L. Shi, and Q. Kan, "EGR1-CCL2 Feedback Loop Maintains Epithelial-Mesenchymal Transition of Cisplatin-Resistant Gastric Cancer Cells and Promotes Tumor Angiogenesis," *Dig Dis Sci*, vol. 67, no. 8, pp. 3702–3713, 2021.

[60] S. Li, J. Lu, Y. Chen et al., "MCP-1-induced ERK/GSK-3β/Snail signaling facilitates the epithelial–mesenchymal transition and promotes the migration of MCF-7 human breast carcinoma cells," *Cellular and Molecular Immunology*, vol. 14, no. 7, pp. 621–630, 2017.

[61] K. Izumi, L. Y. Fang, A. Mizokami et al., "Targeting the androgen receptor with siRNA promotes prostate cancer metastasis through enhanced macrophage recruitment via CCL2/CCR2-induced STAT3 activation," *EMBO Molecular Medicine*, vol. 5, no. 9, pp. 1383–1401, 2013.

[62] Z. Ling, X. Yang, X. Chen, J. Xia, B. Cheng, and X. Tao, "CCL2 promotes cell migration by inducing epithelial-mesenchymal transition in oral squamous cell carcinoma," *Journal of Oral Pathology & Medicine*, vol. 48, no. 6, pp. 477–482, 2019.

[63] X. Cheng, H. Wu, Z. J. Jin et al., "Up-regulation of chemokine receptor CCR4 is associated with Human Hepatocellular Carcinoma malignant behavior," *Scientific Reports*, vol. 7, no. 1, Article ID 12362, 2017.

[64] F. Zhu, X. Li, S. Chen, Q. Zeng, Y. Zhao, and F. Luo, "Tumor-associated macrophage or chemokine ligand CCL17 positively regulates the tumorigenesis of hepatocellular carcinoma," *Medical Oncology*, vol. 33, no. 2, p. 17, 2016.

[65] J. Liu, C. Wang, X. Ma et al., "High expression of CCR5 in melanoma enhances epithelial-mesenchymal transition and metastasis via TGFβ1," *The Journal of Pathology*, vol. 247, no. 4, pp. 481–493, 2019.

[66] F. Meng, W. Li, C. Li, Z. Gao, K. Guo, and S. Song, "CCL18 promotes epithelial-mesenchymal transition, invasion and migration of pancreatic cancer cells in pancreatic ductal adenocarcinoma," *International Journal of Oncology*, vol. 46, no. 3, pp. 1109–1120, 2015.

[67] N. Kapur, H. Mir, C. E. Clark III et al., "CCR6 expression in colon cancer is associated with advanced disease and supports epithelial-to-mesenchymal transition," *British Journal of Cancer*, vol. 114, no. 12, pp. 1343–1351, 2016.

[68] G. Han, D. Wu, Y. Yang, Z. Li, J. Zhang, and C. Li, "CrkL meditates CCL20/CCR6-induced EMT in gastric cancer," *Cytokine*, vol. 76, no. 2, pp. 163–169, 2015.

[69] S. Marsigliante, C. Vetrugno, and A. Muscella, "Paracrine CCL20 loop induces epithelial-mesenchymal transition in breast epithelial cells," *Molecular Carcinogenesis*, vol. 55, no. 7, pp. 1175–1186, 2016.

[70] J. Liu, X. Zheng, H. Deng et al., "Expression of CCR6 in esophageal squamous cell carcinoma and its effects on epithelial-to-mesenchymal transition," *Oncotarget*, vol. 8, no. 70, Article ID 115244, 2017.

[71] B. Xu, M. Zhou, W. Qiu, J. Ye, and Q. Feng, "CCR7 mediates human breast cancer cell invasion, migration by inducing epithelial-mesenchymal transition and suppressing apoptosis through AKT pathway," *Cancer Medicine*, vol. 6, no. 5, pp. 1062–1071, 2017.

[72] J. Zhang, Y. Zhou, and Y. Yang, "CCR7 pathway induces epithelial–mesenchymal transition through up-regulation of

Snail signaling in gastric cancer," *Medical Oncology*, vol. 32, no. 2, p. 17, 2015.

[73] S. Cheng, J. Guo, Q. Yang, and X. Yang, "Crk-like adapter protein regulates CCL19/CCR7-mediated epithelial-to-mesenchymal transition via ERK signaling pathway in epithelial ovarian carcinomas," *Medical Oncology*, vol. 32, no. 3, p. 47, 2015.

[74] Y. Chen, Z. Shao, E. Jiang et al., "CCL21/CCR7 interaction promotes EMT and enhances the stemness of OSCC via a JAK2/STAT3 signaling pathway," *Journal of Cellular Physiology*, vol. 235, no. 9, pp. 5995–6009, 2020.

[75] L. Zhang, D. Wang, Y. Li et al., "CCL21/CCR7 Axis contributed to CD133+ pancreatic cancer stem-like cell metastasis via EMT and Erk/NF-κB pathway," *PLoS One*, vol. 11, no. 8, Article ID e0158529, 2016.

[76] G. Zhong, L. Chen, R. Yin et al., "Chemokine (C-C motif) ligand 21/C-C chemokine receptor type 7 triggers migration and invasion of human lung cancer cells by epithelial-mesenchymal transition via the extracellular signal-regulated kinase signaling pathway," *Molecular Medicine Reports*, vol. 15, no. 6, pp. 4100–4108, 2017.

[77] F. Li, Z. Zou, N. Suo et al., "CCL21/CCR7 axis activating chemotaxis accompanied with epithelial–mesenchymal transition in human breast carcinoma," *Medical Oncology*, vol. 31, no. 9, p. 180, 2014.

[78] G. Li, Y. Yang, S. Xu, L. Ma, M. He, and Z. Zhang, "Erratum to: Slug signaling is up-regulated by CCL21/CCR7 to induce EMT in human chondrosarcoma," *Medical Oncology*, vol. 32, no. 3, p. 58, 2015.

[79] X. Liu, X. Xu, W. Deng et al., "CCL18 enhances migration, invasion and EMT by binding CCR8 in bladder cancer cells [J]," *Molecular Medicine Reports*, vol. 19, no. 3, pp. 1678–1686, 2019.

[80] H. Kong, W. Yu, Z. Chen et al., "CCR9 initiates epithelial–mesenchymal transition by activating Wnt/β-catenin pathways to promote osteosarcoma metastasis," *Cancer Cell International*, vol. 21, no. 1, p. 648, 2021.

[81] J. Park, X. Zhang, S. K. Lee et al., "CCL28-induced RARβ expression inhibits oral squamous cell carcinoma bone invasion," *Journal of Clinical Investigation*, vol. 129, no. 12, pp. 5381–5399, 2019.

[82] H. T. T. Do and J. Cho, "Involvement of the ERK/HIF-1α/EMT pathway in XCL1-induced migration of MDA-MB-231 and SK-BR-3 breast cancer cells," *International Journal of Molecular Sciences*, vol. 22, no. 1, p. 89, 2020.

[83] A. MüLLER, B. Homey, H. Soto et al., "Involvement of chemokine receptors in breast cancer metastasis," *Nature*, vol. 410, no. 6824, pp. 50–56, 2001.

[84] L. Kong, S. Guo, C. Liu et al., "Overexpression of SDF-1 activates the NF-κB pathway to induce epithelial to mesenchymal transition and cancer stem cell-like phenotypes of breast cancer cells," *International Journal of Oncology*, vol. 48, no. 3, pp. 1085–1094, 2016.

[85] A. Orimo, P. B. Gupta, D. C. Sgroi et al., "Stromal fibroblasts present in invasive human breast carcinomas promote tumor growth and angiogenesis through elevated SDF-1/CXCL12 secretion," *Cell*, vol. 121, no. 3, pp. 335–348, 2005.

[86] P. S. H. Soon, E. Kim, C. K. Pon et al., "Breast cancer-associated fibroblasts induce epithelial-to-mesenchymal transition in breast cancer cells," *Endocrine-Related Cancer*, vol. 20, no. 1, pp. 1–12, 2013.

[87] E. T. Roussos, J. S. Condeelis, and A. Patsialou, "Chemotaxis in cancer," *Nature Reviews Cancer*, vol. 11, no. 8, pp. 573–587, 2011.

[88] A. D. Shah, M. J. Bouchard, and A. C. Shieh, "Interstitial fluid flow increases hepatocellular carcinoma cell invasion through CXCR4/CXCL12 and MEK/ERK signaling," *PLoS One*, vol. 10, no. 11, Article ID e0142337, 2015.

[89] J. D. Shields, M. E. Fleury, C. Yong, A. A. Tomei, G. J. Randolph, and M. A. Swartz, "Autologous chemotaxis as a mechanism of tumor cell homing to lymphatics via interstitial flow and autocrine CCR7 signaling," *Cancer Cell*, vol. 11, no. 6, pp. 526–538, 2007.

[90] P. Kukreja, A. B. Abdel-Mageed, D. Mondal, K. Liu, and K. C. Agrawal, "Up-regulation of CXCR4 expression in PC-3 cells by stromal-derivedfactor-1alpha (CXCL12) increases endothelial adhesion and transendothelial migration: role of MEK/ERK signaling pathway-dependentNF-kappaB activation," *Cancer Research*, vol. 65, no. 21, pp. 9891–9898, 2005.

[91] F. Marchesi, P. Monti, B. E. Leone et al., "Increased survival, proliferation, and migration in metastatic human pancreatic tumor cells expressing functional CXCR4," *Cancer Research*, vol. 64, no. 22, pp. 8420–8427, 2004.

[92] X. F. Zhang, X. Jin, S. Malladi et al., "Selection of bone metastasis seeds by mesenchymal signals in the primary tumor stroma," *Cell*, vol. 154, no. 5, pp. 1060–1073, 2013.

[93] R. A. Franklin and M. O. Li, "Ontogeny of tumor-associated macrophages and its Implication in cancer regulation," *Trends in Cancer*, vol. 2, no. 1, pp. 20–34, 2016.

[94] M. Cortés, L. Sanchez-Moral, O. De Barrios et al., "Tumor associated macrophages (TAMs) depend on ZEB1 for their cancer-promoting roles," *Embo j*, vol. 36, no. 22, pp. 3336–3355, 2017.

[95] Q. Liu, J. Song, Y. Pan et al., "Wnt5a/CaMKII/ERK/CCL2 axis is required for tumor-associated macrophages to promote colorectal cancer progression," *International Journal of Biological Sciences*, vol. 16, no. 6, pp. 1023–1034, 2020.

[96] E. N. Arwert, A. S. Harney, D. Entenberg et al., "A Unidirectional transition from migratory to perivascular macrophage is required for tumor cell intravasation," *Cell Reports*, vol. 23, no. 5, pp. 1239–1248, 2018.

[97] M. A. Hauser and D. F. Legler, "Common and biased signaling pathways of the chemokine receptor CCR7 elicited by its ligands CCL19 and CCL21 in leukocytes," *Journal of Leukocyte Biology*, vol. 99, no. 6, pp. 869–882, 2016.

[98] T. Ueno, K. Hara, M. S. Willis et al., "Role for CCR7 ligands in the emigration of newly generated T lymphocytes from the neonatal thymus," *Immunity*, vol. 16, no. 2, pp. 205–218, 2002.

[99] K. Mashino, N. Sadanaga, H. Yamaguchi et al., "Expression of chemokine receptor CCR7 is associated with lymph node metastasis of gastric carcinoma [J]," *Cancer Research*, vol. 62, no. 10, pp. 2937–2941, 2002.

[100] K. GüNTHER, J. Leier, G. Henning et al., "Prediction of lymph node metastasis in colorectal carcinoma by expressionof chemokine receptor CCR7," *International Journal of Cancer*, vol. 116, no. 5, pp. 726–733, 2005.

[101] E. Tutunea-Fatan, M. Majumder, X. Xin, and P. K. Lala, "The role of CCL21/CCR7 chemokine axis in breast cancer-induced lymphangiogenesis," *Molecular Cancer*, vol. 14, no. 1, p. 35, 2015.

[102] A. Issa, T. X. Le, A. N. Shoushtari, J. D. Shields, and M. A. Swartz, "Vascular endothelial growth factor-C and C-C chemokine receptor 7 in tumor cell–lymphatic cross-talk promote invasive phenotype," *Cancer Research*, vol. 69, no. 1, pp. 349–357, 2009.

[103] S. Nisar, P. Yousuf, T. Masoodi et al., "Chemokine-cytokine networks in the head and neck tumor microenvironment,"

International Journal of Molecular Sciences, vol. 22, no. 9, p. 4584, 2021.

[104] X. LEóN, S. Diez, J. GARCíA et al., "Expression of the CXCL12/CXCR4 chemokine axis predicts regional control in head and neck squamous cell carcinoma," *European Archives of Oto-Rhino-Laryngology*, vol. 273, no. 12, pp. 4525–4533, 2016.

[105] C. T. Tan, C. Y. Chu, Y. C. Lu et al., "CXCL12/CXCR4 promotes laryngeal and hypopharyngeal squamous cell carcinoma metastasis through MMP-13-dependent invasion via the ERK1/2/AP-1 pathway," *Carcinogenesis*, vol. 29, no. 8, pp. 1519–1527, 2008.

[106] A. O. Rehman and C. Y. Wang, "CXCL12/SDF-1α activates NF-κB and promotes oral cancer invasion through the Carma3/Bcl10/Malt1 complex," *International Journal of Oral Science*, vol. 1, no. 3, pp. 105–118, 2009.

[107] X. Li, Q. Xu, Y. Wu et al., "A CCL2/ROS autoregulation loop is critical for cancer-associatedfibroblasts-enhanced tumor growth of oral squamous cell carcinoma," *Carcinogenesis*, vol. 35, no. 6, pp. 1362–1370, 2014.

[108] Z. Ling, W. Li, J. Hu et al., "Targeting CCL2-CCR4 axis suppress cell migration of head and neck squamous cell carcinoma," *Cell Death & Disease*, vol. 13, no. 2, p. 158, 2022.

[109] Z. J. Shang, K. Liu, and Z. Shao, "Expression of chemokine receptor CCR7 is associated with cervical lymph node metastasis of oral squamous cell carcinoma," *Oral Oncology*, vol. 45, no. 6, pp. 480–485, 2009.

[110] Z. J. Zhao, F. Y. Liu, P. Li, X. Ding, Z. H. Zong, and C. F. Sun, "CCL19-induced chemokine receptor 7 activates the phosphoinositide-3kinase-mediated invasive pathway through Cdc42 in metastatic squamous cell carcinoma of the head and neck," *Oncology Reports*, vol. 25, no. 3, pp. 729–737, 2011.

[111] N. Guo, F. Liu, L. Yang, J. Huang, X. Ding, and C. Sun, "Chemokine receptor 7 enhances cell chemotaxis and migration of metastatic squamous cell carcinoma of head and neck through activation of matrix metalloproteinase-9," *Oncology Reports*, vol. 32, no. 2, pp. 794–800, 2014.

[112] P. Li, Z. J. Zhao, F. Y. Liu et al., "The chemokine receptor 7 regulates cell adhesion and migration via beta1 integrin in metastatic squamous cell carcinoma of the head and neck," *Oncology Reports*, vol. 24, no. 4, pp. 989–995, 2010.

[113] Z. Xu, X. Zheng, L. Yang et al., "Chemokine receptor 7 promotes tumor migration and invasiveness via the RhoA/ROCK pathway in metastatic squamous cell carcinoma of the head and neck," *Oncology Reports*, vol. 33, no. 2, pp. 849–855, 2015.

[114] W. Wang, Y. Qiao, and Z. Li, "New insights into modes of GPCR activation," *Trends in Pharmacological Sciences*, vol. 39, no. 4, pp. 367–386, 2018.

[115] M. Thelen, P. Peveri, P. Kernen, V. Von Tscharner, A. Walz, and M. Baggiolini, "Mechanism of neutrophil activation by NAF, a novel monocyte-derived peptide agonist," *Faseb j*, vol. 2, no. 11, pp. 2702–2706, 1988.

[116] A. Zlotnik and O. Yoshie, "The chemokine superfamily revisited," *Immunity*, vol. 36, no. 5, pp. 705–716, 2012.

[117] N. Arang and J. S. G. Gutkind, "G Protein Coupled receptors and heterotrimeric G proteins as cancer drivers," *FEBS Letters*, vol. 594, no. 24, pp. 4201–4232, 2020.

[118] R. Iglesias-Bartolome, D. Torres, R. Marone et al., "Inactivation of a Gαs–PKA tumour suppressor pathway in skin stem cells initiates basal-cell carcinogenesis," *Nature Cell Biology*, vol. 17, no. 6, pp. 793–803, 2015.

[119] D. R. Pattabiraman, B. Bierie, K. I. Kober et al., "Activation of PKA leads to mesenchymal-to-epithelial transition and loss of tumor-initiating ability," *Science*, vol. 351, no. 6277, Article ID aad3680, 2016.

[120] W. F. Schwindinger and J. D. Robishaw, "Heterotrimeric G-protein$\beta\gamma$-dimers in growth and differentiation," *Oncogene*, vol. 20, no. 13, pp. 1653–1660, 2001.

[121] E. R. Neptune and H. R. Bourne, "Receptors induce chemotaxis by releasing the $\beta\gamma$ subunit of G_i, not by activating G_q or G_s," *Proceedings of the National Academy of Sciences of the United States of America*, vol. 94, no. 26, Article ID 14489, 1997.

[122] F. M. Davis, I. Azimi, R. A. Faville et al., "Induction of epithelial–mesenchymal transition (EMT) in breast cancer cells is calcium signal dependent," *Oncogene*, vol. 33, no. 18, pp. 2307–2316, 2014.

[123] R. J. Norgard, J. R. Pitarresi, R. Maddipati et al., "Calcium signaling induces a partial EMT," *European Molecular Biology Organization Reports*, vol. 22, no. 9, Article ID e51872, 2021.

[124] J. B. Rubin, "Chemokine signaling in cancer: one hump or two," *Seminars in Cancer Biology*, vol. 19, no. 2, pp. 116–122, 2009.

[125] H. G. Dohlman and J. Thorner, "RGS proteins and signaling by heterotrimeric G proteins," *Journal of Biological Chemistry*, vol. 272, no. 7, pp. 3871–3874, 1997.

[126] M. Thelen, "Dancing to the tune of chemokines," *Nature Immunology*, vol. 2, no. 2, pp. 129–134, 2001.

[127] C. A. Parent and P. N. Devreotes, "A Cell's sense of direction," *Science*, vol. 284, no. 5415, pp. 765–770, 1999.

[128] C. H. Stuelten, C. A. Parent, and D. J. Montell, "Cell motility in cancer invasion and metastasis: insights from simple model organisms," *Nature Reviews Cancer*, vol. 18, no. 5, pp. 296–312, 2018.

[129] T. A. Kohout and R. J. Lefkowitz, "Regulation of G Protein-Coupled receptor kinases and arrestins during receptor desensitization," *Molecular Pharmacology*, vol. 63, no. 1, pp. 9–18, 2003.

[130] R. J. Lefkowitz and S. K. Shenoy, "Transduction of receptor signals by ß-arrestins," *Science*, vol. 308, no. 5721, pp. 512–517, 2005.

[131] L. M. Luttrell, F. L. Roudabush, E. W. Choy et al., "Activation and targeting of extracellular signal-regulated kinases by β-arrestin scaffolds," *Proceedings of the National Academy of Sciences of the United States of America*, vol. 98, no. 5, pp. 2449–2454, 2001.

[132] Y. Daaka, L. M. Luttrell, and R. J. Lefkowitz, "Switching of the coupling of the β2-adrenergic receptor to different G proteins by protein kinase A," *Nature*, vol. 390, no. 6655, pp. 88–91, 1997.

[133] J. S. Smith, T. F. Pack, A. Inoue et al., "Noncanonical scaffolding of G(αi) and β-arrestin by G protein-coupled receptors," *Science*, vol. 371, no. 6534, 2021.

[134] E. R. Neptune, T. Iiri, and H. R. Bourne, "Gαi is not required for chemotaxis mediated by Gi-coupled receptors," *Journal of Biological Chemistry*, vol. 274, no. 5, pp. 2824–2828, 1999.

[135] M. O'Hayre, K. Eichel, S. Avino et al., "Genetic evidence that β-arrestins are dispensable for the initiation of β_2-adrenergic receptor signaling to ERK," *Science Signaling*, vol. 10, no. 484, Article ID eaal3395, 2017.

[136] L. ROSANò, R. Cianfrocca, P. Tocci et al., "Endothelin A receptor/β-arrestin signaling to the wnt pathway renders ovarian cancer cells resistant to Chemotherapy," *Cancer Research*, vol. 74, no. 24, pp. 7453–7464, 2014.

[137] X. Duan, T. Zhang, Z. Kong et al., "β-arrestin1 promotes epithelial-mesenchymal transition via modulating GSK-3β/β-catenin pathway in prostate cancer cells," *Biochemical and Biophysical Research Communications*, vol. 479, no. 2, pp. 204–210, 2016.

[138] S. Pillai, J. Trevino, B. Rawal et al., "β-Arrestin-1 mediates nicotine-induced metastasis through E2F1 target genes that modulate epithelial–mesenchymal transition," *Cancer Research*, vol. 75, no. 6, pp. 1009–1020, 2015.

[139] C. C. Tsai, Y. T. Chou, and H. W. Fu, "Protease-activated receptor 2 induces migration and promotes Slug-mediatedepithelial-mesenchymal transition in lung adenocarcinoma cells," *Biochimica et Biophysica Acta (BBA) - Molecular Cell Research*, vol. 1866, no. 3, pp. 486–503, 2019.

[140] Y. Jiang, X. Zhuo, Y. Wu, X. Fu, and C. Mao, "PAR2 blockade reverses osimertinib resistance in non-small-cell lung cancer cells via attenuating ERK-mediated EMT and PD-L1 expression," *Biochimica et Biophysica Acta (BBA) - Molecular Cell Research*, vol. 1869, no. 1, Article ID 119144, 2022.

[141] R. H. Oakley, S. A. Laporte, J. A. Holt, M. G. Caron, and L. S. Barak, "Differential affinities of visual arrestin, βarrestin1, and βarrestin2 for g protein-coupled receptors delineate two major classes of receptors," *Journal of Biological Chemistry*, vol. 275, no. 22, Article ID 17201, 2000.

[142] T. N. Feinstein, N. Yui, M. J. Webber et al., "Noncanonical control of vasopressin receptor type 2 signaling by retromer and arrestin," *Journal of Biological Chemistry*, vol. 288, no. 39, Article ID 27849, 2013.

[143] S. Ferrandon, T. N. Feinstein, M. Castro et al., "Sustained cyclic AMP production by parathyroid hormone receptor endocytosis," *Nature Chemical Biology*, vol. 5, no. 10, pp. 734–742, 2009.

[144] R. C. Werthmann, S. Volpe, M. J. Lohse, and D. Calebiro, "Persistent cAMP signaling by internalized TSH receptors occurs in thyroid but not in HEK293 cells," *Faseb j*, vol. 26, no. 5, pp. 2043–2048, 2012.

[145] F. Mullershausen, F. Zecri, C. Cetin, A. Billich, D. Guerini, and K. Seuwen, "Persistent signaling induced by FTY720-phosphate is mediated by internalized S1P1 receptors," *Nature Chemical Biology*, vol. 5, no. 6, pp. 428–434, 2009.

[146] A. R. B. Thomsen, B. Plouffe, T. J. Cahill et al., "GPCR-Gprotein-β-arrestin super-complex mediates sustained G protein signaling," *Cell*, vol. 166, no. 4, pp. 907–919, 2016.

[147] A. Cartier and T. Hla, "Sphingosine 1-phosphate: lipid signaling in pathology and therapy," *Science*, vol. 366, no. 6463, Article ID eaar5551, 2019.

[148] S. Angers, A. Salahpour, and M. Bouvier, "Dimerization: an emerging concept for g protein–coupled receptor ontogeny and function," *Annual Review of Pharmacology and Toxicology*, vol. 42, no. 1, pp. 409–435, 2002.

[149] M. Mellado, J. M. RODRíGUEZ-Frade, S. MAñES, and C. Martinez-A, "Chemokine signaling and functional responses: the role of receptor dimerization and TK pathway activation," *Annual Review of Immunology*, vol. 19, no. 1, pp. 397–421, 2001.

[150] Y. Percherancier, Y. A. Berchiche, I. Slight et al., "Bioluminescence resonance energy transfer reveals ligand-induced conformational changes in CXCR4 homo- and heterodimers," *Journal of Biological Chemistry*, vol. 280, no. 11, pp. 9895–9903, 2005.

[151] A. Levoye, K. Balabanian, F. Baleux, F. Bachelerie, and B. Lagane, "CXCR7 heterodimerizes with CXCR4 and regulates CXCL12-mediated G protein signaling," *Blood*, vol. 113, no. 24, pp. 6085–6093, 2009.

[152] R. L. Contento, B. Molon, C. Boularan et al., "CXCR4–CCR5: a couple modulating T cell functions," *Proceedings of the National Academy of Sciences of the United States of America*, vol. 105, no. 29, Article ID 10101, 2008.

[153] L. MARTíNEZ-MUñOZ, R. Barroso, S. Y. Dyrhaug et al., "CCR5/CD4/CXCR4 oligomerization prevents HIV-1 gp120IIIB binding to the cell surface," *Proceedings of the National Academy of Sciences of the United States of America*, vol. 111, no. 19, Article ID E1960, 2014.

[154] D. Sohy, M. Parmentier, and J. Y. Springael, "Allosteric transinhibition by specific antagonists in CCR2/CXCR4 heterodimers," *Journal of Biological Chemistry*, vol. 282, no. 41, Article ID 30062, 2007.

[155] O. M. Pello, L. Martínez-muñoz, V. Parrillas et al., "Ligand stabilization of CXCR4/δ-opioid receptor heterodimers reveals a mechanism for immune response regulation," *European Journal of Immunology*, vol. 38, no. 2, pp. 537–549, 2008.

[156] L. Sánchez-martín, P. Sánchez-Mateos, and C. Cabañas, "CXCR7 impact on CXCL12 biology and disease," *Trends in Molecular Medicine*, vol. 19, no. 1, pp. 12–22, 2013.

[157] M. Mellado, J. M. Rodríguez-Frade, A. J. Vila-Coro et al., "Chemokine receptor homo- or heterodimerization activates distinct signaling pathways," *The EMBO Journal*, vol. 20, no. 10, pp. 2497–2507, 2001.

[158] Y. Kojima, A. Acar, E. N. Eaton et al., "Autocrine TGF-β and stromal cell-derivedfactor-1 (SDF-1) signaling drives the evolution of tumor-promoting mammary stromal myofibroblasts," *Proceedings of the National Academy of Sciences of the United States of America*, vol. 107, no. 46, Article ID 20009, 2010.

[159] C. Akekawatchai, J. D. Holland, M. Kochetkova, J. C. Wallace, and S. R. McColl, "Transactivation of CXCR4 by the insulin-like growth factor-1 receptor (IGF-1R) in human MDA-MB-231 breast cancer epithelial cells," *Journal of Biological Chemistry*, vol. 280, no. 48, Article ID 39701, 2005.

[160] J. P. Hobson, H. M. Rosenfeldt, L. S. Barak et al., "Role of the sphingosine-1-phosphate receptor EDG-1 in PDGF-induced cell motility," *Science*, vol. 291, no. 5509, pp. 1800–1803, 2001.

[161] Z. G. Goldsmith and D. N. Dhanasekaran, "G Protein regulation of MAPK networks," *Oncogene*, vol. 26, no. 22, pp. 3122–3142, 2007.

[162] Z. J. Cheng, J. Zhao, Y. Sun et al., "β-Arrestin differentially regulates the chemokine receptor CXCR4-mediated signaling and receptor internalization, and this implicates multiple interaction sites between β-arrestin and CXCR4," *Journal of Biological Chemistry*, vol. 275, no. 4, pp. 2479–2485, 2000.

[163] M. P. Stemmler, R. L. Eccles, S. Brabletz, and T. Brabletz, "Non-redundant functions of EMT transcription factors," *Nature Cell Biology*, vol. 21, no. 1, pp. 102–112, 2019.

[164] J. H. Tsai, J. L. Donaher, D. A. Murphy, S. Chau, and J. Yang, "Spatiotemporal regulation of epithelial-mesenchymal transition is essential for squamous cell carcinoma metastasis," *Cancer Cell*, vol. 22, no. 6, pp. 725–736, 2012.

[165] D. Hanahan, "Hallmarks of cancer: new dimensions," *Cancer Discovery*, vol. 12, no. 1, pp. 31–46, 2022.

Hindawi
Journal of Oncology
Volume 2022, Article ID 9253938, 15 pages
https://doi.org/10.1155/2022/9253938

Research Article

Unveiling the Noncanonical Autophagy-Independent Role of *ATG7* and *ATG9B* in Head and Neck Squamous Cell Carcinoma (HNSCC)

Yibo Guo,[1,2] Yiting Sun,[2,3] Mingtao Chen,[1,2] Yisheng Feng,[1,2] Xu Zhang,[1,2] Tong Ji,[1,2] Zheqi Liu,[1,2] and Yu Zhang[1,2]

[1]*Department of Oral Maxillofacial-Head Neck Oncology, Shanghai Ninth People's Hospital, Shanghai Jiao Tong University School of Medicine, Shanghai, China*
[2]*College of Stomatology, Shanghai Jiao Tong University, National Center for Stomatology, National Clinical Research Center for Oral Diseases, Shanghai Key Laboratory of Stomatology, Shanghai, China*
[3]*Department of Oral and Cranio-Maxillofacial Surgery, Shanghai Ninth People's Hospital, Shanghai Jiao Tong University School of Medicine, Shanghai, China*

Correspondence should be addressed to Tong Ji; jitong70@sjtu.edu.cn, Zheqi Liu; 734672500@sjtu.edu.cn, and Yu Zhang; zhyzhy1818@sjtu.edu.cn

Received 10 June 2022; Accepted 14 September 2022; Published 10 October 2022

Academic Editor: Qihong Li

The role of autophagy in cancer remains elusive, and nontargeted autophagy inhibitors have limited therapeutic effects in HNSCC. Here, we systematically analyzed the correlation of autophagy-related genes in HNSCC through TCGA and single-cell sequencing data (GSE103322). *ATG9B* and *ATG7* were found to have noncanonical autophagy-independent functions in HNSCC. Specifically, *ATG9B* was a protective factor in HNSCC patients through downregulating cancer cell EMT, and *ATG7* was correlated with the immunosuppressive environment in HNSCC. Mechanistically, single-cell analysis revealed that *ATG9B* increased the epithelial phenotype of cancer cells but did not influence EMT signaling pathways. *ATG7* was strongly correlated with elevated immunosuppressive checkpoints like PD-1, PD-L1, and CTLA4 in HNSCC. Further single-cell analysis and multiple immunofluorescence colocalization analyses indicated that *ATG7* contributed to the high expression of PD-L1 in myeloid cells but not cancer cells. Collectively, our results revealed noncanonical autophagy-independent functions of autophagy-related genes. These results increase understanding of the intricacies of autophagy and may contribute to precision treatment using autophagy-targeted therapies.

1. Introduction

Macroautophagy (referred to throughout this article as autophagy) is a highly conserved catabolic process, which involves the formation of double-membraned vesicles known as autophagosomes that engulf cellular proteins and organelles for delivery to the lysosome. Autophagy is also highly involved in tumor initiation and progression; however, it remains controversial whether it plays a tumor-suppressive or a tumor-promoting role in different tumor types. It is now generally acknowledged that autophagy plays a larger role in tumor inhibition during tumorigenesis and malignant transformation. For example, mice with monoallelic deletion of the autophagy-related gene *beclin1* eventually develop spontaneous tumors [1]. Additionally, mice lacking Atg4 are more prone to chemically-induced fibrosarcoma [2]. However, autophagy may exert an opposite function in established tumors. It can protect tumor cells from metabolic stressors such as glucose and amino acid deficiency [3] as well as help cancer cells survive chemotherapy drugs and targeted therapy drugs [4, 5]. Aside from the canonical functions of autophagy in tumor progression, cumulative evidence shows that autophagy is also involved in other hallmarks of cancer like cancer metabolism [6],

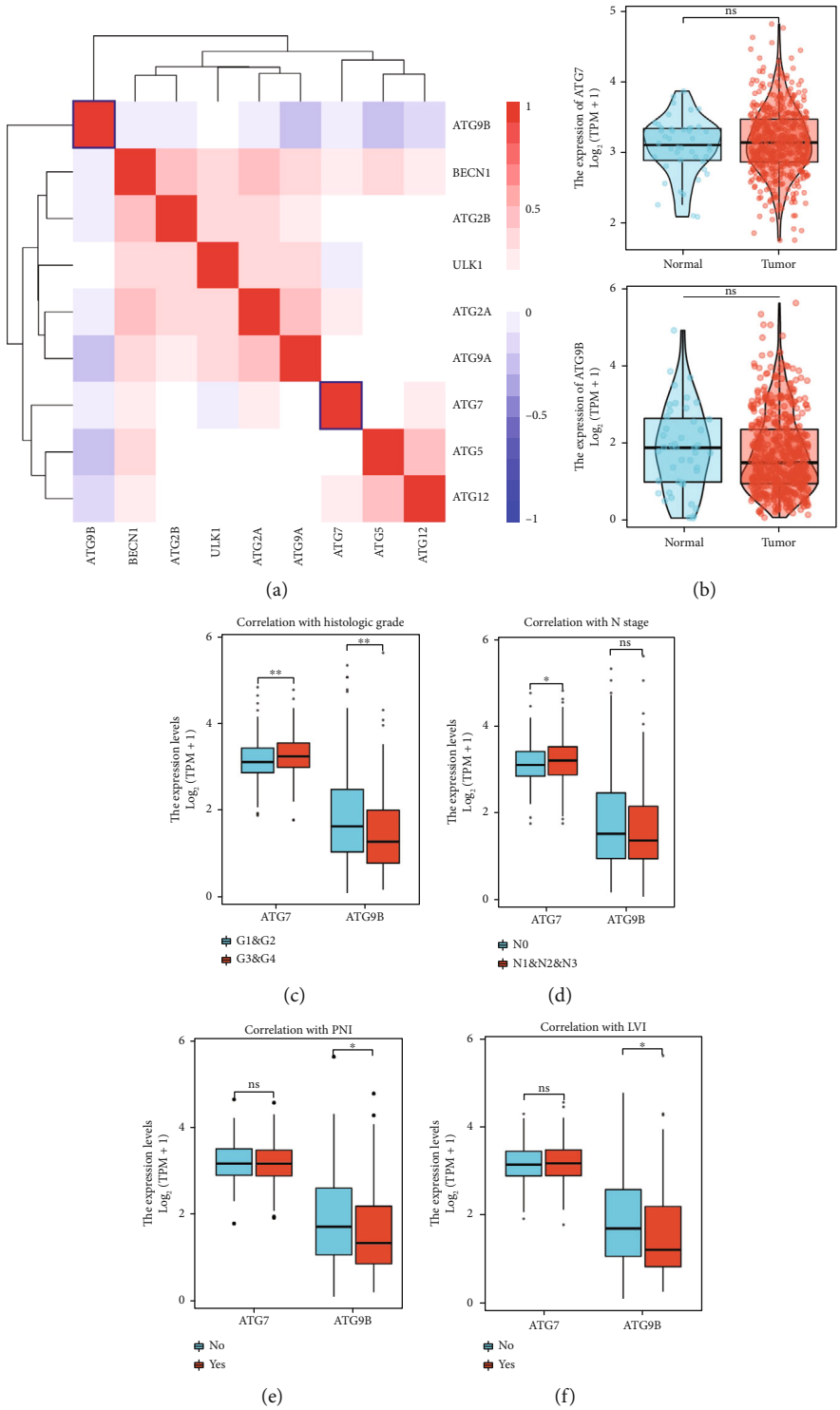

Figure 1: Continued.

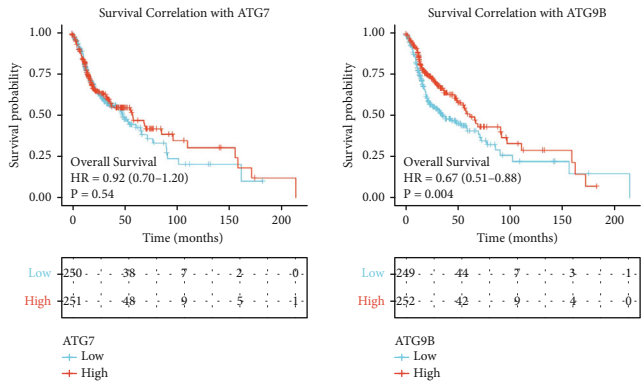

(g)

Figure 1: *ATG7* and *ATG9B* may play autophagy-independent roles in HNSCC. (a) Correlation of different autophagy-related genes with transcription level based on the TCGA database. (b) The mRNA levels of *ATG7* and *ATG9B* in HNSCC tumor and normal tissues. (c–f) The correlation between clinicopathological features and expression of *ATG7* and *ATG9B* in HNSCC patients. (g) Kaplan-Meier analysis of the mRNA expression of *ATG7* and *ATG9B* on the overall survival rate of HNSCC patients.

metastasis, and immune escape [7, 8] depending on the tumor type. The multifaceted effects of autophagy on tumors make targeting autophagy for cancer therapy a significant problem. Mining of the noncanonical functions of autophagy during cancer progression may increase understanding of the intricacies of autophagy and contribute to precision treatment using autophagy-targeted therapies.

Head and neck squamous cell cancer (HNSCC) is a common and aggressive malignancy with a poor 5-year survival rate of 45% [9], and it is closely correlated with overuse of tobacco and alcohol. The role of autophagy in HNSCC remains ambiguous, as it has been implicated in processes from inhibition to overactivation in HNSCC [10]. Despite success in inhibiting cancer cell growth through autophagy inhibition in vitro [11], in vivo curative effects of the nontargeted autophagy inhibitors hydroxychloroquine and 3-MA have been less successful. Furthermore, different autophagy-related genes play different roles beyond their functions in autophagy and autophagy-related membrane-trafficking pathways [12]. Understanding the specific roles of individual autophagy genes will contribute to more accurate autophagy-targeted therapies. In this study, we have explored the noncanonical functions of autophagy-related genes by analyzing The Cancer Genome Atlas (TCGA) database and single-cell HNSCC database (GSE103322). This study provides a new perspective on specific autophagy-related genes in HNSCC, and may aid in the development of more accurate autophagy-targeted therapies.

2. Methods

2.1. RNA-Sequencing Data from TCGA. The gene expression data, including the count and fragments per kilobase of transcript per million mapped reads (FPKM), and related clinical data of The Cancer Genome Atlas (TCGA) HNSC project were downloaded from the UCSC Xena online database (http://xena.ucsc.edu/). For further analysis, the FPKM data were transformed into transcripts per million reads (TPM). This study met the publication guidelines described by TCGA.

2.2. Differential Gene Expression Analysis. Identification of differentially expressed genes (DEGs) between different groups were performed using limma package. Log2 FoldChange > 2 and adjust P value <0.01 were set as the threshold values for DEGs [13].

2.3. Functional Analysis of DEGs. The Gene Ontology (GO) and Kyoto Encyclopedia of Genes and Genomes (KEGG) analyses of correlated neighboring genes were conducted using the enrichGO and enrichKEGG functions of the clusterProfiler package, respectively [14]. GSEA analysis was performed using the GSEA function of clusterProfiler package. Adjusted P values (false-discovery rate [FDR]) lower than 0.05 were considered to indicate statistical significance. Gene set permutations were performed 1000 times for each analysis.

2.4. Tumor Purity Analysis. ESTIMATE is a method that uses gene expression signatures to infer the fraction of stromal and immune cells in tumor samples [15]. The tumor purity of TCGA samples was calculated using the ESTIMATE package in R.

2.5. Analysis of Immune Infiltration. TIMER (http://timer.cistrome.org/) is a reliable and intuitive tool for inferring immune infiltration levels from TCGA datasets [16]. The immune infiltration level scores of TCGA samples, including scores calculated by TIMER, CIBERSORT [17], MCPcounter [18], and EPIC [19], were downloaded from the TIMER database for further analysis.

2.6. Single-Cell Sequencing Data Analysis. Single-cell sequencing data from GSE103322 [20] was downloaded from Gene Expression Omnibus (GEO) database and had already been normalized by the researcher who deposited it. Cancer and noncancer cells were already labelled by the researcher. The matrix was combined in R and converted

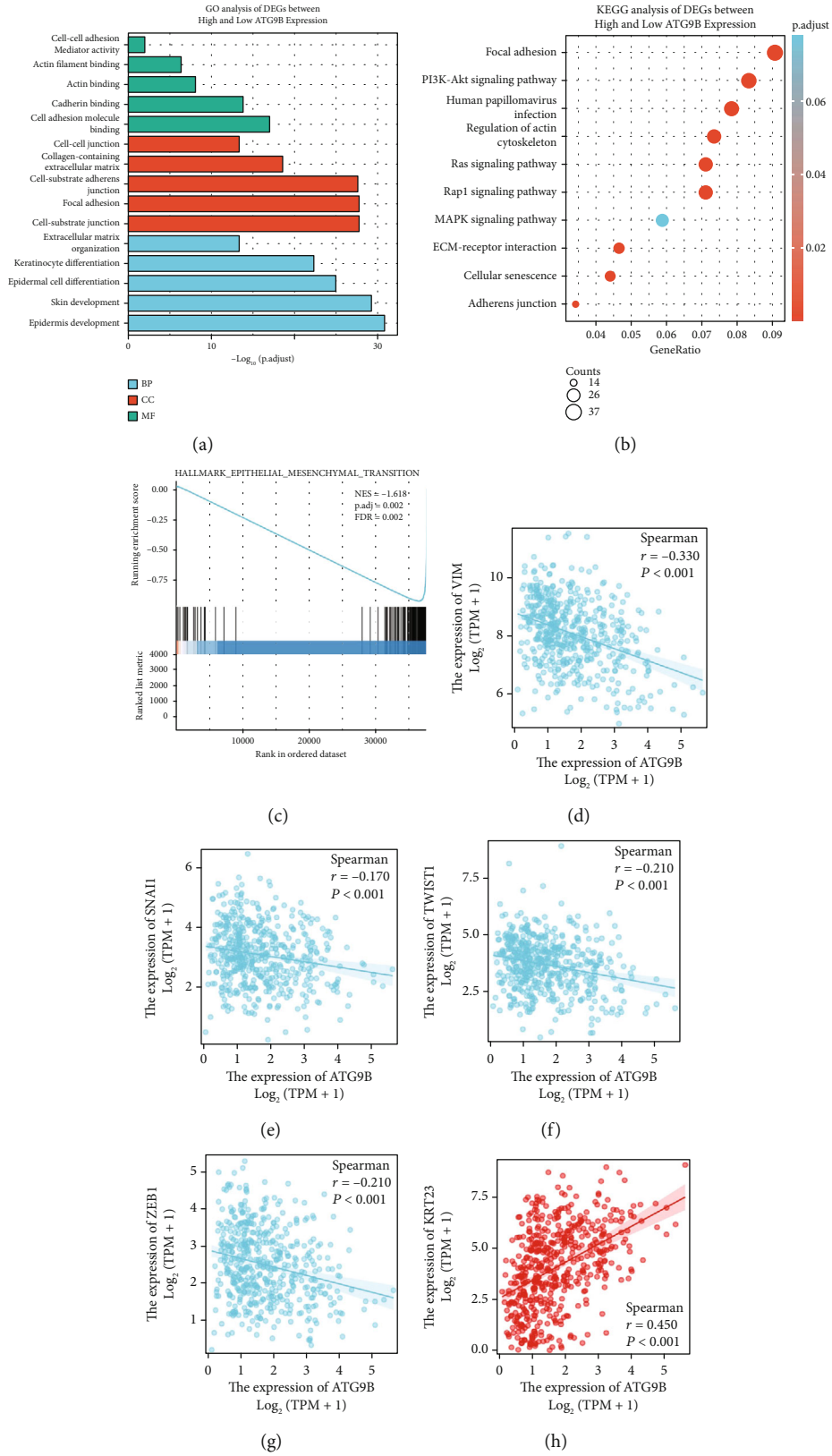

Figure 2: Continued.

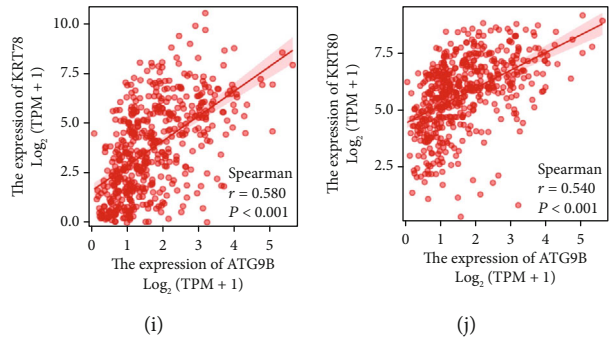

Figure 2: *ATG9B* was negatively correlated with HNSCC EMT in TCGA. (a) GO analysis of different expression genes with a fold change of >1.5 or <0.667 and an FDR < 0.05 based on *ATG9B* mRNA expression. (b) KEGG analysis of different expression genes with a fold change of >1.5 or <0.667 and an FDR < 0.05 based on *ATG9B* mRNA expression. (c) GSEA analysis showed that *ATG9B* was negatively correlated with HNSCC EMT. (d–g) The expression of *ATG9B* was negatively correlated with EMT marker genes. (h–j) The expression of *ATG9B* was strongly correlated with the keratin family.

to a Seurat object using the Seurat R package [21]. To reduce dimensionality, principal component analysis was employed to summarize the resulting variably expressed genes, and then t-SNE dimensionality reduction (RunTSNE function) was used to further summarize principal components. In cancer cells, all the cells were divided into 13 clusters using FindNeighbors and FindClusters functions in Seurat. In noncancer cells, the clusters of each cell type were annotated based on expression of the following gene sets: CD4+ T cells (*CD4* and *IL7R*), Tregs (*CD4*, *FOXP3*, and *IL2RA*), CD8+ T cells (*CD8A* and *CD8B*), exhausted CD8+ T cells (*CD8A*, *CD8B*, *PDCD1*, *CTLA4*, and *LAG3*), myeloid cells (*TPSB2*, *CD1A*, *CD14*, *CD163*, *C1QA*, and *TREM1*), fibroblasts (*COL1A2* and *DCN*), NK cells (*NCAM1*, *KLRD1*, *KLRC1*, and *XCL1*), endothelial cells, (*PECAM1* and *VWF*), and B cells (*CD79A* and *CD19*).

2.7. Cell Culture. The human OSCC cell lines CAL27 cells were purchased from the American Type Culture Collection (ATCC, USA). All of these cells were maintained in Dulbecco's minimum essential medium (Invitrogen, Carlsbad, CA, USA) supplemented with 10% fetal bovine serum (FBS), 100 units/ml penicillin and 100 μg/ml streptomycin incubated in a humidified atmosphere with 5% CO2 at 37°C.

2.8. Western Blot. Western blotting was performed as described previously [9]. The antibodies against the following proteins were used: *ATG7* (1 : 1000, 8558, Cell Signaling Technology), PD-L1 (1 : 1000, 13684, Cell Signaling Technology), β-actin (1 : 5000, 4970, Cell Signaling Technology), and *ATG9B* (1 : 1000, A7406, ABclonal). The immunoreactive bands were visualized using an Odyssey® Infrared Imaging System (Bioscience USA).

2.9. Immunofluorescence. The HNSCC patient paraffin sections were incubated with anti-ATG7, anti-PD-L1 and anti-CD-68 antibodies overnight at 4°C and then washed and incubated for 30 min with an Alexa Fluor 488 donkey anti-rabbit IgG (H+L) (Invitrogen, USA; 1 : 500) or an Alexa Fluor 549 donkey anti-mouse IgG (H+L) (Invitrogen, USA; 1 : 500) at room temperature in the dark. The nuclei were stained with 4′, 6-diamidino-2-phenylindole (DAPI; Invitrogen, USA; 1 : 1000) for 5 min. The cells were imaged using an Axio Vert. A1 microscope (Carl Zeiss, Germany). Prior to the use of the clinical materials for research purpose, patients' written informed consents and approval were obtained. The use of human specimens in this study was approved by the Institutional Research Ethics Committee of Shanghai Ninth People's Hospital.

2.10. Statistical Analysis and Data Visualization. Statistical analysis was performed using R (4.0.2). The Spearman correlation tests were performed to analyze the correlation among the expression of different autophagy related genes. Gene expression of *ATG7*/*ATG9B* was compared using the Wilcoxon rank-sum test. The association between the expression of *ATG7*/*ATG9B* and survival was analyzed using Cox regression models. The relationships between clinical parameters and the expression of *ATG7*/*ATG9B* were analyzed using the Wilcoxon rank-sum test. Correlation analyses between the expression of *ATG7* and tumor purity, the RNA expression of *CD274*, *PDCD1*, and *CTLA4*, or immune infiltration levels were also performed using the Spearman correlation tests. Results were visualized with the ggplot2, pheatmap, clusterProfiler, and Seurat packages.

3. Results

3.1. Different Clusters of Autophagy-Related Genes. To assess the correlation between autophagy-related genes, we downloaded expression profiling datasets for 517 HNSCC patients in TCGA. We analyzed the correlations of the autophagy-related genes *BECN1*, *ULK1*, *ATG2A*, *ATG2B*, *ATG5*, *ATG7*, *ATG9A*, *ATG9B*, and *ATG12*. The results showed that *BECN1*, *ULK1*, *ATG2A*, *ATG2B*, and *ATG9A* had stronger correlation in transcriptomes (thus we named it cluster A), while *ATG5* and *ATG12* were strongly correlated with each other (thus we named it cluster B) (Figure 1(a)). Strikingly, *ATG7* had a weaker correlation with both cluster A and B, and *ATG9B* was the only autophagy-related gene negatively correlated with the other clusters, suggesting it might have other autophagy-independent functions.

These correlations were in accordance with the protein functions in autophagy. *BECN1*, *ULK1*, *ATG2A*, *ATG2B*, and *ATG9A* were more involved in autophagy initiation

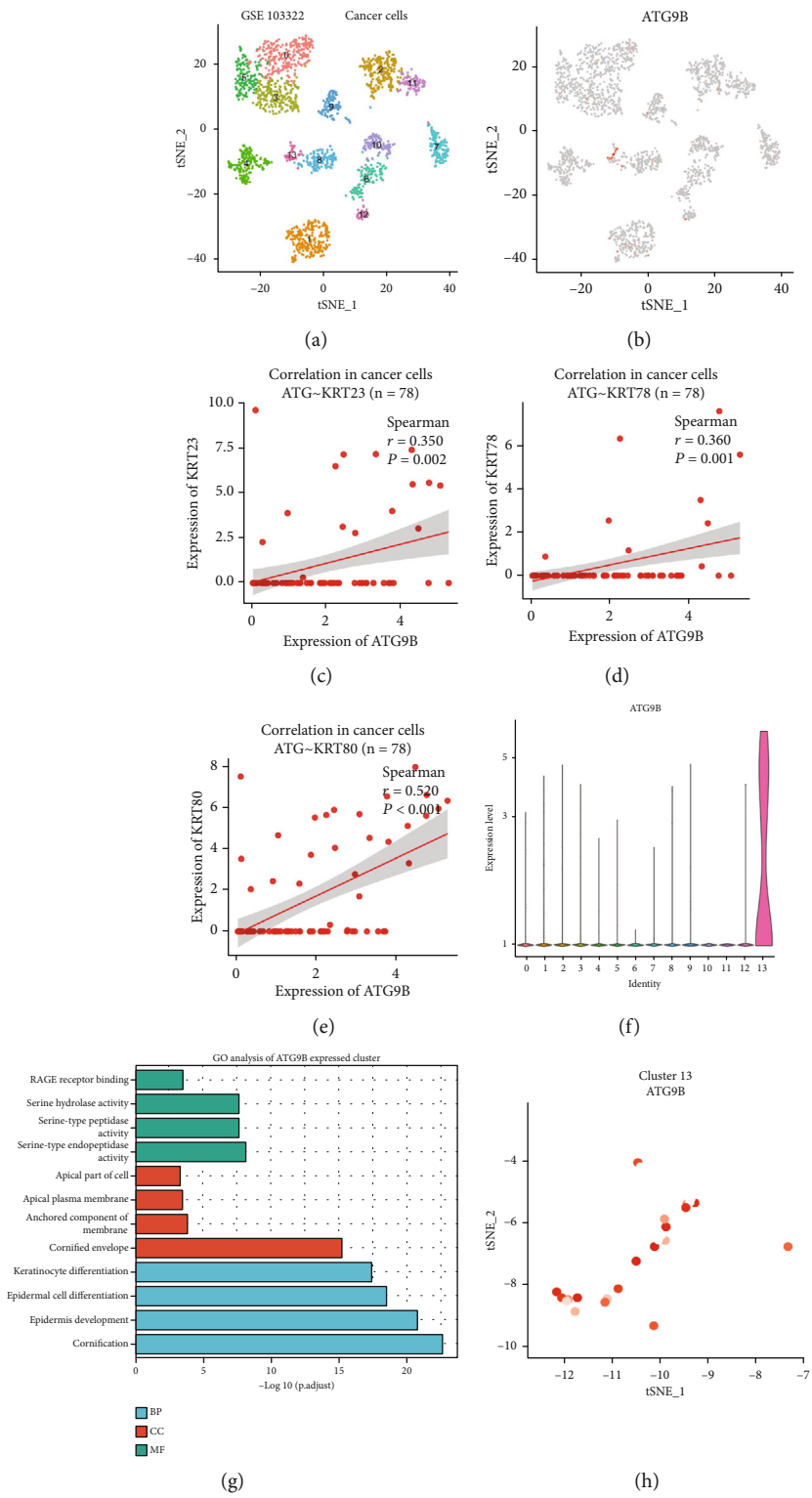

Figure 3: Continued.

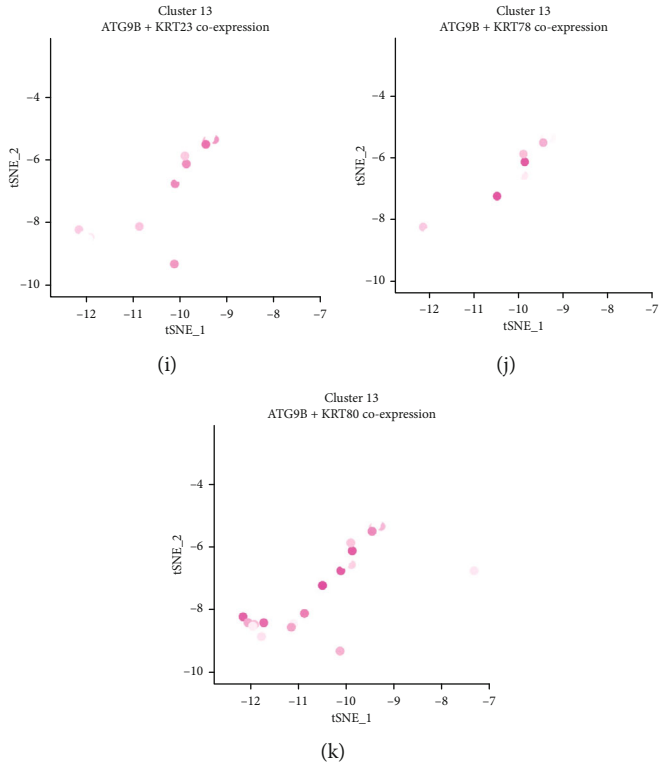

Figure 3: *ATG9B* was negatively correlated with HNSCC EMT in the single-cell database (GSE103322). (a) Different clusters of cancer cells in GSE103322. (b) Expression of ATG9B in cancer cells. (c–e) Correlation of *ATG9B* with *KRT23*, 78, and 80 in cancer cells. (f) *ATG9B* was mainly expressed in cluster 13 of cancer cells. (g) GO analysis of highly expressed genes in cluster 13 cancer cells. (h–k) *ATG9B* was coexpressed with *KRT23*, 78, and 80 in cluster 13 cancer cells.

and phagophore formation, while *ATG5* and *ATG12* were involved in the elongation of phagophores. Therefore, we further investigated the potential autophagy-independent roles of *ATG7* and *ATG9B*. Compared to normal tissues, the *ATG7* mRNA level was slightly upregulated, and the *ATG9B* mRNA level was slightly downregulated in HNSCC tissues in the TCGA database (Figure 1(b)). However, both results were not significantly different. We then analyzed the correlation between the mRNA expression of *ATG7* and *ATG9B* and the clinicopathological features of HNSCC patients in the TCGA database. Higher *ATG7* expression was correlated with high histologic grade ($P < 0.01$) and lymph node metastasis ($P < 0.05$) (Figures 1(c)–1(f)). Strikingly, higher *ATG9B* expression was correlated with lower histologic grade ($P < 0.01$), lower chance of perineural invasion ($P < 0.05$), and lower chance of lymphatic vascular invasion ($P < 0.05$) (Figures 1(c)–1(f)). Kaplan-Meier analysis (KM) showed that HNSCC patients with higher *ATG9B* had better overall survival rates (OS) (HR = 0.67, $P = 0.004$) (Figure 1(g)). Collectively, these results indicated that *ATG7* and *ATG9B* might play autophagy-independent roles in HNSCC. Specifically, *ATG7* might play a role in tumor promotion, while *ATG9B* might be a tumor suppressor.

3.2. ATG9B Was Negatively Correlated with HNSCC Epithelial Mesenchymal Transition (EMT) in TCGA. The transcriptomes of HNSCC patients from the TCGA database were divided into 2 groups according to *ATG9B* mRNA expression. Differential gene expression with a fold change >1.5 or <0.667 and an FDR < 0.05 were identified and underwent GO analysis. GO analysis showed that *ATG9B* was highly involved in the EMT process including cell-cell adhesion mediator activity, cadherin binding, and extracellular matrix organization (Figure 2(a)). KEGG analysis showed similar results like focal adhesion, regulation of the actin cytoskeleton, ECM-receptor interaction, and adherens junction (Figure 2(b)). Gene Set Enrichment Analysis (GSEA) indicated that *ATG9B* was negatively correlated with HNSCC EMT (NES = 1.618, FDR = 0.002) (Figure 2(c)). We further found that *ATG9B* was negatively correlated with the EMT marker genes SNAIL ($r = -0.017$, $P < 0.001$), TWIST ($r = -0.210$, $P < 0.001$), ZEB1 ($r = -0.210$, $P < 0.001$), and VIM ($r = -0.330$, $P < 0.001$) (Figures 2(d)–2(g)). Furthermore, *ATG9B* was strongly correlated with the keratin family, especially KRT23 ($r = 0.450$, $P < 0.001$), *KRT78* ($r = 0.580$, $P < 0.001$), and *KRT80* ($r = 0.540$, $P < 0.001$) (Figures 2(h)–2(j)). These three KRT genes had much lower expression in normal tissues compared to HNSCC (Figure S1). These results showed that cancer cells with higher *ATG9B* expression had a phenotype closer to epithelial cells, which might partially explain the negative correlation between *ATG9B* expression and PNI and lymphatic vascular invasion in HNSCC. Moreover, we explored the protein levels of *ATG9B* in human HNSCC tissues. As expected, there was significantly lower *ATG9B* protein levels in tumor tissues compared to adjacent normal tissues (Supplementary Figure 2).

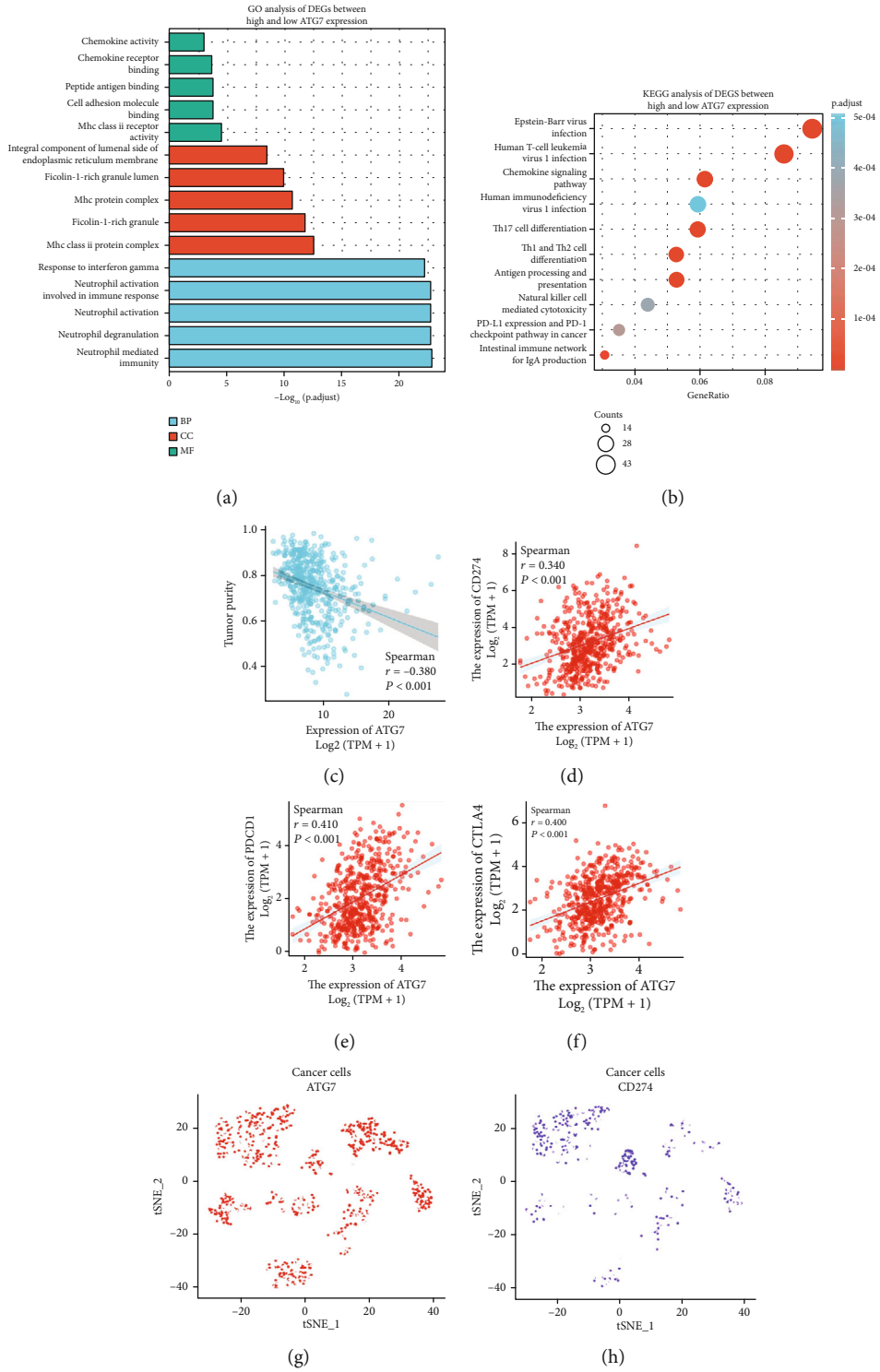

Figure 4: Continued.

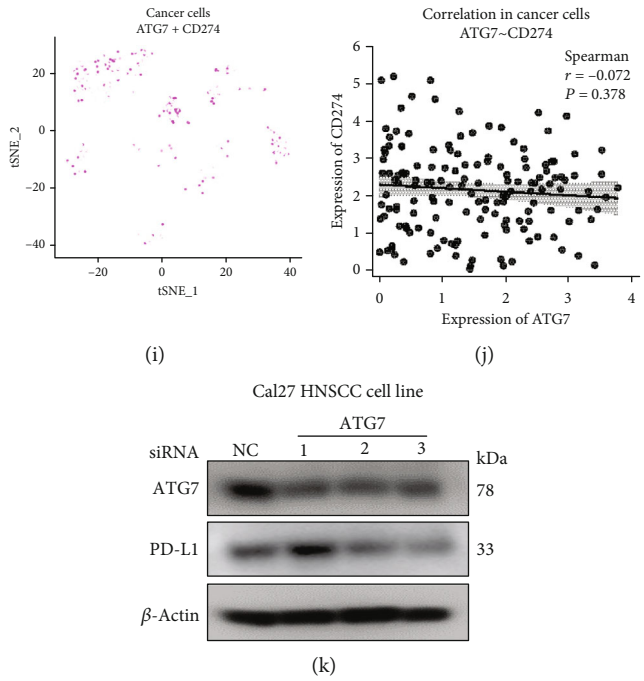

Figure 4: *ATG7* was involved in the tumor immune microenvironment (TIME) in HNSCC, but did not function in cancer cells. (a) GO analysis of different expression genes with a fold change >1.5 or <0.667 and an FDR < 0.05 based on the mRNA expression of *ATG7* in HNSCC in the TCGA database. (b) KEGG analysis of different expression genes with a fold change >1.5 or <0.667 and an FDR < 0.05 based on the mRNA expression of *ATG7* in HNSCC in the TCGA database. (c) The correlation between *ATG7* expression and tumor purity in HNSCC in the TCGA database. (d–f) *ATG7* was positively correlated with PD-L1, PD1, and CTLA4. (g–j) *ATG7* was not correlated with PD-L1 in cancer cells in GSE103322. (k) Knockdown of *ATG7* did not affect the expression of PD-L1 in the Cal27 HNSCC cell line.

Together, these results indicate that high *ATG9B* expression is positively correlated with the epithelial cell phenotype of HNSCC cells, which might contribute to an impaired EMT phenotype.

3.3. Verification of the Function of ATG9B in HNSCC through the Single-Cell Database. To further determine the distribution of *ATG9B* in HNSCC and verify its function in specific cell types, we mined the GSE103322 single-cell database (Figure 3(a)). We found that *ATG9B* was mainly expressed in cancer cells and not in immune and stromal cells (Figure 3(b)). Then, we verified the correlation between *ATG9B* and the KRT family. As expected, *ATG9B* was positively correlated with KRT23 ($r = 0.350$, $P = 0.002$), *KRT78* ($r = 0.360$, $P = 0.001$), and *KRT80* ($r = 0.520$, $P < 0.001$), which again proved that cancer cells with higher expression of *ATG9B* have a phenotype similar to the epithelial cell (Figures 3(c)–3(e)). Then, we focused on the cell cluster with high expression of *ATG9B*. The violin figure shows that *ATG9B* was mainly expressed in cancer cell cluster 13 (Figure 3(f)). We further identified the highly expressed genes in cluster 13 and ran a GO analysis. The results indicated that cancers in cluster 13 had more epidermal development, epidermal cell differentiation, and keratinocyte differentiation (Figure 3(g)). Finally, we identified the cancer cells in cluster 13 and the single cells expressing both *ATG9B* and *KRT23*, *KRT78*, or *KRT80* (Figures 3(i)–3(k)). Collectively, these results indicate that high *ATG9B* expression is positively correlated with the epithelial phenotype of single cancer cells through mining the HNSCC single-cell database.

3.4. ATG7 Was Involved in the Tumor Immune Microenvironment (TIME) in HNSCC, but Did Not Function in Cancer Cells. The transcriptomes of HNSCC patients in TCGA were divided into 2 groups according to *ATG7* mRNA expression. Differential gene expression with a fold change of >1.5 or <0.667 and an FDR < 0.05 was identified and underwent GO analysis. The GO items showed that *ATG7* was highly involved in the tumor immune microenvironment in HNSCC, including chemokine activity, MHC protein procession, and neutrophil activation (Figure 4(a)). KEGG analysis was conducted, and the top 10 items were correlated with immune response (Figure 4(b)). However, the "PD-L1 expression and PD-1 checkpoint pathway in cancer" item caught our attention. We then analyzed the relationship between expression of *ATG7* and tumor purity in HNSCC using the TCGA database. *ATG7* was negatively correlated with tumor purity ($r = -0.038$, $P < 0.001$), suggesting a positive correlation between high ATG expression and high infiltrating immune cells in HNSCC tumors (Figure 4(c)). The increased immune cells in TIME suggested that *ATG7* might enhance the antitumor immune response. However, further analysis of the correction between *ATG7* and immunosuppressive checkpoints showed that high expression of *ATG7* was correlated with high expression of PD-L1 ($r = 0.340$, $P < 0.001$), PD-1 ($r = 0.410$, $P < 0.001$), and

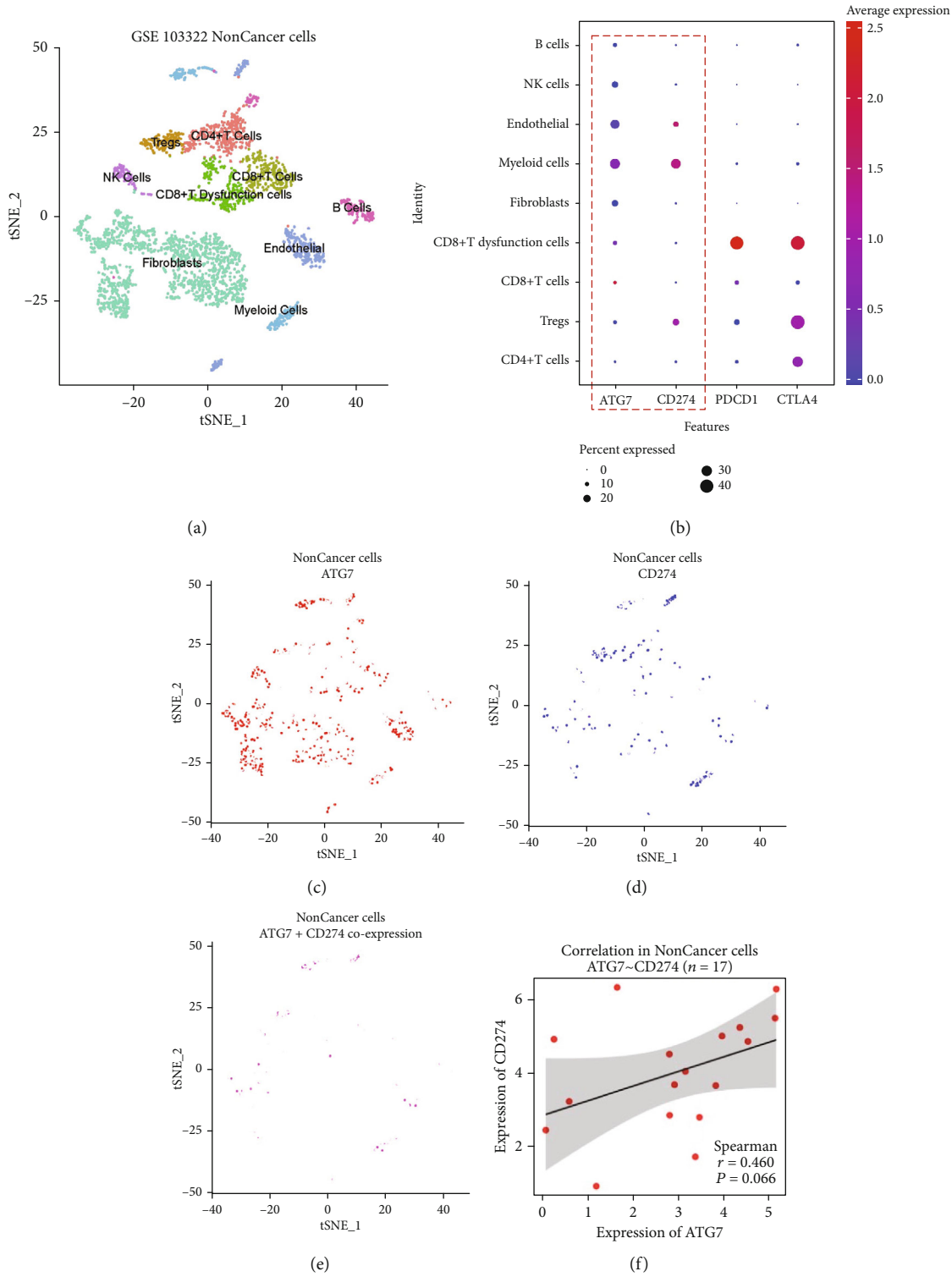

Figure 5: Continued.

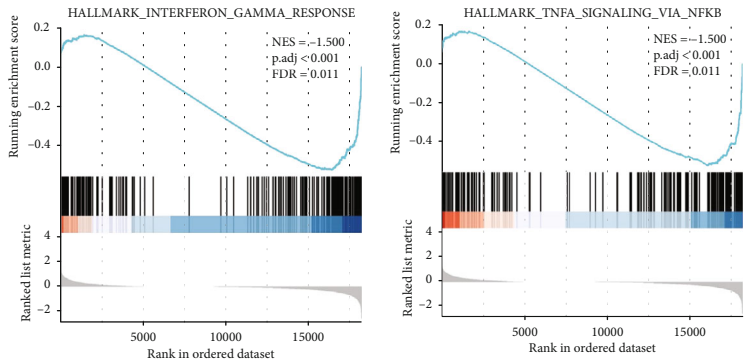

(g) (h)

Figure 5: High *ATG7* expression was correlated with high PD-L1 expression in noncancer cells in HNSCC in GSE103322. (a) Different clusters of noncancer cells in GSE103322. (b) *ATG7* had a similar distribution to PD-L1 but not PD1 or CTLA4 in noncancer cells. (c–f) Cells expressing both *ATG7* and PD-L1 were identified, and *ATG7* had a positive correlation with PD-L1. (g–h) Genes highly expressed in cells expressing both *ATG7* and PD-L1 underwent GSEA analysis.

CTLA4 ($r = 0.400$, $P < 0.001$) in HNSCC, which implied that ATG might be involved in immunosuppression in HNSCC (Figures 4(d)–4(e)).

To further determine whether *ATG7* exerts its immunosuppressive functions in cancer cells or immune cells, we analyzed the single-cell data from GSE103322. It is generally thought that cancer cells express high levels of PD-L1, thus suppressing the anticancer function of the immune system. We identified the cancer cells expressing both *ATG7* and PD-L1 but found no correlation between *ATG7* and PD-L1 in cancer cells (Figures 4(g)–4(j)). Finally, we found that the protein level of PD-L1 was not influenced by knockdown of *ATG7* in the Cal27 HNSCC cell line. Collectively, these data showed that *ATG7* was involved in TIME in HNSCC, and it potentially did not function in cancer cells.

3.5. High ATG7 Expression Was Correlated with High PD-L1 Expression in Noncancer Cells in HNSCC. To further determine the function of *ATG7* in HNSCC TIME, we further explored the correlation of *ATG7* and noncancer cells using GSE103322 (Figure 5(a)). Figure 5(b) shows the expression of ATG7, PD-L1, PD1, and CTLA4 in noncancer cells. We found that *ATG7* had a similar distribution to PD-L1 but not PD1 or CTLA4 in noncancer cells. Cells expressing both *ATG7* and PD-L1 were identified, and *ATG7* had a positive correlation with PD-L1 ($r = 0.460$, $P = 0.0660$) (Figures 5(c)–5(f)). Furthermore, genes highly expressed in cells expressing both *ATG7* and PD-L1 underwent GSEA analysis. Results showed that these cells had a downregulated response to interferonγ (NES = −1.500, FDR = 0.011) and TNFα ($r = 0.46$, $P = 0.066$) (Figures 5(g)–5(h)). These results further proved that *ATG7* exerted its immunosuppressive function in noncancer cells through regulating PD-L1 expression.

3.6. ATG7 Was Correlated with Myeloid Cells in HNSCC TIME. We have already revealed that *ATG7* was correlated with impaired immune function in HNSCC and mainly functioned in noncancer cells. We then investigated the cluster of noncancer cells influenced by ATG7. We mined 4 databases (TIMER, MCPcounter, EPIC, and CIBERSORT), and high *ATG7* expression was correlated with macrophages in 3 databases, dendritic cells in 2 databases, and CD8+T cells in 3 databases based on TCGA analysis (Figures 6(a)–6(d)). Furthermore, the expression of *ATG7* was mainly enriched in myeloid cells in GSE103322 (Figure 6(e)). The myeloid cells were reported to have adverse outcomes in cancer patients according to cancer types. Therefore, we further investigated the influence of myeloid cell proportion on overall survival in HNSCC through Cox regression models. A high proportion of myeloid cells was an adverse prognostic factor in the CIBERSORT (HR = 5.170$P < 0.0001$) and TIMER (HR = 27.2$P < 0.0001$) databases (Figure 6(f)). We next confirmed these correlations in HNSCC patients. The multiple immunofluorescence results showed that cancer cells with a high expression of *ATG7* did not have elevated expression of PD-L1, while CD68(+) myeloid cells had strong coexpression of *ATG7* and PD-L (Figures 7(a)–7(b)). Together, these data highlight a potential role for *ATG7* in myeloid cells, which may contribute to the immune suppressive microenvironment in HNSCC.

4. Discussion

The role of autophagy in cancer remains controversial. It is possible that both autophagy and autophagy-related genes play multifaceted roles depending on the tumor type and stage of the tumor. In HNSCC, Liu et al. revealed higher levels of cytoplasmic p62, suggesting impaired autophagy and its correlation with reduced overall and disease-specific survival [10]. However, elevated endogenous LC3-II expression has been reported in 90 oral cavity tumors, revealing the association of "high" levels of LC3-II with reduced overall survival. This supports the theory of autophagy reactivation during disease progression [22]. This uncertainty makes targeting autophagy for cancer therapy unpredictable. To overcome this challenge, it is important to determine the specific roles of different autophagy-related genes in both autophagy-dependent and -independent pathways. This understanding may contribute to precision autophagy-targeted therapies. In this research, we mined the TCGA

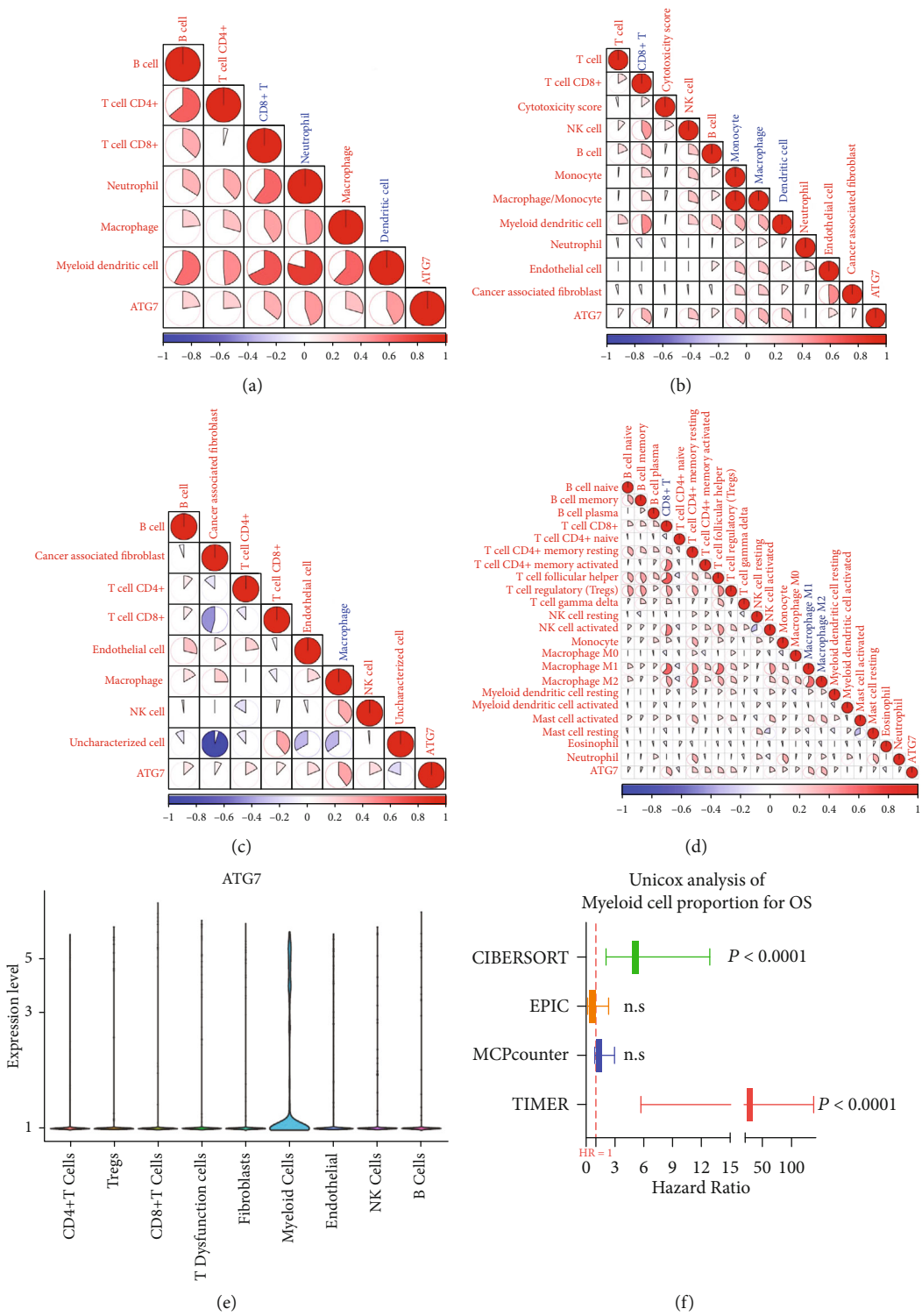

Figure 6: *ATG7* was correlated with high PD-L1 expression in myeloid cells in the HNSCC TIME. (a–d) Correlation between *ATG7* and noncancer immune cells in the TIMER, MCPcounter, EPIC, and CIBERSORT databases according to TCGA. (e) *ATG7* was mainly expressed in myeloid cells in GSE103322. (f) The high proportion of myeloid cell in tumors was correlated with poor overall survival-rates in the CIBERSORT and TIMER databases.

database and found that *ATG9B* and *ATG7* had noncanonical autophagy-independent functions in HNSCC.

We found that ATG9B was a strong protective factor in HNSCC patients. ATG9B downregulation is significantly correlated with high EMT in HNSCC. By mining the HNSCC single-cell database, we further proved that *ATG9B* mainly functions in cancer cells through enhancing the epithelial phenotype of cancer cells. The correlation between

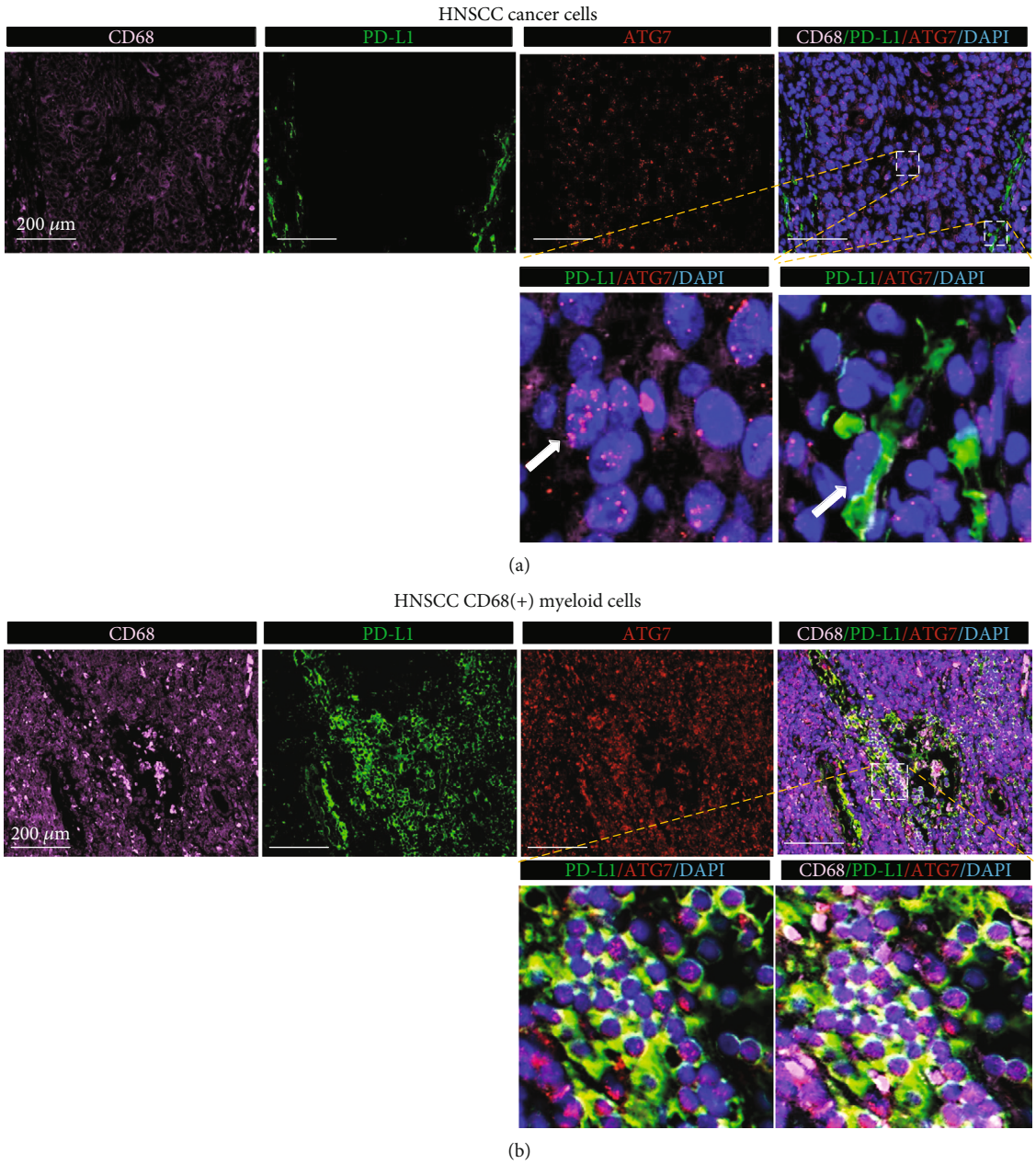

Figure 7: *ATG7* was coexpressed with PD-L1 in CD-68(+) myeloid cells but not cancer cells in HNSCC patient tissues. (a) Cancer cells with high expression of *ATG7* did not show high expression of PD-L1 in HNSCC patient tissues. (b) In CD68(+) myeloid cells, *ATG7* was coexpressed with PD-L1. Representative IHC images from 3 HNSCC tumor tissues.

autophagy and EMT is elusive [23]. On the one hand, cells are dependent on autophagy activation to survive during EMT. On the other hand, autophagy functions as a tumor-suppressive signal, which hinders the early phases of metastasis and activation of EMT [24]. It should be emphasized that in our verification in the single-cell database, *ATG9B* was not correlated with EMT markers (SNAIL, TWIST, and ZEB1), but did have a strong correlation with KRT family members. These results show that instead of influencing canonical EMT pathways like the WNT signaling pathway, *ATG9B* plays a more direct role in maintaining the epithelial phenotype of cancer cells. To our knowledge, there are no reports on *ATG9B* and cancer EMT, and further studies should focus on how *ATG9B* is involved in maintaining the epithelial phenotype of cancer cells instead of participating in EMT signaling pathways.

Another intriguing finding of our research was that *ATG7* had a strong correlation with the high expression of PD-L1 in TIME. Interestingly, *ATG7* seemed to function in myeloid cells instead of cancer cells in TIME. It is widely acknowledged that the upregulation of PD-L1 in cancer cells or upregulation of PD-1 or CTLA4 results in the immunosuppressive environment in TIME. However, it is easy to overlook that the increased expression of PD-L1 in immune

cells can have the same effects. Fleming et al. found that mouse melanoma cells upregulated the expression of PD-L1 on mouse immature myeloid cells, leading to suppression of T-cell activation [25]. Zhang et al. specifically targeted PD-L1 in tumor-associated myeloid cells and showed a large synergistic curative effect with radiation therapy [26]. Increasing numbers of studies are focusing on the contribution of myeloid cell-derived PD-L1 instead of cancer-derived PD-L1 to the immunosuppressive environment in TIME [27, 28]. To our knowledge, there is only one study showing that *ATG7* was correlated with PD-L1 expression in bladder cancer cells [29]. Our findings preliminarily confirm that higher expression of *ATG7* was closely correlated with high PD-L1 expression in myeloid cells in HNSCC. The molecular mechanisms need to be further elucidated. Combined therapy targeting *ATG7* and PD-L1 in HNSCC may be a potential treatment.

There are also some limitations of the present study. Of particular, the correlation between the *ATG7* and PD-L1 expression in myeloid cells should be further verified using biocellular and biomolecular assays. Moreover, the therapeutical efficacy of the combination of ATG7-targeted agents and immune checkpoint blockade therapies can be further explored on multiple preclinical models.

Collectively, we preliminarily verified two noncanonical autophagy-independent functions of *ATG9B* and *ATG7* in HNSCC through the TCGA and single-cell databases. These findings increase understanding of the role of autophagy and autophagy genes in HNSCC and may contribute to precision autophagy-targeted therapies in HNSCC.

Data Availability

The open-access datasets are available through the following URL: GSE103322 (https://www.ncbi.nlm.nih.gov/geo/query/acc.cgi?acc=GSE103322/) and the Cancer Genome Atlas (TCGA) HNSC project (http://xena.ucsc.edu/). All data generated or analyzed during this study are available from the corresponding author on reasonable request.

Conflicts of Interest

The authors declare that there is no conflict of interest regarding the publication of this article.

Authors' Contributions

Yibo Guo and Yiting Sun have contributed equally to this work.

Acknowledgments

This work was supported by the grants from the National Natural Science Foundation of China (No. 81872189).

Supplementary Materials

Figure S1: Expression of KRT genes in tumor and normal tissues in the TCGA-HNSCC cohort. Figure S2: ATG9B protein levels in human HNSCC tissues and paired adjacent normal tissues. *(Supplementary Materials)*

References

[1] V. M. Aita, X. H. Liang, V. V. Murty et al., "Cloning and genomic organization of _beclin 1,_ a candidate tumor suppressor gene on chromosome 17q21," *Genomics*, vol. 59, no. 1, pp. 59–65, 1999.

[2] A. C. Kimmelman, "The dynamic nature of autophagy in cancer," *Genes & Development*, vol. 25, no. 19, pp. 1999–2010, 2011.

[3] J. M. M. Levy, C. G. Towers, and A. Thorburn, "Targeting autophagy in cancer," *Nature Reviews Cancer*, vol. 17, no. 9, pp. 528–542, 2017.

[4] M. H. Lee, D. Koh, H. Na et al., "MTA1 is a novel regulator of autophagy that induces tamoxifen resistance in breast cancer cells," *Autophagy*, vol. 14, no. 5, pp. 812–824, 2018.

[5] K. L. Bryant, C. A. Stalnecker, D. Zeitouni et al., "Combination of ERK and autophagy inhibition as a treatment approach for pancreatic cancer," *Nature Medicine*, vol. 25, no. 4, pp. 628–640, 2019.

[6] A. C. Kimmelman and E. White, "Autophagy and tumor metabolism," *Cell Metabolism*, vol. 25, no. 5, pp. 1037–1043, 2017.

[7] L. Galluzzi, J. M. Bravo-San Pedro, S. Demaria, S. C. Formenti, and G. Kroemer, "Activating autophagy to potentiate immunogenic chemotherapy and radiation therapy," *Nature Reviews. Clinical Oncology*, vol. 14, no. 4, pp. 247–258, 2017.

[8] K. Yamamoto, A. Venida, J. Yano et al., "Autophagy promotes immune evasion of pancreatic cancer by degrading MHC-I," *Nature*, vol. 581, no. 7806, pp. 100–105, 2020.

[9] J. Ferlay, I. Soerjomataram, R. Dikshit et al., "Cancer incidence and mortality worldwide: sources, methods and major patterns in GLOBOCAN 2012," *International Journal of Cancer*, vol. 136, no. 5, pp. E359–E386, 2015.

[10] J. L. Liu, F. F. Chen, J. Lung et al., "Prognostic significance of p62/SQSTM1 subcellular localization and LC3B in oral squamous cell carcinoma," *British Journal of Cancer*, vol. 111, no. 5, pp. 944–954, 2014.

[11] X. H. Ma, S. Piao, D. Wang et al., "Measurements of tumor cell autophagy predict invasiveness, resistance to chemotherapy, and survival in melanoma," *Clinical Cancer Research*, vol. 17, no. 10, pp. 3478–3489, 2011.

[12] B. Levine and G. Kroemer, "Biological functions of autophagy genes: a disease perspective," *Cell*, vol. 176, no. 1–2, pp. 11–42, 2019.

[13] M. E. Ritchie, B. Phipson, D. Wu et al., "Limma powers differential expression analyses for RNA-sequencing and microarray studies," *Nucleic Acids Research*, vol. 43, no. 7, pp. e47–e47, 2015.

[14] G. Yu, L. G. Wang, Y. Han, and Q. Y. He, "clusterProfiler: an R package for comparing biological themes among gene clusters," *OMICS: A Journal of Integrative Biology*, vol. 16, no. 5, pp. 284–287, 2012.

[15] K. Yoshihara, M. Shahmoradgoli, E. Martínez et al., "Inferring tumour purity and stromal and immune cell admixture from expression data," *Nature Communications*, vol. 4, no. 1, p. 2612, 2013.

[16] T. Li, J. Fan, B. Wang et al., "TIMER: a web server for comprehensive analysis of tumor-infiltrating immune cells," *Cancer Research*, vol. 77, no. 21, pp. e108–e110, 2017.

[17] A. M. Newman, C. L. Liu, M. R. Green et al., "Robust enumeration of cell subsets from tissue expression profiles," *Nature Methods*, vol. 12, no. 5, pp. 453–457, 2015.

[18] E. Becht, N. A. Giraldo, L. Lacroix et al., "Estimating the population abundance of tissue-infiltrating immune and stromal cell populations using gene expression," *Genome Biology*, vol. 17, no. 1, p. 218, 2016.

[19] J. Racle, K. de Jonge, P. Baumgaertner, D. E. Speiser, and D. Gfeller, "Simultaneous enumeration of cancer and immune cell types from bulk tumor gene expression data," *eLife*, vol. 6, 2017https://cdn.elifesciences.org/articles/26476/elife-26476-v2.pdf.

[20] S. V. Puram, I. Tirosh, A. S. Parikh et al., "Single-cell transcriptomic analysis of primary and metastatic tumor ecosystems in head and neck cancer," *Cell*, vol. 171, no. 7, pp. 1611–1624.e24, 2017.

[21] T. Stuart, A. Butler, P. Hoffman et al., "Comprehensive integration of single-cell data," *Cell*, vol. 177, no. 7, pp. 1888–1902.e21, 2019.

[22] J. Y. Tang, E. Hsi, Y. C. Huang, N. C. Hsu, P. Y. Chu, and C. Y. Chai, "High LC3 expression correlates with poor survival in patients with oral squamous cell carcinoma," *Human Pathology*, vol. 44, no. 11, pp. 2558–2562, 2013.

[23] H. T. Chen, H. Liu, M. J. Mao et al., "Crosstalk between autophagy and epithelial-mesenchymal transition and its application in cancer therapy," *Molecular Cancer*, vol. 18, no. 1, p. 101, 2019.

[24] M. Gugnoni, V. Sancisi, G. Manzotti, G. Gandolfi, and A. Ciarrocchi, "Autophagy and epithelial-mesenchymal transition: an intricate interplay in cancer," *Cell Death & Disease*, vol. 7, no. 12, pp. e2520–e2520, 2016.

[25] V. Fleming, X. Hu, C. Weller et al., "Melanoma extracellular vesicles generate immunosuppressive myeloid cells by upregulating PD-L1 via TLR4 signaling," *Cancer Research*, vol. 79, no. 18, pp. 4715–4728, 2019.

[26] P. Zhang, J. Miska, C. Lee-Chang et al., "Therapeutic targeting of tumor-associated myeloid cells synergizes with radiation therapy for glioblastoma," *Proceedings of the National Academy of Sciences*, vol. 116, no. 47, pp. 23714–23723, 2019.

[27] Z. C. Ding, X. Lu, M. Yu et al., "Immunosuppressive myeloid cells induced by chemotherapy attenuate antitumor CD4+ T-cell responses through the PD-1-PD-L1 axis," *Cancer Research*, vol. 74, no. 13, pp. 3441–3453, 2014.

[28] J. P. Antonios, H. Soto, R. G. Everson et al., "Immunosuppressive tumor-infiltrating myeloid cells mediate adaptive immune resistance via a PD-1/PD-L1 mechanism in glioblastoma," *Neuro-Oncology*, vol. 19, no. 6, article now287, 2017.

[29] J. Zhu, Y. Li, Y. Luo et al., "A feedback loop formed by ATG7/autophagy, FOXO3a/miR-145 and PD-L1 regulates stem-like properties and invasion in human bladder cancer," *Cancers*, vol. 11, no. 3, p. 349, 2019.

Hindawi
Journal of Oncology
Volume 2022, Article ID 1205353, 14 pages
https://doi.org/10.1155/2022/1205353

Research Article

RBM24 Mediates Lymph Node Metastasis and Epithelial-Mesenchymal Transition in Human Hypopharyngeal Squamous Cell Carcinoma by Regulating Twist1

Yuhong Liu, Min Pan, Tao Lu, Yanshi Li, Dan Yu, Zhihai Wang, and Guohua Hu

Department of Otorhinolaryngology, First Affiliated Hospital of Chongqing Medical University, Chongqing 400016, China

Correspondence should be addressed to Guohua Hu; hghcq@sina.com

Received 23 June 2022; Revised 10 August 2022; Accepted 9 September 2022; Published 29 September 2022

Academic Editor: Zhi-En Feng

Objective. Despite the target RNA regulatory action of RBM24 (RNA Binding Motif 24), a protein implicated in multiple carcinomas, its role in HSCC remains unclear. Our study probed to understand the effect of RBM24 on HSCC. *Materials and Methods.* A combination of qRT-PCR, IHC, and western blot was employed to assess the HSCC tissue level of RBM24. The colony formation and CCK-8 assays were performed to estimate cellular proliferative potential, whereas the transwell assay was conducted to examine invasive and metastatic potential. The FaDu cell motility was assessed via the scratch-wound assay and EMT (epithelial-mesenchymal transition) by adopting qRT-PCR in conjunction with western blot and IF (immunofluorescence). The in-vivo effect of RBM24 on HSCC was investigated through modeling metastasis to the popliteal LNs (lymph nodes). *Results.* Among HSCC patients showing metastasis to LNs, prominent RBM24 downregulation was noted, with an intrinsic association between low RBM24 level and poor outcome. Knocking down RBM24 promoted cell multiplication, migration, and infiltration, while overexpression led to the opposite effects and inhibited the EMT. RBM24's suppressive action against the FaDu cell mobility and invasion was reversed by Twist1 overexpression. RBM24's suppressive actions against the tumor evolution and LN metastasis in HSCC in-vivo were also validated. *Conclusion.* As a carcinoma inhibitor gene, RBM24 regulates Twist1 to achieve LN metastasis and EMT suppression in HSCC.

1. Introduction

As a highly invasive malignancy representing almost 0.4% of carcinomas [1], HSCC (hypopharyngeal squamous cell carcinoma), despite being rare, is prognostically inferior to any cancers of the head and neck, with a relative five-year survival between 25% and 45% [2–5]. According to Ho et al., a chief independent factor linked tightly to the mortality risk among patients with hypopharyngeal carcinomas was the metastatic LN (lymph node) count [6]. Although the diagnostic measures and therapeutic regimes have tremendously improved, the condition in HSCC patients usually progressed to an advanced stage upon initial diagnosis, showing cervical LN or distant metastasis, and the prevalence of LN metastasis was 65-80% [7, 8]. Thus, understanding the malignant progression mechanisms in HSCC with LN metastasis at the molecular level is necessary for early screening biomarkers to enhance diagnostic precision. Implicated in regulating the target RNA substrates nearly over the whole life cycle, RBPs (RNA-binding proteins) may exert a kernel function in gene expression networks [9]. An RBP census in humans demonstrated that 7.5% of genes encode proteins in gene expression modulation [10]. In addition, RBPs are considered carcinogenesis participants [11]. Thus, transcript modulation is achieved by classic RBPs through the formation of RNP (ribonucleoprotein) complexes with corresponding RNA targets through the RBDs (RNA-binding domains), including the hnRNP KH (K homology) domains, the RRMs (RNA recognition motifs), and the S1 domains [12]. An RBP, RBM24 (RNA Binding Motif 24), encompasses a highly conserved RRM consisting of 2 submotifs (RNP1 and RNP2) [13], which could promote the cardiomyocytic differentiation from embryonic stem cells through the alternative splicing modulation [14] and

improve the myogenic differentiation through transcript stability regulation of myogenin mRNA by binding to its 3′-UTR (3′-untranslated region) [15] in mice. Although the role of RBM24 as a carcinoma inhibitor gene has been demonstrated in NPC (nasopharyngeal carcinoma) [16], CRC (colorectal cancer) [17], and hepatic carcinoma [18], its precise function in HSCC is elusive.

Owing to EMT (epithelial-mesenchymal transition), an important event linked tightly to carcinoma progression capable of mediating metastasis, the tumor cells can invade the paracarcinoma tissues and achieve metastasis [19]. Twist1, a member of the basic helix-loop-helix protein family, is a primary regulator of EMT. Upregulation of Twist1 facilitates the malignant progression of HSCC and is related to poor prognosis [20, 21]. In contrast, Twist1 overexpression makes the FaDu cells less chemically sensitive to Taxol [22], despite its unclear function in the LN metastasis in HSCC.

Our work is the first to discover RBM24 downregulation among HSCC patients showing LN metastasis. We aimed to prove the capability of RBM24 to suppress the multiplication and metastasis of HSCC cells both in-vivo and in-vitro. Besides, it could be demonstrated that Twist1 overexpression, RBM24's downstream target, rescues RBM24's suppressive actions against the FaDu cell invasion, migration, and EMT. These outcomes could reveal that RBM24 probably targets Twist1 to achieve metastatic LN inhibition.

2. Materials and Methods

2.1. Patients and Tissue Samples. In this study, fresh HSCC tissues and the corresponding adjacent normal tissues were derived from patients suffering from surgery at the First Affiliated Hospital of Chongqing Medical University and were maintained at −80°C to perform protein and RNA extraction. The surgical specimens for IHC were collected from patients who underwent surgery at the First Affiliated Hospital of Chongqing Medical University from 2015 to 2019. The criteria for inclusion were: (i) diagnosed with HSCC pathologically. (ii) Laryngectomy performed only once. (iii) Completion of Follow-up data and electronic nasopharyngoscopy, CT, or MRI examination was performed every six months after the initial operation. Besides, the exclusion criteria were: (i) preoperative radiotherapy, chemotherapy, or targeted therapy had been performed. (ii) The diagnosis was another type of tumor. Two experienced pathologists performed pathological diagnosis and tumor grading. In the end, 57 patients diagnosed with HSCC were included in the current work.

2.2. Immunohistochemistry (IHC) and Scoring. Paraffin-embedded tissue sections (4 μm) were deparaffinized in xylene and rehydrated in a graded ethanol series. Sections were heated in citrate buffer for 15 min at 100°C for antigen retrieval. Next, slides were rinsed in phosphate-buffered saline (PBS) and treated with peroxidase block at 37°C for 10 min. After blocking with 10% normal goat serum at 37°C for 15 min to minimize nonspecific staining, the slides were incubated with an anti-RBM24 primary antibody (1 : 200; ab94567, Abcam, Cambridge, UK) overnight at 4°C. The next day, the slides were incubated with a horseradish peroxidase (HRP)-conjugated polyclonal goat secondary antibody for 15 min and incubated with diaminobenzidine (DAB) reagents (ZSGB-BIO, Beijing, China) at room temperature for 1 min for detection of antigen-antibody interaction signals. Finally, the slides were counterstained with hematoxylin for 20 sec. Slides incubated with PBS instead of the primary antibody were used as a negative control. All slides were visualized by two experienced pathologists. Determinants of IHC score included the ratio of tumor cells positive for RBM24 and the staining intensity. The first determinant was scored 0 for 0-5%, 1 for 5-25%, 2 for 25-50%, 3 for 50-75%, or 4 for 75-100%. The second determinant was scored 0 if negatively stained, 1 for weakly stained, 2 for moderately stained, or 3 for strongly stained. The product of the preceding two scores constituted the final IHC score. The RBM24 expression classification was accomplished by the ROC curve-based assessment of IHC scores, with a threshold of 4. The expression was considered low if the score < 4, whereas high if ≥ 4.

2.3. Cell Line and Culture. Human HSCC FaDu cells were procured from the Chinese Academy of Sciences (Shanghai, China) and maintained at 37°C and 5% CO_2 conditions in the MEM (minimal essential medium) (Boster, USA) with 10% FBS (PAN-Biotech, Adenbach, Germany) and 1% penicillin-streptomycin.

2.4. Lentiviral Transduction. The GFP (green fluorescent protein)-expressing lentiviral particles for RBM24 overexpression, namely OE-RBM24 and Control, were procured from GeneChem (Shanghai, China). After reaching 20-40% confluency, FaDu cells were plated onto a 6-well microplate, followed by infection using lentiviral particles at a 10 MOI (multiplicity of infection). The cells were screened after 48-72 h of infection using MEM with 2 μg/mL puromycin (Beyotime, Shanghai, China). Cells were further harvested for assessment via qRT (quantitative real-time)-PCR in conjunction with western blot.

2.5. siRNA Transfection. siRNA oligonucleotides against human RBM24 (Si-RBM24, 5′-GAG CUG CAU ACG CAC AAU ATT-3′ and 5′-UAU UGU GCG UAU GCA GCU CTT-3′) and a scrambled siRNA (Si-NC sense, 5′-UUC UCC GAA CGU GUC ACG UTT-3′ and antisense, 5′-ACG UGA CAC GUU CGG AGA ATT-3′) were obtained from GenePharma (Shanghai, China) to knockdown RBM24. In addition, FaDu cells were seeded into a six-well plate, and Lipofectamine RNAiMAX (Invitrogen, CA, USA) was utilized to transfect these siRNAs according to the manufacturer's instructions. In addition, the knockdown efficiency was examined using qRT-PCR and western blotting.

2.6. Plasmid Transfection. A Lipofectamine 3000 system (Invitrogen, Carlsbad, USA) was employed for the transfection of the PCMV (control plasmid) and OE-Twist1 (Twist1

overexpressing plasmid) (Tsingke Biotechnology, Nanjing, China), into the FaDu cells.

2.7. Western Blotting (WB) Analysis and Antibodies. Total proteins were sampled from FaDu cells and tissues via a kit (KeyGen, Nanjing, China). A BCA Assay Kit (Beyotime, Shanghai, China) was utilized to examine the protein concentration. Hybrid proteins were isolated via SDS-PAGE (10%), placed onto the PVDF (polyvinylidene fluoride) membranes (Biosharp, Hefei, China), subjected to a 15-minute blockage using buffer (Beyotime, Shanghai, China), and incubated overnight using 1 : 1000 anti-RBM24 (ab94567), 1 : 5000 anti-Vimentin (ab92547; both Abcam, Cambridge, UK), 1 : 1000 anti-E-cadherin (#3195), 1 : 1000 anti-N-cadherin (#13116; both Cell Signaling Technology, MA, USA), 1 : 1000 anti-Twist1 (AF4009; Affinity, Jiangsu, China), and 1 : 3000 anti-GAPDH (AF1186; Beyotime, Shanghai, China) antibodies at 4°C. Subsequently, 1 h processing of the membranes was accomplished using 1 : 5000 anti-rabbit goat IgG (A0208; Beyotime, Shanghai, China) at ambient temperature. Finally, an XRS+ imaging system (ChemiDoc™; Bio-Rad, CA, USA) was utilized to examine the specific proteins.

2.8. qRT-PCR Analysis. Total RNA was extracted using a Total RNA Kit I (Omega, Norcross, USA). An RT Reagent Kit with gDNA Eraser (Perfect Real Time) (PrimeScript™; Takara, Dalian, China) was employed for complementary DNA synthesis and assessed using qRT-PCR using an SYBR PrimeScript™ RT-PCR Kit (Takara, Dalian, China). The $2^{-\Delta\Delta Ct}$ approach was applied for the mRNA level assessment. Table 1 presents the primer details.

2.9. Cell Proliferation Assay. Cell proliferation was examined using Cell Counting Kit-8 (CCK-8; GlpBio, Montclair, CA, USA) reagent. FaDu cells were plated at 2,000/well onto a 96-well plate. Subsequently, CCK-8 (10 μL) was added to each well, and the 96-well plate was incubated at 37°C containing 5% CO_2 for 1 h. Subsequently, the absorbance was assessed at 450 nm, and data were collected continuously for 96 h.

2.10. Colony Formation Assay. FaDu cells were plated at 1,000/well onto a 6-well microplate and incubated for 2 weeks in 10% FBS-MEM. The cells were then immobilized using methanol, stained with crystal violet (0.5%), and colonies were quantified, comprising a minimum of 50 cells.

2.11. Transwell Migration and Invasion Assays. Transwell assays were performed for the invasive and migratory capacity assessment of FaDu cells. The chambers were filled with membranes (pore size: 8 μm; Corning, NY, USA) coated by Matrigel (BD Biosciences, MA, USA) or noncoated membranes. The upper chambers were added with 5×10^4 cell-involving serum-free MEM (200 μL), whereas the lower chambers with 20% FBS-MEM (600 μL). Further, the cells were immobilized in methanol for 48 h later, subjected to the crystal violet (0.5%) staining, and quantified microscopically.

Table 1: Primer sequences.

Gene name	Primer sequences (5′-3′)
RBM24	Forward: GAA CCT GGC ATA CTT AGG AGC A Reverse: AGG TCT TTG TAT AAG GGC TGG A
E-cadherin	Forward: TGC CCA GAA AAT GAA AAA GG Reverse: GTG TAT GTG GCA ATG CGT TC
N-cadherin	Forward: GAC AAT GCC CCT CAA GTG TT Reverse: CCA TTA AGC CGA GTG ATG GT
Vimentin	Forward: GAG AAC TTT GCC GTT GAA GC Reverse: GCT TCC TGT AGG TGG CAA TC
Twist1	Forward: ACA AGC TGA GCA AGA TTC AGA CC Reverse: TCC AGA CCG AGA AGG CGT AG
Snail	Forward: GCG AGC TGC AGG ACT CTA AT Reverse: CCT CAT CTG ACA GGG AGG TC
Slug	Forward: TGA TGA AGA GGA AAG ACT ACAG Reverse: GCTCACATATTCCTTGTCACAG
ZEB1	Forward: TGC ACT GAG TGT GGA AAA GC Reverse: TGG TGA TGC TGA AAG AGA CG
GAPDH	Forward: GGA GTC CAC TGG CGT CTT CA Reverse: GTC ATG AGT CCT TCC ACG ATA CC

2.12. Wound Healing Assay. Linear scratches were created in the single layers of confluent FaDu cells, kept in 6-well microplates, using 200-μL disinfected pipette tips. PBS (Phosphate Buffer Saline) was used to clear the cellular debris, and microscopic monitoring of the wound closure was accomplished separately at 0 h and 24 h following injury.

2.13. Immunofluorescence (IF) Assay. In a 24-well microplate, FaDu cells were inoculated on coverslips, fixed in paraformaldehyde (4%) for 15 min, and, where necessary, permeabilized for 20 min using Triton X-100 (0.5%). The coverslips were incubated overnight in 1 : 100 anti-E-cadherin (#3195), 1 : 100 anti-N-cadherin (#13116; both Cell Signaling Technology, Danvers, USA) together with 1 : 500 anti-Vimentin (ab92547, Abcam, Cambridge, UK) antibodies at 4°C after a 1 h blockage in goat serum (Beyotime, Shanghai, China). On the following day, these coverslips were processed for 1 h using a 1 : 250 fluorescent secondary antibody (ab150078, Abcam, Cambridge, UK) and subsequent 5 min processing with DAPI (Beyotime, Shanghai, China) at ambient temperature. After applying the antifade mounting medium to slow the fluorescent quenching, a laser scanning confocal microscope was utilized to surveil and photograph the coverslips.

2.14. Animal Experiments. Murine models of popliteal LN metastasis were created using nude male BALB/c mice aged 5 weeks (Tengxin, Chongqing, China), reared in the Animal Laboratory of Chongqing Medical University under SPF conditions. The mice were categorized randomly into two groups (5 mice per group) and exposed to injection in the footpads with 2×10^6 FaDu cells transfected with empty vector (FaDu-Control cells) or FaDu cells with stable overexpression of RBM24 (FaDu-OE-RBM24 cells) suspended in 30 μL PBS. A caliper was utilized to quantify the tumor dimensions, and the murine body weight was evaluated at

5 d intervals. Fifteen days following cellular implantation, an Indigo 2.0.5.0 (Berthold Technologies, Germany) was utilized to assess the tumor evolution and LN metastasis through in-vivo imaging. The mice were killed twenty-five days later, and their primary tumor tissues, along with LNs, were harvested for embedding in paraffin. The computational formula for tumor volume was $0.5 \times \text{length} \times \text{width}^2$. For IHC tissues staining, 1 : 200 anti-RBM24 (ab94567), 1 : 250 anti-Vimentin (ab92547; both Abcam, Cambridge, UK), 1 : 100 anti-Twist1 (AF4009, Affinity), and 1 : 400 anti-E-cadherin (#3195, Cell Signaling Technology, MA, USA) antibodies were adopted. H&E (hematoxylin and eosin) staining was used for LNs. Moreover, the murine experiments' approval was acquired from the First Affiliated Hospital of Chongqing Medical University's Ethics Committee.

2.15. Statistical Analysis. This study utilized SPSS 22.0 (IBM Corp, Armonk, NY, USA) and GraphPad Prism 8.0 (GraphPad, San Diego, USA) to perform statistical analysis. Student's *t*-test or the Mann–Whitney *U* test was used to assess the significance of differences between two groups, while one-way ANOVA was used to compare three or more groups. Correlations between the IHC expression of RBM24 and clinicopathological characteristics were assessed using Pearson's chi-squared test or Fisher's exact test. The Kaplan-Meier analysis with the logrank test was adopted to evaluate overall survival (OS). The data are represented as the mean ± standard error of the mean (SEM) values, and a *p*value < 0.05 was regarded as statistically significant.

3. Results

3.1. RBM24 Was Downregulated in HSCC Patients with LN Metastasis. In this study, transcriptome sequencing was performed to identify the differentially expressed genes (DEmRNAs) in HSCC patients who had or did not have LN metastasis in our former research [23, 24]. RBM24 was identified as one downregulated gene in the LN metastasis group. Several members of RRM family have been reported to play vital role in cancer metastasis [25, 26], and a bioinformatics study based on data from TCGA database suggested RBM24 might be a prognostic-related gene in head and neck squamous cell carcinoma [27]. But, the role of RBM24 in HSCC has not been expounded yet. Subsequently, this study detected the RBM24 expression at the mRNA and protein levels. Our study found that the mRNA level of RBM24 in eight LN metastasis cases was lower than in both the eight adjacent normal cases ($p < 0.01$) and the 8 cases that did not have LN metastasis ($p < 0.05$) (Figure 1(a)). Consequently, the RBM24 protein level was lower in five LN metastasis cases than in the other two groups (five cases without LN metastasis and five corresponding adjacent normal tissues) through WB analysis ($p < 0.05$) (Figure 1(b)). In addition, RBM24 expression in tissues was examined by IHC analysis. Figure 1(c) showed the differential staining of RBM24 in HSCC tissues and the staining of RBM24 in non-LN metastatic tissues was stronger than those in LN metastatic tissues. The proportion of tissues with low RBM24 expression was higher in those undergoing LN metastasis (25/41 [61.0%]) than those without LN metastasis (2/16 [12.5%]) ($p < 0.001$; Table 2). Moreover, this study evaluated the associations between RBM24 expression and clinical characteristics in 57 HSCC patients and found that RBM24 expression was correlated with tumor stage ($p < 0.01$) as well as LN stage ($p < 0.001$) but not with age, sex, or pathological stage (Table 3). According to Kaplan-Meier survival analysis, those who had low RBM24 expression had poor overall survival ($p < 0.05$) (Figure 1(d)). All the findings suggested that RBM24 was downregulated in HSCC patients with LN metastasis, showing a close association with poor prognosis.

3.2. Inhibition of RBM24 Stimulated the Proliferation, Migration, and Invasion of FaDu Cells. qRT-PCR combined with WB analysis was conducted to validate the expression of RBM24 to investigate RBM24 biofunctionality in FaDu cells. The RBM24 siRNA#1, #2, and #3, together with the Si-NC (control siRNA), were used to transfect the FaDu cells. The knockdown of RBM24 was found to be most efficient with siRNA#3 (Si-RBM24) (Supplementary Figures 1(a) and 1(b), Figures 2(a) and 2(b)) and chosen for further investigations. According to the colony formation and proliferation assay, the FaDu cell multiplication was facilitated by suppressing RBM24 (Figures 2(c) and 2(d)). Next, more FaDu cells went through the upper chambers in the Si-RBM24 group compared with the Control and Si-NC group according to transwell migration and invasion assays (Figure 2(e)), indicating the RBM24 knockdown improved the invasiveness and motility of FaDu cells. Besides, the wound healing assay showed knockdown of RBM24 increased the migration speed of FaDu cells at 24 hours after injury (Figure 2(f)), suggesting the RBM24 knockdown enhanced wound healing capacity of FaDu cells. In conclusion, deletion of RBM24 could promote the proliferation, invasion, and migration of FaDu cells.

3.3. Overexpression of RBM24 Restrained the Proliferation, Migration as well as Invasion of FaDu Cells. This study generated FaDu-OE-RBM24 cells by infection with lentiviral particles and evaluated the RBM24 overexpression efficiency using qRT-PCR (Figure 3(a)) and WB (Figure 3(b)) analyses. As the colony formation and proliferation assays indicated, the RBM24 overexpression in FaDu cells led to multiplication reduction (Figures 3(c) and 3(d). The transwell assay exhibited less FaDu cells went through the upper chambers in the OE-RBM24 group compared with the Control group (Figure 3(e)), indicating RBM24 overexpression led to invasive and migratory inhibition of FaDu cells. Besides, wound healing assay showed the RBM24 overexpression decreased the migration speed of FaDu cells at 24 hours after injury (Figure 3(f)), suggesting overexpression of RBM24 led to migratory inhibition of FaDu cells. These findings suggested the regulatory role of RBM24 in the FaDu cell multiplicative, invasive, and migratory potential.

3.4. Overexpression of RBM24 Downregulated Twist1 and Hindered EMT in FaDu Cells. The pivotal effects of EMT on head and neck squamous cell carcinoma metastasis

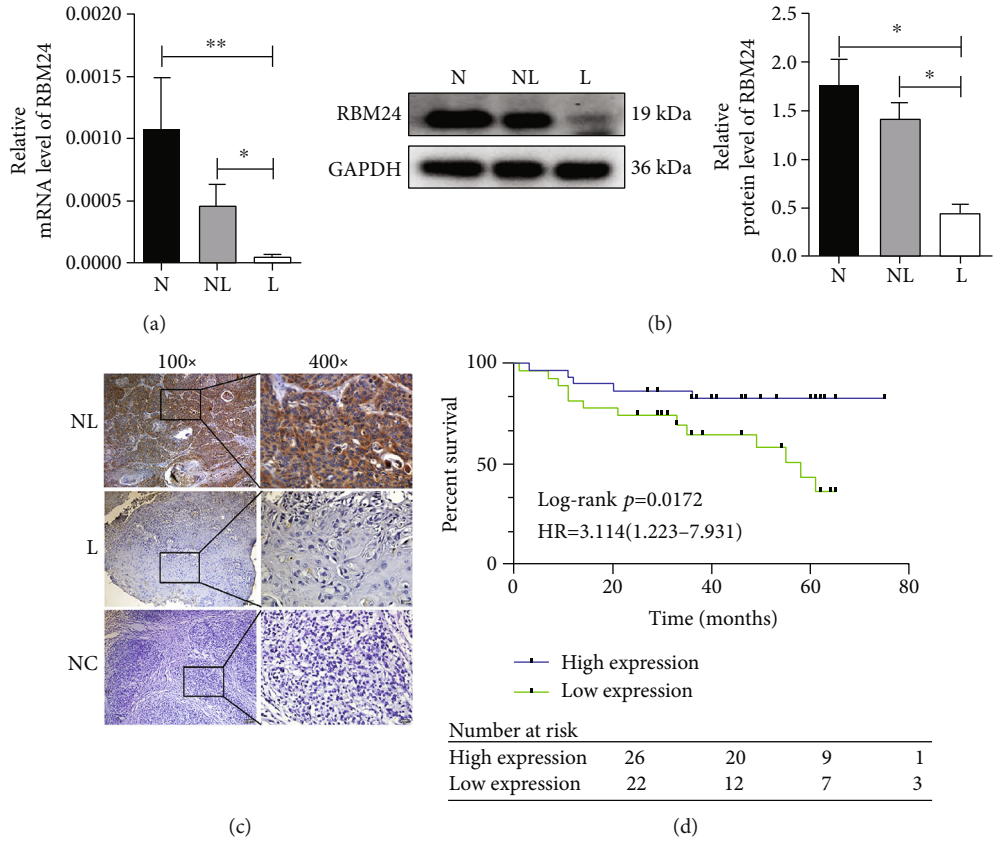

Figure 1: Downregulated RBM24 among the HSCC patients presenting LN metastasis was linked to poor outcomes. (a and b) The qRT-PCR and WB outcomes for RBM24 level in HSCC. (c) Typical IHC outcomes for RBM24; staining of HSCC tissue specimens from the LN metastatic and nonmetastatic populations. PBS served as the negative control to substitute for the primary antibody, where the magnification was 100× for the left panel and 400× for the right panel. (d) Kaplan-Meier overall survival plots for HSCC patients ($n = 57$) expressing RBM24 highly and lowly. $^{*}p < 0.05$, $^{**}p < 0.01$. Abbreviations: N stands for normal tissues; NL represents the tumor tissues from the non-LN metastatic population; L represents the tumor tissues from LN metastatic population; NC stands for negative control.

Table 2: The immunohistochemical expression of RBM24 in HSCC patients with lymphatic metastasis and without metastasis.

Tissue	Number of patients	Expression of RBM24		P value
		High	Low	
Lymphatic metastasis	41	16 (39.0%)	25 (61.0%)	<0.001
Non-lymphatic metastasis	16	14 (87.5%)	2 (12.5%)	

P values are from χ^2 test or Fisher's exact test and were statistically significant when < 0.05.

have been established universally [28], and extensive studies have reported the role of TGFβ as a potent elicitor of EMT [29]. In our work, loss of RBM24 was found to elicit the malignant HSCC progression. Hence, the linkage of RBM24 to the TGFβ-triggered EMT was investigated. After eliciting EMT in FaDu cells through a 48 h treatment using TGFβ (20 ng/mL), more FaDu-Control cells showed spindle shape and loss of intercellular adhesion (Figure 4(a)), indicating FaDu-Control cells underwent EMT. Then the mRNA levels of EMT-TFs (EMT-triggering transcriptional factors) were assessed to clarify the responders to the overexpression of RBM24. As displayed in Figure 4(b), Twist1 was RBM24's downstream effector, while changes in the Slug, Snail, and ZEB1 expressions were inapparent. RBM24 overexpression contributed to a decline in Twist1 protein expression (Figure 4(d)). Correspondingly, the mRNA and protein expressions of E-cadherin were elevated in FaDu-OE-RBM24 cells, whereas N-cadherin and Vimentin declined (Figures 4(c) and 4(d), implying TGFβ-triggered EMT suppression by the RBM24 overexpression. A further confocal immunofluorescent assay showed the fluorescent signal of E-cadherin was stronger while the fluorescent signals of N-cadherin and Vimentin were weaker in the FaDu-OE-RBM24 cells compared with the FaDu-Control cells (Figure 4(e)), which revealed that the RBM24 overexpression increased E-cadherin and decreased N-cadherin and Vimentin. As indicated by the preceding findings, RBM24 was capable

Table 3: Relationship between RBM24 expression and clinicopathological characteristics of 57 HSCC patients.

Category	Number of patients	Expression of RBM24		*P* value
		High	Low	
Age (years old)				0.63
(i) <60	23	13	10	
(ii) ≥60	34	17	17	
Gender				1
(i) Male	56	29	27	
(ii) Female	1	1	0	
T stage				<0.01
(i) T1 + T2	11	10	1	
(ii) T3 + T4	46	20	26	
N stage				<0.001
(i) N0 + N1	24	20	4	
(ii) N2 + N3	33	10	23	
Pathological stage				0.82
(i) High differentiation	14	7	7	
(ii)Moderate or poor differentiation	43	23	20	

P values are from χ^2 test or Fisher's exact test and were statistically significant when < 0.05. Abbreviations: T stage, tumor stage; N stage, lymph node stage.

of suppressing the TGFβ-triggered EMT event and lowered the Twist1 level.

3.5. Overexpression of Twist1 Could Reverse the Inhibitory Impacts of RBM24 on Invasion, Migration, and EMT in FaDu Cells. Given the essential function of Twist1 in the HSCC evolution, our study explored whether it is indispensable for RBM24's actions in HSCC cells by transfecting a Twist1-expressing plasmid and a control plasmid (PCMV) into the FaDu-OE-RBM24 cells. The expression of Twist1 was validated by qRT-PCR combined with WB analysis (Figures 5(a) and 5(b). Transwell and wound healing assays showed the cellular invasiveness, motility were repressed, and WB analysis showed the protein level of E-cadherin was elevated whereas the levels of N-cadherin and Vimentin declined by RBM24 overexpression. However, the Twist1 overexpression reversed these effects (Figures 5(c)–5(e)). Thus, the RBM24 overexpression was capable of inhibiting the cellular migratory/invasive potential and EMT process through adverse Twist1 modulation.

3.6. Overexpression of RBM24 Hindered HSCC Tumor Growth as well as LN Metastasis In-Vivo. The nude male BALB/c mice were inoculated with FaDu-OE-RBM24 or FaDu-Control cells at the footpads to investigate RBM24 level impacts on the HSCC evolution and metastasis to LNs in-vivo (Figure 6(a)). Both groups exhibited distinct fluorescent signals in the murine footpads (Figure 6(b)). Nevertheless, these signals were noted in the popliteal fossa, indicating metastasis to LNs in the FaDu-Control group. Slower tumor growth was detected in the FaDu-OE-RBM24 mice compared to the FaDu-Control mice (Figure 6(d)). Besides, the FaDu-OE-RBM24 group also exhibited lower tumor volumes (Figure 6(c)). The metastatic cell counts in LNs were reduced by the stable RBM24 overexpression (Figure 6(e)). According to Figure 6(f), metastasis to LNs was noted in one-fifth of the FaDu-OE-RBM24 mice, while it was absent in three-fourths of the FaDu-Control mice. IHC assay found higher RBM24 and E-cadherin levels yet lower Twist1 and Vimentin levels in the FaDu-OE-RBM24 group's tumors compared to the FaDu-Control tumors (Figure 6(g)). Thus, based on the in-vitro surveillance, it was presumed that the RBM24 overexpression downregulated Twist1 in-vivo.

4. Discussion

RBPs exert crucial functions in regulating pathways involved in numerous aspects of RNA metabolism, including transcription, alternative splicing, modification, stability, subcellular localization, translation, and decay [11, 30]. The implication of abnormal RBPs expression (critical gene regulatory proteins) or their mutations and binding sites in RNA targets has been reported in diverse human diseases containing carcinomas [31]. According to the latest review, RBPs exert a role in carcinoma metastasis through mechanotransduction modulation [32].

RBM24, an RRM family member, is a p53 pathway participant through stability modulation of p21 mRNA and interplay with p53 in diverse human carcinoma cells [13, 33]. The modulator role of RBM24 in the p63 expression is achieved by intrinsic mRNA stability [34]. The antitumor role of RBM24 in a few carcinomas is noteworthy [16–18]. Despite these, there is insufficient knowledge about its effects on carcinogenesis and evolution, particularly in hypopharyngeal carcinomas. In our preliminary work, the genes showing altered expression were investigated through RNA sequencing among HSCC patients with or without metastasis to LNs, and RBM24 was one of the downregulated genes. The downregulation of RBM24 was confirmed among

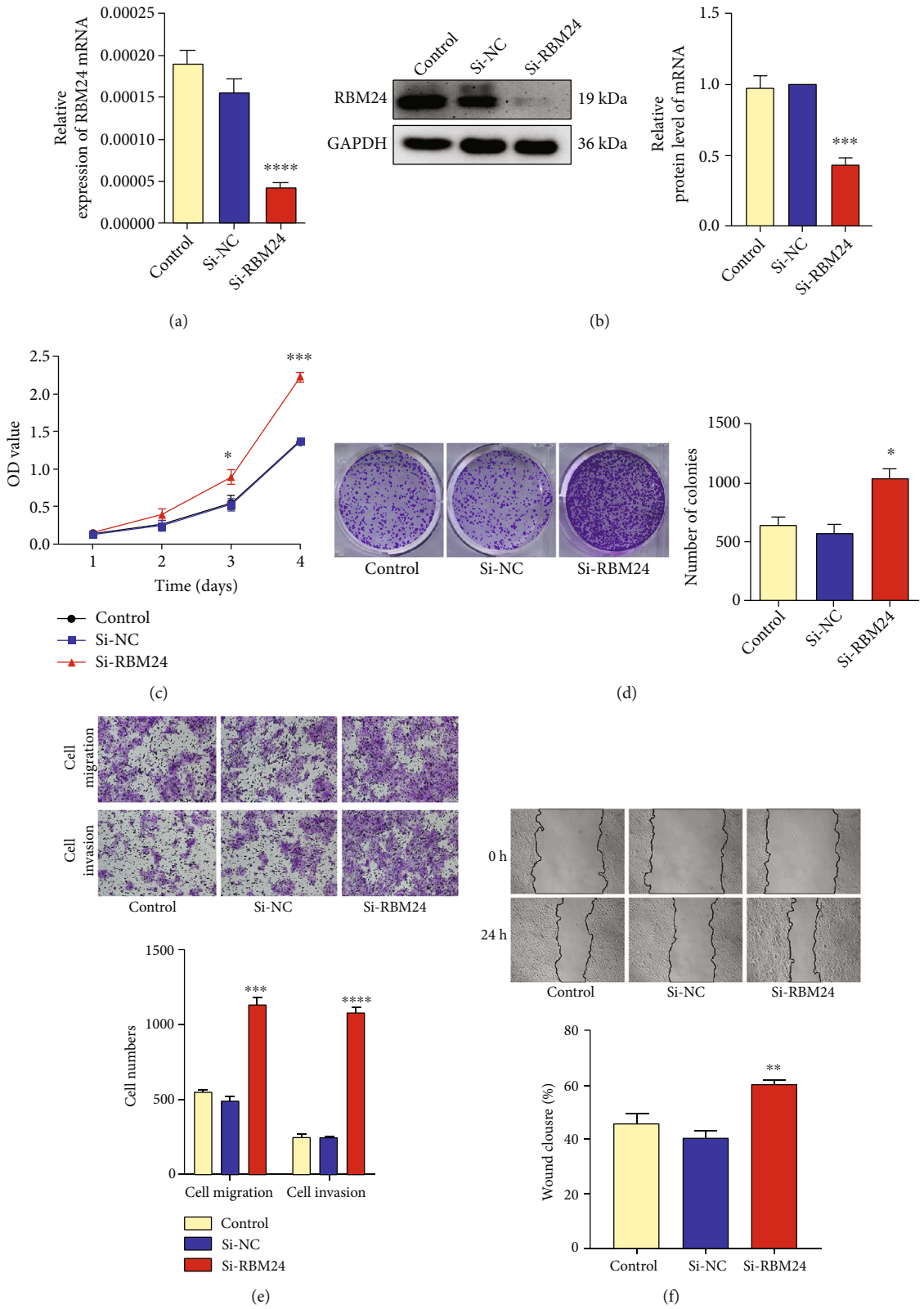

Figure 2: Facilitation of the FaDu cell multiplication, motility, and invasiveness by the RBM24 knockdown. (a and b) Lowered protein and mRNA expressions of RBM24 in the FaDu cells silenced for RBM24. (c) CCK-8 assay outcomes for the FaDu cell vitality at four varying time points. (d) Colony formation assay outcomes for the multiplicative potential of FaDu cells. (e) Transwell assay outcomes for the invasive and migratory potential of FaDu cells under a magnification of 100×. $^{*}p < 0.05$, $^{**}p < 0.01$, $^{***}p < 0.001$, $^{****}p < 0.0001$. The data are represented as the mean ± SEM values from no less than three independently experiments.

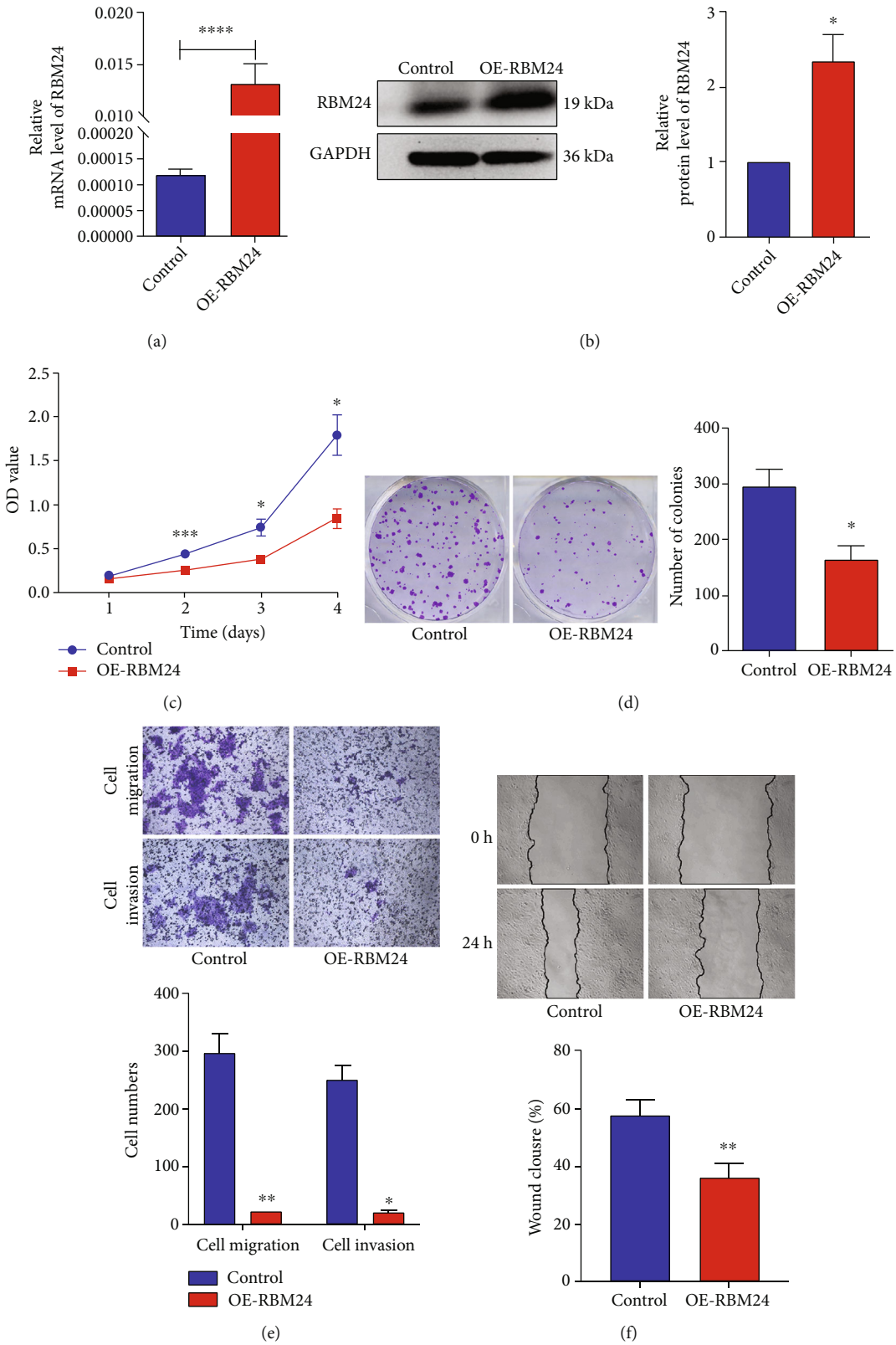

Figure 3: Suppression of the FaDu cell multiplication, motility, and invasiveness by the RBM24 overexpression. (a and b) Elevated protein and mRNA expressions of RBM24 in the FaDu-OE-RBM24 cells. (c) CCK-8 assay outcomes for the FaDu cell vitality at four varying time points. (d) Colony formation assay outcomes for the multiplicative potential of FaDu cells. (e) Transwell assay outcomes for the FaDu cell invasive and migratory potential under 100× magnification. (f) Wound healing assay outcomes for the FaDu cell motility under 100× magnification. $^{*}p < 0.05$, $^{**}p < 0.01$, $^{****}p < 0.0001$. The data are represented as the mean ± SEM values from no less than three independently experiments.

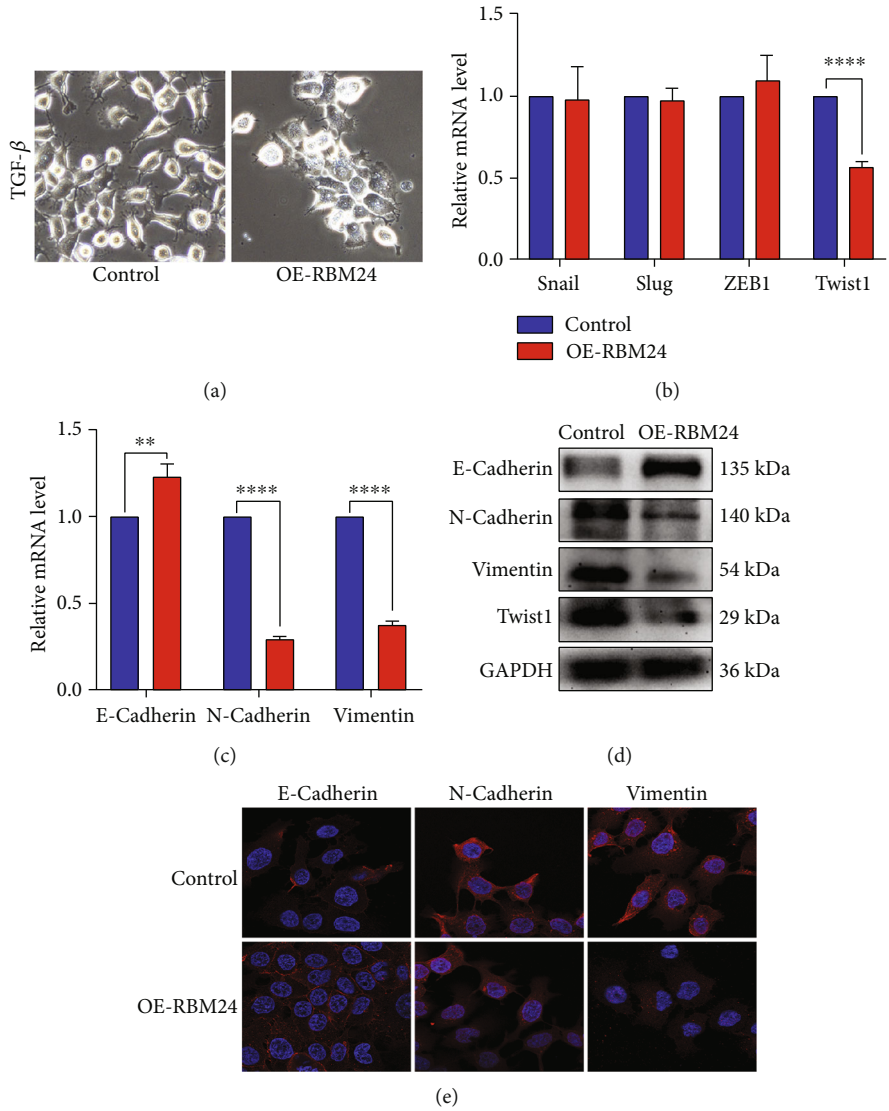

Figure 4: Twist1 downregulation and EMT suppression in FaDu cells led by the RBM24 overexpression. (a) Representative images of cell morphology after 48 h treatment using TGFβ (200× magnification). (b) The qRT-PCR outcomes for Slug, Snail, ZEB1, and Twist1 mRNA expressions in the FaDu-OE-RBM24 and FaDu-Control cells. (c) The qRT-PCR outcomes for N-cadherin, E-cadherin, and Vimentin mRNA expressions in the FaDu-OE-RBM24 and FaDu-Control cells. (d) The WB outcomes for the N-cadherin, E-cadherin, Vimentin, and Twist1 protein expressions. (e) The confocal immunofluorescent microscopy-based observations of N-cadherin, E-cadherin, and Vimentin levels under a magnification of 400×. $^{**}p < 0.01$, $^{****}p < 0.0001$. The data are represented as the mean ± SEM values from no less than three independently experiments.

HSCC patients showing metastasis to LNs. Besides, lower expression of RBM24 was related to several clinicopathological characteristics and worse overall survival, indicating that RBM24 could be both a biomarker for early diagnosis and a potential target for treating HSCC. For the in-vitro biofunctionality evaluation of RBM24, its level was adjusted in FaDu cells with lentiviral particles and siRNAs. The results verified that RBM24 could suppress the cellular multiplicative, migratory, and invasive potential and the EMT event in-vitro. Most importantly, the probable function of RBM24 was as a tumor inhibitor against the HSCC evolution.

Upon initial diagnosis, metastasis to cervical LNs was usually detected in the HSCC patients, resulting in therapeutic failure and dissatisfied overall survival [3, 35–37]. Thus, it is imperative to explore the mechanisms concerning HSCC evolution and LN metastasis. The pivotal effects of EMT on carcinoma progression have been established universally. The features of EMT include the polarity depletion of epithelial cells and their phenotypic transformation into mesenchymal [38]. Because of the previous processes, cancer cells can escape from the original site to metastasize distantly. EMT is defined by lowered E-cadherin (epithelial marker) and elevated Vimentin and N-cadherin (mesenchymal markers) levels [39]. EMT has recently been linked tightly to LN metastasis [40, 41]. EMT-TFs are the chief EMT regulators, Twist1 being a kernel factor [29]. According to the latest research, Twist1 is an oncogene whose aberrant overexpression promotes carcinogenesis, evolution, and

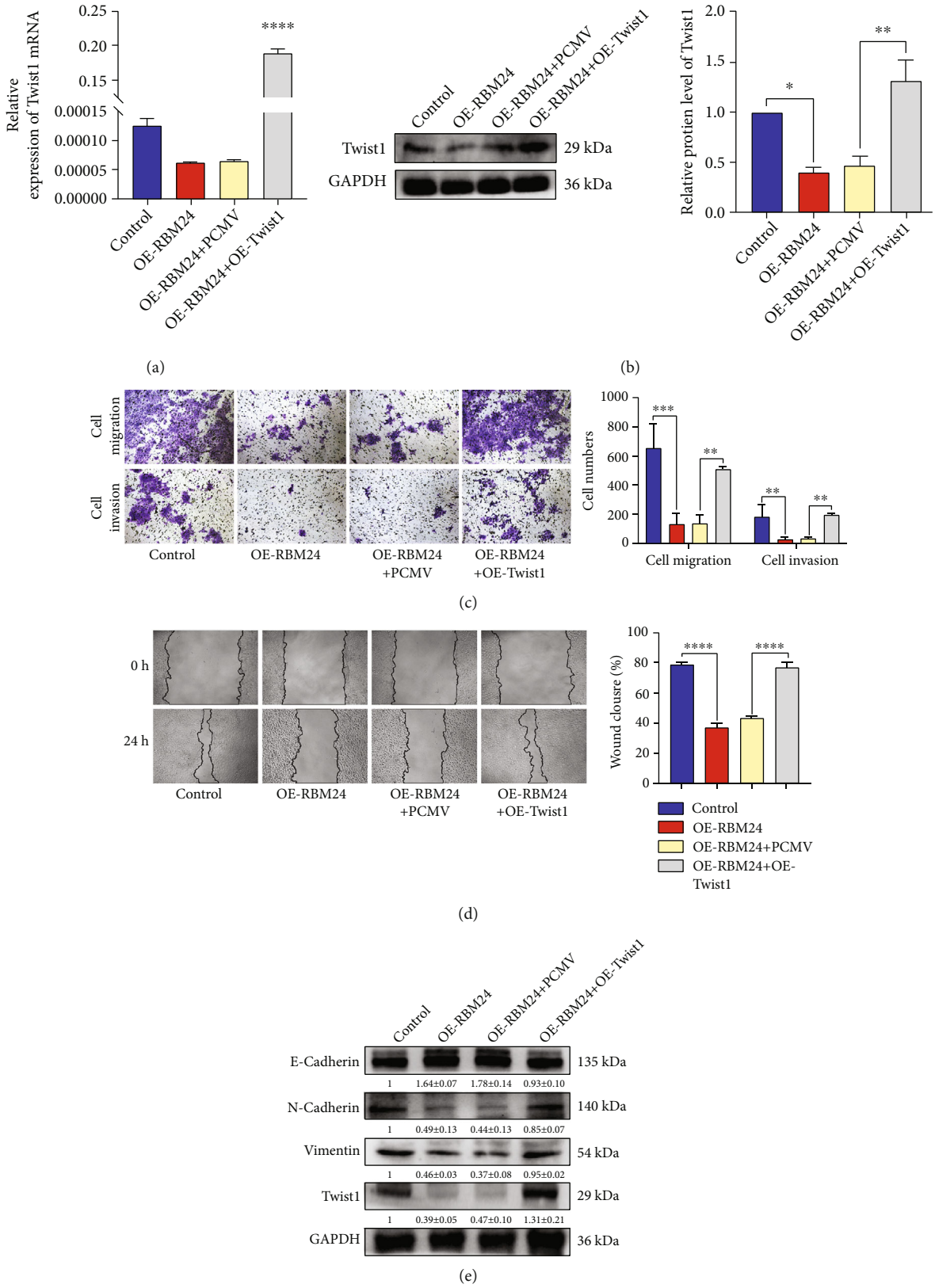

Figure 5: Reversal of RBM24's suppressive actions against the FaDu cell migration, invasiveness, and EMT by Twist1 overexpression. (a and b) Protein and mRNA expressions of Twist1 in the investigated cells. (c) Transwell assay outcomes for the FaDu cell invasive and migratory potential under 100× magnification. (d) Wound healing assay outcomes for the FaDu cell motility under 100× magnification. (e) N-cadherin, E-cadherin, Vimentin, and Twist1 protein levels in the investigated cells. $^{*}p < 0.05$, $^{**}p < 0.01$, $^{***}p < 0.001$, $^{****}p < 0.0001$. The data are represented as the mean ± SEM values from no less than three independently experiments.

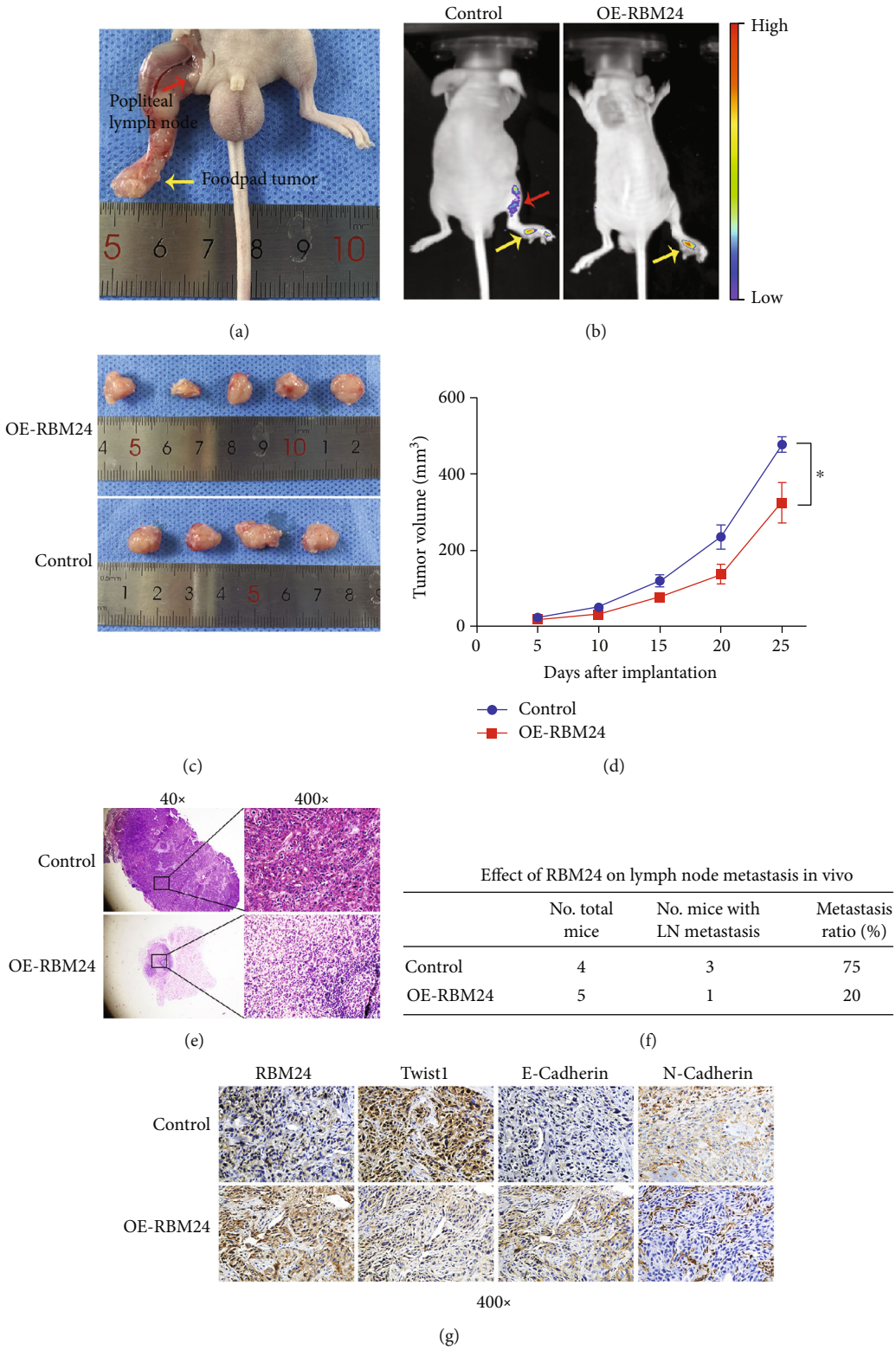

	No. total mice	No. mice with LN metastasis	Metastasis ratio (%)
Control	4	3	75
OE-RBM24	5	1	20

Figure 6: In-vivo inhibition of the HSCC evolution and metastasis to LNs by the RBM24 overexpression. (a) Typical model illustrating the metastasis to popliteal LNs. (b) Typical fluorescence micrographs of FaDu-OE-RBM24 and FaDu-Control cell-inoculated mice. The footpad tumors are represented by yellow arrows, whereas red arrows represent the metastases to popliteal LNs. (c) Excised tumor images of the FaDu-OE-RBM24 cell-inoculated mice ($n = 5$) and the corresponding FaDu-Control mice ($n = 4$). (d) Tumor growth graphs of the FaDu-OE-RBM24 group ($n = 5$) and the FaDu-Control group ($n = 4$). (e) Typical H&E-stained micrographs of metastatic LNs for the FaDu-OE-RBM24 mice ($n = 5$) and the FaDu-Control mice ($n = 4$), where the magnification was 40× for the left panel and 400× for the right panel. (f) Percentages of LN metastatic mice in the FaDu-OE-RBM24 group ($n = 5$) versus the FaDu-Control group ($n = 4$). (g) Typical micrographs of IHC-stained tumor cells in the FaDu-OE-RBM24 and FaDu-Control groups. $^*p < 0.05$.

metastasis. Twist1 can facilitate carcinoma evolution through the cancer cell multiplication enhancement and apoptosis inhibition, leading to strengthened chemotherapy susceptibility of cancer cells and an extended colony of cancer stem cells to prompt the metastasis and invasiveness [42, 43]. Our study investigated the links between RBM24 expression and TGFβ-induced EMT, given the significance of EMT in tumor metastasis and former research showing that RBM24 overexpression could upregulate E-cadherin expression but downregulate Vimentin expression in HCT116 human CRC cells [17]. The present study validated on HSCC FaDu cells that the expressions of a few representative EMT markers, along with Twist1, could be modulated by RBM24. Thus, RBM24 may target Twist1 to suppress the TGFβ-triggered EMT and HSCC metastasis to LNs. Rescue experiments were conducted where Twist1 was overexpressed in FaDu cells to validate this assumption. Reversal of cellular invasiveness, migration, and EMT was found after Twist1 overexpression. Besides, RBM24 overexpression inhibited HSCC evolution and metastasis to LNs in-vivo.

Further IHC staining revealed the corresponding alterations in a few EMT markers and Twist1 levels. Thus, RBM24 overexpression probably suppresses the HSCC evolution and diminishes the LN metastasis through Twist1 level repression. However, further explorations are required to validate the Twist1-binding ability of RBM24 and clarify the precise mechanism. Deeper probing is required to specify the mechanisms of RBM24 and Twist1 interaction to modulate the LN metastasis and the EMT.

5. Conclusion

To conclude, RBM24, as a novel tumor inhibitor gene, inhibits the LN metastasis and EMT by the downregulation of the Twist1 in HSCC. Hence, the RBM24 and Twist1 probably serve as diagnostic biomarkers and therapeutic targets for HSCC patients presenting LN metastasis.

Data Availability

The corresponding author, on reasonable request, offered the obtained data.

Ethical Approval

This work was carried out following the requirements of the Declaration of Helsinki. Besides, ethics approval was granted by the Ethics Committee of the First Affiliated Hospital of Chongqing Medical University. The animal research was approved by the Ethics Committee of the First Affiliated Hospital of Chongqing Medical University.

Consent

All the involved individual participants approved the informed consent.

Disclosure

This manuscript was submitted as a preprint in the link https://www.researchsquare.com/article/rs-1167348/v1 [44].

Conflicts of Interest

The authors declare that there is no conflict of interest regarding the publication of this article.

Authors' Contributions

YL, MP, and GH designed this study. YL carried out the experiments, analyzed the data, and completed the study. TL, DY, and YL revised the present study. GH and ZW verified the authenticity of all the raw data. The final version of this manuscript was checked and approved by all authors.

Acknowledgments

This work was supported by the National Natural Science Foundation of China (No. 81902776) and the Natural Science Foundation of Chongqing (cstc2019jcyj-msxm0325, 2020MSXM091).

Supplementary Materials

Supplementary Figure 1 SiRNA#3 (Si-RBM24) exhibited the highest RBM24 knockdown efficiency. (a) mRNA level of RBM24 in FaDu cells transfected with RBM24 siRNAs. (b) Protein expression level of RBM24 in FaDu cells transfected with RBM24 siRNAs. $^{**}p < 0.01$. *(Supplementary Materials)*

References

[1] F. Bray, J. Ferlay, I. Soerjomataram, R. L. Siegel, L. A. Torre, and A. Jemal, "Global cancer statistics 2018: GLOBOCAN estimates of incidence and mortality worldwide for 36 cancers in 185 countries," *CA: a Cancer Journal for Clinicians*, vol. 68, no. 6, pp. 394–424, 2018.

[2] G. Gatta, R. Capocaccia, L. Botta et al., "Burden and centralised treatment in Europe of rare tumours: results of RARECARE-net–a population-based study," *The Lancet Oncology*, vol. 18, no. 8, pp. 1022–1039, 2017.

[3] S. Grasl, S. Janik, T. Parzefall et al., "Lymph node ratio as a prognostic marker in advanced laryngeal and hypopharyngeal carcinoma after primary total laryngopharyngectomy," *Clinical Otolaryngology*, vol. 45, no. 1, pp. 73–82, 2020.

[4] S. Tian, Q. Li, R. Li et al., "Development and validation of a prognostic nomogram for hypopharyngeal carcinoma," *Frontiers in Oncology*, vol. 11, article 696952, 2021.

[5] J. C. Garneau, R. L. Bakst, and B. A. Miles, "Hypopharyngeal cancer: a state of the art review," *Oral Oncology*, vol. 86, pp. 244–250, 2018.

[6] A. S. Ho, S. Kim, M. Tighiouart et al., "Association of quantitative metastatic lymph node burden with survival in hypopharyngeal and laryngeal cancer," *JAMA Oncology*, vol. 4, no. 7, pp. 985–989, 2018.

[7] H. E. Eckel and P. J. Bradley, "Treatment options for hypopharyngeal cancer," *Advances in Oto-Rhino-Laryngology*, vol. 83, pp. 47–53, 2019.

[8] H. Wang, R. Wu, X. Huang et al., "The pattern of cervical lymph node metastasis and risk factors of retropharyngeal lymph node metastasis based on magnetic resonance imaging in different sites of hypopharyngeal carcinoma," *Cancer Management and Research*, vol. 12, pp. 8581–8587, 2020.

[9] P. Babitzke, Y. J. Lai, A. J. Renda, and T. Romeo, "Posttranscription initiation control of gene expression mediated by bacterial RNA-binding proteins," *Annual Review of Microbiology*, vol. 73, no. 1, pp. 43–67, 2019.

[10] S. Gerstberger, M. Hafner, and T. Tuschl, "A census of human RNA-binding proteins," *Nature Reviews. Genetics*, vol. 15, no. 12, pp. 829–845, 2014.

[11] B. Pereira, M. Billaud, and R. Almeida, "RNA-binding proteins in cancer: old players and new actors," *Trends in Cancer*, vol. 3, no. 7, pp. 506–528, 2017.

[12] B. M. Lunde, C. Moore, and G. Varani, "RNA-binding proteins: modular design for efficient function," *Nature Reviews Molecular Cell Biology*, vol. 8, no. 6, pp. 479–490, 2007.

[13] Y. Jiang, M. Zhang, Y. Qian, E. Xu, J. Zhang, and X. Chen, "Rbm24, an RNA-binding protein and a target of p53, regulates p21 expression via mRNA stability∗," *The Journal of Biological Chemistry*, vol. 289, no. 6, pp. 3164–3175, 2014.

[14] T. Zhang, Y. Lin, J. Liu et al., "Rbm24 regulates alternative splicing switch in embryonic stem cell cardiac lineage differentiation," *Stem Cells*, vol. 34, no. 7, pp. 1776–1789, 2016.

[15] D. H. Jin, K. Hidaka, M. Shirai, and T. Morisaki, "RNA-binding motif protein 24 regulates myogenin expression and promotes myogenic differentiation," *Genes To Cells*, vol. 15, no. 11, pp. 1158–1167, 2010.

[16] W. F. Hua, Q. Zhong, T. L. Xia et al., "RBM24 suppresses cancer progression by upregulating miR-25 to target MALAT1 in nasopharyngeal carcinoma," *Cell Death & Disease*, vol. 7, no. 9, article e2352, 2016.

[17] R. M. Xia, T. Liu, W. G. Li, and X. Q. Xu, "RNA-binding protein RBM24 represses colorectal tumourigenesis by stabilising PTEN mRNA," *Clinical and Translational Medicine*, vol. 11, no. 10, article e383, 2021.

[18] J. H. Choi, S. M. Kwon, S. U. Moon et al., "TPRG1-AS1 induces RBM24 expression and inhibits liver cancer progression by sponging miR-4691-5p and miR-3659," *Liver International*, vol. 41, no. 11, pp. 2788–2800, 2021.

[19] J. M. Lee, S. Dedhar, R. Kalluri, and E. W. Thompson, "The epithelial-mesenchymal transition: new insights in signaling, development, and disease," *The Journal of Cell Biology*, vol. 172, no. 7, pp. 973–981, 2006.

[20] T. D. Way, J. T. Huang, C. H. Chou, C. H. Huang, M. H. Yang, and C. T. Ho, "Emodin represses TWIST1-induced epithelial-mesenchymal transitions in head and neck squamous cell carcinoma cells by inhibiting the β-catenin and Akt pathways," *European Journal of Cancer*, vol. 50, no. 2, pp. 366–378, 2014.

[21] S. Ardalan Khales, E. Ebrahimi, E. Jahanzad, S. Ardalan Khales, and M. M. Forghanifard, "MAML1 and TWIST1 co-overexpression promote invasion of head and neck squamous cell carcinoma," *Asia-Pacific Journal of Clinical Oncology*, vol. 14, no. 5, pp. e434–e441, 2018.

[22] S. Lu, L. Yu, Y. Mu et al., "Role and mechanism of Twist1 in modulating the chemosensitivity of FaDu cells," *Molecular Medicine Reports*, vol. 10, no. 1, pp. 53–60, 2014.

[23] Y. Li, M. Pan, T. Lu et al., "RAF1 promotes lymphatic metastasis of hypopharyngeal carcinoma via regulating LAGE1: an experimental research," *Journal of Translational Medicine*, vol. 20, no. 1, p. 255, 2022.

[24] T. Lu, Y. Li, M. Pan et al., "TBC1D14 inhibits autophagy to suppress lymph node metastasis in head and neck squamous cell carcinoma by downregulating macrophage erythroblast attacher," *International Journal of Biological Sciences*, vol. 18, no. 5, pp. 1795–1812, 2022.

[25] X. Wang, L. Tian, Y. Li et al., "RBM15 facilitates laryngeal squamous cell carcinoma progression by regulating TMBIM6 stability through IGF2BP3 dependent," *Journal of Experimental & Clinical Cancer Research*, vol. 40, no. 1, p. 80, 2021.

[26] J. Wu, X. J. Zhou, X. Sun et al., "RBM38 is involved in TGF-β-induced epithelial-to-mesenchymal transition by stabilising zonula occludens-1 mRNA in breast cancer," *British Journal of Cancer*, vol. 117, no. 5, pp. 675–684, 2017.

[27] Y. Jin and X. Qin, "Comprehensive analysis of the roles and prognostic value of RNA-binding proteins in head and neck squamous cell carcinoma," *DNA and Cell Biology*, vol. 39, no. 10, pp. 1789–1798, 2020.

[28] D. E. Johnson, B. Burtness, C. R. Leemans, V. W. Y. Lui, J. E. Bauman, and J. R. Grandis, "Head and neck squamous cell carcinoma," *Nature Reviews. Disease Primers*, vol. 6, no. 1, p. 92, 2020.

[29] S. Lamouille, J. Xu, and R. Derynck, "Molecular mechanisms of epithelial-mesenchymal transition," *Nature reviews Molecular cell biology.*, vol. 15, no. 3, pp. 178–196, 2014.

[30] F. Gebauer, T. Schwarzl, J. Valcarcel, and M. W. Hentze, "RNA-binding proteins in human genetic disease," *Nature Reviews Genetics*, vol. 22, no. 3, pp. 185–198, 2021.

[31] B. Kechavarzi and S. C. Janga, "Dissecting the expression landscape of RNA-binding proteins in human cancers," *Genome Biology*, vol. 15, no. 1, p. R14, 2014.

[32] Y. Zhang and Z. Li, "RNA binding proteins: linking mechanotransduction and tumor metastasis," *Cancer Letters*, vol. 496, pp. 30–40, 2021.

[33] M. Zhang, Y. Zhang, E. Xu et al., "Rbm24, a target of p53, is necessary for proper expression of p53 and heart development," *Cell Death & Differentiation.*, vol. 25, no. 6, pp. 1118–1130, 2018.

[34] E. Xu, J. Zhang, M. Zhang, Y. Jiang, S. J. Cho, and X. Chen, "RNA-binding protein RBM24 regulates p63 expression via mRNA stability," *Molecular Cancer Research*, vol. 12, no. 3, pp. 359–369, 2014.

[35] N. D. Wycliffe, R. S. Grover, P. D. Kim, and A. Simental Jr., "Hypopharyngeal cancer," *Topics in Magnetic Resonance Imaging*, vol. 18, no. 4, pp. 243–258, 2007.

[36] R. P. Takes, P. Strojan, C. E. Silver et al., "Current trends in initial management of hypopharyngeal cancer: the declining use of open surgery," *Head & Neck*, vol. 34, no. 2, pp. 270–281, 2012.

[37] H. Suzuki, T. Matoba, N. Hanai et al., "Lymph node ratio predicts survival in hypopharyngeal cancer with positive lymph node metastasis," *European Archives of Oto-Rhino-Laryngology*, vol. 273, no. 12, pp. 4595–4600, 2016.

[38] J. P. Thiery, H. Acloque, R. Y. Huang, and M. A. Nieto, "Epithelial-mesenchymal transitions in development and disease," *Cell*, vol. 139, no. 5, pp. 871–890, 2009.

[39] I. Pastushenko and C. Blanpain, "EMT transition states during tumor progression and metastasis," *Trends in Cell Biology*, vol. 29, no. 3, pp. 212–226, 2019.

[40] Y. Morita, K. Hata, M. Nakanishi et al., "Cellular fibronectin 1 promotes VEGF-C expression, lymphangiogenesis and lymph node metastasis associated with human oral squamous cell carcinoma," *Clinical & Experimental Metastasis*, vol. 32, no. 7, pp. 739–753, 2015.

[41] B. Liu, X. Li, C. Li, R. Xu, and X. Sun, "miR-25 mediates metastasis and epithelial-mesenchymal-transition in human esophageal squamous cell carcinoma via regulation of E-cadherin signaling," *Bioengineered.*, vol. 10, no. 1, pp. 679–688, 2019.

[42] J. Srivastava, O. Rho, R. M. Youssef, and J. DiGiovanni, "Twist1 regulates keratinocyte proliferation and skin tumor promotion," *Molecular Carcinogenesis*, vol. 55, no. 5, pp. 941–952, 2016.

[43] Q. Qin, Y. Xu, T. He, C. Qin, and J. Xu, "Normal and disease-related biological functions of Twist1 and underlying molecular mechanisms," *Cell Research*, vol. 22, no. 1, pp. 90–106, 2012.

[44] Y. Liu, T. Lu, M. Pan, D. Yu, Y. Li, and G. Hu, "PSR: Unified Framework of Parameter-Learning-Based MR Image Superresolution," *Journal of Healthcare Engineering*, vol. 2021, Article ID 5591660, 14 pages, 2021.

Hindawi
Journal of Oncology
Volume 2022, Article ID 2676367, 7 pages
https://doi.org/10.1155/2022/2676367

Research Article

Unicystic Mucoepidermoid Carcinoma: A Pitfall for Clinical and Pathologic Diagnosis

Xi Wang,[1,2] Wei Li,[1,2] Yanrui Feng,[3] Lingchao Liu,[4] Huiying He,[4] and Binbin Li[1,2]

[1]*Department of Oral Pathology, Peking University School and Hospital of Stomatology & National Center of Stomatology & National Clinical Research Center for Oral Diseases & National Engineering Research Center of Oral Biomaterials and Digital Medical Devices, Beijing 100081, China*
[2]*Research Unit of Precision Pathologic Diagnosis in Tumors of the Oral and Maxillofacial Regions, Chinese Academy of Medical Sciences (2019RU034), China*
[3]*Central Laboratory, Peking University School and Hospital of Stomatology & National Center of Stomatology & National Clinical Research Center for Oral Diseases & National Engineering Research Center of Oral Biomaterials and Digital Medical Devices, Beijing 100081, China*
[4]*Department of Pathology, School of Basic Medical Sciences, Third Hospital, Peking University Health Science Center, Beijing, China*

Correspondence should be addressed to Huiying He; huiyinghe@bjmu.edu.cn and Binbin Li; kqlibinbin@bjmu.edu.cn

Received 8 July 2022; Accepted 30 August 2022; Published 13 September 2022

Academic Editor: Tiancheng Li

Unicystic mucoepidermoid carcinoma (UC-MEC) is a rare MEC variant, and its diagnosis is frequently problematic. This study is aimed at summarizing its clinicopathologic characteristics, treatment, and prognosis and proposing key points to avoid missed diagnosis and misdiagnosis in clinical and pathological conditions. This retrospective study included 30 UC-MEC cases, and the clinical findings were collected from the clinical medical records. Radiographic features, histologic behaviors, MAML2 rearrangement by fluorescence in situ hybridization (FISH), and follow-up data were analyzed. Moreover, glandular odontogenic cyst (GOC) and cytadenoma (CA) were used as controls. In the UC-MEC group, 19 patients were female (63%), and 11 were male (37%). The mean patient age was 39.5 (range, 7–72 years). The affected locations included the jaw (8 maxillary, 3 mandibular) and salivary glands (7 parotid, 11 palates, and 1 floor of the mouth). The chief complaint was swelling; the lesions were all cystic, among which 66.7% were well circumscribed and 33.3% poorly defined. Microscopic examination showed two UC-MEC histologic subtypes. Type A presented as a single cyst with mural thickening (8/30, 27%) lined predominantly by epidermoid cells with interspersed intermediate and mucinous cells, and type B (22/30, 73%) showed infiltrative tumor islands in the cystic wall or the surrounding tissue. FISH analysis suggested that approximately 66.7% of UC-MEC harbored a MAML2 rearrangement. During the median follow-up period of 42 months (range, 6–120 months), all type A patients and 68% of type B patients who underwent complete surgical resection lived without relapse. Seven cases with type B cancer that underwent curettage initially had local recurrence. Clinicians and pathologists hardly recognize UC-MEC owing to its cystic architecture. Specific epidermoid, mucous, and intermediate tumor cells, and MAML2 fusion testing, are essential to avoid potential diagnostic pitfalls. Prompting and completing resection surgery with negative margins would have a favorable prognosis.

1. Introduction

Mucoepidermoid carcinoma (MEC) is the most common malignancy of the salivary glands, accounting for 30% of salivary gland tumors and 2–4% of jaw tumors [1]. Although the majority of MEC are typical in histology, unicystic MEC (UC-MEC), a rare variant of MEC, poses a great diagnostic and treatment challenge for clinicians and pathologists. To date, only 20 cases of UC-MEC have been reported in the English literature [2–9], which means that

more cases are needed to study the clinicopathological features and appropriate treatment choices.

In practice, the large cystic architecture of UC-MEC may be a pitfall in diagnosis. On computed tomography (CT) or contrast-enhanced CT, UC-MEC is commonly characterized by well-circumscribed unilocular radiolucency mimicking benign cysts or tumors. Histologically, an insufficiently deep or bread incisional biopsy, such as fine-needle aspiration biopsy (FNAB), may miss the key diagnostic portion of the tumor because large cysts may sometimes develop in the superficial aspect of the tumor and show only an innocuous part [10, 11].

Recent studies have demonstrated that 33.7–86.6% of MECs harbor CREB-regulated transcriptional coactivator 1- (CRTC1-) mastermind-like gene family-2 (MAML2) translocation [12]. Owing to its high specificity [13], the MAML2 rearrangement is considered a useful ancillary diagnostic tool for MEC diagnosis. However, there are no published reports on MAML2 rearrangement in UC-MEC.

The Armed Forces Institute of Pathology (AFIP) grading criteria for typical MEC (TMEC) generally show a good correlation with clinical outcomes and are considered applicable to UC-MEC [14]. The management of UC-MEC should be tailored to its type, location, and histological grading. However, there are still many disputes regarding their disposal. Some researchers thought the UC-MEC qualifies as a low-grade tumor with indolent clinical behavior and may be more conservatively treated [2]. Generally, low-grade MEC requires surgical treatment only, whereas high-grade MEC requires adjuvant radiation and neck dissection [15]. However, some pathologists have emphasized the importance of radical surgery and adjuvant treatment [8]. The recurrence rate was around 40% for conservative treatment such as enucleation and debridement and 4% for radical treatment such as segmental resection with/without associated adjuvant therapy [16]. In the published cohort, 86% of patients were treated with regional surgical excision. Of these patients, 14% underwent extra lymph node dissection and adjuvant radiotherapy. In order to solve these disputes above, we reported the largest number of 30 UC-MEC cases to date and described the clinicopathologic characteristics, diagnosis, and prognosis of UC-MEC to gain a comprehensive understanding of this unique MEC variant.

2. Materials and Methods

2.1. Study Population Selection and Follow-Up. The study was approved by the Institutional Review Board of Peking University, School and Hospital of Stomatology (PKUSSIRB-201948111). In the head and neck region, 635 cases of MEC were identified from the surgical pathology database between January 2005 and October 2021. All hematoxylin and eosin- (H&E-) stained slides were reviewed and regraded by two head and neck pathologists (Binbin Li and Huiying He). Inclusion criteria for MEC were proposed when the lesion was showing unicystic architecture and composed of varying proportions of epidermoid cells, mucocytes, and intermediate cells. Patients with metastatic MEC from other primary lesions were excluded. Diagnostic hematoxylin and eosin (H&E) slides, and formalin-embedded (FFPE) blocks were retrieved from the surgical pathology archives.

Glandular odontogenic cyst (GOC) is a developmental odontogenic cyst, while cystadenomas (CA) is a rare benign salivary gland tumor. Both share numerous histopathological features with UC-MEC, such as mucous and eosinophilic cuboidal cells [14, 15]. Thus, six GOC and 19 CA samples were selected as the negative control for MAML2 test [17, 18].

Clinical characteristics were obtained from the electronic medical records, including age at the time of diagnosis, sex, tumor site, symptoms and signs, interval between the initial symptoms and histologic verification, image manifestations, surgical treatment (local recision, complete revision with or without neck lymph node dissection), and adjuvant treatment (radiation therapy, chemotherapy, and/or I^{125} seed implantation). Tumors were staged according to the American Joint Committee on Cancer (Cancer Staging Manual, 8th edition) [19]. Long-term follow-up was available for all patients. Local recurrence and distant metastases were confirmed by clinical examination, imaging, and pathological diagnosis of tissue biopsy. The status at the last follow-up was classified as follows: no evidence of disease, alive with disease, or death from disease. Clinical follow-up information was available for all patients.

2.2. Histology. Tumor samples were examined microscopically and graded using the histologic grading system of the AFIP [20]. HE staining, tumor size, growth pattern (well-defined or peripheral growth in nests and islands), mitoses, tumor necrosis, atypical mitoses, nuclear pleomorphism, perineural, bone, vascular, and muscle invasions, lymph node, and distant metastasis were evaluated.

2.3. Fluorescent In Situ Hybridization. The paraffin sections were labeled with MAML2 probes for in situ fluorescence hybridization (FISH). A dual-color break probe was used. One end was a 680 kb fragment of the 5′MAML2 gene labeled with ZyGreen, and the other was a 370 kb fragment of the 3′MAML2 gene labeled with ZyOrange (Z-2014-200, Zytovision, Bremerhaven, Germany). One hundred randomly selected nonoverlapping tumor cells were evaluated for the presence of orange, green, or yellow fluorescent signals. A normal situation is defined as the distance between two signal points being smaller than the diameter of one point, and signals separated by a distance greater than a single signal width are regarded as split signals. Rearrangement was considered positive if the split signal was above 15%. Each assay was accompanied by internal and external controls to monitor the correct performance of processed specimens and test reagents.

2.4. Statistical Analysis. Statistical analyses were performed using Spearman's correlation and Fishers exact test. Statistical programming was completed in R Studio (version 4.0.0) and GraphPad Prism (version 9.0), using packages "ggplot2." $P < 0.05$ was considered a statistical significance.

3. Results

3.1. Clinical Features. Thirty patients with UC-MEC arising from the head and neck were selected. Among them, 19 patients were female (63%), and 11 were male (37%). The age at diagnosis ranged from 7 to 72 years (mean age: 39.5 years old), with approximately 40% of these cases presenting during the third and fourth decades. Nineteen lesions were in the salivary gland; of those, seven were in the parotid gland, eleven in the palatal gland, and one on the floor of the mouth. Approximately 37% lesions were in the jaw, including eight in the maxilla and three in the mandible. Eight maxillary lesions were found in the premolar and molar regions. The mandibular lesion involved an angle extending to the premolar region on the same side. Swelling was the principal finding in all the patients. None of the patients showed any signs of lower lip/facial numbness.

3.2. Imaging Features. All lesions behaved as cystic masses on computed tomography (CT). In the UC-MEC group, the average tumor size was 1.7 cm (range 0.7–2.6 cm). In total, 66.7% (20/30) of the lesions were well circumscribed. An unclear definition was present in 33.3% of patients with UC-MEC. In the control group, CT imaging showed circular or oval lesions with well-defined borders in all GOC and CA lesions. The tumor sizes in the control groups ranged from 1.0 to 4.5 cm, with a mean size of 1.8 cm. The average tumor size in the UC-MEC group was smaller than that in the GOC and CA groups; however, the differences were not statistically significant ($P > 0.05$) among them.

3.3. Histologic Features. On gross examination of UC-MEC, the masses were generally unencapsulated, and a large cystic space was demonstrated in all cases.

Microscopically, in the UC-MEC group, the cyst was lined by tumor-forming cells (epidermoid cells and clusters of mucus-secreting cells interspersed with intermediate cells), areas of mural thickening, and infiltrative components. Oncocytic proteinaceous material and (pre) calcified bodies were detectable within the cavity. In some cases, papillary projections consisting of epidermoid and mucinous cells are observed inside the inner cystic wall. Notably, proliferative clusters of epithelial cells were observed in the subepithelial area of the fibrocollagenous wall in some of these cases. This cluster was composed of intermediate cells with markedly hyperchromatic nuclei, scattered mucous cells, and polygonal cells showing epidermoid differentiation. Nuclear pleomorphism and anaplasia were minimal; mitosis was rare; and necrosis, perineural invasion, and lymphovascular invasion were undetectable. Detailed clinicopathological data of all UC-MEC are presented in Table 1. Based on the morphological features of UC-MEC, GOC and CA could be considered in the differential diagnosis. The presence of distinct and frequently prevalent clusters of epidermoid and intermediate cells help to rule out CA, respectively. GOC may closely mimic UC-MECs, but epithelial spheres or whorl is a vital character for GOC diagnosis.

Taken together, UC-MEC is usually low-grade according to the AFIP grading system, except for one intermediate grade. Cysts occasionally rupture and release mucus into the cyst wall, which may evoke a florid inflammatory and sometimes a granulomatous response or local fibrous repair reaction. Screening of all slides of UC-MEC can be classified into two histologic subtypes. In type A, the tumor was a simple cyst ($n = 8$, 26.7%) with lining epithelium, showing features of an MEC with/without intraluminal tumor nodules. Type B tumors ($n = 22$, 73.3%) contained infiltrative tumor islands in the cyst wall (capsule) or connective tissue. A schematic representation of types A and B cystic MEC is shown in Figure 1.

3.4. FISH Results. In the UC-MEC group, 66.7% (20/30) of patients harbored the MAML2 rearrangement, including 62.5% of type A (5/8) and 68.2% (15/22) type B cases.

Six GOC and 19 CA cases were negative for MAML2 gene rearrangements. Representative FISH and histological images are shown in Figures 2(a)–2(h).

3.5. Treatment and Follow-Up. Twenty-three patients underwent the extensive resection without recurrence, but 7 cases underwent curettage and recurred (Table 1). Follow-up studies ranging from 6 to 120 months were available for all patients. The overall local recurrence (LR) rate was 23.3% (7/30), and the 5-year LR rate was 16.7% (5/30), of which 2 had an LR beyond five years. The average time to the first LR was 50.8 months (range, 3–108 months). Distal metastases were not observed.

It is worth mentioning that all relapsed UC-MEC patients were type B and underwent curettage initially; the recurred CT and histology images are shown in Figure 3.

4. Discussion

UC-MEC, a MEC variant first described by Raslan [21] in 1998, has been reported as a low-grade tumor with a favorable prognosis. A literature review revealed 20 cases of UC-MEC in the maxillofacial region [2–9]. The average age of these UC-MEC patients was 41.7 (range, 20–80) years. Overall, women ($n = 16$) were more frequently affected than men ($n = 5$). The most frequent primary site was the minor salivary gland ($n = 18$; 9 hard palates, 2 retromolar trigones, 2 mandibles, 2 buccal, 2 soft palates, and 1 mandible), followed by the parotid gland ($n = 3$). Our data confirmed that UC-MEC occurs at an earlier age (mean, 40.3 years) than TMEC (mean, 49 years) [22]. A female predilection in our cohort (63%) was observed, which was consistent with previous reports.

Clinically, the diagnosis of UC-MEC is problematic because of the large number of potential mimics. Swelling was the common cause of hospital visits in patients with UC-MEC, without any malignant indication, and 66.7% of UC-MEC cases were characterized by well-circumscribed unilocular radiolucency with well-defined borders and no signs of malignancy. Therefore, it is difficult for clinicians to distinguish between UC-MEC and benign lesions using only clinical and imaging examinations. In addition, FNAB usually fails to provide sufficient information owing to its cystic nature and insufficient sampling [11]. One recurrent

Table 1: Clinicopathological characteristics of patients with UC-MEC.

ID	Subtype	Age	Gender	Location	AFIP grading	FISH result	Treatment	Status
Case1	A	27	Male	Palate gland	LG	-	ER	Live, nr
Case2		29	Male	Palate gland	LG	+	ER	Live, nr
Case3		37	Female	Palate gland	LG	+	ER	Live, nr
Case4		7	Female	Palate gland	LG	+	ER	Live, nr
Case5		39	Female	Palate gland	LG	+	ER	Live,nr
Case6		30	Female	Parotid gland	LG	-	ER	Live, nr
Case7		40	Male	Parotid gland	LG	-	ER	Live,nr
Case8		30	Female	Mandibular	LG	+	ER	Live, nr
Case9		67	Female	Palate gland	LG	+	ER	Live, nr
Case10		49	Male	Palate gland	LG	-	ER	Live, nr
Case11		24	Female	Palate gland	LG	-	ER	Live, nr
Case12		52	Male	Palate gland	LG	-	ER	Live, nr
Case13		46	Female	Palate gland	LG	+	EN	Live,re
Case14		69	Male	Palate gland	LG	+	ER	Live,nr
Case15	B	58	Male	Parotid gland	LG	-	ER	Live, nr
Case16		50	Female	Parotid gland	LG	+	ER	Live, nr
Case17		72	Female	Parotid gland	LG	+	ER	Live,nr
Case18		33	Male	Parotid gland	LG	+	ER	Live,nr
Case19		38	Female	Parotid gland	LG	+	EN	Live,re
Case20		45	Male	Floor of the mouth	LG	+	EN	Live,re
Case21		28	Male	Maxillary	LG	+	ER	Live, nr
Case22		40	Female	Maxillary	LG	-	ER	Live, nr
Case23		49	Female	Maxillary	LG	-	ER	Live, nr
Case24		30	Male	Maxillary	IntG	+	EN	Live, re
Case25		23	Female	Maxillary	LG	+	ER	Live, nr
Case26		30	Female	Maxillary	LG	+	ER	Live, nr
Case27		26	Female	Maxillary	LG	-	EN	Live, re
Case28		30	Female	Maxillary	LG	+	ER	Live, re
Case29		57	Female	Mandibular	LG	+	ER	Live, nr
Case30		30	Female	Mandibular	LG	+	EN	Live, re

Note: UC-MEC: unicystic mucoepidermoid carcinoma; LG: low grade; IntG: intermediate grade; ER: extensive resection; EN: enucleation; Live, nr: live, no recurrence; Live, re: live, recurrence.

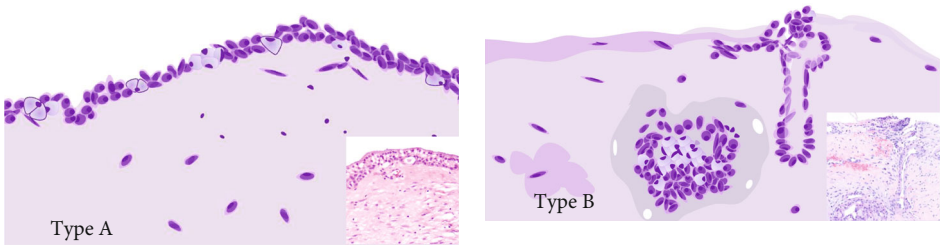

(a) (b)

Figure 1: A schematic representation of the types A and B of UC-MEC. Note: UC-MEC: unicystic mucoepidermoid carcinoma.

case in our cohort experienced multiple attempts at FNAB over 12 years and failed to identify the malignant nature of the lesion. Incisional biopsy usually consists of only small fragments of the cyst wall, and some nonspecific epithelial lining may not reflect the true nature of the entire lesion. Thus, the negative findings on FNAB do not exclude the possibility of a neoplastic cystic lesion. Therefore, a careful histopathological evaluation of the excised tissue should be performed.

GOC and CA share some histopathological features with UC-MEC, including a cystic architecture lined by epithelium consisting of epidermoid and mucous cells. These

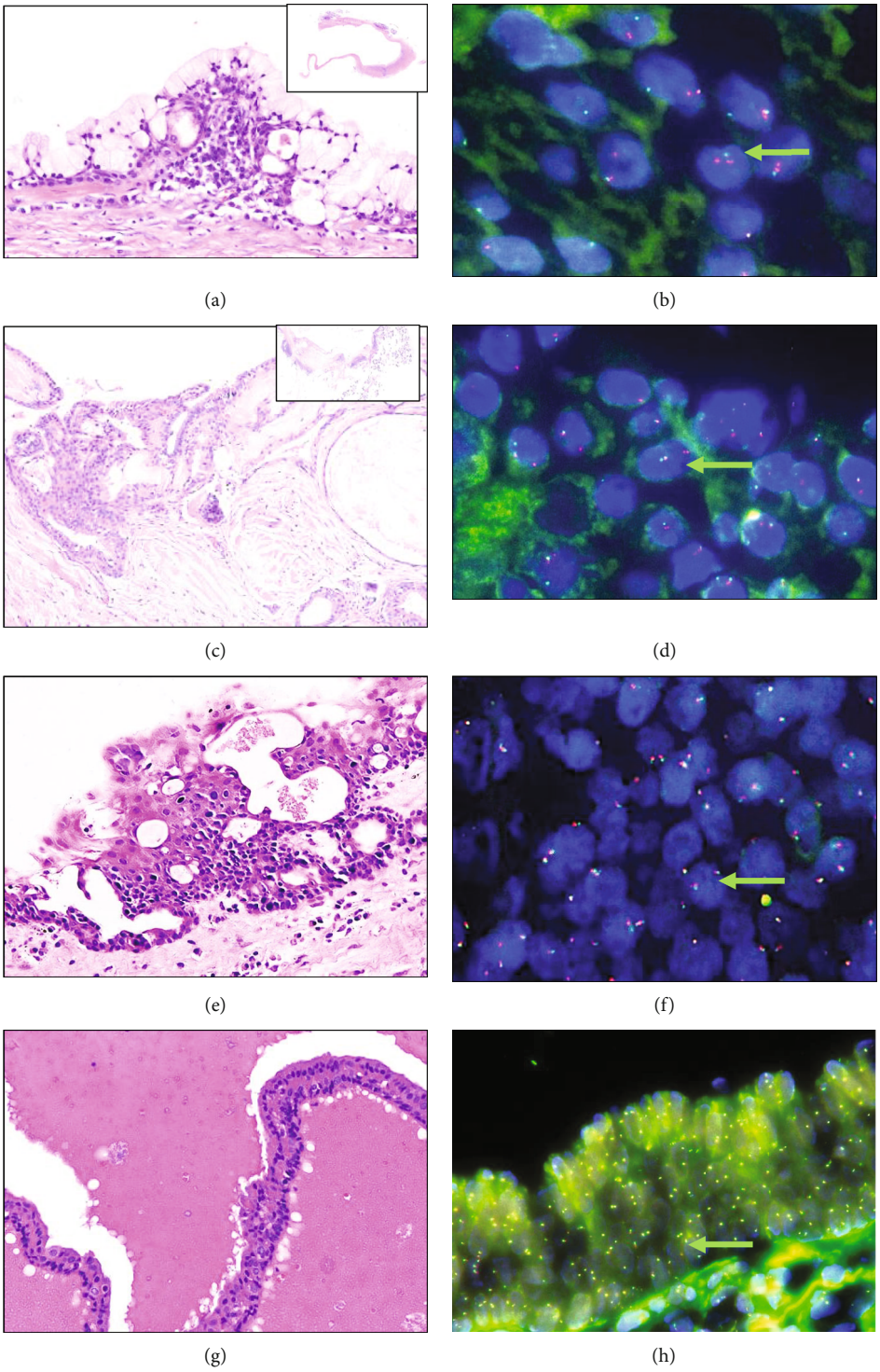

Figure 2: Histological and molecular features of type A, type B MEC, GOC, and CA. (a) Type A UC-MEC (HE ×20); (b) MAML-2 fusion positive in type A UC-MEC (×40), arrowheads indicate MAML2-positive cells; (c) type B UC-MEC (HE ×20); (d) MAML-2 fusion positive in type B UC-MEC (×40), arrowheads indicate MAML2-positive cells; (e) GOC (HE ×20); (f) MAML-2 fusion negative in GOC (×40), arrowheads indicate MAML2-nagetive cells. (g) CA (HE ×40); (h) MAML-2 fusion negative in CA (×40), arrowheads indicate MAML2-nagetive cells.

morphological similarities make the diagnosis difficult [18]. Apart from the specific features of epithelial plaques in GOC, MAML2 rearrangement tested by FISH or NGS was helpful for differential diagnosis. The most frequent chromosomal translocation in TMEC is t (11; 19) (q21; p12-13), which generates a CRTC1-MAML2 fusion gene. Saade et al. found 77% low- and intermediate-grade MEC harboring MAML2 fusion, and only 23% of high-grade MEC

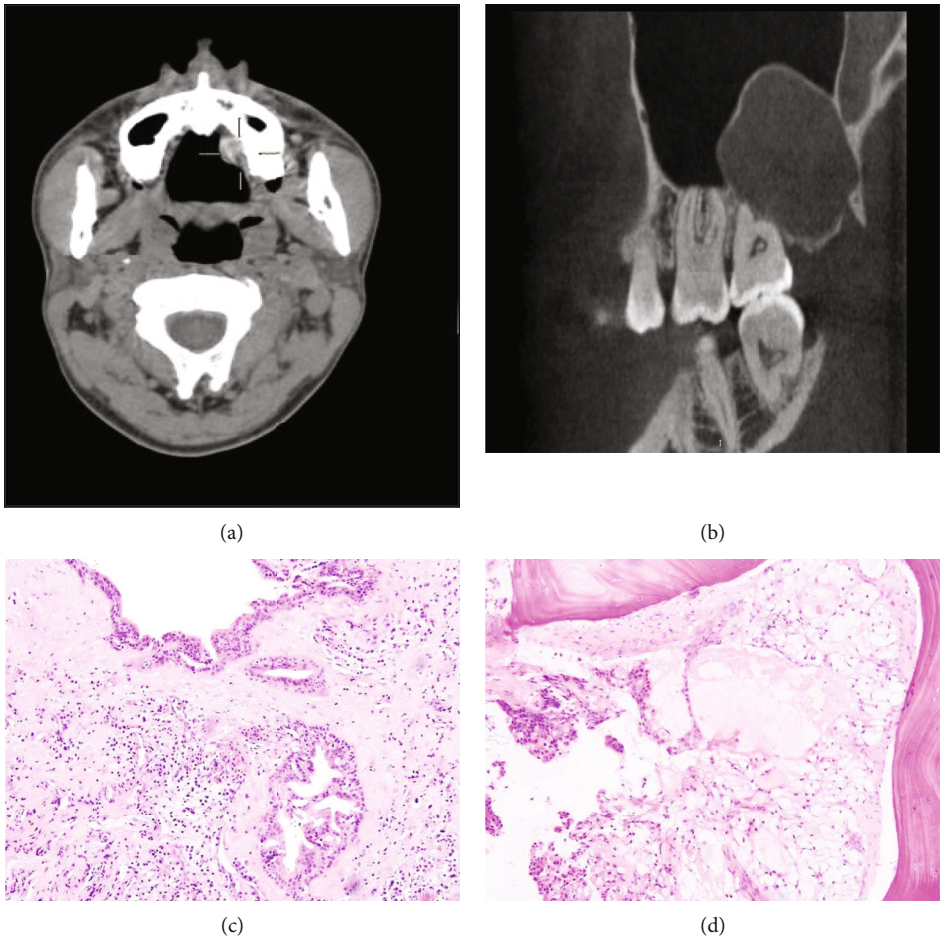

Figure 3: The CT images and histology images of one recurred patient of type B UC-MEC. (a) Contrast-enhanced CT scan of the primary lesion showed that it was cystic and well outlined on the hard palate. (b) 2 years later, CT scan of the recurred lesion showed a well-circumscribed lesion. (c) The proliferative clusters of epithelial cells were observed in the subepithelial area of the fibro-collagenous wall in the primary lesion (HE 10x). (d) The epithelial clusters were invasive into jaw bone in the recurrent lesion (HE 10x).

harbored the MAML2 fusion [23]. In our study, MAML2 rearrangement was detected in 55% of UC-MECs, but in none of the GOCs and CAs, which is similar to a previous study [17, 24]. The high specificity of MAML2 rearrangement for UC-MECs points to its utility as a diagnostic adjunct in separating UC-MEC from mucinous cystic lesions in the jaw and salivary glands.

The AFIP grading systems cited by the WHO (2017 vision) have been commonly adopted and proven useful for prognostic purposes. This system considers the extension of the intracystic component, the presence of neural invasion and necrosis, mitotic index, and cellular anaplasia. Based on the features of exclusive intracystic growth, minimal nuclear pleomorphism, mitotic figures, and absence of perineural invasion and necrosis, UC-MEC was assigned to low-grade tumors. Furthermore, according to invasiveness, we subtyped UC-MEC into types A and B, showing distinctive behavioral differences within its own histopathologic spectrum. In type A, none of the patients had postoperative recurrence mimicking in situ carcinoma. In type B, infiltrative tumor islands were recognized as exhibiting a higher risk of recurrence than those in type A. The management of UC-MEC should be tailored to its grade, histological subtype, and location. For both types A and B, surgery aims to obtain complete resection with negative surgical margins.

5. Conclusions

We collected and analyzed 30 cases of UC-MEC over a long term and clarified the key factors influencing diagnosis and local recurrence. UC-MEC showed two histologic subtypes. In equivocal cases of UC-MEC, FISH for MAML2 rearrangement helps to resolve a differential diagnostic dilemma. Complete surgical resection is a promising treatment option for UC-MEC. The present unique subtype further emphasizes the intralesional heterogeneity of MEC, which may lead to the diagnostic and treatment confusion.

Data Availability

The data used to support the findings of this study are available from the corresponding author upon request.

Conflicts of Interest

The authors declare that the research was conducted in the absence of any commercial or financial relationships that could be construed as a potential conflict of interest.

Acknowledgments

This study received funding from the CAMS Innovation Fund for Medical Sciences (2019-I2M-5-038) and the Fundamental Research Funds for the Central Universities: Special Projects for Strengthening Basic Research of Peking University (BMU2019JC001).

References

[1] A. El-Naggar, J. Chan, and T. Takata, *WHO Classification of Tumours*, IARC Press, Pathology and genetics of head and neck tumours, Lyon, 2017.

[2] S. Capodiferro, G. Ingravallo, L. Limongelli et al., "Intra-cystic (in situ) mucoepidermoid carcinoma: a clinico-pathological study of 14 cases," *Journal of Clinical Medicine*, vol. 9, no. 4, p. 1157, 2020.

[3] S. Saxena, S. Kumar, and J. Kharbanda, "Swelling of the submandibular gland region: cystic or neoplastic entity?," *J Oral Maxillofac Pathol*, vol. 23, no. 3, pp. 468–471, 2019.

[4] N. Ata and H. Ünverdi, "Parotid mucoepidermoid carcinoma mimicking a large mucocele," *The Journal of Craniofacial Surgery*, vol. 29, no. 3, pp. e295–e296, 2018.

[5] R. K. Verma, S. K. Sunku, A. Bal, and N. K. Panda, "Giant cystic primary mucoepidermoid carcinoma of mandible: a rare case and literature review," *Otolaryngologia Polska*, vol. 68, no. 6, pp. 328–332, 2014.

[6] B. R. Spoorthi, R. S. Rao, P. B. Rajashekaraiah, S. Patil, S. S. Venktesaiah, and P. Purushothama, "Predominantly cystic central mucoepidermoid carcinoma developing from a previously diagnosed dentigerous cyst: case report and review of the literature," *Clinics and Practice*, vol. 3, no. 2, article e19, 2013.

[7] A. Qannam, I. O. Bello, M. Al-Kindi, and M. Al-Hindi, "Unicystic mucoepidermoid carcinoma presenting as a salivary duct cyst," *International Journal of Surgical Pathology*, vol. 21, no. 2, pp. 181–185, 2013.

[8] N. Goldman, S. Shuja, R. Makary, and R. L. Griffin, "Mucoepidermoid carcinoma presenting as a large cyst of the parotid gland in HIV disease," *Ear, Nose, & Throat Journal*, vol. 92, no. 7, pp. 310-311, 2013.

[9] M. K. Ranganath, V. Matmari, U. D. Narayanaswamy, and R. M. Bavle, "Mucoepidermoid carcinoma presenting as a retromolar mucocele," *Ann Maxillofac Surg*, vol. 1, no. 1, pp. 66–69, 2011.

[10] E. F. Brachtel, B. Z. Pilch, U. Khettry, A. Zembowicz, and W. C. Faquin, "Fine-needle aspiration biopsy of a cystic pleomorphic adenoma with extensive adnexa-like differentiation: differential diagnostic pitfall with mucoepidermoid carcinoma," *Diagnostic Cytopathology*, vol. 28, no. 2, pp. 100–103, 2003.

[11] P. C. Edwards and P. Wasserman, "Evaluation of cystic salivary gland lesions by fine needle aspiration: an analysis of 21 cases," *Acta Cytologica*, vol. 49, no. 5, pp. 489–494, 2005.

[12] S. I. Chiosea, S. Dacic, M. N. Nikiforova, and R. R. Seethala, "Prospective testing of mucoepidermoid carcinoma for the MAML2 translocation: clinical implications," *Laryngoscope*, vol. 122, no. 8, pp. 1690–1694, 2012.

[13] N. A. Cipriani, J. J. Lusardi, J. McElherne et al., "Mucoepidermoid carcinoma a comparison of histologic grading systems and relationship to MAML2 rearrangement and prognosis," *American Journal of Surgical Pathology*, vol. 43, no. 7, pp. 885–897, 2019.

[14] R. K. Goode, P. L. Auclair, and G. L. Ellis, "Mucoepidermoid carcinoma of the major salivary glands," *Cancer*, vol. 82, no. 7, pp. 1217–1224, 1998.

[15] R. R. Seethala, "Histologic grading and prognostic biomarkers in salivary gland carcinomas," *Advances in Anatomic Pathology*, vol. 18, no. 1, pp. 29–45, 2011.

[16] R. Tucci, L. F. Matizonkas-Antonio, A. A. de Carvalhosa, P. H. Castro, F. D. Nunes, and Pinto DD Jr, "Central mucoepidermoid carcinoma: report of a case with 11 years' evolution and peculiar macroscopical and clinical characteristics," *Medicina Oral, Patología Oral y Cirugía Bucal*, vol. 14, no. 6, pp. E283–E286, 2009.

[17] J. A. Bishop, R. Yonescu, D. Batista, G. R. Warnock, and W. H. Westra, "Glandular odontogenic cysts (GOCs) lack MAML2 rearrangements: a finding to discredit the putative nature of GOC as a precursor to central mucoepidermoid carcinoma," *Head and Neck Pathology*, vol. 8, no. 3, pp. 287–290, 2014.

[18] R. Reddy, M. N. Islam, I. Bhattacharyya, D. M. Cohen, S. G. Fitzpatrick, and S. Ganatra, "The reliability of _MAML2_ gene rearrangement in discriminating between histologically similar glandular odontogenic cysts and intraosseous mucoepidermoid carcinomas," *Oral Surgery, Oral Medicine, Oral Pathology, Oral Radiology*, vol. 127, no. 6, pp. e136–e147, 2019.

[19] R. R. Seethala and G. Stenman, "Update from the 4th edition of the World Health Organization classification of head and neck tumours: tumors of the salivary gland," *Head and Neck Pathology*, vol. 11, no. 1, pp. 55–67, 2017.

[20] P. L. Auclair, R. K. Goode, and G. L. Ellis, "Mucoepidermoid carcinoma of intraoral salivary glands. Evaluation and application of grading criteria in 143 cases," *Cancer*, vol. 69, no. 8, pp. 2021–2030, 1992.

[21] W. F. Raslan, D. R. Sawyer, and L. G. Mercuri, "Central mucoepidermoid carcinoma," *Journal of the Canadian Dental Association*, vol. 64, no. 6, pp. 420–424, 1998.

[22] A. Peraza, R. Gómez, J. Beltran, and F. J. Amarista, "Mucoepidermoid carcinoma. An update and review of the literature," *J Stomatol Oral Maxillofac Surg*, vol. 121, no. 6, pp. 713–720, 2020.

[23] R. E. Saade, D. Bell, J. Garcia, D. Roberts, and R. Weber, "Role of CRTC1/MAML2 translocation in the prognosis and clinical outcomes of mucoepidermoid carcinoma," *JAMA OTOLARYNGOLOGY-HEAD & NECK SURGERY*, vol. 142, no. 3, pp. 234–240, 2016.

[24] M. H. Toper and S. Sarioglu, "Molecular pathology of salivary gland neoplasms: diagnostic, prognostic, and predictive perspective," *Advances in Anatomic Pathology*, vol. 28, no. 2, pp. 81–93, 2021.

Hindawi
Journal of Oncology
Volume 2022, Article ID 7283946, 8 pages
https://doi.org/10.1155/2022/7283946

Research Article

Efficacy and Safety of Pembrolizumab Monotherapy for Recurrent/Unresectable/Metastatic Oral Squamous Cell Carcinoma: A Single-Center Study in China

Jieying Li,[1,2] Zongxuan He,[1,2] Yueqin Tao,[1] Xiaochen Yang,[1,2] Shengyou Ge,[1,2] Haoyue Xu,[1,2] Wei Shang,[1,2] and Kai Song[1,2]

[1]*Department of Oral and Maxillofacial Surgery, The Affiliated Hospital of Qingdao University, Qingdao, Shandong Province, China*
[2]*School of Stomatology, Qingdao University, Qingdao, Shandong Province, China*

Correspondence should be addressed to Wei Shang; liweishang@126.com and Kai Song; assongkai@163.com

Received 13 June 2022; Accepted 4 August 2022; Published 28 August 2022

Academic Editor: Wei Cao

Background. Although pembrolizumab is recommended as a first-line treatment for advanced recurrent/unresectable/metastatic (R/U/M) head and neck squamous carcinoma, the differences in its efficacy among different populations need to be investigated. *Methods*. We reviewed 15 consecutive patients with R/U/M oral squamous cell carcinoma (OSCC) treated with pembrolizumab monotherapy at the Affiliated Hospital of Qingdao University between February 2021 and May 2022. All the 15 patients had known programmed death-ligand 1 expression and received multiple cycles of pembrolizumab monotherapy as first-line treatment. We evaluated and analyzed patients' basic characteristics, time to first remission, the clinical efficacy of pembrolizumab monotherapy, and treatment-related adverse reactions. *Results*. The objective response rate of the 15 patients was 60%. Six patients (40.0%) achieved partial response, while three patients (20.0%) achieved complete response. In our study, the objective response status of the patients was observed in two to five cycles (mean, 3.6 cycles). For patients who responded well to immunotherapy, the mean Karnofsky Performance Status (KPS) score after treatment was significantly higher than that before treatment ($P < 0.001$). The progression-free survival rates were 66.9% and 50.1% at 6 months and 1 year, respectively. Eight adverse events were observed, comprising four cases of rash and one case each of hypothyroidism, interstitial pneumonia, cheilitis, and cerebral thrombosis. *Conclusion*. Our study suggests that pembrolizumab is beneficial to the most responsive patients with R/U/M OSCC in our single-center study and may shed light on the management of OSCC.

1. Introduction

Oral squamous cell carcinoma (OSCC) is a common subtype of head and neck squamous cell carcinoma (HNSCC), with a 5-year survival rate of approximately 50% [1, 2]. In the past decade, cetuximab plus platinum-fluorouracil chemotherapy has been the primary first-line treatment option for recurrent or metastatic OSCC as it helps in local control and improves overall survival in some patients; however, the overall prognosis of patients with advanced OSCC remains poor [3–6]. Therefore, for patients with advanced recurrent/unresectable/metastatic (R/U/M) OSCC, prolonging life expectancy and improving quality of life remains challenging for oncologists.

Immunotherapy has caused a paradigm shift in cancer treatment. In particular, immune checkpoint inhibitors targeting programmed cell death 1 (PD-1) have been effective in treating certain cancer types. Presently, immunotherapy has shown good efficacy for more than 10 solid tumors, including melanoma and lung cancer [7, 8]. A KEYNOTE-024 randomized controlled trial (pembrolizumab) conducted on patients with metastatic non-small-cell lung cancer indicated that the 5-year survival rate of patients treated with pembrolizumab significantly

improved from 16.3% to 31.9% compared to those subjected to platinum-based chemotherapy [9].

Recently, the clinical benefits of immunotherapy in patients with HNSCC have been reported. In a KEYNOTE-048 prospective randomized controlled study on patients expressing programmed death-ligand 1 (PD-L1), pembrolizumab monotherapy or a combination of chemotherapy was reportedly superior to the EXTREME regimen in terms of meaningful improvements in overall survival (OS), progression-free survival (PFS), and objective response rate (ORR) [10]. According to the 2021 National Comprehensive Cancer Network guidelines for Head and Neck Cancer (published on November 9, 2020), pembrolizumab was first proposed as the first-line treatment for advanced R/U/M HNSCC [11]. Subsequently, pembrolizumab monotherapy was approved by the National Medicine Products Administration (NMPA) of China for treating patients with advanced R/U/M HNSCC and PD-L1 combined positive score (CPS) ≥ 20. Although immunotherapy has revolutionized HNSCC treatment, the efficacy and safety of pembrolizumab varies by geographic region and ethnicity [10, 12]. Moreover, limited data are available on pembrolizumab efficacy in the Chinese population with HNSCC, especially OSCC. In the present study, we evaluated 15 patients with advanced R/U/M OSCC who were treated with pembrolizumab to evaluate its antitumor efficacy and safety among the Chinese OSCC population. We hope that the results of our study will be a useful reference for the immunotherapy of patients with advanced OSCC.

2. Materials and Methods

2.1. Patients and Treatments. Based on the NCCN guidelines (Version 1.2021), the inclusion criterion of R/U/M was summarized as follows: R, loco-regional recurrence (recurrence of the primary tumor or the draining lymph nodes) or persistent disease; U, newly diagnosed T4b, N0–3, M0, or unresectable nodal disease, or unfit for surgery; M, distant metastases [11]. In our study, we reviewed 15 consecutive patients with R/U/M OSCC who were treated with pembrolizumab monotherapy at Affiliated Hospital of Qingdao University between February 2021 and May 2022. All the patients were histopathologically confirmed to have OSCC and tested positive for PD-L1 expression based on CPS testing of HNSCC [13]. All the patients received first-line pembrolizumab monotherapy (200 mg) intravenously every 3 weeks [10, 14]. The treatment regimen was re-evaluated when any of the following issues were noted: grade 4-5 adverse reactions (AEs), progressive disease, or no positive response by the fifth cycle. In addition, 20 patients with no surgery or radiotherapy option received the conventional chemotherapy regime (platinum and 5-fluorouracil or paclitaxel) with or without cetuximab in the CPS of 1 or more populations. These populations with chemotherapy were used as the control group for the evaluation of PFS without pembrolizumab in our study. All the patients were followed up until the end of the study (May 1, 2022). This study was approved by the review board of the Affiliated Hospital of Qingdao University and conducted in accordance with the Declaration of Helsinki (1964). This manuscript is available as a preprint at https://www.researchsquare.com/article/rs-1708624/v1 [15].

2.2. Data Collection and Evaluation. Patients' demographic and clinical data, medical history, PD-L1 expression, and Karnofsky performance status (KPS) score were obtained [16]. Follow up was conducted regularly by telephone calls or during clinic visits. Patients' quality of life (QoL) was evaluated using the KPS scale, which had a maximum score of 100; the higher the score, the better the health status of the patient [16]. Response to pembrolizumab monotherapy was assessed by regular imaging examination and observation of objective tumor response according to the suggestions of the multidisciplinary team (MDT) and Response Evaluation Criteria in Solid Tumors version 1.1 (RECIST 1.1) [17]. Data were collected from the initiation of pembrolizumab monotherapy to the end of our study on May 1, 2022. Immune-related adverse events (irAEs) were evaluated according to the Common Terminology Criteria for Adverse Events, version 5.0 [18].

2.3. Data Analysis. A paired *t*-test was conducted to compare the KPS scores before and after pembrolizumab monotherapy [19]. PFS was determined using the Kaplan–Meier method. Data were analyzed using the SPSS version 25.0 (International Business Machines Corp., Chicago, IL, USA). The results with $P < 0.05$ were considered statistically significant.

3. Results

3.1. Demographic and Clinical Data of Patients. Fifteen patients (five female and ten male) with OSCC who were receiving pembrolizumab monotherapy as first-line treatment were enrolled in the study (Figure 1). The median age was 69 years (range: 48–89 years). The primary sites of the OSCC were the tongue ($n = 4$, 26.7%), gingiva ($n = 6$, 40.0%), buccal mucosa ($n = 3$, 20.0%), floor of mouth ($n = 1$, 6.67%), and hard palate ($n = 1$, 6.67%). Among the 15 patients, four cases were of recurrent OSCC, nine of unresectable primary OSCC, and two of metastatic OSCC. Thirteen patients had a CPS ≥ 20 while two patients had 1 ≤ CPS ≤ 19.

3.2. Efficacy of Pembrolizumab as First-Line Treatment. PFS analysis showed that four patients (26.7%) had disease progression at 6-months posttreatment and five patients (33.3%) had disease progression at 1-year posttreatment. The PFS rates were 66.9% and 50.1% at 6 months and 1 year, respectively (Figure 2). Additionally, we found that the PFS rates in the chemotherapy group were 58.7% and 37.3% at 6 months and 1-year posttreatment, respectively. When compared with the chemotherapy group (patients who received conventional chemotherapy without pembrolizumab), the pembrolizumab alone group did not observe significantly improved PFS in the PD-L1 CPS of 1 or more population ($P = 0.906$; Figure 2). Nine of 15 patients

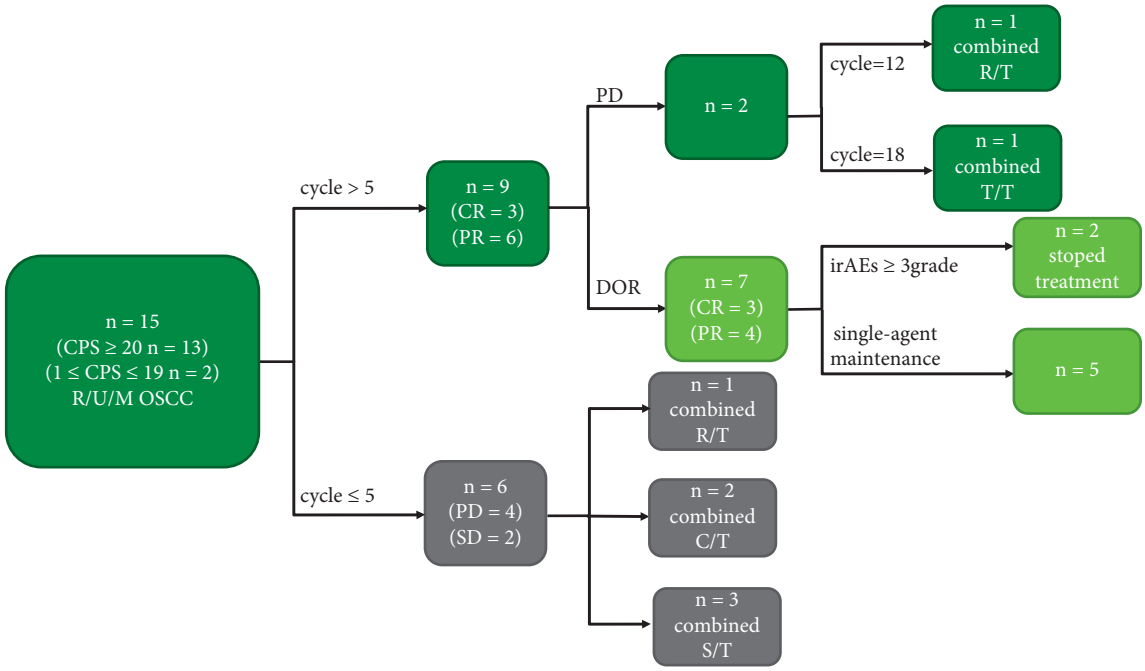

Figure 1: Treatment schema roadmap of all patients in our study. The efficacy of monotherapy in patients with OSCC was assessed according to Response Evaluation Criteria in Solid Tumors version 1.1. CR = complete response; PR = partial response; SD = stable disease; PD = progressive disease; DOR = duration of response; irAEs = immune-related adverse events; *C*/*T* = chemotherapy; *R*/*T* = radiotherapy; *S*/*T* = surgical treatment; and *T*/*T* = targeted therapy.

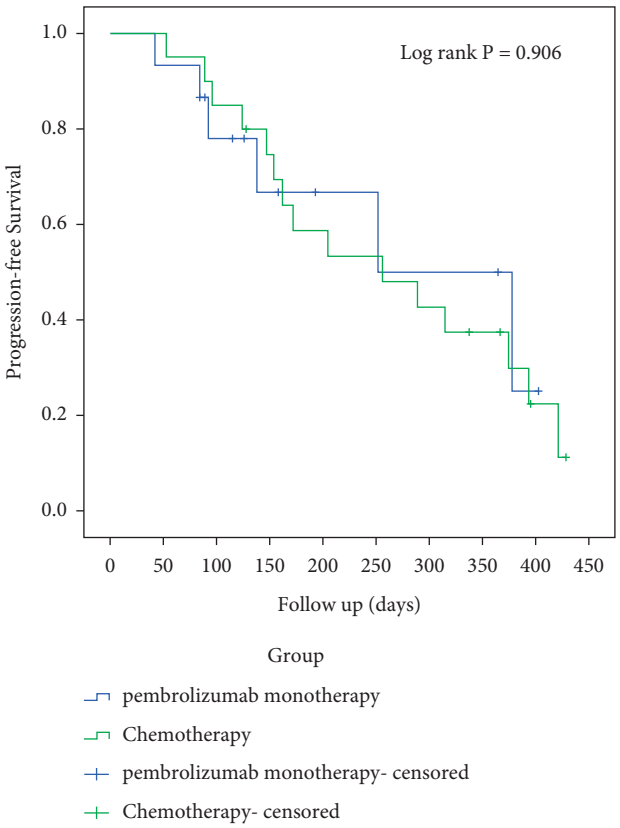

Figure 2: Kaplan–Meier survival curves for progression-free survival of patients with recurrent/unresectable/metastatic oral squamous cell carcinoma treated with pembrolizumab or chemotherapy.

responded well to single-agent immunotherapy with a median follow-up duration of 9.6 months (range: 3–13.5 months). For the total patients (15/15) with immunotherapy, the median follow-up duration was 6.4 months (range: 2.8–13.5 months). Until the end of the study, the fifteen included patients were all alive and follow-up studies were ongoing. A swimmer plot of outcomes for each of the 15 patients is displayed in Figure 3. The ORR was 60% (9/15). Nine patients started showing positive response to pembrolizumab monotherapy (time to first remission) between two to five cycles (mean: 3.6). The imaging examinations and biopsies after treatment showed that three patients (20%) achieved a complete response, whereas six patients (40%) achieved a partial response (PR). Among them, one patient each transitioned to progressive disease status on the 12th and 18th cycles, respectively. For the patients who responded well to immunotherapy, the mean KPS score after treatment was significantly higher than that before treatment (58.89 ± 13.64 to 85.56 ± 10.14; $P < 0.001$).

3.3. Pembrolizumab Treatment-Related Adverse Events. The adverse reactions observed during the immunotherapy are listed in Table 1. Eight adverse events were observed: four (26.7%) cases of rash and one case each of hypothyroidism, interstitial pneumonia, cheilitis, and cerebral thrombosis (each 6.7%). Among these adverse events, one patient suffered concurrent rash and interstitial pneumonia, whereas another had concurrent rash and cheilitis. The emergency management of severe irAEs should be given attention because it would be life-threatening for patients. In our study, one patient developed breath-holding and coughing

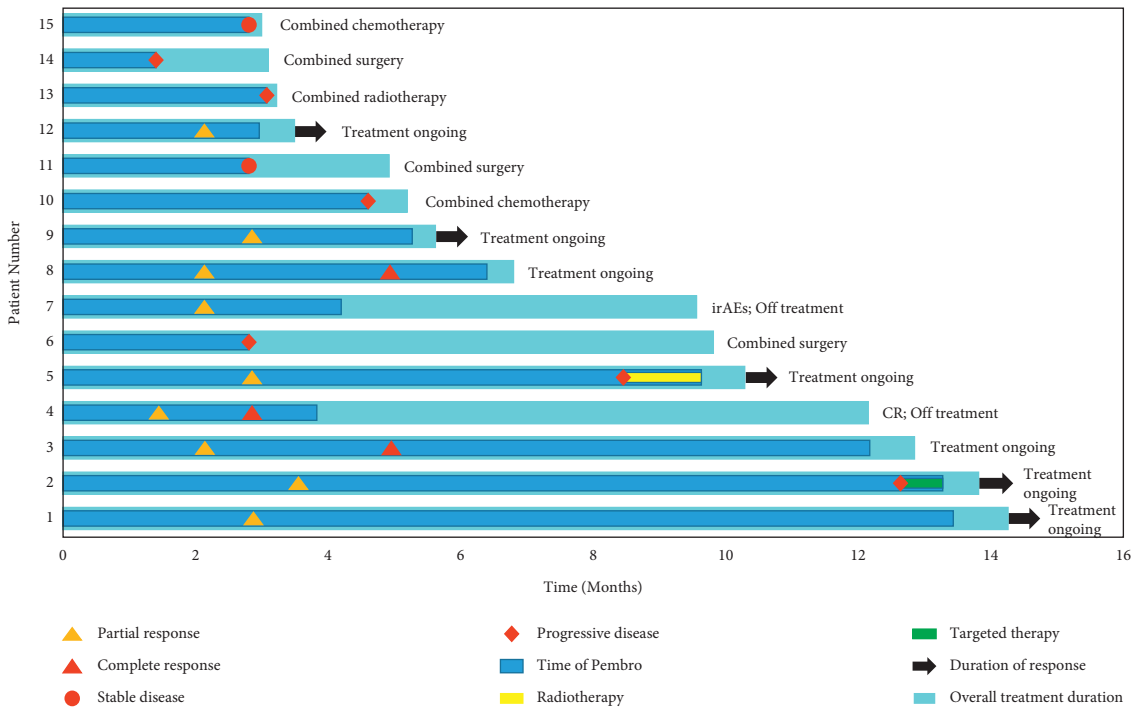

Figure 3: Swimmer plot for a treatment duration of the 15 patients enrolled in our study. CR = complete response; irAEs = immune-related adverse events. The "overall treatment duration" in the swimmer plot referred to the time for pretreatment assessments (including physical examination, imaging study, CPS evaluation, and MDT), pembrolizumab treatment, and subsequent follow-up.

Table 1: Adverse events in 15 patients who were enrolled in our study.

Adverse event	1–2 Grade	3–5 Grade
Rash	4 (26.7%)	0
Hypothyroidism	1 (6.7%)	0
Arrhythmia	0	0
Pneumonitis	0	1 (6.7%)
Stomatitis	1 (6.7%)	0
Liver dysfunction	0	0
Gastroenteritis	0	0
Cerebral thrombosis	0	1 (6.7%)

and was admitted with grade IV interstitial pneumonia after seven cycles of pembrolizumab. The patient's symptoms were significantly alleviated after 1-week of treatment with the intervention of a high dose of intravenous methylprednisolone and maintenance of airway patency. This patient maintained PR status even after cessation of anti-PD-1 immunotherapy (Figure 4). In another case of severe irAE, the patient had a history of thrombosis and developed symptoms of cerebral thrombosis on the seventh treatment cycle. Despite the permanent cessation of anti-PD-1 immunotherapy, the recurrence of either vascular thrombosis or tumor was not observed during the follow-up of this patient.

4. Discussion

Patients with R/U/M OSCC have a poor prognosis, with a median survival of 6–12 months [3, 20]. In recent years, the benefits of immunotherapy in HNSCC have caused a paradigm shift in the treatment of OSCC. On December 11, 2020, pembrolizumab monotherapy was approved by the NMPA of China for treating patients with advanced R/U/M HNSCC with PD-L1 expression (CPS ≥ 20). However, the efficacy and safety of pembrolizumab in Chinese patients with R/U/M HNSCC, especially OSCC, has not been reported adequately due to the relatively short clinical treatment duration. Hence, our case series evaluated the efficacy and safety of pembrolizumab for OSCC treatment in a single-center in China.

Immunotherapy allows the re-establishment of the immune system and is a promising therapy for advanced OSCC. In a KEYNOTE-048 study on HNSCC, 23% (31/133) participants showed an objective response (OR) were reported in the pembrolizumab alone group with PD-L1 expression (CPS ≥ 20) [10]. In our study, the ORR of patients with OSCC was reduced from 60% (9/15) on the fifth cycle to 46.67% (7/15) on the 18th cycle. This change in patients' ORR suggests that a longer follow-up might be more useful for determining pembrolizumab efficacy. O'Donnell et al. [21–23]reported that the acquired immune resistance could lead to tumor progression or recurrence, which may also be related to changes in ORR. Additionally, in 2019, the European Society of Medical Oncology meeting declared that the efficacy of pembrolizumab for HNSCC was much better in the Asian group than in the non-Asian group [10]. In our study, although the time of the first remission of immunotherapy was inconclusive, the OR was observed between two and five cycles (mean: 3.6 cycles). Currently, there are no guidelines describing the time for modifying the treatment

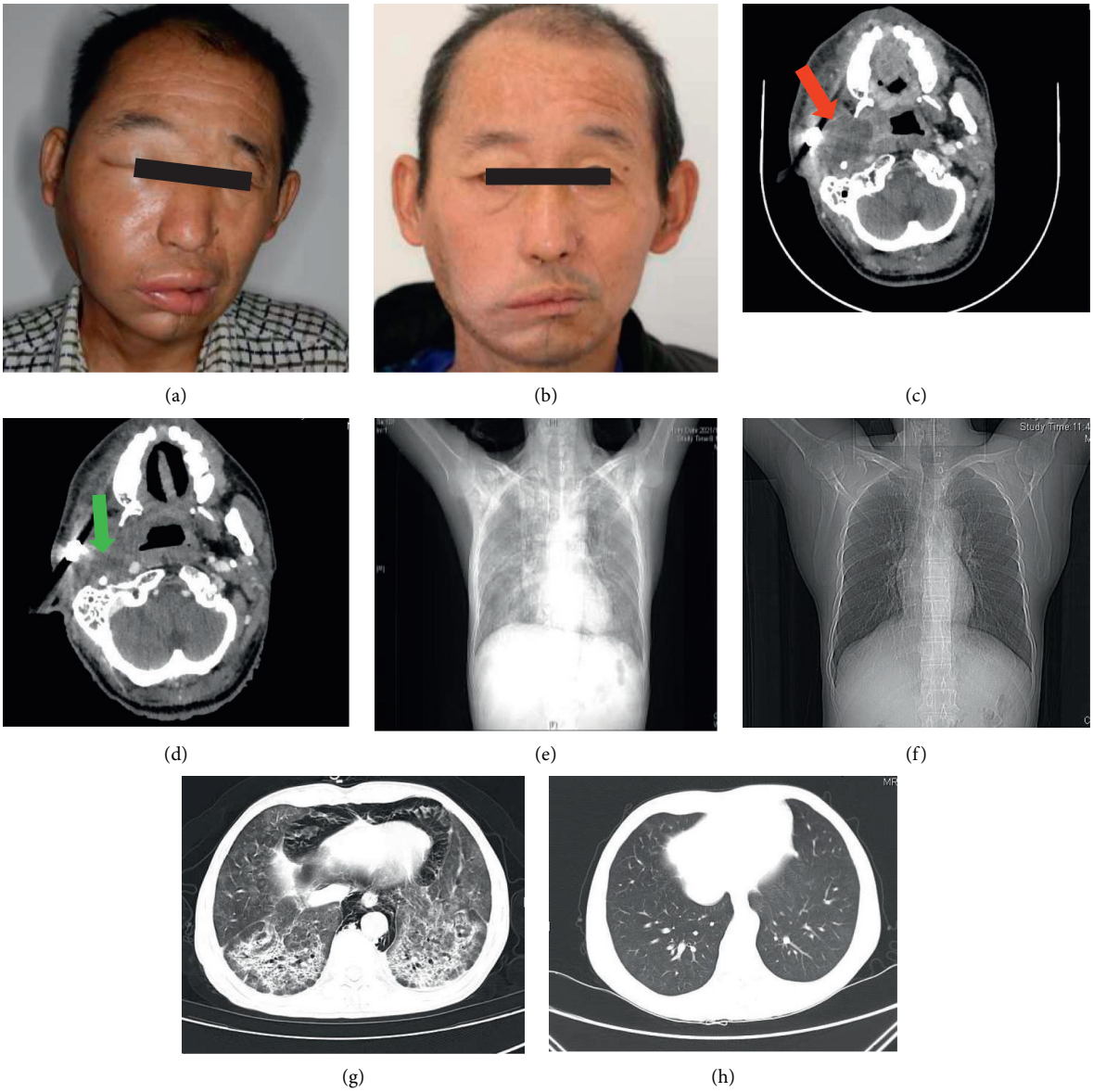

Figure 4: Patient No. 7 experienced tumor recurrence on the right maxilla and an invasion into the pterygoid plate ((a); (c) red arrow). Partial response occurred after four cycles of pembrolizumab treatment ((b); (d) green arrow). Interstitial pneumonia in both lungs was observed after seven cycles of pembrolizumab treatment ((e) chest radiograph; (g) chest computed tomography). The serial images indicate that the immune-related adverse events were controlled following seven days of methylprednisolone treatment ((f) chest radiograph; (h) chest computed tomography).

regimens for patients receiving single-agent immunotherapy. According to MDT evaluations and our single-center experiences with pembrolizumab, combination therapy may be recommended if patients show no positive response to the single-agent immunotherapy by the fifth cycle.

The management of cancer patients aims to prolong life expectancy and improve QoL. So far, none of the studies have concluded that immunotherapy can significantly improve the PFS and OS of oral cancer patients. In our study, the longest follow-up period for the single-agent immunotherapy was more than 18 cycles (13 months) in patients with good responses. Although there were no PFS benefits by comparing the pembrolizumab group with the chemotherapy group without pembrolizumab in the PD-L1 CPS ≥ 1 population in our study, our patients with pembrolizumab treatment showed a better PFS than those subjected to the chemotherapy regimen in an open-label Phase II trial reported by Chang [24]. Due to the lack of data on the long-termfollow-up of efficacy, it is insufficient to evaluate OS. Indeed, to a certain extent, the QoL of patients with OSCC is considered as important as survival. Advanced oral cancer significantly impacts patients' QoL by adversely influencing their communication and appearance and inducing intractable pain and dysphagia [25–27]. In recent years, immunotherapy has significantly improved QoL for patients with different cancers. In the KEYNOTE-024 study,

pembrolizumab was useful for improving or maintaining QoL by relieving symptoms such as cough, chest pain, and dyspnea in lung cancer patients, compared to chemotherapy [28]. In patients responding well to single-agent immunotherapy, the mean KPS score before and after treatment improved from 58.89 ± 13.64 to 85.56 ± 10.14 ($P < 0.001$), suggesting that immunotherapy significantly improved their physical and mental health.

Although immunotherapy has led to a paradigm shift in OSCC treatment, the risk of irAEs in immunotherapy cannot be avoided completely. In our study, we found that mild irAEs (grades 1-2) were predominant compared to severe irAEs (grades 3–5). For patients undergoing immunotherapy, the emergency management of severe irAEs should be established, because they would be life-threatening for patients. Pneumonitis, organizing pneumonia, interstitial pneumonitis, and nonspecific interstitial pneumonia, have been underscored as grade 3–5 irAEs in case reports and clinical studies [29, 30]. Immune-related pneumonitis is a rare but life-threatening adverse reaction that accounts for 35% of PD-1/PD-L1 inhibitor-related deaths [31]. Once PD-1inhibitor-related pneumonitis is recognized, treatment should be immediately stopped and glucocorticoid administration should be considered [32]. In our study, one patient developed severe respiratory failure after seven cycles of pembrolizumab and was diagnosed with immune-related pneumonitis (interstitial pneumonitis). The patient's symptoms were significantly alleviated after administering high doses of intravenous methylprednisolone and maintaining airway patency for one week. In addition, immunotherapy may increase the risk of irAEs, such as thrombosis. Although the correlation between thrombosis and immunotherapy has not been well reported in recent years, it has been reported that checkpoint blockers in patients with cancer could induce accelerated inflammation and lead to an increased risk of thromboembolism and cardiovascular complications [33–36]. In our study, a patient with a history of thrombosis developed symptoms of cerebral thrombosis on the seventh treatment cycle. Despite the permanent cessation of anti-PD-1 immunotherapy, the recurrence of either vascular thrombosis or tumor was not observed during the follow-up period. Our case may contribute to the expanding evidence for the correlation between anti-PD-1-related immunotherapy and the risk of thrombosis.

5. Conclusion

MDT is important for single-agent immunotherapy in patients with R/U/M OSCC and should be recommended throughout the treatment period. Existing data lacks a long-termfollow-up to conclusively evaluate the efficacy or OS. However, in our study, patients responding well to anti-PD-1 single-agent immunotherapy showed obvious improvement in QoL. The emergency management of severe irAEs should be established because the risk of irAEs in immunotherapy cannot be avoided completely. Nevertheless, some limitations should be acknowledged in our study. Since our findings came from a single-center study, clinically relevant differences may be found among hospitals. Additionally, a larger sample size should be designed to increase the significance of the results. Overall, we hope that our data can provide a clinical reference for immunotherapy in Chinese patients with R/U/M OSCC.

Data Availability

No data were used to support this study.

Ethical Approval

Ethics approval for this study was provided by the Research Ethics Board of Qingdao University.

Consent

A written informed consent was obtained from each patient before treatment.

Disclosure

This manuscript has been presented in Research Square as a preprint according to the following link: https://www.researchsquare.com/article/rs-1708624/v1.

Conflicts of Interest

The authors declare there are no conflicts of interest.

Authors' Contributions

Jieying Li and Zongxuan He contributed equally to this study.

Acknowledgments

This work was supported by the National Natural Science Foundation of China (grant no. 81502340). The authors acknowledge the help by Dr. Guizhong Li in data collection.

References

[1] M. N. M. R. Petruzzi, K. Cherubini, F. G. Salum, and M. A. Z. de Figueiredo, "Role of tumour-associated macrophages in oral squamous cells carcinoma progression: an update on current knowledge," *Diagnostic Pathology*, vol. 12, no. 1, p. 32, 2017.

[2] D. Baraniya, V. Jain, R. Lucarelli et al., "Screening of health-associated oral bacteria for anticancer properties in vitro," *Frontiers in Cellular and Infection Microbiology*, vol. 10, Article ID 575656, 2020.

[3] J. B. Vermorken, R. Mesia, F. Rivera et al., "Platinum-based chemotherapy plus cetuximab in head and neck cancer," *New England Journal of Medicine*, vol. 359, no. 11, pp. 1116–1127, 2008.

[4] Y. Wang, W. Zhang, P. Sun et al., "A novel multimodal NIR-II nanoprobe for the detection of metastatic lymph nodes and targeting chemo-photothermal therapy in oral squamous cell carcinoma," *Theranostics*, vol. 9, no. 2, pp. 391–404, 2019.

[5] Q. Tang, M. Xie, S. Yu et al., "Periodic oxaliplatin administration in synergy with PER2-mediated PCNA transcription

repression promotes chronochemotherapeutic efficacy of OSCC," *Advanced Science*, vol. 6, no. 21, Article ID 1900667, 2019.

[6] R. Wang, X. Lu, and R. Yu, "lncRNA MALAT1 promotes EMT process and cisplatin resistance of oral squamous cell carcinoma via PI3K/AKT/m-TOR signal pathway," *Onco-Targets and Therapy*, vol. 13, pp. 4049–4061, 2020.

[7] K. Margolin, M. S. Ernstoff, O. Hamid et al., "Ipilimumab in patients with melanoma and brain metastases: an open-label, phase 2 trial," *The Lancet Oncology*, vol. 13, no. 5, pp. 459–465, 2012.

[8] A. S. Mansfield, R. S. Herbst, G. de Castro et al., "Outcomes with pembrolizumab monotherapy in patients with programmed death-ligand1-positive NSCLC with brain metastases: pooled analysis of KEYNOTE-001, 010, 024, and 042," *JTO Clinical and Research Reports*, vol. 2, no. 8, Article ID 100205, 2021.

[9] F. Li and X. Dong, "Pembrolizumab provides long-term survival benefits in advanced non-small cell lung cancer: the 5-year outcomes of the KEYNOTE-024 trial," *Thorac Cancer*, vol. 12, no. 23, pp. 3085–3087, 2021.

[10] B. Burtness, K. J. Harrington, R. Greil et al., "Pembrolizumab alone or with chemotherapy versus cetuximab with chemotherapy for recurrent or metastatic squamous cell carcinoma of the head and neck (KEYNOTE-048): a randomised, open-label, phase 3 study," *Lancet*, vol. 394, no. 10212, pp. 1915–1928, 2019.

[11] D. G. Pfister and S. Spencer, "NCCN clinical practice guidelines in head and neck cancers," *Official Journal of the National Comprihensive Cancer Network*, vol. 18, 2020.

[12] R. Mehra, T. Y. Seiwert, S. Gupta et al., "Efficacy and safety of pembrolizumab in recurrent/metastatic head and neck squamous cell carcinoma: pooled analyses after long-termfollow-up in KEYNOTE-012," *British Journal of Cancer*, vol. 119, no. 2, pp. 153–159, 2018.

[13] D. Evrard, M. Hourseau, A. Couvelard et al., "PD-L1 expression in the microenvironment and the response to checkpoint inhibitors in head and neck squamous cell carcinoma," *OncoImmunology*, vol. 9, no. 1, Article ID 1844403, 2020.

[14] E. B. Garon, N. A. Rizvi, R. Hui et al., "Pembrolizumab for the treatment of non-small-cell lung cancer," *New England Journal of Medicine*, vol. 372, no. 21, pp. 2018–2028, 2015.

[15] J. Li, Z. He, Y. Tao, X. Yang, S. Ge, and H. Xu, *Efficacy and Safety of Pembrolizumab Monotherapy for Recurrent/unresectable/metastatic Oral Squamous Cell Carcinoma: A Single-Centre Study in China. Research Square*, Preprint, 2022.

[16] A. H. Friendlander and R. L. Ettinger, "Karnofsky performance status scale," *Special Care in Dentistry*, vol. 29, no. 4, pp. 147-148, 2009.

[17] E. A. Eisenhauer, P. Therasse, J. Bogaerts et al., "New response evaluation criteria in solid tumours: revised RECIST guideline (version 1.1)," *European Journal of Cancer*, vol. 45, no. 2, pp. 228–247, 2009.

[18] M. Lv, M. Chen, R. Zhang et al., "Manganese is critical for antitumor immune responses via cGAS-STING and improves the efficacy of clin ical immunotherapy," *Cell Research*, vol. 30, no. 11, pp. 966–979, 2020.

[19] G. Raffa, M. C. Quattropani, G. Marzano et al., "Mapping and preserving the visuospatial Network by repetitive nTMS and DTI tractography in patients with right parietal lobe tumors," *Frontiers Oncology*, vol. 11, Article ID 677172, 2021.

[20] A. Argiris, K. J. Harrington, M. Tahara et al., "Evidence-based treatment options in recurrent and/or metastatic squamous cell carcinoma of the head and neck," *Frontiers Oncology*, vol. 7, p. 72, 2017.

[21] J. S. O'Donnell, M. W. L. Teng, and M. J. Smyth, "Cancer immunoediting and resistance to T cell-based immunotherapy," *Nature Reviews Clinical Oncology*, vol. 16, no. 3, pp. 151–167, 2019.

[22] A. Kalbasi and A. Ribas, "Tumour-intrinsic resistance to immune checkpoint blockade," *Nature Reviews Immunology*, vol. 20, no. 1, pp. 25–39, 2020.

[23] G. Herbreteau, A. Vallée, A.-C. Knol et al., "Circulating tumor DNA early kinetics predict response of metastatic melanoma to anti-PD1 immunotherapy: validation study," *Cancers*, vol. 13, no. 8, p. 1826, 2021.

[24] P. M. H. Chang, H. J. Lu, L. W. Wang et al., "Effectiveness of incorporating cetuximab into docetaxel/cisplatin/fluorouracil induction chemotherapy and chemoradiotherapy for inoperable squamous cell carcinoma of the oral cavity: a phase II study," *Head & Neck*, vol. 39, no. 7, pp. 1333–1342, 2017.

[25] J. Breeze, A. Rennie, D. Dawson et al., "Patient-reported quality of life outcomes following treatment for oral cancer," *International Journal of Oral and Maxillofacial Surgery*, vol. 47, no. 3, pp. 296–301, 2018.

[26] M. K. Oba, L. M. A. R. Innocentini, G. Viani et al., "Evaluation of the correlation between side effects to oral mucosa, salivary glands, and general health status with quality of life during intensity-modulated radiotherapy for head and neck cancer," *Supportive Care in Cancer*, vol. 29, no. 1, pp. 127–134, 2021.

[27] D. Adkins, J. Ley, P. Oppelt et al., "Impact on health-related quality of life of induction chemotherapy compared with concurrent cisplatin and radiation therapy in patients with head and neck cancer," *Clinical Oncology*, vol. 31, no. 9, pp. e123–e131, 2019.

[28] J. R. Brahmer, D. Rodríguez-Abreu, A. G. Robinson et al., "Health-related quality-of-life results for pembrolizumab versus chemotherapy in advanced, PD-L1-positive NSCLC (KEYNOTE-024): a multicentre, international, randomised, open-label phase 3 trial," *The Lancet Oncology*, vol. 18, no. 12, pp. 1600–1609, 2017.

[29] V. Leroy, C. Templier, J. B. Faivre et al., "Pembrolizumab-induced pneumonitis," *ERJ Open Research*, vol. 3, no. 2, pp. 00081–2016, 2017.

[30] S. L. Topalian, F. S. Hodi, J. R. Brahmer et al., "Safety, activity, and immune correlates of anti-PD-1 antibody in cancer," *New England Journal of Medicine*, vol. 366, no. 26, pp. 2443–2454, 2012.

[31] D. Y. Wang, J. E. Salem, J. V. Cohen et al., "Fatal toxic effects associated with immune checkpoint inhibitors: a systematic review and meta-analysis," *JAMA Oncology*, vol. 4, no. 12, pp. 1721–1728, 2018.

[32] M. Nishino, N. H. Ramaiya, M. M. Awad et al., "PD-1inhibitor-related pneumonitis in advanced cancer patients: radiographic patterns and clinical course," *Clinical Cancer Research*, vol. 22, no. 24, pp. 6051–6060, 2016.

[33] J. Roopkumar, S. Swaidani, A. S. Kim et al., "Increased incidence of venous thromboembolism with cancer immunotherapy," *Medicus Plus*, vol. 2, no. 4, pp. 423–434.e3, 2021.

[34] J. Tsukamoto, M. Monteiro, S. Vale et al., "Thromboembolic events related to treatment with checkpoint inhibitors: report of two cases," *Case Rep Oncol*, vol. 11, no. 3, pp. 648–653, 2018.

[35] C. Fu, G. Wang, and W. Yang, "Vascular thrombosis and anti-PD-1 therapy: a series of cases," *Cancer Management and Research*, vol. 13, pp. 8849–8853, 2021.

[36] Y. Ando, T. Hayashi, R. Sugimoto et al., "Risk factors for cancer-associated thrombosis in patients undergoing treatment with immune checkpoint inhibitors," *Investigational New Drugs*, vol. 38, no. 4, pp. 1200–1206, 2020.

Hindawi
Journal of Oncology
Volume 2022, Article ID 5227771, 6 pages
https://doi.org/10.1155/2022/5227771

Research Article

Risk Factors for Esophageal Squamous Cell Carcinoma in Patients with Head and Neck Squamous Cell Carcinoma

Lei Wang,[1,2,3] **Wenjing Pang**,[1,2,3] **Kun Zhou**,[1,2,3] **Lei Li**,[1,2,3] **Feng Wang**,[4] **Wei Cao**,[5,6,7,8] **and Xiangjun Meng**[1,2,3]

[1]*Department of Gastroenterology, Shanghai Ninth Peoples' Hospital, Shanghai Jiao Tong University School of Medicine, Shanghai 200011, China*
[2]*Center for Digestive Diseases Research and Clinical Translation of Shanghai Jiao Tong University, Shanghai 200011, China*
[3]*Shanghai Key Laboratory of Gut Microecology and Associated Major Diseases Research, Shanghai 200011, China*
[4]*Department of Thoracic Surgery, Shanghai Ninth Peoples' Hospital, Shanghai Jiao Tong University School of Medicine, Shanghai 200011, China*
[5]*Department of Oral and Maxillofacial-Head and Neck Oncology, Shanghai Ninth Peoples' Hospital, Shanghai Jiao Tong University School of Medicine, Shanghai 200011, China*
[6]*National Clinical Research Center for Oral Diseases, Shanghai 200011, China*
[7]*Shanghai Key Laboratory of Stomatology & Shanghai Research Institute of Stomatology, Shanghai 200011, China*
[8]*Research Unit of Oral and Maxillofacial Regenerative Medicine, Chinese Academy of Medical Sciences, Shanghai 200011, China*

Correspondence should be addressed to Wei Cao; caowei561521@hotmail.com and Xiangjun Meng; meng_xiangjun@yahoo.com

Received 12 June 2022; Revised 9 July 2022; Accepted 18 July 2022; Published 27 August 2022

Academic Editor: Dali Zheng

Background. Esophageal squamous cell carcinoma (ESCC) is a common second primary neoplasia in patients with a history of head and neck squamous cell carcinoma (HNSCC). The aim of this study was to provide further information and novel insights into the risk factors for ESCC in patients with HNSCC. *Methods*. We retrospectively analyzed 98 HNSCC patients diagnosed from 2007 to 2017, 30 HNSCC patients suffering from ESCC, who had undergone endoscopic examination because of positive imaging examinations or symptoms, and 68 HNSCC patients who had no ESCC occurrence for at least six years post-HNSCC diagnosis. Associated clinicopathological data and lifestyle information of the ESCC group and the without ESCC group were collected, and a case-control study of risk factors was analyzed between the two groups. *Results*. The majority (83.4%) of the cases with HNSCC esophageal cancers were male patients over 50 years. We established that 93.75% (30/32) of the ESCC occurred within six years after HNSCC diagnosis. HNSCC location, stage, and radiotherapy history had no significant association with the development of ESCC. High Ki67 labeling index (Ki67 LI) (>46) patients tended to be 3.1 times (95% CI = 1.3–7.6) more likely to develop ESCC compared to low Ki67 LI (≤45) patients ($P < 0.05$). Drinkers with alcohol flushing response were at a 3.3 times higher risk to have ESCC (95% CI = 1.0–10.4) than drinkers without flush response ($P < 0.05$). *Conclusions*. HNSCC patients, especially drinkers with an alcohol flushing response, as well as those with high Ki67 LI of HNSCC tissue, were more likely to develop ESCC.

1. Introduction

Head and neck squamous cell carcinoma (HNSCC) patients have a high risk of developing second primary carcinoma in their upper gastrointestinal tract, most commonly in the esophagus [1, 2]. Reportedly, approximately 5%–15% of HNSCC patients develop esophageal squamous cell carcinoma (ESCC), which is higher than the general population [3–7]. Due to the usual absence of early clinical symptoms associated with esophageal malignant tumors, ESCC often leads to treatment failure in HNSCC, which is associated with a poor prognosis [8–10].

With advances in endoscopy, such as NBI in combination with magnifying endoscopy, early detection of esophageal cancer is possible. Thus, routine esophageal screening in asymptomatic patients with HNSCC has been

recommended [11–17]. However, there is no consensus reached on the criteria for screening patients with a higher risk for esophageal cancer [18, 19]. Hence, a retrospective comparative case-control study between the ESCC group and the without ESCC group of HNSCC patients was conducted to investigate the associated risk factors of second primary ESCC in patients with HNSCC.

2. Materials and Methods

2.1. Study Design. We retrospectively reviewed the medical records of 98 HNSCC patients diagnosed for the first time at the Department of Oral and Maxillofacial Head and Neck Oncology, Shanghai Ninth Peoples' Hospital, Shanghai Jiaotong University (Shanghai, China), from 2007 to 2017. Thirty HNSCC patients suffering from synchronous or metachronous ESCC within or after six months following HNSCC diagnosis were included. Synchronous cancers were defined as the occurrence of a second primitive cancer within the first six months following the detection of first cancer, whereas metachronous cancers appeared within more than six months. Sixty-eight HNSCC patients without ESCC occurrence for at least six years after HNSCC diagnosis were included as a control group. The inclusion criteria were as follows: HNSCC patients were first diagnosed based on pathological postoperative confirmation, esophageal lesions were observed by upper gastrointestinal endoscopy with the NBI mode, and the histopathology of the esophageal lesions was confirmed as ESCC or high-grade intraepithelial neoplasia. The following exclusion criteria were applied: patients who had a history of esophageal cancer or other malignancies before HNSCC diagnosis, HNSCC patients who were not newly diagnosed in our hospital, and patients who had prior gastrointestinal surgery before HNSCC diagnosis. The study was conducted in accordance with the Declaration of Helsinki (as revised in 2013) and was approved by the Ethics Committee of Shanghai Ninth People's Hospital, Shanghai Jiao Tong University School of Medicine (No.: SH9H-2020-T189-1). Individual consent for this retrospective analysis was waived.

2.2. Information of HNSCC Patients. Associated clinicopathological data and lifestyle information of all HNSCC patients were collected. All HNSCC patients underwent surgical treatment at the Department of Oral and Maxillofacial Head and Neck Oncology, Shanghai Ninth Peoples' Hospital, Shanghai Jiao Tong University (Shanghai, China). Histopathological diagnoses were made at the department of oral pathology of our hospital. HNSCC was graded based on the surgical histopathological results and the TNM staging system for lip and oral cancer (AJCC, eighth edition) [20]. The Ki67 labeling index (Ki67 LI) was assessed based on immunohistochemical evaluation from histopathological reports of HNSCC operation tissues. IHC staining was performed following the standard procedure. Ki67-positive neoplastic epithelial cell counts were carried out in five randomly selected fields at 400 × magnification. Ki67 LI was derived as the number of Ki67-positive cells multiplied by 100 and divided by the total number of the observed neoplastic epithelial cells. The Ki67 antigen expression levels were categorized into the following categories: low, Ki67 LI ≤ 45; high, Ki67 LI > 45. Drinkers were defined as those consuming any alcoholic beverage at least once per week for a minimum of six months and smokers as those smoking ten cigarettes or more per week for at least six months [21]. Information on whether the drinkers experienced flushing in response to alcohol was collected. The radiotherapy history of each HNSCC patient was also reviewed.

2.3. Endoscopic Examination of Esophageal Cancer. Endoscopic examination was performed at the initial HNSCC diagnosis or at the postoperative follow-up based on positive imaging examination or the presence of symptoms such as progressive dysphagia or pain behind the sternum. Endoscopy of the upper gastrointestinal tract (GIF-H290; Olympus, Japan) was performed through the mouth by a physician experienced in endoscopy. Once in the oral cavity, the NBI mode was turned on for observation of the pyriform sinus and esophageal mucosa, focusing on any suspected esophageal lesions. Biopsy was next performed when a definitive pathological diagnosis was needed. Esophageal cancer was classified according to AJCC eighth edition guidelines [20].

2.4. Patient Follow-Up. All HNSCC patients were followed up by trained medical personnel by telephone or WeChat for follow-up treatment and a second primary cancer diagnosis. HNSCC patients were followed up to the time of esophageal cancer diagnosis or at least six years after HNSCC diagnosis.

2.5. Statistical Analysis. Comparisons between the ESCC group and the without ESCC group of HNSCC patients were performed using the χ^2 test or Fisher's exact test. Logistic regression analysis was conducted using the data for sex, age, HNSCC site, HNSCC stage, Ki67 labeling, radiotherapy history, smoking history, drinking history, and flush response. Odds ratios and 95% confidence intervals were calculated. Statistical analysis was performed using GraphPad Prism 6. P values <0.05 were considered to indicate statistically significant differences.

3. Results

3.1. Characteristics of ESCC Cases in HNSCC Patients. Thirty HNSCC patients suffering from ESCC were included in this study. Of them, two HNSCC patients had recurrent cases of ESCC. The average interval time between ESCC and HNSCC diagnosis was 36.0 ± 39.2 months; the longest interval time was 180 months. There were 8 (25%) cases of synchronous carcinoma with an interval time within 6 months, 13 (40.6%) cases from 6 months to 3 years, 9 (28.1%) cases from 3 years to 6 years, and 2 (6.3%) case more than 6 years. Overall, 93.75% (30/32) of ESCC occurred within 6 years after HNSCC diagnosis.

The most common ESCC location was in the middle thoracic segment of the esophagus (13 cases) (40.6%), followed by 9 (28.1%) cases in the upper thoracic esophagus, 7 (21.9%) in the lower thoracic esophagus, and 3 (9.4%) in the cervical esophagus. There were 5 (15.6%) cases with early ESCC and 27 (84.4%) cases with advanced ESCC. In terms of endoscopic morphology, 1 (3.1%) case of early ESCC was 0-Is type and 4 (12.5%) cases were 0-IIb type, and the 27 cases of advanced ESCC were mass type (7 cases) (21.9%), mass infiltration type (10 cases) (31.3%), ulcer type (1 case) (3.1%), ulcer infiltration type (6 cases) (18.8%), and constriction type (3 cases) (9.4%). The endoscopic morphology of ESCC consisted mainly of the mass and mass infiltration types (Table 1).

Table 1: Characteristics of ESCC cases in HNSCC patients.

	ESCC cases ($n = 32$), N (%)
Interval time (months)	
≤6 months	8 (25)
6 months–3 years	13 (40.6)
3–6 years	9 (28.1)
>6 years	2 (6.3)
ESCC location	
Neck	3 (9.4)
Upper thoracic	9 (28.1)
Middle thoracic	13 (40.6)
Lower thoracic	7 (21.9)
ESCC stage	
Early	5 (15.6)
Developed	27 (84.4)
Endoscopic morphology	
Early	
0-Is	1 (3.1)
0-IIb	4 (12.5)
Developed	
Mass type	7 (21.9)
Mass infiltration type	10 (31.3)
Ulcer type	1 (3.1)
Ulcer infiltration type	6 (18.8)
Peripheral constriction type	3 (9.4)

3.2. Risk Factors Associated with ESCC Occurrence in HNSCC Patients. The case-control study was performed on HNSCC patients suffering from synchronous or metachronous ESCC and HNSCC patients without ESCC occurrence. Ninety-eight HNSCC patients were retrospectively reviewed in this research, 30 HNSCC patients with ESCC were enrolled in the ESCC group, and 68 HNSCC patients were in the without ESCC group. Although no significant differences in gender and age were observed between the ESCC and the without ESCC groups, of the 30 HNSCC patients with ESCC, 25 (83.4%) were over 50 years, and 28 (93.3%) of the patients were male. We found that male patients were 3.3 times (95% CI = 0.7–15.4) more likely to develop ESCC than female patients. The risk remained to be 1.3 times (95% CI = 0.4–3.7) and 2.1 times (95% CI = 0.6–6.8), respectively, as the age of patients increased by 10 years.

Concerning the clinicopathological risk factors, the most common HNSCC location in the ESCC group was the tongue (33.3%), followed by the soft palate (23.3%), the mouth floor (20.0%), gingiva (16.7%), and the lip and the larynx (3.3%), with no significant differences in the HNSCC location distribution of the without ESCC group. About the HNSCC stage, for the ESCC group, there were 10 (33.3%) cases with stage I, 7 (23.3%) cases with stage II, 8 (26.7%) cases with stage III, and 5 (16.7%) cases with stage IV. In the without ESCC group, there were 26 (38.2%) cases with stage I, 15 (22.1%) cases with stage II, 14 (20.6%) cases with stage III, and 13 (19.1%) cases with stage IV of the disease. The HNSCC stage was not significantly associated with ESCC development. Ki67 immunohistochemical expression was analyzed in specimens of HNSCC operation tissues. The results showed that in the ESCC group, 16 (53.3%) cases had low Ki67 LI (≤45) and 14 (46.7%) cases had high Ki67 LI (>46). In the without ESCC group, 53 (77.9%) cases had low Ki67 LI and 15 (22.1%) cases had high Ki67 LI. HNSCC patients with ESCC tended to have significantly higher Ki67 LI levels than HNSCC patients without ESCC ($P < 0.05$). Additionally, high Ki67 LI (>46) patients tended to be 3.1 times (95% CI = 1.3–7.6) more likely to develop ESCC than low Ki67 LI (≤45) patients (Figure 1). We established that 14 (46.7%) HNSCC with ESCC patients and 40 (58.8%) HNSCC without ESCC patients underwent postoperative radiotherapy, with no significant differences in radiotherapy history between the two groups.

Regarding lifestyle risk factors, smoking was not significantly associated with the occurrence of ESCC. Alcohol drinkers were 1.9 times (95% CI = 0.7–4.8) more likely to develop ESCC than nondrinkers, despite the lack of a statistically significant difference. Furthermore, drinkers with alcohol flushing response were more likely to develop ESCC than drinkers without flush response ($P < 0.05$). HNSCC patients were exposed to a 3.3 times higher risk to develop ESCC (95% CI = 1.0–10.4) if they had alcohol flush response (Table 2).

4. Discussion

In recent years, field cancerization has attracted considerable research attention [22–24]. Esophageal and oral mucosa epithelial cells are both squamous epithelial cells, which are exposed to similar environments. Hence, HNSCC patients are at high risk for second primary carcinoma of ESCC [25]. Previous studies established a 5%–15% incidence of esophageal cancer in HNSCC patients, which was significantly higher than that in the general population [3–7].

We found that the period of ESCC manifestation was large, ranging from concurrence with HNSCC to many years after HNSCC. However, 93.75% (30/32) of the ESCC cases occurred within six years after HNSCC diagnosis. Due to the long timespan of second primary ESCC, the selection of HNSCC patients and targeted upper gastrointestinal endoscopy are critical to the improvement of the early diagnosis rate of synchronous and metachronous ESCC. To clarify the associated risk factors of ESCC in patients with

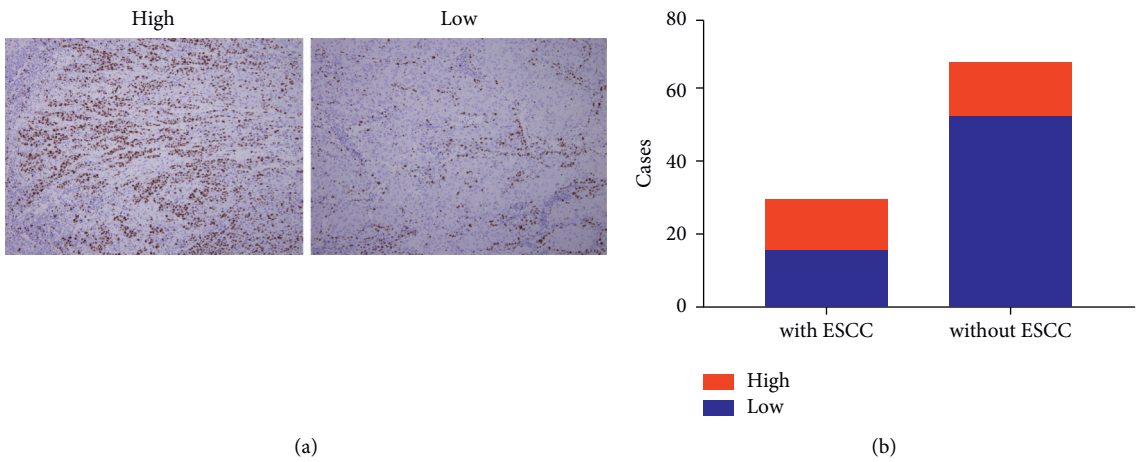

Figure 1: Ki67 immunohistochemical expression (Ki67 labeling index, Ki67 LI) in HNSCC operation tissues with or without secondary ESCC. (a) High Ki67 LI (>45) and low Ki67 LI (≤45) in HNSCC operation tissues (immunohistochemistry; magnification ×100). (b) Bar plots representing high Ki67 LI in HNSCC with ESCC patients compared to HNSCC without ESCC patients.

Table 2: Risk factors associated with ESCC occurrence in HNSCC patients.

	With ESCC ($n = 30$), N (%)	Without ESCC ($n = 68$), N (%)	Total ($n = 98$), N (%)	P	OR (95% CI)
Sex				0.1390	
Female	2 (6.7)	13 (19.1)	15 (15.3)		1
Male	28 (93.3)	55 (80.9)	83 (84.7)		3.3 (0.7, 15.4)
Age (years)				0.4618	
40–50	5 (16.7)	16 (23.5)	21 (21.4)		1
51–60	14 (46.7)	35 (51.5)	49 (50.0)		1.3 (0.4, 3.7)
>60	11 (36.7)	17 (25.0)	28 (28.6)		2.1 (0.6, 6.8)
HNSCC site				0.7129	
Lip	1 (3.3)	5 (7.4)	6 (6.1)		1
Gingiva	5 (16.7)	8 (11.8)	13 (13.3)		3.1 (0.3, 43.3)
Larynx	1 (3.3)	7 (10.3)	8 (8.2)		0.7 (0.0, 16.1)
Mouth floor	6 (20.0)	12 (17.6)	18 (18.4)		2.5 (0.3, 33.8)
Soft palate	7 (23.3)	19 (27.9)	26 (26.5)		1.8 (0.3, 24.5)
Tongue	10 (33.3)	17 (25.0)	27 (27.6)		2.9 (0.4, 37.7)
HNSCC stage				0.9051	
Stage I	10 (33.3)	26 (38.2)	36 (36.7)		1
Stage II	7 (23.3)	15 (22.1)	22 (22.4)		1.2 (0.4, 4.1)
Stage III	8 (26.7)	14 (20.6)	22 (22.4)		1.5 (0.5, 4.9)
Stage IV	5 (16.7)	13 (19.1)	18 (18.4)		1.0 (0.3, 3.2)
Ki67 labeling index				0.0177	
Low (≤45)	16 (53.3)	53 (77.9)	69 (70.4)		1
High (>45)	14 (46.7)	15 (22.1)	29 (29.6)		3.1 (1.3, 7.6)
Radiotherapy				0.2802	
No	16 (53.3)	28 (41.2)	44 (44.9)		1
Yes	14 (46.7)	40 (58.8)	54 (55.1)		0.6 (0.3, 1.5)
Smoking habits				0.7727	
Nonsmoker	5 (16.7)	13 (19.1)	18 (18.4)		1
Smoker	25 (83.3)	55 (80.9)	80 (81.6)		1.2 (0.4, 3.3)
Drinking habits				0.2452	
Nondrinker	7 (23.3)	25 (36.8)	32 (32.7)		1
Drinker	23 (76.7)	43 (63.2)	66 (67.3)		1.9 (0.7, 4.8)
Flush				0.0401	
Without flush	6 (20.0)	23 (33.8)	29 (29.6)		1
With flush	17 (56.7)	20 (29.4)	37 (37.8)		3.3 (1.0, 10.4)

HNSCC, we retrospectively analyzed HNSCC cases with ESCC who were diagnosed by upper gastrointestinal endoscopy in our hospital from 2007 to 2017. A case-control study was performed with these patients without ESCC occurrence for at least six years after HNSCC diagnosis.

Of the 30 HNSCC patients with recurrent ESCC in our present study that developed esophageal secondary primary cancer, 25 (83.4%) were aged over 50 years and 28 (93.3%) were male. Despite the lack of significant differences between the two groups included in our study, male and old-age HNSCC patients were at a higher risk to develop ESCC. These results may be due to the limited sample size of our investigation and the fact that HNSCC and ESCC patients had similar characteristics in terms of gender and age. Previous reports showed that older age (over 65 years) was significantly higher in patients with second primary esophageal cancer than in patients without esophageal cancer [26].

Our case-control study revealed that HNSCC cases with ESCC and without ESCC were similar and most commonly in the tongue and soft palate. Other research findings established no association between esophageal cancers and HNSCC location [27]. However, a larger number of esophageal secondary primary cancers were reportedly detected in patients with hypopharyngeal and oropharyngeal cancers [1]. The reasons for the different outcomes in these localizations remain to be elucidated, partly because the conclusions might have been obscured by the small sample size and the approaches employed to locate HNSCC. Furthermore, we found no significant relationship between ESCC recurrence and HNSCC staging. However, an earlier study showed that patients with esophageal recurrent cancer had earlier HNSCC staging, which may be because HNSCC patients with earlier stages had adequate time to develop recurrence [28].

Ki67 is a large nonhistone protein present in the nucleus and nucleolar region, which is observed in proliferating cells. The expression of Ki67 is a diagnostic and poor prognostic biomarker for HNSCC patients [29]. Here, we established that the Ki67 LI was significantly higher in HNSCC patients with ESCC. Therefore, it may be suggested that quantitative measurements of Ki67-positive neoplastic epithelial cells in HNSCC can be used to reveal the potential risks of recurrent ESCC. Further research is recommended with a large cohort of HNSCC patients to validate the predictive value of Ki67 LI.

The consumption of alcohol and cigarettes is a significant risk factor for HNSCC and esophageal cancer [30, 31]. A prospective study found that high-dose drinkers of HNSCC with a flush reaction were at a significantly higher risk of developing synchronous ESCC; drinkers with a higher daily average or cumulative amount were also exposed to a significantly higher risk for the development of ESCC [4]. Similar to previous studies, the present study further confirmed that alcohol flushing response is a risk factor of ESCC in patients with HNSCC. We also found that the risk for ESCC development in alcohol drinkers was 1.9 times higher than that in nondrinkers, but the impact of the cumulative dose of alcohol consumption was difficult to clarify in this retrospective study. Alcohol flushing response is associated with inherited deficiencies in the enzyme aldehyde dehydrogenase 2 (ALDH2), resulting in accumulation of acetyl aldehyde. The East Asian-specific dysfunctional ALDH2 $*$ 2 missense mutation is a genetic risk factor for upper aerodigestive tract (UADT) cancer. An earlier epidemiological study clearly showed that ALDH2 $*$ 2 was associated with increased susceptibility to synchronous and metachronous UADT cancers and was highly represented in the majority of such cancer patients, who also had faster cancer progression and poor prognosis [32].

5. Conclusions

In the present study, we found that HNSCC patients, especially drinkers with an alcohol flushing response, as well as those with high Ki67 LI in their HNSCC tissues were more likely to develop ESCC. Nevertheless, the conclusions that can be drawn have limited representativeness to make as this study was retrospective and with a very small sample size. Therefore, further prospective research is needed to confirm our present findings.

Data Availability

No data were used to support this study.

Additional Points

The authors have completed the STROBE reporting checklist.

Ethical Approval

The study was conducted in accordance with the Declaration of Helsinki (as revised in 2013). The study was approved by the Ethics Committee of Shanghai Ninth People's Hospital, Shanghai Jiao Tong University School of Medicine (No.: SH9H-2020-T189-1).

Consent

Individual consent for this retrospective analysis was waived.

Conflicts of Interest

The authors declare that there are no conflicts of interest.

Authors' Contributions

Lei Wang and Xiangjun Meng conceptualized and designed the study. Feng Wang and Wei Cao involved in provision of study materials or patients. Wenjing Pang and Kun Zhou collected and assembled data. Lei Li analyzed and interpreted data. All authors wrote the manuscript and provided the final approval.

Acknowledgments

The authors thank Pro Jiang Li of Department of Oral Pathology, Ninth People's Hospital, Shanghai Jiao Tong University School of Medicine, for pathological assistance.

References

[1] O. Bugter, S. E. M. van de Ven, J. A. Hardillo, M. J. Bruno, A. D. Koch, and R. J. Baatenburg de Jong, "Early detection of esophageal second primary tumors using Lugol chromoendoscopy in patients with head and neck cancer: a systematic review and meta-analysis," *Head & Neck*, vol. 41, no. 4, pp. 1122–1130, 2019.

[2] K. Onochi, H. Shiga, S. Takahashi et al., "Risk factors linking esophageal squamous cell carcinoma with head and neck cancer or gastric cancer," *Journal of Clinical Gastroenterology*, vol. 53, no. 4, pp. e164–e170, 2019.

[3] T. Matsui, T. Okada, K. Kawada et al., "Detection of second primary malignancies of the esophagus and hypophraynx in oral squamous cell carcinoma patients," *Laryngoscope Investigative Otolaryngology*, vol. 3, no. 4, pp. 263–267, 2018.

[4] Y. K. Wang, Y. S. Chuang, T. S. Wu et al., "Endoscopic screening for synchronous esophageal neoplasia among patients with incident head and neck cancer: prevalence, risk factors, and outcomes," *International Journal of Cancer*, vol. 141, no. 10, pp. 1987–1996, 2017.

[5] C. S. Chung, W. C. Lo, M. H. Wen, C. H. Hsieh, Y. C. Lin, and L. J. Liao, "Long term outcome of routine image-enhanced endoscopy in newly diagnosed head and neck cancer: a prospective study of 145 patients," *Scientific Reports*, vol. 6, no. 1, Article ID 29573, 2016.

[6] Y. C. Huang, Y. C. Lee, P. H. Tseng et al., "Regular screening of esophageal cancer for 248 newly diagnosed hypopharyngeal squamous cell carcinoma by unsedated transnasal esophagogastroduodenoscopy," *Oral Oncology*, vol. 55, pp. 55–60, 2016.

[7] J. A. S. Atienza and C. A. Dasanu, "Incidence of second primary malignancies in patients with treated head and neck cancer: a comprehensive review of literature," *Current Medical Research and Opinion*, vol. 28, no. 12, pp. 1899–1909, 2012.

[8] Y. Hamada, T. Mizuno, K. Tanaka et al., "Esophageal squamous cell neoplasia is an independent negative prognostic factor for head and neck cancer patients," *International Journal of Clinical Oncology*, vol. 23, no. 2, pp. 243–248, 2018.

[9] M. Morita, A. Egashira, Y. U. Nakaji et al., "Treatment of squamous cell carcinoma of the esophagus synchronously associated with head and neck cancer," *In Vivo*, vol. 31, no. 5, pp. 909–916, 2017.

[10] H. H. Ko, S. L. Cheng, J. J. Lee et al., "Factors influencing the incidence and prognosis of second primary tumors in patients with oral squamous cell carcinoma," *Head & Neck*, vol. 38, no. 10, pp. 1459–1466, 2016.

[11] E. J. Gong, D. H. Kim, J. Y. Ahn et al., "Routine endoscopic screening for synchronous esophageal neoplasm in patients with head and neck squamous cell carcinoma: a prospective study," *Diseases of the Esophagus*, vol. 29, no. 7, pp. 752–759, 2016.

[12] D. Blanchard, B. Barry, D. De Raucourt et al., "Guidelines update: posttreatment follow-up of adult head and neck squamous cell carcinoma: screening for metastasis and metachronous esophageal and bronchial locations," *European Annals of Otorhinolaryngology, Head and Neck Diseases*, vol. 132, no. 4, pp. 217–221, 2015.

[13] H. Lim, D. H. Kim, H. Y. Jung et al., "Clinical significance of early detection of esophageal cancer in patients with head and neck cancer," *Gut Liver*, vol. 9, no. 2, pp. 9159–9165, 2015.

[14] D. H. Kim, E. J. Gong, H. Y. Jung et al., "Clinical significance of intensive endoscopic screening for synchronous esophageal neoplasm in patients with head and neck squamous cell carcinoma," *Scandinavian Journal of Gastroenterology*, vol. 49, no. 12, pp. 1486–1492, 2014.

[15] W. L. Wang, C. P. Wang, H. P. Wang et al., "The benefit of pretreatment esophageal screening with image-enhanced endoscopy on the survival of patients with hypopharyngeal cancer," *Oral Oncology*, vol. 49, no. 8, pp. 808–813, 2013.

[16] Y. Y. Su, W. C. Chen, H. C. Chuang et al., "Effect of routine esophageal screening in patients with head and neck cancer," *JAMA Otolaryngol Head Neck Surg*, vol. 139, pp. 350–354, 2013.

[17] C. T. Lee, C. Y. Chang, Y. C. Lee et al., "Narrow-band imaging with magnifying endoscopy for the screening of esophageal cancer in patients with primary head and neck cancers," *Endoscopy*, vol. 42, no. 08, pp. 613–619, 2010.

[18] J. S. Kim and B. W. Kim, "Esophageal cancer and head and neck cancer: the earlier, the better," *Gut Liver*, vol. 9, pp. 131-132, 2015.

[19] P. J. Bradley and P. T. Bradley, "Searching for metachronous tumours in patients with head and neck cancer: the ideal protocol!" *Current Opinion in Otolaryngology & Head and Neck Surgery*, vol. 18, no. 2, pp. 124–133, 2010.

[20] M. B. Amin, S. B. Edge, F. L. Greene et al., *AJCC Cancer Staging Manual*, Springer, Berlin, Germany, 2017.

[21] C. H. Lee, J. M. Lee, D. C. Wu et al., "Independent and combined effects of alcohol intake, tobacco smoking and betel quid chewing on the risk of esophageal cancer in Taiwan," *International Journal of Cancer*, vol. 113, no. 3, pp. 475–482, 2005.

[22] K. Curtius, N. A. Wright, and T. A. Graham, "An evolutionary perspective on field cancerization," *Nature Reviews Cancer*, vol. 18, no. 1, pp. 19–32, 2018.

[23] Y. Baba, T. Ishimoto, J. Kurashige et al., "Epigenetic field cancerization in gastrointestinal cancers," *Cancer Letters*, vol. 375, no. 2, pp. 360–366, 2016.

[24] P. V. Angadi, J. K. Savitha, S. S. Rao, and Y. Sivaranjini, "Oral field cancerization: current evidence and future perspectives," *Oral and Maxillofacial Surgery*, vol. 16, no. 2, pp. 171–180, 2012.

[25] The Cancer Genome Atlas Research Network, "Integrated genomic characterization of oesophageal carcinoma," *Nature*, vol. 541, no. 7636, pp. 169–175, 2017.

[26] T. Iwatsubo, R. Ishihara, T. Morishima et al., "Impact of age at diagnosis of head and neck cancer on incidence of metachronous cancer," *BMC Cancer*, vol. 19, no. 1, p. 3, 2019.

[27] H. Ikawa, M. Tonogi, G. Y. Yamane et al., "Upper gastrointestinal tract cancers as double-cancers in elderly patients with oral squamous cell carcinoma," *The Bulletin of Tokyo Dental College*, vol. 53, no. 1, pp. 9–16, 2012.

[28] O. Bugter, D. L. Iwaarden, E. A. C. Dronkers et al., "Survival of patients with head and neck cancer with metachronous multiple primary tumors is surprisingly favorable," *Head & Neck*, vol. 41, no. 6, pp. 1648–1655, 2019.

[29] A. R. Gadbail, S. C. Sarode, M. S. Chaudhary et al., "Ki67 Labelling Index predicts clinical outcome and survival in oral squamous cell carcinoma," *Journal of Applied Oral Science*, vol. 29, Article ID e20200751, 2021.

[30] Y. Liu, H. Chen, Z. Sun, and X. Chen, "Molecular mechanisms of ethanol-associatedoro-esophageal squamous cell carcinoma," *Cancer Letters*, vol. 361, no. 2, pp. 164–173, 2015.

[31] C. S. Chung, L. J. Liao, W. C. Lo et al., "Risk factors for second primary neoplasia of esophagus in newly diagnosed head and neck cancer patients: a case-control study," *BMC Gastroenterology*, vol. 13, no. 1, p. 154, 2013.

[32] C. H. Chen, W. L. Wang, M. H. Hsu, and D. Mochly-Rosen, "Alcohol consumption, ALDH2 polymorphism as risk factors for upper aerodigestive tract cancer progression and prognosis," *Life*, vol. 12, no. 3, p. 348, 2022.